

UNRAVELING THE GENETIC EFFECTS AND DECIPHERING THE
MOLECULAR MECHANISMS UNDERLYING THE TOLERANCE TO
PHOSPHORUS DEFICIENCY IN POPCORN PLANTS

ROSIMEIRE BARBOZA BISPO

UNIVERSIDADE ESTADUAL DO NORTE FLUMINENSE
DARCY RIBEIRO – UENF

CAMPOS DOS GOYTACAZES - RJ
FEBRUARY – 2024

UNRAVELING THE GENETIC EFFECTS AND DECIPHERING THE
MOLECULAR MECHANISMS UNDERLYING THE TOLERANCE TO
PHOSPHORUS DEFICIENCY IN POPCORN PLANTS

ROSIMIERE BARBOZA BISPO

“Thesis presented to the Centro de Ciências e
Tecnologias Agropecuárias of the Universidade
Estadual do Norte Fluminense Darcy Ribeiro, as
part of the requirements for obtaining the title of
Doctor of Science in Genetics and Plant
Breeding.”

Advisor: Prof. Antônio Teixeira do Amaral Junior

CAMPOS DOS GOYTACAZES - RJ
FEBRUARY – 2024

FICHA CATALOGRÁFICA

UENF - Bibliotecas

Elaborada com os dados fornecidos pela autora.

B622

Bispo, Rosimeire Barboza.

Unraveling the genetic effects and deciphering the molecular mechanisms underlying the tolerance to phosphorus deficiency in popcorn plants / Rosimeire Barboza Bispo. - Campos dos Goytacazes, RJ, 2024.

154 f. : il.

Bibliografia: 63 - 75.

Tese (Doutorado em Genética e Melhoramento de Plantas) - Universidade Estadual do Norte Fluminense Darcy Ribeiro, Centro de Ciências e Tecnologias Agropecuárias, 2024.
Orientador: Antonio Teixeira do Amaral Junior.

1. Estresse nutricional. 2. Análise dialéctica. 3. Proteômica. 4. *Zea mays L. var. everta*. I. Universidade Estadual do Norte Fluminense Darcy Ribeiro. II. Título.

CDD - 631.5233

UNRAVELING THE GENETIC EFFECTS AND DECIPHERING THE
MOLECULAR MECHANISMS UNDERLYING THE TOLERANCE TO
PHOSPHORUS DEFICIENCY IN POPCORN PLANTS

ROSIMEIRE BARBOZA BISPO

“Thesis presented to the Centro de Ciências e
Tecnologias Agropecuárias of the Universidade
Estadual do Norte Fluminense Darcy Ribeiro, as
part of the requirements for obtaining the title of
Doctor of Science in Genetics and Plant
Breeding.”

Approved on February 23rd, 2024.

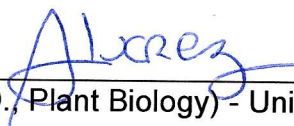
Examining committee:




Prof. Vitor Batista Pinto (D.Sc. Genetics and Breeding) - UENF



Prof. Ricardo Enrique Bressan-Smith (D.Sc. Plant Production) - UENF



Dr. Sophie Alvarez (Ph.D. Plant Biology) - University of Nebraska- Lincoln/UNL



Prof. Antônio Teixeira do Amaral Junior (D.Sc, Genetics and Breeding) - UENF
(Advisor)

DEDICATION

"It's not what the world holds for you, but what you bring to the world."

Anne with an E

ACKNOWLEDGMENTS

To God, for placing such wonderful people in my life and for all the opportunities I've had.

To everyone in my family who is always by my side and believes in me, especially my grandparents Luiz (*In memoriam*) and Joséfa, my parents Alírio and Maria and my sisters Marciele, Rosieli, Liliane and Rosimara (my soulmate).

To my advisor, Professor Dr. Antônio Teixeira do Amaral Junior, for the opportunity, trust, friendship, and all the support over these years, you were essential to this achievement.

To Professors Eliemar Campostrini and Vitor Batista Pinto for their contributions and co-orientation in this study.

To the friends of the Popcorn Breeding Group, Divino, Valter, Samuel, Jhean, Uéliton, Bruna, and others, for their company, trust, help and friendship. Especially Talles de Oliveira Santos, for his partnership in the laboratory and in the travels, thank you for everything.

To my laboratory colleagues at the University of Nebraska - Lincoln, Mike, Anne, and especially to Professor Sophie Alvarez, for all the teachings and learning during my sandwich Ph.D.

To my friends from Lincoln, Nebraska, Ana, Felipe, Rafael, and Raissa, thank you for all the moments together, and especially to Denny and Roy, for being like a family during this time.

To the secretary of the Graduate Program in Genetics and Plant Breeding, José Daniel, for all his support throughout the years.

To the Universidade Estadual do Norte Fluminense Darcy Ribeiro and the Graduate Program in Genetics and Plant Breeding for the opportunity of education and completion of my Ph.D.

To CAPES, for granting me a scholarship, and to other research funding organizations that contributed to my education.

This study was financed in part by the Coordenação de Aperfeiçoamento de Pessoal de Nível Superior - Brasil (CAPES) – Finance Code 001.

SUMMARY

| | |
|------------------------------------------------------------------------------------------------------------|------|
| ABSTRACT | xi |
| RESUMO | xiii |
| 1. INTRODUCTION | 1 |
| 2. OBJECTIVES | 3 |
| 2.1 Objectives of the first chapter | 3 |
| 2.2 Objective of the second chapter | 3 |
| 3. CHAPTERS | 4 |
| 3.1 MORPHOPHYSIOLOGICAL APPROACH TO HETEROSIS IN PHOSPHORUS USE EFFICIENCY IN POPCORN | 4 |
| 3.1.1 INTRODUCTION | 4 |
| 3.1.2 LITERATURE REVIEW | 6 |
| 3.1.2.1 General aspects of popcorn..... | 6 |
| 3.1.2.2 Improving maize for phosphorus use efficiency..... | 8 |
| 3.1.3 MATERIALS AND METHODS | 10 |
| 3.1.3.1 Genotypes and growing conditions..... | 10 |
| 3.1.3.2 Traits evaluated | 12 |
| 3.1.3.2.1 Morphological traits | 12 |
| 3.1.3.2.2 Concentration, utilization rates, and efficiency of P | 12 |
| 3.1.3.2.3 Chlorophyll fluorescence measurements..... | 13 |
| 3.1.3.2.4 Leaf pigments | 13 |
| 3.1.3.2.5 Gas exchange measurements..... | 13 |
| 3.1.3.2.6 Estimating heterosis | 14 |
| 3.1.3.2.7 Statistical analysis | 14 |
| 3.1.4 RESULTS | 15 |
| 3.1.4.1 Plant growth traits and phosphorus use efficiency..... | 15 |
| 3.1.4.2 Chlorophyll fluorescence, leaf pigments, and exchange measurements..... | 19 |

| | |
|-------------------------------------------------------------------------------------------------------------------------------------------------------------------------------|----|
| 3.1.5 DISCUSSION | 22 |
| 3.1.5.1 Impact of P availability on growth traits and P use efficiency in popcorn genotypes | 22 |
| 3.1.5.2 Effect of P supply on chlorophyll fluorescence, leaf pigments, and gas exchange measurements in popcorn genotypes | 25 |
| 3.1.5.3 How can genetic gains be maximized in popcorn under P deficiency?..... | 27 |
| 3.1.6 CONCLUSION | 28 |
| 3.2 UNRAVELING THE MECHANISMS OF EFFICIENT PHOSPHORUS UTILIZATION IN POPCORN (<i>Zea mays</i> L. VAR. EVERTA): INSIGHTS FROM PROTEOMICS AND METABOLITES ANALYSIS | 30 |
| 3.2.1 INTRODUCTION | 30 |
| 3.2.2 LITERATURE REVIEW | 32 |
| 3.2.2.1 Phosphorus within Plants: Uptake, Utilization and Remobilization..... | 32 |
| 3.2.2.2 Proteomic approaches to P use efficiency..... | 34 |
| 3.2.3 MATERIALS AND METHODS | 36 |
| 3.2.3.1 Plant materials and treatment..... | 36 |
| 3.2.3.2 Physiological measurements | 38 |
| 3.2.3.2.1 Leaf gas exchange measurements | 38 |
| 3.2.3.2.2 Leaf chlorophyll content..... | 38 |
| 3.2.3.2.3 Dry matter..... | 38 |
| 3.2.3.2.4 Phosphorus concentration..... | 38 |
| 3.2.3.2.5 P utilization and efficiency indexes | 39 |
| 3.2.3.2.6 Statistical analysis | 39 |
| 3.2.3.3 Proteomics..... | 39 |
| 3.2.3.3.1 Material handling | 39 |
| 3.2.3.3.2 Protein extraction and digestion | 40 |
| 3.2.3.3.3 Proteomic analysis | 40 |
| 3.2.3.3.4 Gene ontology and enrichment pathway analysis | 42 |
| 3.2.3.4 Metabolomic Analysis..... | 42 |
| 3.2.3.4.1 Sample Preparation for LC-MS/MS | 42 |
| 3.2.3.4.2 LC-MS/MS, polyphenols and phytohormones analysis | 43 |
| 3.2.3.4.3 Statistical analysis | 43 |
| 3.2.4 RESULTS | 44 |
| 3.2.4.1 Physiological responses of popcorn to phosphorus deficiency..... | 44 |
| 3.2.4.2 Proteome profile of popcorn leaves | 47 |

| | | |
|--------------|-----------------------------------------------------------------------------------------------------|-----------|
| 3.2.4.3 | Functional analysis of DEPs involved in the response to P deficiency..... | 49 |
| 3.2.4.4 | Metabolite analysis | 56 |
| 3.2.5 | DISCUSSION | 58 |
| 3.2.5.1 | Effects of P deficiency and adaptation mechanisms..... | 58 |
| 3.2.5.2 | P deficiency impacts the photosynthesis, electron transfer chain and energy metabolism in L80 | 58 |
| 3.2.5.3 | P starvation affects ribosomal protein biosynthesis | 60 |
| 3.2.5.4 | Protective mechanisms involved in the oxidative stress response..... | 61 |
| 3.2.6 | CONCLUSIONS | 62 |
| | REFERENCES | 63 |
| | APPENDIX | 76 |

LIST OF FIGURES

- Figure 1.** Average, maximum, and minimum temperature ($^{\circ}\text{C}$), relative humidity (RH, %), and photosynthetically active radiation (PAR, $\mu\text{mol m}^{-2} \text{s}^{-1}$) over the dates and phenological stages (V) of popcorn plant growth in two conditions of P availability (May to July 2021)11
- Figure 2.** Importance (expressed as %) of the quadratic components related to general (ϕ_g) and specific combining ability (ϕ_s) and reciprocal effects (ϕ_{rc}) and residual effects for the traits.....18
- Figure 3.** Importance (expressed as %) of quadratic components related to general (ϕ_g) and specific combining ability (ϕ_s), reciprocal (ϕ_{rc}), and residual effects for traits related to photosynthesis, chlorophyll fluorescence, and leaf pigments.....22
- Figure 4 -** Average, maximum, and minimum temperature ($^{\circ}\text{C}$), relative humidity (RH, %) and photosynthetically active radiation (PAR, $\mu\text{mol m}^{-2} \text{s}^{-1}$) along the dates and phenological stages (V) of growth of popcorn plants under two conditions of P availability.....37
- Figure 5.** Dry matter accumulation (**A**) P content (**B**) and PUE (**C**) in shoot in the two popcorn inbred lines L80 and P7 under high (HP) and low (LP) phosphorus levels.....44
- Figure 6. A-** Line L80 under low P supply. **B-** Line P7 under low P supply.....45

| | |
|-----------------------------------------------------------------------------------------------------------------------------------------------------------------------------------------------------------------------------------------------------------------------------------------------------------------------------------------------------------------------|----|
| Figure 7. Photosynthetic traits in two popcorn inbred lines L80 and P7 under high (HP) and low (LP) phosphorus levels. A- net CO ₂ assimilation rate (A); <i>g_s</i> - stomatal conductance (B); <i>E</i> - transpiration (C); <i>C_i</i> - internal CO ₂ concentration (D)..... | 46 |
| Figure 8. Chlorophyll (A) flavonoid (B) and anthocyanin content (C) in the leaves of the two popcorn inbred lines L80 and P7 under high (HP) and low (LP) phosphorus levels..... | 47 |
| Figure 9. Heatmap of the 2549 proteins identified and quantified in L80 and P7 under high P and low P conditions..... | 48 |
| Figure 10. Venn diagram analysis of differentially expressed proteins (DEPs) in L80_LP/L80_HP and P7_LP/P7_HP, broken down as up- and down-regulated..... | 49 |
| Figure 11. GO enrichment analysis of DEPs uniquely down-regulated in L80_LP or P7_LP..... | 50 |
| Figure 12. GO enrichment analysis of DEPs uniquely up-regulated in L80 or P7..... | 52 |
| Figure 13. KEGG pathway enrichment analysis of the DEPs uniquely down- and up-regulated in L80 and P7..... | 53 |
| Figure 14. Polyphenols (A) and phytohormones (B) accumulation pattern in leaves of L80 and P7 lines in high and low P supply. Concentration in ng/g..... | 57 |

LIST OF TABLES

| | |
|-------------------------------------------------------------------------------------------------------------------------------------------------------------------------------------------------------------------------------------------------------------------------------------------------------------------------------------------|----|
| Table 1. Summary of the joint and individual analyses of variance, means, standard deviations, and heterosis (H %) for morphological traits and P use efficiency in popcorn inbred lines and hybrids in diallel grown under contrasting conditions of P availability..... | 17 |
| Table 2. Summary of the joint and individual analyses of variance, means, standard deviations, and heterosis (H %) of physiological traits associated with gas exchange, chlorophyll fluorescence, and leaf pigment measurements of popcorn lines and hybrids in diallel grown under contrasting conditions of P availability..... | 20 |
| Table 3. Selected differentially expressed proteins (DEPs) in leaves of popcorn lines treated with high and low P availability from the major enriched pathways identified by KEGG enrichment analysis..... | 54 |

ABSTRACT

Bispo, Rosimeire Barboza; D.Sc.; Universidade Estadual do Norte Fluminense Darcy Ribeiro; February 2024; Unraveling the genetic effects and deciphering the molecular mechanisms underlying the tolerance to phosphorus deficiency in popcorn plants; Advisor: Antônio Teixeira do Amaral Junior; Counselors: Eliemar Campostrini and Vitor Batista Pinto.

Agriculture expansion combined with the need for sustainable farming activities is a major drive for breeders to introduce plant cultivars better adapted to abiotic stress conditions such as nutrient deficiency. Phosphorus (P) plays a crucial role in photosynthesis and, consequently, in plant growth. Moreover, P is a non-renewable resource, requiring the extraction of limited reserves of phosphate rocks. This instigates considerable interest in the development of crop varieties capable of providing higher yields while utilizing available soil P more efficiently. In this context, the objective of this study is to investigate the genetic effects governing growth traits, phosphorus use efficiency (PUE), foliar gas exchange, and photochemical efficiency in four S₇ popcorn lines (P2 and P7, efficient and responsive to P; L75 and L80, inefficient and unresponsive to P) and their respective 12 F_{1s} hybrids under two contrasting P conditions: high P (100% - 31.00 mg NH₄H₂PO₄ L⁻¹) and low P (0.5% - 0.15 mg NH₄H₂PO₄ L⁻¹). Additionally, the study aims to investigate the differential expression of proteins and the production of metabolites in two popcorn lines (P7 and L80) to elucidate the molecular mechanisms involved in the response to P deficiency. The first chapter focused on estimating the genetic effects influencing

the control of morphophysiological traits associated with PUE in four popcorn lines subjected to contrasting P conditions. Utilizing the diallel analysis proposed by Griffing (1956), additive, non-additive, and reciprocal genetic effects governing these traits were calculated. In both P conditions, non-additive genetic effects were more prominent, indicating that exploiting heterosis represents the most viable strategy for developing cultivars with greater PUE efficiency. Additionally, the concentration of flavonoids emerged as a promising trait for differentiating genotypes in both P conditions. In the second chapter, physiological, proteomic, and comparative metabolomic approaches were employed to unravel differences in the response to P availability in two contrasting lines for PUE, P7 and L80, under low (LP) and high (HP) P conditions, as described in the first chapter. Under LP conditions, chlorophyll and anthocyanin concentrations were not significant between P7 and L80, while the concentration of flavonoids was almost twice as high in P7. Comparative proteomic analysis revealed differentially expressed proteins (DEPs) associated with photosynthesis, protein biosynthesis, secondary metabolites, and energy metabolism exclusively under LP conditions. Furthermore, distinct mechanisms of redox regulation and oxidative stress were identified in the two lines. Enzymes such as glutathione transferase, involved in detoxifying reactive oxygen species (ROS), ascorbate dehydratase, chalcone-flavanone isomerase, and glycosyltransferase related to flavonoid biosynthesis were accumulated exclusively in the P7 line. Additionally, metabolomic analysis data revealed that flavonoids such as apigenin, luteolin, kaempferol, quercetin, and syringic acid were more abundantly accumulated in P7. These results highlight significant differences in response mechanisms between the lines, paving the way for future research and agronomic improvements aimed at developing popcorn varieties more resistant to low P conditions.

Keywords: Nutritional stress, Diallel analysis, Proteomics, *Zea mays* L. var. *everta*

RESUMO

Bispo, Rosimeire Barboza; D.Sc.; Universidade Estadual do Norte Fluminense Darcy Ribeiro; February, 2024; Unraveling the genetic effects and deciphering the molecular mechanisms underlying the tolerance to phosphorus deficiency in popcorn plants; Orientador: Antônio Teixeira do Amaral Junior; Conselheiros: Eliemar Campostrini e Vitor Batista Pinto.

A expansão da agricultura, aliada à necessidade de práticas agrícolas sustentáveis, constitui um forte estímulo para os melhoristas introduzirem variedades de plantas mais adaptadas às condições de estresse abiótico, como a deficiência de nutrientes. O fósforo (P) desempenha um papel crucial na fotossíntese e, por conseguinte, no crescimento das plantas. Além disso, o P é um recurso não renovável, requerendo extração de reservas limitadas de rochas fosfáticas. Isso instiga um interesse considerável no desenvolvimento de variedades de culturas capazes de proporcionar maiores rendimentos enquanto utilizam de maneira mais eficiente o P disponível no solo. Neste sentido, o objetivo deste estudo é investigar os efeitos genéticos que regem às características de crescimento, eficiência no uso de P (PUE), as trocas gasosas foliares e eficiência fotoquímica em quatro linhagens S₇ de milho-pipoca (P2 e P7 eficientes e responsivas ao P; L75 e L80 ineficientes e não responsivas ao P) e os respectivos 12 híbridos F_{1s}, em duas condições contrastantes de P: alto P (100% - 31,00 mg NH₄H₂PO₄ L⁻¹) e baixo P (0,5% - 0,15 mg NH₄H₂PO₄ L⁻¹). Além disso, o estudo visa investigar a expressão diferencial de proteínas e a produção de metabólitos de duas linhagens de milho-pipoca (P7 e

L80) a fim de elucidar os mecanismos moleculares envolvidos na resposta à deficiência de P. O primeiro capítulo concentrou-se na estimativa dos efeitos genéticos que influenciam o controle de características morfofisiológicas associadas à PUE em quatro linhagens de milho-pipoca submetidas a condições contrastantes de P. Utilizando a análise dialélica proposta por Griffing (1956), foram calculados os efeitos genéticos aditivos, não-aditivos e recíprocos que regem essas características. Em ambas as condições de P, os efeitos genéticos não-aditivos foram mais proeminentes, indicando que a exploração da heterose representa a estratégia mais viável para o desenvolvimento de cultivares com maior eficiência em PUE. Além disso a concentração de flavonóides surgiu como uma característica promissora na diferenciação de genótipos em ambas as condições de P. No segundo capítulo abordagens fisiológicas, de proteômica e metabolômica comparativa foram empregadas com o objetivo de desvendar as diferenças na resposta à disponibilidade de P em duas linhagens contrastante para a PUE, P7 e L80, sob baixo (LP) e alto (HP) P, conforme descrito no primeiro capítulo. Em condições de LP, a concentração de clorofila e antocianinas não apresentou diferenças significativas entre P7 e L80, enquanto a concentração de flavonoides foi quase duas vezes maior em P7. A análise de proteômica comparativa revelou que proteínas diferencialmente expressas (DEPs) associadas à fotossíntese, biossíntese de proteínas, metabólitos secundários e metabolismo energético foram observadas exclusivamente na condição de LP. Além disso, foram identificados mecanismos distintos de regulação redox e estresse oxidativo nas duas linhagens. Enzimas como glutathione transferase, envolvidas na desintoxicação de espécies reativas de oxigênio (ROS), arogenato desidratase, chalcona-flavonona isomerase e glicosiltransferase relacionadas à biossíntese de flavonoides foram acumuladas exclusivamente na linhagem P7. Adicionalmente, os dados da análise metabolômica revelou que flavonoides como apigenina, luteolina, kaempferol, quercetina e o ácido fenólico siríngico foram mais abundantemente acumulados em P7. Esses resultados evidenciam diferenças significativas nos mecanismos de resposta entre as linhagens. Isso abre caminho para futuras pesquisas e aprimoramentos agronômicos, com o objetivo de desenvolver variedades de milho-pipoca mais resistentes a condições de baixo teor de P.

Palavras-chave: Estresse nutricional, Análise dialélica, Proteômica, *Zea mays* L. var. *everta*

1. INTRODUCTION

The expansion of agriculture, along with the need for sustainable cultivation, represents one of the major challenges for the scientific community working on the development of new cultivars adapted to abiotic stress conditions (Gerhardt et al., 2017; Silva et al., 2019). Among the stressors, the low availability of phosphorus (P) is of great importance because its natural source is finite, and deficiency of this mineral limits plant growth and development (Zhang et al., 2014; Sun et al., 2018; Schegoscheski Gerhardt et al., 2019).

It is estimated that less than 20% of phosphate fertilizer applied to soils is taken up by crops due to factors such as plant uptake capacity, soil buffering effects, or the duration of mineral contact with roots (Cordell and White, 2014). A significant portion of the applied mineral that is not available to crops leaches into lakes and rivers, resulting in severe environmental impacts (Mpanga et al., 2019).

An alternative to mitigate the consequences associated with excessive P use is to develop materials/cultivars more efficiently in both acquisition and internal use. Studies have attempted to understand the physiological and genetic basis of morphological traits related to plant responses to low soil P, using model species as well as maize. Methods available for such studies and the generation of novel genotypes include diallel crosses (DoVale and Fritsche-Neto, 2013; Colombo et al., 2018). These represent genetic designs for generating combinations of contrasting genotypes, allowing the identification of progeny that include traits such as P use efficiency and productivity, as well as allelic interactions (Gerhardt et al., 2017; Schegoscheski Gerhardt et al., 2019).

Genotypes obtained from diallels are a valuable source of material, where trait variances have already been resolved and interactions have been studied. Such genotypes, which differ in P use efficiency, differ in their success in triggering different adaptive mechanisms that can be contrasted with traits previously studied in the diallel. These mechanisms work to enhance P uptake and utilization and involve changes at the physiological, morphological, and molecular levels, including changes in gene expression and subsequent protein expression (Ayadi et al., 2015; Zhan et al., 2019; Luo et al., 2020).

The main morphological and physiological changes in response to low P occur in the roots and consist of: reduction in primary root growth and the development of longer and denser root hairs (Lan et al., 2018); release of organic acids and acid phosphatases to liberate inorganic phosphate (Pi) from organic sources (López-Arredondo et al., 2014; Zhang et al., 2014); and activation of high-affinity Pi transporter genes (Liu et al., 2016; Mlodzińska and Zboińska, 2016; Zhan et al., 2019). Molecular mechanisms involved in P use efficiency in plants have identified proteins involved in different pathways, such as photosynthesis, carbohydrate metabolism, energy metabolism, secondary metabolism, signal transduction, protein synthesis, and defense mechanisms (Li et al., 2014; Zhang et al., 2014).

Proteins involved in the ethylene pathway are important because they may be associated with cell expansion and capillary root development (Song et al., 2016; Shibata and Sugimoto, 2019). Ethylene also plays a role in mediating the response to nutrient deficiency (García et al., 2015; Dubois et al., 2018; Huang et al., 2020). In addition, acid phosphatases and cysteines are important proteins as they contribute to internal Pi homeostasis (Huang et al., 2019; Mo et al., 2019; Ruan et al., 2019). Proteins involved in the sucrose pathway may interfere with the activity of ribulose-1,5-bisphosphate carboxylase/oxygenase (Rubisco), which are essential for photosynthetic processes in response to Pi deficiency (Li et al., 2017).

Therefore, a more comprehensive investigation of the response among different genotypes at the proteomic level may provide insight into whether the efficiency of P use is related to the efficiency of its acquisition or internal utilization (Zhang et al., 2016). However, a significant amount of this information remains unclear for popcorn.

2. OBJECTIVES

2.1 Objectives of the first chapter

- To analyze the genetic mechanisms underlying the differences in growth traits, P use efficiency, leaf gas exchange, and photochemical efficiency in popcorn genotypes under two phosphorus supply conditions; and
- To investigate the effects of heterosis on the phenotypic expression of these traits.

2.2 Objective of the second chapter

- To investigate the response mechanisms of two popcorn inbred lines, one P-efficient and one P-inefficient, under low and high phosphorus availability through proteomic and metabolite analysis

3. CHAPTERS

3.1 MORPHOPHYSIOLOGICAL APPROACH TO HETEROSIS IN PHOSPHORUS USE EFFICIENCY IN POPCORN

3.1.1 INTRODUCTION

Studies reveal that 30% of the world's arable soils face phosphorus (P) deficiency (MacDonald et al., 2011; Alewell et al., 2020). The lack of this nutrient in such areas can reduce crop yields by 30% to 40% (Malhotra et al., 2018). Tropical regions are particularly affected due to the presence of highly weathered and acidic soils, with strong capacity to sequester iron and aluminum ions, thereby limiting the availability of phosphorus for plant absorption (Yadav et al., 2017; Mabagala, 2022).

As a result, less than 20% of the phosphate fertilizer applied to soils is absorbed by plants and the reasons for the low efficiency are the buffering of the soil, or the lack of adequate contact between the mineral and the roots (Cordell and White, 2014). Faced with this limitation to maintain crop productivity, farmers have employed extensive applications of phosphate fertilizers derived from phosphate rock. However, this resource is finite, non-renewable, and plays a fundamental role in sustaining global food production (Scholz et al., 2013; Yang et al., 2017; Grieger et al., 2023). In high yield cropping systems, intensive fertilization with inorganic

phosphate (Pi) has been associated to significant water pollution (Mpanga et al., 2019), while in low yield systems, prevailing in developing countries, the scarcity of Pi availability is a major constraint on agricultural production (Galindo-Castaños et al., 2018; Langhans et al., 2022).

Therefore, the pursuit of cultivars with enhanced P utilization is crucial for three primary reasons: firstly, fertilizers represent a substantial portion of agricultural production costs; secondly, the indiscriminate and excessive application of fertilizers exert a significant environmental impact, resulting in contamination of water sources; and lastly, the production of phosphate fertilizers relies on non-renewable mineral sources (Parentoni et al., 2012). Consequently, researchers and breeders are seeking timely strategies to enhance the phosphorus use efficiency and mitigate the adverse effects associated with its excessive use in agriculture. To achieve this goal, ongoing studies are focused on the development of crops that enhance both the acquisition (Lynch, 2007) and utilization (Taghinasab et al., 2018; Wacker-Fester et al., 2019; Santos et al., 2022) of P. This research aims the reduction of production costs, preserve the environment, and ensure the sustained availability of this essential nutrient in agriculture.

Identifying genotypes that produce more biomass per unit of P applied is an alternative for sustainable agricultural production. Studies on different crops have used physiological traits associated with the photosynthetic process to select genotypes displaying superior growth performance in phosphorus deficient soils (Carstensen et al., 2019; Chea et al., 2021; Kumar et al., 2021; Kayoumu et al., 2023). The aim is to identify varieties with greater efficiency in using available P, thereby reducing the dependence on phosphate fertilizers, and promoting sustainable agricultural practices.

Breeding programs play a role in the development of cultivars with enhanced phosphorus use efficiency (PUE) in the soil, taking into account the genetic action linked to agronomic and physiological traits. Studies carried out with corn and popcorn plants reveal that the genetic action of dominance significantly influences the expression of PUE under conditions of P deficiency (Fritsche-Neto et al., 2010; Caixeta et al., 2013; Almeida et al., 2018; Gerhardt et al., 2019). Nevertheless, further research is essential to understand how heterosis manifests itself in the initial stages of plant development and to investigate the physiological mechanisms underlying this performance under conditions of P deficiency. Additionally, exploring

the influence of genetic control on traits associated with carbon assimilation, water loss, leaf pigmentation, and photochemical efficiency will contribute to a more comprehensive understanding of how popcorn genotypes respond to the expression of PUE.

With these considerations in mind, this study aimed to analyze the genetic mechanisms responsible for the discrepancies in growth traits, P use efficiency, leaf gas exchange, and photochemical efficiency, under optimal conditions and in scenarios of phosphorus deficiency in the rhizosphere. Furthermore, it was sought out to investigate the effects of heterosis on the phenotypic expression of these traits.

3.1.2 LITERATURE REVIEW

3.1.2.1 General aspects of popcorn

Popcorn, scientifically known as *Zea mays* L. var. *everta* (Sturtev) L.H. Bailey (Galinat, 1979), is a subspecies of *Zea mays* L. It is a monocotyledonous plant belonging to the family Poaceae, tribe Maydeae, genus *Zea*, and species *mays* (*Zea mays* L.) (Goodman and Smith, 1987). Like common corn, both have the same number of chromosomes ($n = 10$) (Ranum et al., 2014).

Currently, five major types of maize are known: flint, dent, popcorn, sweet, and floury. This classification is due to differences in the quantity, quality, and composition of the grain endosperm (Noor and Iqbal, 2017). In addition to grain differences, popcorn differs from common corn in other characteristics. Popcorn plants have thinner stalks, generally fewer leaves, and smaller but more numerous ears that are positioned higher, making them more prone to lodging and stalk breakage and more susceptible to diseases such as stalk rot, ear rot, and grain rot (Sawazaki, 2001).

However, the primary characteristic that distinguishes popcorn from all other types of maize is the formation of large flakes when the kernels explode in response to heating (Ziegler, 2000). This characteristic is referred to as "expansion" or "popping" capacity (Larish and Brewbaker, 1999). The expansion capacity of

popcorn is simply the ratio of the volume of expanded popcorn to the initial volume or weight of the grains subjected to popping (Guadagnin, 1996). When the kernels are exposed to temperatures above 180°C, they expand due to the presence of oil and moisture in the kernel (Silva et al., 1993). The higher the expansion capacity, the better the quality of the popcorn (Sawazaki, 2001).

In addition, popcorn kernels can vary in shape (round, flat, pointed), size, and color (pink, cream, red, purple, black, blue), with white and yellow being the most common colors. The round, pearl-like popcorn with yellow to orange endosperm is the most commercially accepted variety (Sawazaki, 2001).

Regarding the geographic origin of maize, some believe that it was one of the first plants cultivated by farmers between 7,000 and 10,000 years ago. Evidence of maize as a food source has been found in some archaeological sites in Mexico, where small maize cobs estimated to be over 5,000 years old have been found in caves (Ranum et al., 2014).

Despite the historical evidence, various hypotheses have been proposed regarding the origin of maize. Some authors suggest that maize originated from a wild grass called teosinte, which is quite different from modern maize (Beadle, 1939). Others suggest the formation of a hybrid between two wild grasses - a perennial subspecies of teosinte, *Zea diploperennis*, and a species of *Tripsacum* (Ranum et al., 2014).

Similarly, the origin of popcorn is not fully understood. Mangelsdorf and Smith (1949) collected evidence of an ancient popcorn specimen found at the "Bat Cave" archaeological site in New Mexico, dated to 2,500 B.C., which sparked discussions about the origin of popcorn and its relationship to other maize species (Ziegler, 2000). Since then, several hypotheses have been proposed regarding the origin of popcorn. Erwin (1950) proposed that popcorn arose from a mutation of flint endosperm maize. On the other hand, Brunson (1955), based on archaeological evidence, found that popcorn popping is a quantitative trait controlled by many genes, making Erwin's hypothesis unlikely. Thus, the debate over the origin of popcorn continues to this day. However, the most widely accepted hypothesis today is that maize originated in central Mexico about 9,000 years ago from a wild grass called teosinte (Iltis, 1983).

In economic terms, popcorn stands out as a snack with significant economic value added (Jele et al., 2014), and its popularity continues to grow on a global scale. The Global Popcorn Market 2021 report predicts a remarkable increase, estimating

that the popcorn market will reach an impressive US\$16.9 billion by 2027. Notably, the United States and China dominate the global production rankings, underscoring the widespread appeal of this delicious treat. Nationally, the state of Mato Grosso is the largest producer of this cereal, with 268,402 thousand tons produced in a cultivated area of 60,017 hectares during the 2018 agricultural year, the largest in recent years (Kist, 2019). In addition to Mato Grosso, Rio Grande do Sul also contributes to the popcorn supply, with the average yield ranging from 5,500 to 7,200 kilograms per hectare during the 2018/19 harvest.

3.1.2.2 Improving maize for phosphorus use efficiency

It is estimated that 90% of phosphate rock is used for food production, with 82% going to fertilizer, 5% to animal feed, and only 2-3% to food additives (Schroder, 2010). Furthermore, phosphorus resources are unevenly distributed among users, with Morocco controlling 40% of the estimated remaining global reserves (Cordel and White 2014; Scholz and Wellmer, 2015).

In addition, studies indicate that 30% of the world's arable soils are deficient in phosphorus and require mineral fertilization to improve crop yields (MacDonald et al., 2011). To maintain high crop productivity, continuous application of inorganic phosphorus (Pi) to the soil is required (Jiang et al., 2017). In the absence of alternatives, farmers use significant amounts of non-renewable rock phosphate-derived Pi fertilizers (Heuer et al., 2017; Yang et al., 2017).

However, in high-input cropping systems, intensive P fertilization leads to significant water pollution (Mpanga et al., 2019), while in low-input systems common in developing countries, low phosphorus availability is a major constraint to agricultural production (Galindo-Castañeda et al., 2018). Given this scenario, one strategy to mitigate the impacts associated with P use is to develop crops that enhance both phosphorus acquisition (Lynch, 2007) and utilization (Jiang et al., 2017; Taghinasab et al., 2018; Schegoscheski-Gherardt et al., 2019; Wacker-Fester et al., 2019).

Breeding programs have worked to develop cultivars that respond more efficiently to phosphorus deficiency. Studies on genetic variability and selection of maize genotypes for phosphorus use efficiency have been conducted (Machado et al., 1999; Brasil et al., 2007; Fidelis et al., 2010; Reais et al., 2017). However, for a deeper understanding of the factors involved in phosphorus use efficiency in maize,

approaches to investigate the type of gene action associated with this ability have become more frequent.

Fritsche-Neto et al. (2010) investigated the genetic effects controlling the inheritance of traits associated with phosphorus use efficiency in 15 maize hybrids and found that non-additive effects were more important for these traits, suggesting that selection should be made in hybrid combinations. In another study analyzing root system length and aboveground dry matter accumulation in 41 maize hybrids under high and low phosphorus availability, DoVale and Fritsche-Neto (2013) showed that efficient phosphorus acquisition by the plant led to more efficient phosphorus use, with non-additive genetic effects also being more important. Similarly, Colombo et al. (2018) also found a predominance of non-additive effects on grain yield at different levels of phosphate fertilization and identified superior materials that were efficient and responsive to both high and low phosphorus levels.

Heterosis, often manifested by vigorous growth in F_{1s} hybrids, can be exploited to improve crop yield under conditions of low P availability. In the case of maize breeding, heterosis has been widely used for decades to increase yield potential and improve adaptation to stress (Araús et al., 2010; Chairi et al., 2016). Nevertheless, the genetic effects and physiological mechanisms associated with heterosis performance under P deficiency conditions require further investigation. Furthermore, unlike common corn, popcorn remains relatively underexplored and lacks studies aimed at improving phosphorus use efficiency (PUE).

Knowing the type of gene action associated with a particular trait helps breeders choose the best selection strategy, leading to greater gains. A common strategy used by breeders in breeding programs is diallel analysis (Meirelles et al., 2016; Liu et al., 2018). This involves crossing parents that carry favorable genes for a particular trait of interest, and through the expression of heterosis, superior hybrids can be obtained. In addition, diallel crosses involving reciprocal parents allow inference of reciprocal effects that may be under the influence of extrachromosomal genes (Cruz et al., 2014).

Diallel analysis has shown great promise in various corn studies. For example, Meirelles et al. (2016) used the diallel approach to identify superior materials that were efficient and responsive to low phosphorus levels. On the other hand, Liu et al. (2018) evaluated the influence of root traits in six inbred lines and their hybrids in a complete diallel for higher productivity under low and high phosphorus levels.

In popcorn, Schegoscheski-Gerhardt et al. (2019) used diallel analysis to evaluate 28 hybrids and their parents at two locations and under two contrasting soil

phosphorus conditions. The authors found that the best strategy for obtaining efficient and responsive genotypes under low phosphorus conditions is to exploit heterosis, using parents with higher expression of expansion capacity. Promising hybrids identified included P7 × L80, P7 × L59, P7 × L76, and P6 × L80, and they can be considered as options for cultivation in phosphorus-deficient soils.

However, despite the progress made in genetic breeding to understand the genetic mechanisms involved in efficient phosphorus use, little attention has been paid to this relationship in popcorn cultivation. In Brazil, for example, only two public research centers (IAC – Instituto Agronômico de Campinas - and UENF – Universidade Estadual do Norte Fluminense Darcy Ribeiro) have cultivars registered with the Ministério da Agricultura, Pecuária e Abastecimento (MAPA), with thirteen from IAC and fifteen from UENF. Of the fifteen varieties registered by UENF, three (UENF P-01, UENF P-02, UENF P-03) are efficient under low soil phosphorus levels, highlighting the importance of research institutions in developing materials that benefit both the economic and environmental sectors.

3.1.3 MATERIALS AND METHODS

3.1.3.1 Genotypes and growing conditions

Four inbreeding lines (S_7) of popcorn - P2, P7, L75, and L80 - and their respective 12 F_{1s} hybrids, including reciprocal combinations, were evaluated. The P2 line is derived from the CMS-42 composite, adapted to the tropical climate; P7 comes from the hybrid IAC112, adapted to temperate and tropical climates; and L75 and L80 are derived from the open-pollinated variety 'Viçosa', adapted to temperate and tropical climates. These lines were selected based on previous studies in conditions of P limitation in the soil and classified agronomically as efficient (P2 and P7) and inefficient (L75 and L80) in the use of phosphorus in field conditions (Gerhardt et al., 2017). Additionally, there was a selection for the P use efficiency (PUE) in the greenhouse, based on the content of phosphorus in the plant and dry matter (Silva et al., 2019). Following the order of the female and male parents, hybrids P2×P7, P2×L75, P2×L80, P7×P2, P7×L75, P7×L80, L75×P2, L75×P7, L75×L80, L80×P2, L80×P7 and L80×L75 were used.

An experiment was carried out at the North Fluminense State University Darcy Ribeiro facility (21°9'23" S; 41°10'40" W, 14 m altitude) from May to July 2021. The experimental set up took place in a greenhouse with a system of lysimeters comprised of PVC tubes split lengthways and sealed at the bottom. The cultivation was carried out under protected conditions, with the greenhouse covered by transparent plastic and shade. The lysimeters were filled with a substrate of sand washed in deionized water.

The experiment was arranged in a randomized complete block in a factorial design with two levels of phosphorus availability with three replications per genotype. Initially, three seeds were sown per tube, and ten days after germination the seedlings were thinned out, leaving just one plant per tube. The spacing between plants was 25 cm, while the distance between rows was set at 1 m, corresponding to a planting density of 40,000 plants ha⁻¹. To monitor the climatic conditions inside the greenhouse, temperature, air humidity, and photosynthetically active radiation data were collected using a WatchDog 2000 Series mini climatological station from Spectrum Technologies Inc., Aurora, IL, USA (Figure 1).

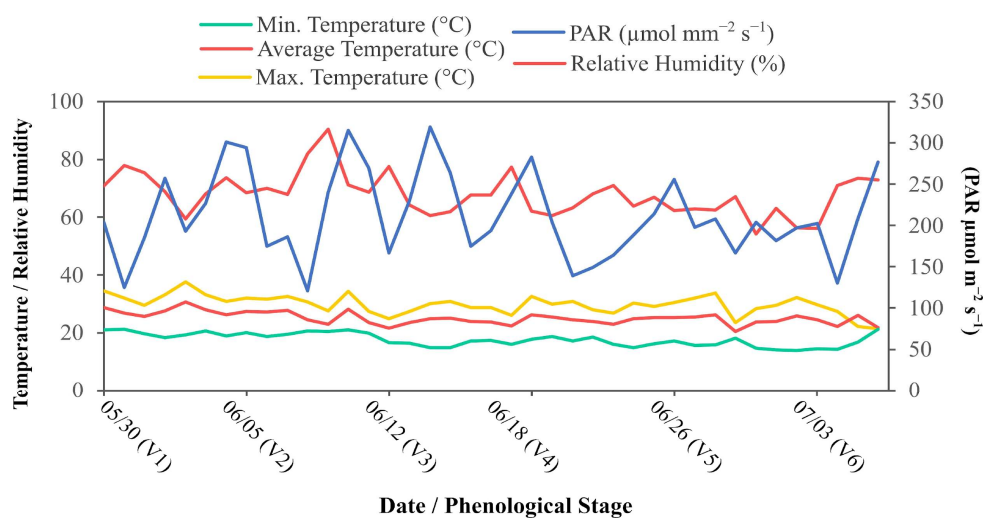


Figure 1. Average, maximum, and minimum temperature (°C), relative humidity (RH, %), and photosynthetically active radiation (PAR, μmol m⁻² s⁻¹) over the dates and phenological stages (V) of popcorn plant growth in two conditions of P availability (May to July 2021).

Two phosphorus (P) availability conditions were established in the substrate based on the Hoagland and Arnon (1950) nutrient solution, with modifications to the

P supply through $\text{NH}_4\text{H}_2\text{PO}_4$. Under the high P condition, the substrate received 100% of the P supply (31.00 mg L^{-1}); in contrast, the low P condition received only 0.5% of the P supply, equivalent to 0.15 mg L^{-1} . Each tube containing one plant received 100 mL of deionized water daily. In the high P condition, the plants were supplied with 158.00 mg L^{-1} of P, whereas those in the low P condition received 0.68 mg L^{-1} of P. The nutrient solution was applied daily from the V2 stage to the V6 stage of the plants. The pH was kept between 5.5 and 5.9. In their respective treatments, the nutrient solution was applied to acclimatize the seedlings to P metabolism at 25% strength for three days and at 50% strength for two days. After the acclimatization period, the plants in the high P condition received 200 mL of the nutrient solution daily with 31.00 mg L^{-1} of P (100% of the strength), whereas the plants in the low P condition received 0.15 mg L^{-1} of P (100% of the strength).

3.1.3.2 Traits evaluated

3.1.3.2.1 Morphological traits

At the end of the experiment, which means 45 days after sowing, measurements were taken to assess various plant traits. Plant height (PH) was measured from the soil surface to the last developed leaf. Stalk diameter (SD) was assessed in the middle third of the plants. Leaf area (LA) was calculated by multiplying the maximum leaf length (LL) by its maximum width (LW) and multiplying the result by 0.75 (Pearce et al., 1975). The leaf dry matter (LDM), stalk (SDM), and roots (RDM) were determined after separating and drying these plant parts in an oven at $65 \text{ }^\circ\text{C}$ for 72 hours. The shoot dry mass (STDM) was obtained by adding the dry mass of the leaves and the stalk. The root/shoot ratio (R/S) was calculated by dividing the dry mass of the roots by the dry mass of the shoots.

3.1.3.2.2 Concentration, utilization rates, and efficiency of P

After the drying process, the leaf, stem, and root samples were ground to quantify phosphorus concentration in 1g of dry matter. For this, extraction was performed by sulfuric digestion (HNO_3 and H_2O_2), and in the extract, P was determined by spectrophotometry (Specord 2010, Analytik Jena, Jena, Germany) using the molybdate method (da Silva Santos et al., 2014). Phosphorus content was

determined by multiplying the concentration of phosphorus in 1 g of dry matter of each sample by the corresponding dry weight (mg P/ plant).

The P accumulation was calculated by multiplying the P concentration obtained in 1g of dry matter from each sample by its corresponding dry weight. Based on the P concentration, the following estimates were obtained: i) P use efficiency (PUE: dry mass of the shoot divided by the total P applied); ii) P absorption efficiency (PUpE: P concentration in the plant divided by the total P applied); and iii) P utilization efficiency (PUtE: dry mass of the shoot divided by the P content in the plant).

3.1.3.2.3 Chlorophyll fluorescence measurements

Chlorophyll fluorescence was assessed one day before the end of the experiment (44 days after sowing). Measurements were taken in the middle third of the last expanded leaf, which is the first leaf counted from the apex of the plant. The evaluation period occurred between 11:30 a.m. and 1:30 p.m., using the MultispeQ v2.0 (Michigan State University, USA). Through the MultispeQ, the following estimates were obtained: PSII electron transport quantum yield (Φ_{PSII}), non-photochemical quenching parameter (NPQt) (Tietz et al., 2017), non-regulated energy dissipation (Φ_{NO}), and regulated energy dissipation (Φ_{NPQ}) (Kramer et al., 2004). In addition, the ratio between non-photochemical extinction efficiency and non-regulated energy dissipation (NPQt/ Φ_{NO}) was calculated.

3.1.3.2.4 Leaf pigments

The leaf chlorophyll levels (Chl), flavonoids (Flav), and nitrogen balance index (NBI) were measured in the same leaf area where chlorophyll fluorescence was assessed using a Dualex® portable leaf pigment meter (FORCE-A, Orsay, France).

3.1.3.2.5 Gas exchange measurements

Gas exchange assessments were carried out 45 days after sowing, specifically at the V6 stage, between 9:00 and 11:00 am. The first fully expanded leaf was measured from the apex of the plant, in the middle third of the leaf, in an area of approximately 600 mm². An Infra-Red Gas Analyzer - IRGA (model LI-6400, LI-COR, Lincoln, NE) was used for this purpose. During the evaluations, the

photosynthetically active radiation (PAR) was maintained at $600 \mu\text{mol m}^{-2} \text{s}^{-1}$, the CO_2 concentration inside the LI-6400 chamber was kept at $400 \mu\text{mol mol}^{-1}$, and the relative air humidity and temperature were kept at 60% and $25 \text{ }^\circ\text{C}$, respectively.

The gas exchange traits evaluated were net CO_2 assimilation rate (A), transpiration (E), stomatal conductance (g_s), and intercellular CO_2 concentration (C_i). In addition, two relative efficiencies were calculated: the instantaneous carboxylation efficiency (A/C_i), representing the ratio between the net CO_2 assimilation rate (A) and the intercellular CO_2 concentration (C_i); and the carboxylation efficiency index and the leaf phosphorus content (A/LPC), defined as the ratio between the net CO_2 assimilation rate (A) and the leaf phosphorus content (LPC).

3.1.3.2.6 Estimating heterosis

For each trait, heterosis (H) was calculated by the difference between the average value obtained by the hybrid (F_1) and the average values obtained by its parents (MP), expressed in percentage, according to the following expression: $H = \left(\frac{F_1 - MP}{MP} \right) \times 100$ (Hallauer et al., 2010).

3.1.3.2.7 Statistical analysis

An individual analysis of variance was carried out for each trait studied, considering the different conditions of phosphorus availability. The statistical model used was: $Y_{ij} = \mu + G_i + B_j + \varepsilon_{ij}$, in which Y_{ij} is the observed value of the i -th genotype in the j -th block; μ is the general constant; G_i is the effect attributed to the i -th genotype; B_j is the effect of block j ; and ε_{ij} is the experimental error associated with the observation Y_{ij} .

A joint analysis of variance was conducted using the following statistical model: $Y_{ijk} = \mu + G_i + B/Pj_k + P_j + GP_{ij} + \varepsilon_{ijk}$, in which Y_{ijk} is the observation of the i -th genotype in the j -th P condition in the k -th block; μ is the general constant; G_i is the fixed effect of the i -th genotype; B/Pj_k is the random effect of the k -th block within the P j condition; P_j is the fixed effect of the j -th P condition; GP_{ij} is the fixed effect of the interaction between the i -th genotype and the j -th P condition; and ε_{ijk} is the average experimental random error associated with the observation Y_{ijk} with NID $(0, \sigma^2)$. The effects of the genitors and hybrids were partitioned for each trait.

Statistical analyses were conducted using SAS 9.4 software (SAS Institute Inc., Cary, NC, USA).

Combinatorial abilities were analyzed using method I of diallel analysis proposed by Griffing (1956). The effects of the genitors, hybrids, and reciprocals were evaluated, considering the effect of the genotypes to be fixed. The general combining ability (GCA) and specific combining ability (SCA) of the genotypes were obtained using the following model: $Y_{ij} = \mu + g_i + g_j + s_{ij} + r_{ij} + \varepsilon_{ij}$, in which Y_{ij} is the mean value of the hybrid combination ($i \neq j$) or the genitor ($i = j$); μ is the overall mean; g_i, g_j are the effects of the general combining ability of the i -th or j -th genitor ($i, j = 1, 2, 3, \text{ and } 4$); s_{ij} is the effect of specific combining ability for crosses between genitors of order i and j ; r_{ij} is the reciprocal effect that quantifies the differences resulting from genitor i or j when used as the male or female genitor in cross ij ; and ε_{ij} is the average experimental error associated with the observation of order ij .

The quadratic components expressing the genetic variability associated with GCA (ϕ_g), SCA (ϕ_s), and reciprocal effects (ϕ_{rc}) were estimated. These components were calculated using the following formulas: $\phi_g = \frac{QMG-Q}{2p}$, $\phi_s = QMS - QMR$, and $\phi_{rc} = \frac{QMRC-QMR}{2}$. In this formula, QMG represents the mean square of the general combining ability, QMS is the mean square of the specific combining ability, QMRC is the mean square of the reciprocal effect, QMR is the mean square of the residue and p is the number of parents.

The effects of the quadratic components were converted into percentages of the total effects. Statistical-genetic analyses were carried out using Genes software (Cruz, 2013).

3.1.4 RESULTS

3.1.4.1 Plant growth traits and phosphorus use efficiency

The joint analysis revealed significant effects for both phosphorus level (P) and genotypes (G), and a significant $G \times P$ interaction for all plant growth traits, P

accumulation, and efficiency. When comparing the two conditions of P availability, it became clear that the deficiency of this nutrient had a more pronounced negative impact on the parent lines, significantly affecting all the growth traits and P accumulation (Table 1).

Significant reductions between the two P conditions were exhibited in the parent lines, surpassing 80.00% in traits such as leaf area (LA, 83.27%), leaf dry matter (LDM, 93.84%), stalk dry matter (SDM, 95.17%), and root dry matter (RDM, 86.67%). The hybrids also showed marked reductions in these traits, reaching values of 78.20%, 90.37%, 88.06%, and 77.19%, respectively (Table 1).

Regarding P accumulation in both parent lines and hybrids, remarkable reductions exceeding 90% were observed as a consequence of P deficiency. In contrast, the plants from the parent lines exhibited an average accumulation of 0.61 and 0.07 mg P/plant in the shoot and root, respectively, while the hybrids achieved a higher average accumulation of 1.06 and 0.11 mg P/plant (Table 1). An increase in P efficiency for both the parent lines and hybrids, with a significant increase in the P use efficiency (PUE), P absorption efficiency (PUpE), and P utilization efficiency (PUtE), was observed. Average increases of 92.86%, 86.46%, and 93.44% were observed for these traits in the parent lines, while the hybrids exhibited even more significant increases, reaching 96.34%, 91.41%, and 95.76%, respectively (Table 1).

Under high phosphorus (P) condition, no significant differences in plant growth traits and P use efficiency were observed between lines and hybrids (III), except for P accumulation in the leaf (LPC) and root (RPC) (Table 1). However, in low P condition, significant differences were identified for most of these traits, except for leaf width (LW), root/shoot ratio (R/S), and P absorption efficiency (PUpE) (Table 1).

Due to the greater impact of low P conditions on the lines, the heterosis for the evaluated traits was more pronounced under these conditions. Significant heterosis percentages were observed for SDM and RDM, with 86.82% and 105.25%, respectively (Table 1). Traits related to P content, such as shoot P content (SPC) and root P content (RPC), also exhibited substantial heterosis percentages, reaching 77.83% and 103.50%, respectively. Furthermore, regarding P efficiency, the PUE and PUtE exhibited significant heterosis rates of 78.07% and 89.09%, respectively (Table 1).

Table 1. Summary of the joint and individual analyses of variance, means, standard deviations, and heterosis (H %) for morphological traits and P use efficiency in popcorn inbred lines and hybrids in diallel grown under different P availability.

| Traits | Joint Analysis | | | High P | | | | Low P | | | |
|--------|----------------|----|-------|----------------------------|-------------------------------|-------------|-------|----------------------------|------------------|-------------|--------|
| | G | P | G × P | Lines (I) | Hybrids (II) | L × H (III) | H % | Lines (I) | Hybrids (II) | L × H (III) | H % |
| PH | ** | ** | ** | 28.22 ± 3.43** | 30.30 ± 3.70** | ns | 11.56 | 11.44 ± 1.27* | 13.70 ± 1.23** | ** | 20.94 |
| SD | ** | ** | ** | 12.26 ± 1.24** | 12.53 ± 1.14** | ns | 5.98 | 3.81 ± 0.42 ^{ns} | 4.60 ± 0.48* | ** | 25.32 |
| LL | ** | ** | ** | 68.91 ± 4.16** | 71.59 ± 6.87** | ns | 0.25 | 37.51 ± 2.12 ^{ns} | 42.48 ± 2.73** | ** | 14.42 |
| LW | * | ** | * | 3.74 ± 0.35 ^{ns} | 3.69 ± 0.42 ^{ns} | ns | -5.64 | 2.58 ± 0.17 ^{ns} | 2.72 ± 0.25** | ns | 3.16 |
| LA | ** | ** | ** | 632.93 ± 88.35** | 668.50 ± 104.26 ^{ns} | ns | 6.33 | 96.32 ± 4.74 ^{ns} | 117.96 ± 10.68** | ** | 21.75 |
| LDM | ** | ** | ** | 3.41 ± 0.51** | 3.74 ± 0.62** | ns | 18.11 | 0.21 ± 0.01** | 0.36 ± 0.03** | ** | 70.50 |
| SDM | ** | ** | ** | 2.07 ± 0.41** | 2.01 ± 0.48** | ns | 6.04 | 0.10 ± 0.01** | 0.24 ± 0.05** | ** | 86.82 |
| RDM | ** | ** | ** | 1.05 ± 0.15** | 1.14 ± 0.20** | ns | 14.88 | 0.14 ± 0.01* | 0.26 ± 0.04** | ** | 105.25 |
| R/S | ** | ** | ** | 0.20 ± 0.04 ^{ns} | 0.20 ± 0.05 ^{ns} | ns | -2.94 | 0.45 ± 0.04* | 0.46 ± 0.06** | ns | 18.50 |
| LPC | ** | ** | ** | 11.59 ± 1.24** | 13.08 ± 1.69** | ** | 18.83 | 0.46 ± 0.07 ^{ns} | 0.74 ± 0.12** | ** | 63.71 |
| SPC | ** | ** | ** | 7.35 ± 0.99** | 7.42 ± 1.26** | ns | 4.28 | 0.15 ± 0.06* | 0.32 ± 0.07** | ** | 77.83 |
| STPC | ** | ** | ** | 18.94 ± 1.95** | 20.50 ± 2.81** | ns | 12.78 | 0.61 ± 0.11 ^{ns} | 1.06 ± 0.16** | ** | 62.53 |
| RPC | ** | ** | ** | 1.09 ± 0.11** | 1.35 ± 0.16** | ** | 37.81 | 0.07 ± 0.01** | 0.11 ± 0.01** | ** | 103.50 |
| PUE | ** | ** | ** | 0.035 ± 0.003** | 0.037 ± 0.008** | ns | 13.84 | 0.42 ± 0.05* | 0.82 ± 0.11** | ** | 78.07 |
| PUpE | ** | ** | ** | 0.13 ± 0.025 ^{ns} | 0.14 ± 0.02** | ns | 14,84 | 0.96 ± 0.28 ^{ns} | 1.53 ± 0.33** | ns | 64,57 |
| PUtE | ** | ** | ** | 0.042 ± 0.006** | 0.046 ± 0.007** | ns | 14,06 | 0.61 ± 0.07 ^{ns} | 1.17 ± 0.14** | ** | 89,09 |

G – genotypes; P - phosphorus conditions; PH – plant height (cm); SD – stalk diameter (mm); LL – leaf length (cm); LW – leaf width (cm); LA – leaf area (cm²); LDM – leaf dry mass (g); SDM – stalk dry mass (g); RDM – root dry mass (g); R/S – root to shoot ratio; LPC – leaf phosphorus content; SPC – stalk phosphorus content; STPC – shoot phosphorus content; RPC – root phosphorus content; PUE – phosphorus use efficiency; PUpE – phosphorus uptake efficiency; and PUtE – phosphorus utilization efficiency. The values in the Lines and Hybrids columns represent the means ± standard deviations of the respective evaluated genotypes and their statistical differences within the parent lines and hybrids; L × H – statistical differences between the lines and hybrids according to the partition of line and hybrid effects. Factor Analysis: genotype (G), phosphorus availability condition (P), and genotype x phosphorus availability condition (G × P). I, II, and III represent the level of significance between lines, between hybrids, and between lines and hybrids, respectively. Significance levels: * $p < 0.05$; ** $p < 0.01$; and ns = not significant.

Although significance was observed in the quadratic components associated with general combining ability (ϕ_g) and the reciprocal effect (ϕ_{rc}) for most of the growth traits, P accumulation and P efficiencies, the most crucial component influencing these traits and explaining the majority of the genetic variability was the quadratic component linked to specific combining ability (ϕ_s). Therefore, dominance effects were more pronounced in both conditions of P availability.

Under the low P conditions, traits exhibited the most significant influence of the genetic effects of dominance (ϕ_s) were LL (69.3%), LDM, SDM, and RDM (65.6%, 66.2% and 70.6%, respectively), SPC and RPC (68.6% and 73.4%, respectively), PUE (70.2%) and PUE (77.5%). Conversely, in the high P condition, traits demonstrating the greatest impact of dominance genetic effects were: LDM and RDM (43.1% and 49.7%, respectively), LPC, SPC, APC, and RPC (56.8%, 43.4%, 51.1%, and 65.5%, respectively), and PUE (46.9%) and PUE (50.5%) (Figure 2).

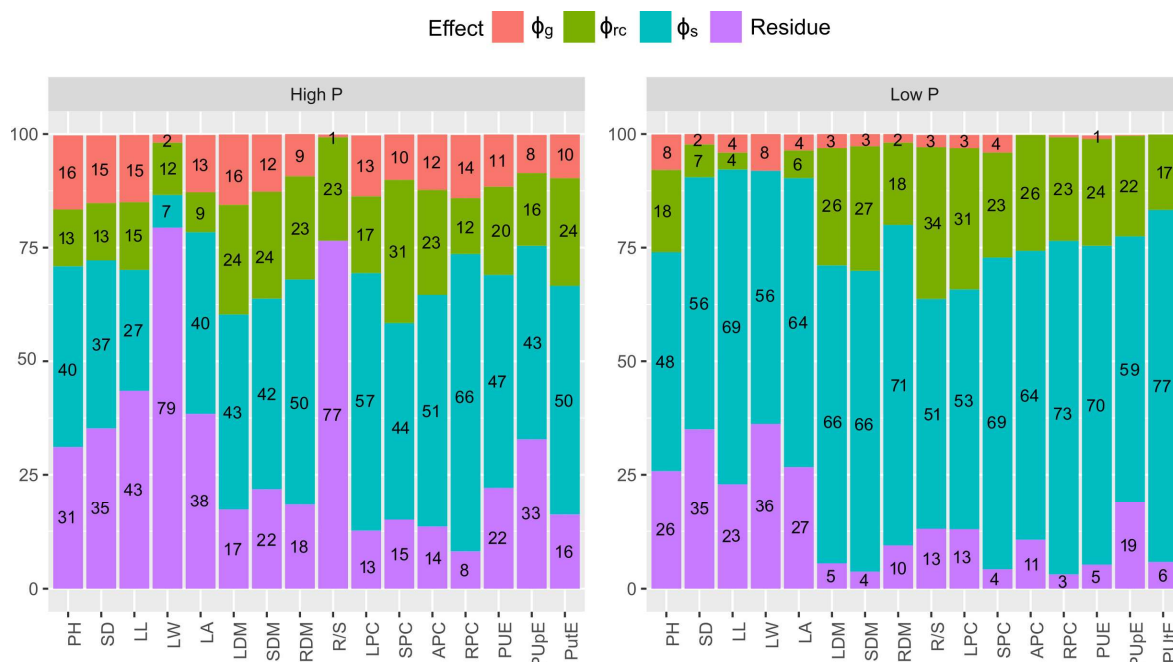


Figure 2. Importance (expressed as %) of the quadratic components related to general (ϕ_g) and specific combining ability (ϕ_s) and reciprocal effects (ϕ_{rc}) and residual effects for the traits: PH – plant height (cm); SD – stalk diameter (mm); LL – leaf length (cm); LW – leaf width (cm); LA – leaf area (cm²); LDM – leaf dry mass (g); SDM – stalk dry mass (g); RDM – root dry mass (g); R/S – root to shoot ratio; LPC – leaf phosphorus content; SPC – stalk phosphorus content; APC – aboveground phosphorus content; RPC – root phosphorus content; PUE – phosphorus use efficiency; PUpE – phosphorus uptake efficiency; and PUE – phosphorus utilization efficiency.

3.1.4.2 Chlorophyll fluorescence, leaf pigments, and exchange measurements

Among the traits related to chlorophyll fluorescence, only NPQt, Φ NO, and NPQt/ Φ NO exhibited significance for genotypes (G), phosphorus conditions (P), and the G \times P interaction (Table 2). For leaf pigments and gas exchange traits, significant differences were identified between G and P and the interaction between G \times P for all the traits analyzed, except for *gs* (Table 2).

P deficiency negatively impacted the Φ PSII and Φ NO traits, resulting in reductions of 79.07% and 48.48% in the parent lines and 78.05% and 69.44% in the hybrids, respectively (Table 2). However, the traits NPQt, Φ NPQ, and the NPQt/ Φ NO ratio increased in both parent lines and hybrids in response to the lack of P (Table 2). Significant reductions were also observed in chlorophyll (Chl) and the nitrogen balance index (NBI), with values of 57.80% and 65.84% in the lines and 50.52% and 77.78% in the hybrids, respectively. On the other hand, the flavonoid content (Flav) increased under low phosphorus conditions in both lines and hybrids.

Under P deficiency, significant reductions in *A* of 75.66%, *gs* of 66.67%, and instantaneous carboxylation efficiency (*A/Ci*) of 88.89% were observed in the parent lines, representing the most substantial losses (greater than 60.00%). In the hybrids, the reductions were approximately 72.11%, 61.11%, and 90.00%, respectively (Table 2). On the other hand, *Ci* and the carboxylation efficiency index concerning the leaf phosphorus content (*A/LPC*) increased with P deficiency by 59.24% and 88.89% in the parent lines and by 51.20% and 78.77% in the hybrids, respectively.

When comparing the parent lines to the hybrids (III; Table 2), a significant difference was observed for NPQt and NPQt/ Φ NO in the high P condition and for NPQt, Φ NO, and NPQt/ Φ NO in the low P condition (Table 2). Chlorophyll concentration (Chl) was significantly different in the low P condition, while the gas exchange traits (*A*, *Ci*, and *A/Ci*) were significant in both P conditions (Table 2).

Table 2. Summary of the joint and individual analyses of variance, means, standard deviations, and heterosis (H %) of physiological traits associated with gas exchange, chlorophyll fluorescence, and leaf pigment measurements of popcorn lines and hybrids in diallel grown under contrasting conditions of P availability.

| Traits | Joint Analysis | | | High P | | | | Low P | | | |
|-----------------|----------------|----|-------|------------------------------|------------------------------|-------------|--------|------------------------------|------------------------------|-------------|--------|
| | G | P | G × P | Lines (I) | Hybrids (II) | L × H (III) | H % | Lines (I) | Hybrids (II) | L × H (III) | H % |
| NPQt | ** | ** | ** | 0.69 ± 0.05 ^{ns} | 0.64 ± 0.06 ^{ns} | * | -4.68 | 5.55 ± 0.86 ^{**} | 8.59 ± 1.35 ^{**} | ** | 140.71 |
| ΦPSII | ns | ** | ** | 0.43 ± 0.06 ^{ns} | 0.41 ± 0.07 ^{ns} | ns | -3.73 | 0.43 ± 0.02 ^{ns} | 0.09 ± 0.02 ^{**} | ns | -28.27 |
| ΦNO | ** | ** | ** | 0.33 ± 0.03 ^{ns} | 0.36 ± 0.04 ^{ns} | ns | 6.00 | 0.17 ± 0.05 [*] | 0.11 ± 0.02 ^{**} | ** | -68.78 |
| ΦNPQ | ns | ** | ns | 0.23 ± 0.04 ^{ns} | 0.23 ± 0.03 ^{ns} | ns | -2.06 | 0.75 ± 0.08 ^{ns} | 0.79 ± 0.07 ^{**} | ns | 14.74 |
| NPQt/ΦNO | ** | ** | ** | 2.12 ± 0.36 ^{ns} | 1.82 ± 0.25 [*] | ** | -10.71 | 52.30 ± 5.96 ^{**} | 154.77 ± 20.70 ^{**} | ** | 529.56 |
| Chl | ** | ** | ** | 36.90 ± 2.34 ^{ns} | 37.71 ± 1.86 ^{ns} | ns | 2.87 | 15.57 ± 2.95 ^{ns} | 18.66 ± 2.65 ^{**} | ** | 22.63 |
| Flav | ** | ** | ** | 0.22 ± 0.05 ^{**} | 0.16 ± 0.03 ^{**} | ** | -15.99 | 0.27 ± 0.08 [*] | 0.43 ± 0.06 ^{**} | ** | 64.87 |
| NBI | ** | ** | ** | 212.52 ± 53.26 ^{ns} | 371.06 ± 71.83 ^{**} | ** | 41.19 | 72.60 ± 10.00 ^{**} | 82.44 ± 34.35 ^{**} | ns | -20.45 |
| A | ** | ** | ** | 18.24 ± 2.27 ^{ns} | 19.47 ± 1.68 ^{**} | * | 8.70 | 4.44 ± 1.02 [*] | 5.43 ± 1.01 ^{**} | ** | 18.07 |
| gs | ** | ** | ns | 0.18 ± 0.05 ^{ns} | 0.18 ± 0.04 ^{**} | ns | 7.28 | 0.06 ± 0.01 ^{ns} | 0.07 ± 0.01 ^{**} | ns | 6.53 |
| E | ** | ** | ** | 0.84 ± 0.11 ^{ns} | 0.86 ± 0.14 [*] | ns | 1.57 | 0.50 ± 0.05 ^{ns} | 0.49 ± 0.08 ^{**} | ns | -3.85 |
| Ci | ** | ** | ** | 205,70 ± 28,03 ^{ns} | 190,35 ± 19,77 ^{**} | * | -0,14 | 509.66 ± 55,62 ^{**} | 398.16 ± 51,32 ^{**} | ** | -21,56 |
| A/Ci | ** | ** | ** | 0.09 ± 0.01 ^{ns} | 0.10 ± 0.01 ^{**} | ** | 8.72 | 0.001 ± 0.003 [*] | 0.01 ± 0.006 ^{**} | ** | 85.79 |
| A/LPC | ** | ** | ** | 1.75 ± 0.23 ^{**} | 1.69 ± 0.31 ^{**} | ns | -12.02 | 10.06 ± 2.88 [*] | 7.96 ± 2.19 ^{**} | ** | -31.35 |

G – genotypes; P - phosphorus conditions; NPQt – non-photochemical quenching parameter; ΦPSII – PSII electron transport quantum yield; ΦNO – non-regulated energy dissipation; ΦNPQ – regulated energy dissipation; NPQt/ΦNO- non-photochemical quenching to non-regulated energy dissipation efficiency ratio; Chl – relative chlorophyll content; Flav – relative flavonoid content; and NBI – nitrogen balance index; A – net CO₂ assimilation rate (μmol CO₂ m⁻² s⁻¹); g_s – stomatal conductance (mol H₂O m⁻² s⁻¹); E – transpiration (mmol H₂O m⁻² s⁻¹); Ci – internal CO₂ concentration (μmol CO₂ m⁻² s⁻¹); A/Ci – instantaneous carboxylation efficiency; A/LPC – carboxylation efficiency ratio to leaf phosphorus content. The values in the Lines and Hybrids columns represent the means ± standard deviations of the respective evaluated genotypes and their statistical differences within the parent lines and hybrids; L x H – statistical differences between the parent lines and hybrids according to the partition of line and hybrid effects. Factor Analysis: genotype (G), phosphorus availability condition (P), and genotype x phosphorus availability condition (G × P). I, II, and III represent the level of significance between lines, between hybrids, and between lines and hybrids, respectively. Significance levels: * *p* < 0.05; ** *p* < 0.01; and ns = not significant.

In the low P condition, the heterosis estimates were negative for Φ_{NO} (-68.78%), while they were positive for NPQt and Φ_{NPQ}/Φ_{NO} , with values of 140.41%, and 529.56%, respectively (Table 2). The heterosis estimates for Chl and Flav were 22.63% and 64.87%, respectively, in the low P condition (Table 2). Concerning the gas exchange traits, there was no significant impact of heterosis for g_s and E in both P conditions. For A, and A/C_i , the heterosis estimates were 8.70% and 8.72% for high P, respectively, and 18.07% and 85.79% for low P. On the other hand, negative heterosis estimates were observed for the other traits (Table 2).

The analysis of variance revealed that under optimum P conditions, the components related to general (ϕ_g) and specific (ϕ_s) combining ability were not statistically significant ($P > 0.05$) for most physiological traits due to the high residual contribution (Supplementary Table 2 and Figure 3). However, under low P conditions, the quadratic components ϕ_s and ϕ_{rc} were statistically significant ($P > 0.05$), and these are the main components responsible for the genetic variability of the gas exchange, chlorophyll fluorescence and leaf pigment traits (Supplementary Table 2 and Figure 3).

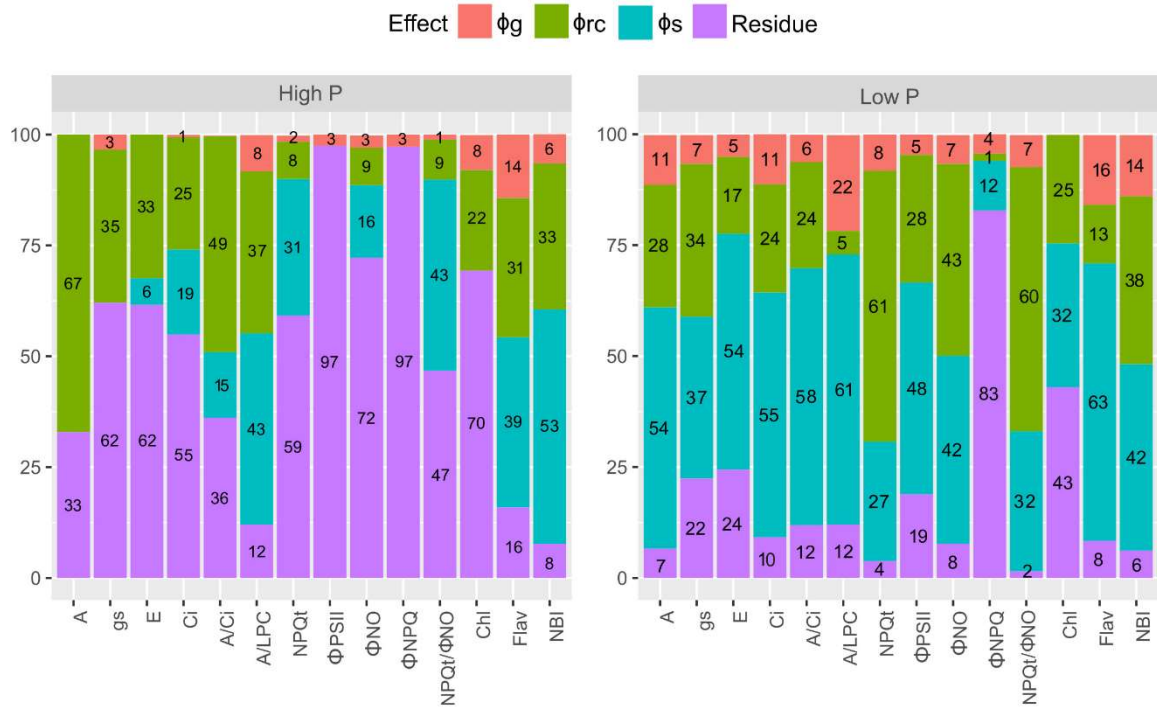


Figure 3. Importance (expressed as %) of quadratic components related to general (ϕ_g) and specific combining ability (ϕ_s), reciprocal (ϕ_{rc}), and residual effects for traits related to photosynthesis, chlorophyll fluorescence, and leaf pigments. A – net CO₂ assimilation rate ($\mu\text{mol CO}_2 \text{ m}^{-2} \text{ s}^{-1}$); gs – stomatal conductance ($\text{mol H}_2\text{O m}^{-2} \text{ s}^{-1}$); E – transpiration ($\text{mmol H}_2\text{O m}^{-2} \text{ s}^{-1}$); Ci – internal CO₂ concentration ($\mu\text{mol CO}_2 \text{ m}^{-2} \text{ s}^{-1}$); A/Ci – instantaneous carboxylation efficiency; A/LPC – carboxylation efficiency ratio to leaf phosphorus content; NPQt – non-photochemical quenching parameter; ΦPSII – PSII electron transport quantum yield; ΦNO – non-regulated energy dissipation; ΦNPQ – regulated energy dissipation; NPQt/ΦNO – non-photochemical quenching to non-regulated energy dissipation efficiency ratio; Chl – relative chlorophyll content; Flav – relative flavonoid content; and NBI – nitrogen balance index.

3.1.5 DISCUSSION

3.1.5.1 Impact of P availability on growth traits and P use efficiency in popcorn genotypes

Adequate phosphorus availability is crucial for plant growth and development, playing an essential role in photosynthesis and plant biomass production (Carstensen et al., 2018; Dusenge et al., 2019; Kayoumu et al., 2023). In the case

of cereals such as corn, seedlings utilize P reserves from the seed during the initial days after sowing (Nadeem et al., 2011; Nadeem et al., 2012). From this period onwards, the supply of inorganic phosphate (Pi) and its absorption by the roots become essential for continued plant growth and development. Pi, along with CO₂, and water, constitutes the primary products of photosynthesis (Rychter, 2005). Consequently, low levels of Pi in the chloroplast diminish ATP production, affect CO₂ assimilation in the Calvin cycle and impede the conversion of NADPH to NADP⁺, resulting in reduction of plant biomass production (Dusenge et al., 2019; Suzuki et al., 2022).

Although the P deficiency significantly reduced the growth of all the plants, the hybrids exhibited a remarkable ability to accumulate greater amounts of this nutrient, as indicated by the values of the P contents accumulated in the lines (Table 1). This distinctive accumulation pattern aligns with findings of previous studies, such as millet genotypes exposed to various P supplements (Maharajan et al., 2019), as well as rice (Pinit et al., 2020) and cotton (Kayoumu et al., 2023) cultivars exhibiting diverse traits of Pi accumulation. Hence, the difference observed in P accumulation capacity between the lines and the hybrids suggests that the hybrids, although affected by the limited availability of P, are coping better than their parents.

The leaf plays a key role in photosynthesis, generating the majority of the carbohydrates essential for plant growth and development (Wang et al., 2018). In contrast to some studies reporting no significant differences in leaf area (LA) in response to P levels in other crops, such as soybeans, cowpeas, wheat, and corn (Bechtaoui et al., 2021), the present study revealed that LA was affected by the lack of P. The observed greater leaf length (LL) in the hybrids may confer an advantage to their overall performance, by increasing the surface area for sunlight capture, thereby favoring photosynthesis and, consequently, plant growth. Additionally, we found that P availability slightly influenced the leaf width (LW), suggesting that it was not a primary response of the plants to cope with this nutritional limitation.

Under low P conditions, we observed drastic reductions in biomass in all the plants, accompanied by an increase in the root/shoot ratio (R/S) in both the parent lines and hybrids (Table 1). This response is commonly observed in certain crops, including corn when exposed to P deficiency (Zhang et al., 2014c; Kumar et al., 2021; Liu et al., 2021). In a study by Wen et al. (2017), critical P concentrations affected the growth of corn seedlings, triggering morphological adaptations in the

roots associated with P acquisition, such as an increase in total root length and R/S ratio. Moreover, some crops adapt to phosphorus deficiency by exploiting the soil at minimal metabolic cost (Lynch, 2007). This adaptation involves allocating more biomass to root classes that are metabolically efficient at absorbing phosphorus, such as adventitious roots and root hairs (Ramaekers et al., 2010). In the present study, despite observing an increase in the R/S ratio, no significant difference in this variable was found. Consequently, this trait did not emerge as a determining factor in the superiority of the hybrids over the lines. Other factors are supposed to contribute more significantly to the hybrids' ability to accumulate more phosphorus under the conditions evaluated.

Phosphorus use efficiency (PUE) refers to the ability of plants to acquire and use phosphorus from the soil to produce biomass and grains (Manske et al., 2000). It comprises phosphorus absorption efficiency (PUpE) and phosphorus utilization efficiency (PUtE). PUpE represents the ability of plants to absorb phosphorus from the soil, while PUtE indicates the ability to convert absorbed phosphorus into biomass or grain (Manske et al., 2000; Gu et al., 2016). Thus, improving PUE can be achieved by improving phosphorus absorption efficiency (PUpE) and, more economically, by improving phosphorus utilization efficiency (PUtE) in plants (Clemens et al., 2016).

The findings of this study reveal that under low P conditions, popcorn hybrids demonstrate a remarkable ability to optimize the efficiency with which they use this nutrient. This was evident in the significant increase in the shoot and the roots biomass and a considerable improvement in the PUE compared to the parent lines (Table 1). This efficiency was primarily attributed to an efficient internal utilization of phosphorus (PUtE) rather than absorption of this nutrient (PUpE), as no significant differences were observed between the parent lines and hybrids under conditions of low P supply (Table 1). The greater contribution from PUtE aligns with the findings of Li et al. (2021), whose study demonstrated that the corn hybrids evaluated exhibited superior performance in biomass production and PUE compared to the lines. These results align with other studies highlighting the significance of efficient translocation and reuse of stored phosphorus for achieving higher PUE (Wang et al., 2010; Abbas et al., 2018; Irfan et al., 2020). A strategy for mobilizing P within the plant involves recycling Pi from mature/senescent plant parts to actively growing tissues (Van de Wiel et al., 2016; Wang et al., 2021). This recycling process can

occur in mechanisms in which plants replace membrane phospholipids with non-phospholipids, such as P free lipids galactolipids (MGDG and GDGD) and sulfolipids (SQDG) (Moellering and Benning, 2011; Mehra et al., 2018). Furthermore, studies have demonstrated that different plant species and even cultivars of the same species can exhibit adaptive responses allowing them to increase external phosphate absorption or prioritize internal use under conditions of low P in the soil (Iqbal et al., 2019; Gerhardt et al., 2017).

Despite the investigated lines displaying differences in P efficiency, discerning marked differences in the aspects related to PUE and PUpE under conditions of low P availability up to the V6 evaluation stage was challenging (Table 1). Therefore, within the scope of this study, the results suggest that in critical circumstances of P deficiency, the primary discrepancies observed between the lines can be attributed to their genetic origins, with physiological factors playing a crucial role in promoting higher PUE and consequently greater biomass accumulation, thus favoring superior performance in the hybrids.

3.1.5.2 Effect of P supply on chlorophyll fluorescence, leaf pigments, and gas exchange measurements in popcorn genotypes

In plants responding to stress, various traits related to photosynthesis are often measured to assess their physiological status. The chlorophyll fluorescence-related traits obtained in this study, such as Φ NPQ, NPQt, Φ NO, and Φ PSII, are associated with different aspects of photosynthetic performance.

Our results reveal that both hybrids and parent lines significantly increased Φ NPQ and NPQt under low P conditions, demonstrating a greater activation of photosynthetic protection mechanisms. These findings align with other studies that have also reported an increase in Φ NPQ in plants exposed to low P supply stress (Patel et al., 2020; Nguyen et al., 2021). However, the hybrids exhibited a higher NPQt/ Φ NO ratio, suggesting a greater allocation of resources to photoprotection and antioxidant protection, which was also confirmed by the higher concentration of flavonoids (Table 2). On the other hand, the parent lines demonstrated greater efficiency in dissipating non-regulated energy about photoprotection, suggesting a less efficient allocation of energy to CO₂ assimilation and carbohydrate production.

This differentiated resource allocation may have negatively impacted plant growth and development, resulting in a lower net CO₂ assimilation rate (*A*).

The heterosis estimates for NPQt and NPQt/ Φ NO showed positive and high values under low P conditions, and these traits were statistically significant for comparisons I, II, and III (Table 2). Hence, the relevance of these traits as indicators capable of distinguishing genotypes and the importance of photosynthetic protection mechanisms activated under conditions of P deficit are highlighted. Other studies have highlighted the importance of NPQt in genetic improvement for enhancement of crop photoprotection (Wei et al., 2022; Hussain et al., 2023).

In crop plants, the measurement of chlorophyll content serves as an indicator of leaf health and, consequently, of the correct activity of the photosynthesis. The reduction in chlorophyll and the increase in flavonoids in response to P deficiency in popcorn lines and hybrids suggest that the absence of this essential nutrient induces alterations in the biosynthetic pathway of these pigments. These changes may be related to plant adaptation mechanisms in response to phosphorus scarcity, potentially affecting photosynthetic efficiency and the plant's ability to protect against oxidative damage (Kayoumu et al., 2023).

Furthermore, flavonoids are one of the traits that significantly showed differences in all comparisons I, II, and III under high and low P content conditions. Studies have previously revealed that flavonoids play an important role in protecting against abiotic stresses, such as P deficiency (Trejo-Téllez et al., 2019; Lou et al., 2019; Liu et al., 2020). Therefore, measuring chlorophyll and flavonoid content can be a useful approach to assess leaf health and provide valuable information on the ability of plants to respond to P nutrient stress.

Regarding gas exchange, the decrease in net CO₂ assimilation rate (*A*), stomatal conductance (*g_s*), and transpiration (*E*), coupled with the increase in intercellular CO₂ concentration (*C_i*) in parent lines and hybrids, aligns with the hypothesis that non-stomatal factors play a substantial role in photosynthesis during P deprivation (Rao et al., 1989; Reich et al., 2009; Zhang et al., 2014b; Kayoumu et al., 2023).

P_i plays a crucial role in photosynthesis, particularly in the dark phase or Calvin cycle. In this phase, carbon dioxide is fixed and converted to triose-phosphate through enzymatic reactions (McClain and Sharkey, 2019), which is an essential step in the production of carbohydrates such as sucrose, an essential

molecule for the plant growth and development (Wingler and Henriques, 2022). Sucrose is a sugar that is transported from leaves to other parts of the plant, where it is used to provide energy and carbon for the growth and activity of tissues and reserve organs (Aluko et al., 2021). Previous studies have demonstrated that P deficiency can impact the production of triose-phosphate transporters (Thuynsma et al., 2016; Chu et al., 2018). Therefore, P deficiency may have influenced sucrose synthesis in popcorn leaves, limiting the availability of energy and carbon needed for healthy development.

In both P availability conditions, no significant differences in g_s and E between the parent lines and hybrids (III; Table 2) were observed. This suggests that the intercellular CO_2 concentration (C_i) was one major factor responsible for the variations in net CO_2 assimilation rate (A) in this comparison (Table 2). Furthermore, a higher A/C_i ratio in the hybrids compared to the lines indicates that the hybrids are more efficient in adaptive responses to P deficiency, with a greater capacity to convert carbon into biomass (Sherin et al., 2022).

3.1.5.3 How can genetic gains be maximized in popcorn under P deficiency?

The low availability of P allowed for a clearer distinction among the studied genotypes. The hybrids exhibited distinct responses from the parent lines, with higher heterosis values observed under low P condition, as indicated in Tables 1 and 2. Furthermore, a predominance of quadratic components associated with dominance effects (ϕ_s) in controlling plant growth traits, P accumulation, and P efficiency in both conditions was observed (Supplementary Table 2 and Figure 2). This implies that the predominant mode of genetic action remains consistent for both P conditions, suggesting that similar breeding strategies can be applied.

In support of this finding, a previous study (Silva et al., 2019) evaluated 29 popcorn lines, including four lines assessed in the present study. They found strong genetic correlations between P availability and shoot and root growth. They suggested that selecting for individuals with high growth in one environment results in a similar increase in the other environment. Therefore, this correlation can be attributed to the quadratic component, with the largest contribution to the genetic variance in the growth and P use efficiency traits being the same in both P availability conditions (Figure 2). Furthermore, the selection of the most suitable

genitors, given the contribution of the quadratic component associated with the reciprocal effect (ϕ_{rc}) evidenced in both P conditions, and the formation of promising hybrids can be carried out at the juvenile stage of the plants. This is because, in the corn crop, the early stages of growth have been identified as critical in terms of the demand for this nutrient (Li et al., 2021).

Regarding the physiological traits, we found that under high P conditions, these traits were significantly influenced by the environment (Figure 3). This indicates that when P is readily available in sufficient amounts, environmental conditions play a major role in determining the physiological traits of popcorn plants. On the other hand, when the plants were subjected to conditions of low P availability, a notable change in dynamics was observed (Figure 3). Genetic factors emerged as the critical elements that most significantly influenced these traits. The quadratic components that contributed most to the variability observed in the traits were the effects of dominance (ϕ_s) and reciprocity (ϕ_{rc}) (Figure 3). While the quadratic component associated with ϕ_s is related to allelic complementation, the quadratic component associated with ϕ_{rc} is related to the action of mitochondrial and chloroplast genes, and nuclear genes from the maternal parent (Cruz et al., 2014). Therefore, exploring heterosis and using female genitors with significant averages for these traits can maximize genetic gains. The main traits to be studied would be: NPQt, Φ NO, and NPQt/ Φ NO related to chlorophyll fluorescence; Flav related to leaf pigments; and *A* and *Ci* related to gas exchange.

Finally, the results provide valuable insights for the improvement of popcorn through the strategic choice of genitors, the exploitation of heterosis, and the selection of specific photosynthetic traits, taking into account the different conditions of P availability.

3.1.6 CONCLUSION

In this study, higher phosphorus use efficiency (PUE) was associated with greater accumulation of this nutrient in the aerial part and roots of the plants, along with a better *A/Ci* and NPQt/ Φ NO ratios. In addition, the concentration of flavonoids proved to be promising for differentiating genotypes under both phosphorus

availability conditions, useful for identifying genotypes with potential and for detecting levels of P deficiency at juvenile stages. Genetic gains for PUE can be achieved by exploiting heterosis in the different traits evaluated in this study, highlighting the importance of this strategy in the genetic improvement of popcorn in the face of P deficiency.

3.2 UNRAVELING THE MECHANISMS OF EFFICIENT PHOSPHORUS UTILIZATION IN POPCORN (*Zea mays* L. VAR. EVERTA): INSIGHTS FROM PROTEOMICS AND METABOLITES ANALYSIS

3.2.1 INTRODUCTION

Phosphorus (P) is a critical nutrient among the essential elements for plant health and growth. Insufficient availability of this mineral acts as a limiting factor for normal plant development (Heuer et al., 2017; Sun et al., 2018). This is due to the indispensable role of inorganic phosphate (Pi) in numerous vital plant functions. Pi acts as a phosphate group donor during phosphorylation, pivotal for activating key molecules and enzymes essential in processes like adenosine triphosphate (ATP) synthesis. ATP, the primary energy carrier molecule in cells, is crucial for fueling various cellular activities in plants (Song, 2021; Fontecilla-Camps, 2022). Furthermore, Pi plays a pivotal role as a fundamental component of nucleic acids, such as DNA and RNA, which are crucial for genetic expression and regulation (Malhotra et al., 2018).

P exists in several forms in soil, with the phosphate anion H_2PO_4^- being the primary form assimilated by plants (Kumar et al., 2021). However, due to its chemical properties, the concentration of P soil solution available for root uptake is low, typically around 10-5 μM (Roberts and Johnston, 2015). When P is applied as fertilizer, it rapidly undergoes fixation processes in the soil, rendering it inaccessible for uptake (Riskin et al., 2013; Delgado et al., 2016). Unlike nitrogen (N), which can

be replenished by fertilizers and nitrogen-fixing plants (Curatti and Rubio, 2014; Sahoo et al., 2014), P is a non-renewable resource. It cannot be replaced or artificially synthesized and must be extracted from limited reserves, mainly phosphate rock deposits (Cordell and White, 2011; Wellmer and Scholz, 2017). Therefore, there is considerable interest in developing crop varieties that can achieve higher yields while using less soil phosphorus.

To address the need to reduce P use while avoiding future Pi depletion, plant breeding is emerging as a viable avenue to increase phosphorus use efficiency (PUE) through genetic improvement (Heuer et al., 2017). However, breeders face a formidable challenge due to the complexity of PUE, which involves multiple traits (van de Wiel et al., 2016). As a result, several methods have been used to identify genotypes with enhanced responsiveness to phosphorus deficiency. These approaches include molecular techniques such as QTL identification (Chen et al., 2008; Yuan et al., 2017; Mahender et al., 2018), transcriptomic analysis (Zeng et al., 2016; Silva et al., 2019a; Liu et al., 2020a), and proteomic profiling (Zhang et al., 2014; Vengavasi et al., 2017), as well as phenotyping methods that assess physiological traits (Patel et al., 2020; Bhatta et al., 2021).

Proteomic and metabolic studies offer valuable insights into how different genotypes respond to stress conditions, revealing essential molecular switches and pathways involved in stress responses and adaptation. For example, under P starvation, maize roots of tolerant inbred lines activated a higher number of genes related to plant hormone signaling, acid phosphatase, and metabolite (Jiang et al., 2017). In addition, proteins associated with carbon metabolism, cell proliferation, and sugar metabolism play a crucial role in enhancing tolerance to low P conditions (Li et al., 2008). In maize leaves, the response to P deficiency alters the regulation of proteins involved in photosynthesis, carbohydrate metabolism, energy metabolism, secondary metabolism, signal transduction, and protein synthesis (Zhang et al. 2014). Despite these insightful studies in common maize, there is a lack of exploration of the molecular regulation of popcorn (*Zea mays* L. var. *everta*) to P deficiency.

Research regarding the effects of P deficiency on popcorn has mainly focused on efforts to identify the most effective breeding strategies that can lead to the development of more P-efficient and productive popcorn varieties (Almeida et al., 2018; Schegoscheski Gerhardt et al., 2019; Santos et al., 2022). This focus is

driven by the economic importance of popcorn as a snack food (Jele et al., 2014), and the significant impact that P deficiency can exert on crop yield. Furthermore, most studies of PUE in popcorn are based only on agronomic traits, and an integrative strategy using molecular tools is needed for a comprehensive understanding of the plant response to P deficiency. The integration of high throughput approaches, such as mass spectrometry-based proteomics, with physiological measurements, can unravel novel players related to tolerance to P starvation and provide a platform with potential candidates to use in popcorn molecular breeding programs.

Thus, the objective of this study was to investigate the responses of two contrasting popcorn inbred lines to PUE under low and high P availability to elucidate the molecular mechanisms of P deficiency tolerance.

3.2.2 LITERATURE REVIEW

3.2.2.1 Phosphorus within Plants: Uptake, Utilization and Remobilization

Phosphorus (P) is an essential element for plant growth and development, with structural (nucleic acids, phospholipids), metabolic (energy transfer), and regulatory functions (Liu et al., 2015; Kleinert et al., 2017; Vengavasi et al., 2017). Despite being a macronutrient, it is one of the least accessible elements due to its low solubility and limited mobility in the soil solution (Ouyang et al., 2016; Liu et al., 2020).

Despite its very low concentration in soil (ranging from 1 to 10 μM) (Yhang et al., 2017; Lambers and Plaxton, 2018), phosphate concentration in plant tissues is relatively high, around 5 to 20 mM (Raghothama, 1999). This is because phosphorus is a fundamental element in essential biomolecules such as DNA, RNA, ATP, NADPH, and membrane phospholipids (Maharajan et al., 2018; Pang et al., 2018). In addition, it plays a critical role in life-sustaining processes in plants, including photosynthesis, respiration, and protein activation through phosphorylation (Li et al., 2014; Muneer and Jeong, 2015).

The molecular mechanisms regulating the expression of genes encoding phosphate transporters and signaling pathways in plants include the coexistence of

high- and low-affinity phosphate transport systems in plant roots (Nussaume et al., 2011; Gu et al., 2016). High-affinity transporters are plasma membrane proteins responsible for the uptake of phosphate from soil at low concentrations (Lopez-Arredondo et al., 2014; Mlodzińska and Zboińska 2016; He et al., 2019). These proteins are encoded by members of the *PHT1* (phosphate transporter) gene family and have significant potential to improve soil phosphate acquisition (Schroder et al., 2013).

The first report of Pi transporters in plants was made for *Arabidopsis thaliana* (Muchhal et al., 1996). Subsequently, various other Pi transporters have been identified not only in *Arabidopsis* but also in other crops such as rice (*Oryza sativa* L.) (Srivastava et al., 2018; Victor et al., 2019), maize (*Zea mays* L.) (Walder et al., 2015; Liu et al., 2016; Wang et al., 2020), and wheat (*Triticum aestivum* L.) (Guo et al., 2014; Teng et al., 2017; De Souza Campos et al., 2019).

A total of thirteen *PTH1* transporters have been identified in maize (Walder et al., 2015; Liu et al., 2016; Liu et al., 2018; Wang et al., 2020). Transporters *ZmPHT1; 1*, *ZmPHT1; 3*, *ZmPHT1; 4*, *ZmPHT1; 8*, and *ZmPHT1; 9* are mainly expressed in roots and leaves and play an important role in phosphate uptake and redistribution. On the other hand, transporters *ZmPHT1; 2*, *ZmPHT1; 4*, *ZmPHT1; 6*, *ZmPHT1; 7*, *ZmPHT1; 9*, and *ZmPHT1; 11* are positively regulated by arbuscular mycorrhizal fungi (AMF), and these genes may be involved in mediating phosphate absorption and/or transport in maize.

After absorption in root cells, Pi is subsequently used to synthesize P-containing compounds such as ATP or phospholipids or can enter the vacuole where it is stored (Mlodzińska and Zboińska, 2016). Thus, in vegetative cells, when there is an excess of available Pi, it is absorbed and stored in vacuoles in the form of orthophosphate (Liu et al., 2015), whereas in seeds, Pi is stored in specialized protein storage vacuoles in the form of phytate (Yang et al., 2017).

Since Pi may not be available at optimal concentrations throughout the plant life cycle, the Pi supply is operated by the vacuolar Pi pool whenever the cytosolic Pi concentration decreases (Liu et al., 2015). Therefore, optimizing Pi influx and efflux from vacuoles is essential for maintaining Pi homeostasis in other organelles, tissues, and at the whole-plant level (Srivastava et al., 2018). Zhang et al. (2016) showed that remodeling the lipid composition of membranes by increasing V-ATPase activity - an enzyme responsible for generating a proton gradient and

pumping stored Pi out of the vacuole (Forgac, 2009) - increased intracellular Pi recycling in a maize mutant under low P deprivation. This may have improved chlorophyll biosynthesis and the levels and activities of several enzymes involved in the Calvin cycle and CO₂ pumps. This mechanism of response to P deficiency is crucial because Pi is used in numerous metabolic processes, including photosynthesis. Therefore, efficient utilization of internal Pi for photosynthesis is essential to ensure an adequate supply of photoassimilates for growth and shoot translocation (Chea et al., 2021).

One strategy for remobilizing phosphate (P) within the plant is to recycle P from mature/senescent plant parts to actively growing tissues (Wiel et al., 2016). This recycling can occur through mechanisms by which plants replace membrane phospholipids with non-phospholipids, specifically phosphorus-free lipids such as galactolipids (MGDG and GDGD) and sulfolipids (SQDG) (Moellering and Benning, 2011; Mehra et al., 2018). Lipids in cell membranes carry approximately one-third of the total cellular organic P (Pant et al., 2015). Thus, membrane lipid remodeling allows phospholipid hydrolysis to release Pi for essential cellular processes with minimal or no damage to membrane function (Verma et al., 2021). Mehra et al. 2018, highlight the importance of galactolipid-mediated lipid remodeling (GDGD) in improving low Pi tolerance in rice, simultaneously targeting Pi utilization and Pi acquisition efficiency. Wang et al. (2020), through lipid analysis in maize leaves and roots under low phosphate conditions, observed an increase in non-phospholipids (MGDG, DGDG, and SQDG) and a decrease in phospholipids, mainly in leaf tissues.

3.2.2.2 Proteomic approaches to P use efficiency

In the last few years, several transcription factors have been discovered and characterized that are involved in the regulation of low-P stress. The MYB family transcription factor *PHR1* has been characterized in Arabidopsis (Bari et al., 2006) as a key regulator of low-P-responsive gene transcription in the root. In addition to *PHR1*, several transcription factors involved in the low-P response have been identified, such as *OsPHR1*, *OsPHR2*, *OsPHR3*, and *OsPHR4* in rice (Wu et al., 2013; Ruan et al, 2017), *WRKY75*, *MYB62*, and *AtPHR1* in Arabidopsis (Devaiah

et al., 2007; Devaiah et al., 2009; Wu et al., 2013), and *OsPTF1* and *ZmAPRG* in maize (Li et al., 2011; Yu et al., 2019).

However, transcriptional studies do not provide direct estimates of protein abundance (Li et al., 2008). Furthermore, many biological questions can only be addressed at the protein level, as the presence of a gene or its mRNA does not guarantee a role in cellular activity (Quirino et al., 2010; Li et al., 2014). Therefore, protein determination and quantification are essential for understanding the mechanisms involved in cellular metabolic control (Lan et al., 2018). Quantitative proteomics has been a good tool for investigating the molecular mechanisms of plant responses to stress. In the field of breeding, its application ranges from the identification of proteins present in tissues, such as leaves/roots (Xiao et al., 2020; Cheng et al., 2021), to specialized organs, such as grains/seeds (Li et al., 2021).

Comparative proteomic studies of maize roots have provided valuable insights into genotypes with different levels of low-P tolerance (Li et al., 2007; Li et al., 2014). Responses included both changes in phosphorylation and changes in the abundance of proteins involved in numerous metabolic and cellular pathways. Changes in protein abundance led to several changes in carbon flux in metabolic processes, including sucrose and other downstream sugar metabolism pathways. In addition, changes in some key enzymes, such as sucrose synthase and malate dehydrogenase, were observed.

The study conducted by Zhang et al. (2014) provided a new perspective on how maize responds to low-P stress through changes in leaf metabolism. The proteins identified by the authors are involved in various metabolic pathways, including photosynthesis, carbohydrate metabolism, energy metabolism, secondary metabolism, signal transduction, protein synthesis, and defense. Under low-P conditions, there was a negative regulation of proteins involved in CO₂ enrichment, the Calvin cycle, and the electron transport system, resulting in reduced photosynthesis. Consequently, with restricted electron transport for photosynthesis, there was a positive regulation of antioxidant contents to eliminate reactive oxygen species (ROS) in response to peroxide accumulation.

In maize, through physiological and comparative proteomic analyses of leaves from Qi319-96 mutant and wild-type Qi319 plants treated with high and low P, Zhang et al. (2016) showed that although shoot phosphorus levels did not differ between genotypes, the Qi319-96 mutant had a higher rate of CO₂ photosynthetic

fixation and plant biomass compared to wild-type Qi319. Proteomic changes included 29 (high-P) and 71 (low-P) differentially expressed proteins involved in a variety of metabolic processes. Under low-P conditions, the levels of Rubisco, NADP-malic enzyme, pyruvate orthophosphate dicinase, delta-aminolevulinic acid dehydratase, sucrose-phosphate phosphatase, cytoplasmic phosphoglucomutase, fructose bisphosphate, aldolase, NADP-glyceraldehyde-3-phosphate dehydrogenase, NADPH-dihydroethidium, plastoquinone dehydrogenase, and chlorophyll a/b binding protein were significantly increased compared to Qi319. Based on these results, the authors suggest that increased internal Pi use efficiency was the primary reason for the higher low-P tolerance in the mutant compared to the wild type.

Although physiological studies related to proteomics in response to low-P stress have been conducted in maize (Li et al., 2007; Li et al., 2014; Zhang et al., 2016; Jiang et al., 2017; Sun et al., 2018), there is a lack of research using these approaches in popcorn.

3.2.3 MATERIALS AND METHODS

3.2.3.1 Plant materials and treatment

Two popcorn inbred lines (S_7) were evaluated: P7 (derived from hybrid IAC112, adapted to temperate and tropical climates) and L80 (derived from open-pollinated variety Viçosa, adapted to temperate and tropical climates). These lines were selected based on previous studies under soil P limiting conditions and were agronomically classified as efficient (P7) and inefficient (L80) in phosphorus use under field conditions (Gerhardt et al., 2017), as well as in P use efficiency in the greenhouse, based on plant phosphorus content and dry matter (Silva et al., 2019b). The experiment was carried out in a lysimeter system, i.e., polyvinyl chloride (PVC) pipes (150 cm deep and 10 cm in diameter) under protected growing conditions in a greenhouse. Temperature, humidity, and photosynthetically active radiation data followed the seasonal pattern and were obtained using the WatchDog 2000 Series Experimental Station (Spectrum Technologies Inc., Aurora, IL, USA) (Figure 4).

Plants were grown under two phosphorus availability conditions based on the nutrient solution according to the methodology of Hoagland and Arnon (1950) with a modified P supply in the form of $\text{NH}_4\text{H}_2\text{PO}_4$. To supplement the ammonium source (NH_4), 1 mol L^{-1} of NH_4Cl was added to the nutrient solution, in order to prevent additional stress from low nitrogen in the plants. The pH of the solution was maintained between 5.5 and 5.8 by adding HCl or NaOH. The high P (HP) and control condition corresponded to 100% P supply (31.00 mg L^{-1}), while the low P (LP) and stress condition corresponded to 0.5% P (0.15 mg L^{-1}). The plants were irrigated daily with deionized water and the nutrient solution (100 mL) was applied from the V2 stage until reaching the V4 stage, with the pH maintained between 5.5 and 5.9. For acclimation of seedlings, from V2 onward, 100 mL of nutrient solution was applied at 25% strength (25% of total concentration) for three days, 50% strength (50% of total concentration) for two days, and 100% strength (100% of total concentration) until the end of the experiment.

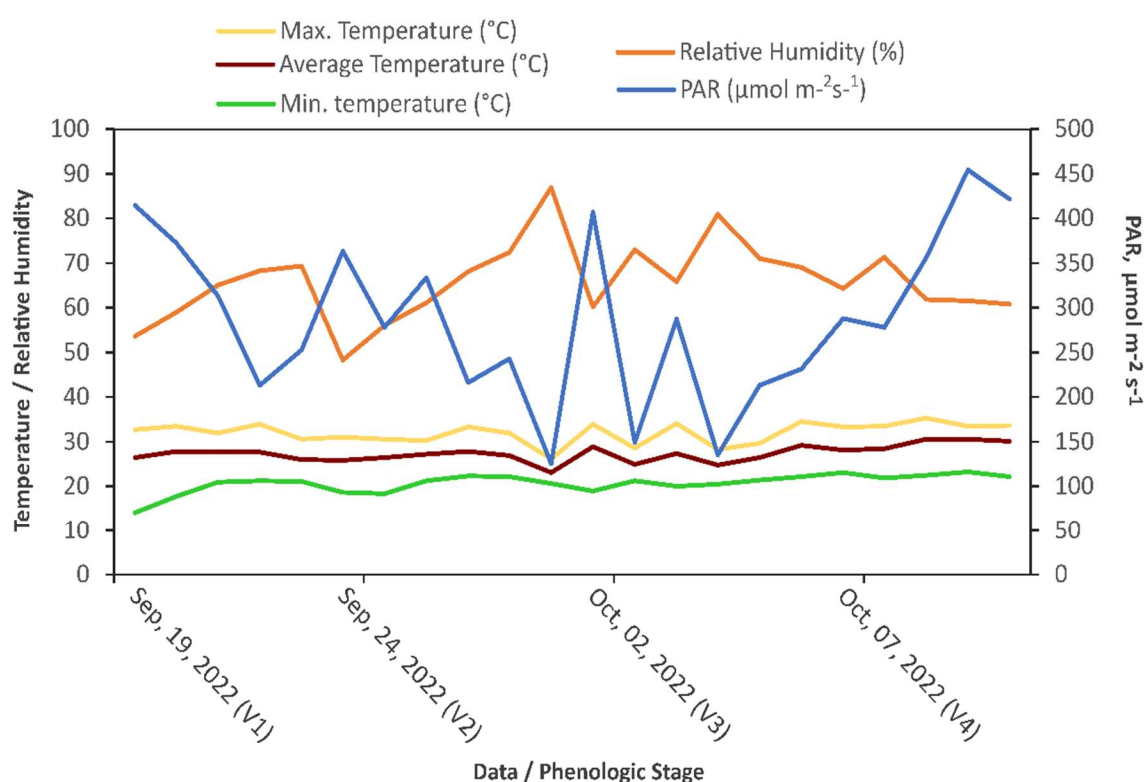


Figure 4 - Average, maximum, and minimum temperature ($^{\circ}\text{C}$), relative humidity (RH, %) and photosynthetically active radiation (PAR, $\mu\text{mol m}^{-2} \text{s}^{-1}$) along the dates and phenological stages (V) of growth of popcorn plants under two conditions of P availability.

3.2.3.2 Physiological measurements

3.2.3.2.1 Leaf gas exchange measurements

Gas exchange was assessed 24 days after sowing (V4) between 9:00 and 11:00 a.m. Measurements were taken in the middle third of the last developed leaf on 6 plants in each treatment over an area of 600 mm². An infrared gas analyzer - IRGA (model LI-6400, LI-COR, Lincoln, NE) was used. During the analyses, the photosynthetically active radiation (PAR) was fixed at 600 $\mu\text{mol m}^{-2} \text{s}^{-1}$, the CO₂ concentration in the LI-6400 chamber was 400 $\mu\text{mol mol}^{-1}$, and the relative humidity and temperature were 60% and 25°C, respectively. Gas exchange parameters analyzed included net CO₂ assimilation rate (*A*), transpiration (*E*), stomatal conductance (*g_s*), and intercellular CO₂ concentration (*C_i*).

3.2.3.2.2 Leaf chlorophyll content

Leaf chlorophyll content was measured in the middle third of the last developed leaf, one day before the end of the experiment (23 days after sowing) using a portable leaf pigment meter model Dualex® (FORCE-A, Orsay, France). Leaf pigment was assessed in the same leaf area (600 mm²) where gas exchange was assessed.

3.2.3.2.3 Dry matter

At the end of the experiment (24 days after sowing), the leaves and stalks of the same plants on which the physiological measurements were performed were separated from the roots and placed in paper bags for drying in an oven at 65 °C for 72 h for the determination of leaf dry matter (LDM - g) and stalk dry matter (SDM - g).

3.2.3.2.4 Phosphorus concentration

After drying, the leaf and stem samples were ground for quantification of phosphorus concentration in 1 g of dry matter. For this, extraction was performed by sulfuric digestion (HNO₃ and H₂O₂), and in the extract, P was determined by spectrophotometry (Specord 2010, Analytik Jena, Jena, Germany) using the molybdate method (da Silva Santos et al., 2014). Phosphorus content was

determined by multiplying the concentration of phosphorus in 1 g of dry matter of each sample by the corresponding dry weight (mg P/ plant).

3.2.3.2.5 P utilization and efficiency indexes

Based on the P concentration obtained in 1g of dry mass and on the dry mass weight, we estimated: i) the P use efficiency (PUE: ADM/total P applied), where ADM is the aerial dry matter in g; ii) P uptake efficiency (PUPE: APC/total P applied) where APC is the concentration of P in the aerial part; and iii) P utilization efficiency (PUtE: ADM/aerial P content) (Moll et al., 1982).

3.2.3.2.6 Statistical analysis

For each trait studied, an individual analysis of variance was performed for each phosphorus availability condition according to the following statistical model: $Y_{ij} = \mu + G_i + B_j + \varepsilon_{ij}$, where Y_{ij} is the observed value of the i-th genotype in the j-th block; μ is the general constant; G_i is the effect attributed to the i-th genotype; B_j is the effect of block j; and ε_{ij} is the experimental error associated with observation Y_{ij} .

Subsequently, combined analysis of variance was performed based on the following statistical model: $Y_{ijk} = \mu + B_k + G_i + P_j + GP_{ij} + \varepsilon_{ijk}$, where Y_{ijk} is the observation of the i-th genotype in the j-th availability of P in the k-th block; μ is the general constant; B_k is the random effect of the k-th block; G_i is the fixed effect of the i-th genotype; P_j is the fixed effect of the j-th P condition; GP_{ij} is the fixed effect of the interaction between the i-th genotype and the j-th P condition; and ε_{ijk} is the average experimental random error associated with observation Y_{ijk} with NID (0, σ^2). The results were subjected to analysis of variance and the means were compared using Tukey's test with a significance level of 5% probability. Statistical analyses were performed using GENES software (Cruz, 2013).

3.2.3.3 Proteomics

3.2.3.3.1 Material handling

At V4 stage, three biological replicates of the last fully expanded leaf were collected for proteomic analysis and stored immediately in liquid nitrogen. Each replicate consisted of a pool of leaves from three individual plants. Leaves were macerated with a mortar and pestle in liquid nitrogen and transferred to 2 mL

microtubes. The microtubes were sealed with parafilm, punctured with a needle, and placed in a lyophilizer (model L101) at -55°C under vacuum for 48 hours and then stored in a freezer at -80°C until further use.

3.2.3.3.2 Protein extraction and digestion

The overall protocol was adapted from Alvarez et al. (2011) with minor modifications. Briefly, total protein was extracted from lyophilized popcorn leaf samples (~ 0.12 mg) using 600 μL Tris-buffered phenol (pH 8.8) and 600 μL 0.1 M Tris-HCl containing 10 mM EDTA, 0.4% 2-mercaptoethanol, and 0.9 M sucrose. Samples were vortexed, placed on a shaker at 4°C and 800 rpm for 1 hour (vortexing every 10 minutes), centrifuged at 16,000g for 20 minutes, and the phenolic phase was then collected. The phenolic phase (~ 350 μL) was precipitated overnight in five volumes of 0.1 M ammonium acetate in 100% methanol at -20°C . The protein was collected by centrifugation at 16,000g and washed once with 0.1 M ammonium acetate in 100% methanol, once with 80% acetone, and once with 70% methanol. The protein pellet was briefly air dried and then resuspended in 100 μL 7M urea/2M thiourea, 5mM dithiothreitol (DTT), 0.1M Tris pH 7.7 and reduced for 1h30min at 37°C . Protein concentration was determined using the CB-X protein assay (Genotech, St. Louis, MO, USA) according to the manufacturer's protocol.

Then, 50 μg of proteins were alkylated with 10 μL of 100mM iodoacetamide (IAM) in 0.1M Tris, pH 7.8 and incubated in the dark for 30 minutes. Subsequently, 10 μL of 0.1M DTT in Tris, pH 7.8 was added to quench the IAM. Lysine and trypsin were used for digestion. Samples were first diluted in 80 μL of 25 mM Tris buffer containing Lys-C enzyme at a 1:10 protein ratio (0.5 $\mu\text{g}/\mu\text{L}^{-1}$) and incubated for 6 hours. Following this, 300 μL of 25 mM Tris buffer containing trypsin enzyme at a protein ratio of 1:25 (100 ng/ μL) was added and the mixture was incubated at 37°C for 18 hours overnight.

3.2.3.3.3 Proteomic analysis

Liquid chromatography-tandem mass spectrometry (LC-MS/MS) analysis was performed using an Ultimate 3000 RSLCnano system coupled to an Orbitrap Eclipse mass spectrometer (Thermo Fisher Scientific, Rockford, IL, USA). The peptides were acidified with trifluoroacetic acid (TFA) to 0.5%. 5 μL of the samples were first injected onto a trap column (Acclaim PepMap™ 100, 75 μm x 2 cm,

ThermoFisher Scientific) and desalted for 6.0 min at a flow rate of 5 $\mu\text{L min}^{-1}$, before switching in line with the main column. Separation was performed on a C18 nano column (Acquity UPLC® M-class, Peptide CSH™ 130A, 1.7 μm 75 μm x 250mm, Waters Corp, Milford, MA, USA) at 300 nL/min with a linear gradient from 5-22% over 69 min. The LC aqueous mobile phase contained 0.1% (v/v) formic acid in water and the organic mobile phase contained 0.1% (v/v) formic acid in 100% (v/v) acetonitrile. Mass spectra for the eluted peptides were acquired in the Orbitrap using the data-dependent mode with a mass range of m/z 375–1500, resolution 120,000, AGC (automatic gain control) target 4×10^6 , maximum injection time 50 ms for the MS1. Data-dependent MS2 spectra were acquired by HCD in the ion trap with a normalized collision energy (NCE) set at 30%, AGC target set to 5×10^4 and a maximum injection time of 100 ms.

The raw data files were processed using the Proteome Discoverer software package (Version 2.4; Thermo Fisher Scientific) and analyzed using the MASCOT search engine (Version 2.7.0; Matrix Science, London, UK). The search was performed against an in-house modified version of the cRAP database (124 entries) and the *Zea mays* database obtained from UniProt (ID: UP000007305, www.uniprot.org), assuming the digestion enzyme trypsin and a maximum of 2 missed cleavages. MASCOT search was performed with a fragment ion mass tolerance of 0.06 Da and a parent ion tolerance of 10.0 ppm. Deamidated of asparagine and glutamine, oxidation of methionine was specified in Mascot as variable modifications, while carbamidomethyl of cysteine was fixed. Peptides were validated by Percolator with a 0.01 posterior error probability (PEP) threshold. The data were searched using a decoy database to set the false discovery rate (FDR) to 1% (high confidence). Only proteins identified with a minimum of 2 unique peptides and 5 peptide-spectrum matches (PSM) were further analyzed for quantitative changes. The peptides were quantified using the precursor abundance based on intensity. The peak abundance was normalized using total peptide amount. The peptide group abundances are summed for each sample and the maximum sum for all files is determined. The normalization factor used is the factor of the sum of the sample and the maximum sum in all files. The protein ratios are calculated using the summed abundance for each replicate separately, and the geometric median of the resulting ratios is used as the protein ratios. The significance of differential expression is tested using a t-test which provides a *p*-

value and an adjusted p -value using the Benjamini-Hochberg method for all the calculated ratios. To identify differentially expressed proteins (DEPs) involved in the phosphorus stress response for each genotype (L80_LP/L80_HP and P7_LP/P7_HP), a p -value less than 0.05 and a log₂ fold change greater than 1 and less than -1 were considered. The mass spectrometry proteomics data have been deposited to the ProteomeXchange Consortium via the PRIDE (Perez-Riverol et al., 2022) partner repository with the dataset identifier PXD044106 (Username: reviewer_pxd044106@ebi.ac.uk; Password: cWLYnh52).

3.2.3.3.4 Gene ontology and enrichment pathway analysis

The Gene Ontology (GO) analysis was performed using a web-based tool PlantRegMap (http://plantregmap.gao-lab.org/go_result.php) and the pathway enrichment analysis was performed using KOBAS 3.0 (<http://kobas.cbi.pku.edu.cn/genelist/>). For both analyses p -values were adjusted with Benjamini-Hochberg correction for multiple testing. Only pathways with p -values or q -values under a threshold of 0.05 were considered significant. A web-based tool Venny 2.1 was used to generate Venn diagrams (<https://bioinfogp.cnb.csic.es/tools/venny/index.html>). Aesthetic modifications to the graphs were made using Inkscape (<https://inkscape.org/>).

3.2.3.4 Metabolomic Analysis

3.2.3.4.1 Sample Preparation for LC-MS/MS

The same leaf samples used for proteomics analysis were used for polyphenol and phytohormone analysis. Briefly, a mixture of stable isotope labeled hormones was used as an internal standard for the assay of phytohormones in the samples, and the synthetic strigolactone GR24 was used for the flavonoid assay. Samples were extracted using a previously described method (Vu and Alvarez, 2021). Briefly, compounds were extracted using 100% methanol and homogenized using a TissueLyzer II (Qiagen, Hilden, Germany) for 15 minutes at 10 Hz and then centrifuged at 4°C for 10 minutes at 16,000 rpm. Samples were dried in a SpeedVac.

To resuspend the samples, 100 μ L of 30% methanol was added to each tube. The tubes were then placed on a shaker for 30 minutes and centrifuged at 16,000 rpm for 25 minutes. Blank tubes were extracted alongside the samples to use as negative control.

3.2.3.4.2 LC-MS/MS, polyphenols and phytohormones analysis

For the polyphenols analysis, samples were separated as detailed in Vu and Alvarez (2021) with an Eclipse XDB C18 (100 \times 3.0 mm; 3.5 μ m; Agilent Technologies, Santa Clara, CA, USA) column at a flow rate of 0.4 mL/min at room temperature using a gradient of mobile phases A (2% acetic acid) and B (100% acetonitrile). The phytohormones analysis followed the same specifications used by Lopez-Guerrero et al. (2022). Briefly, the samples were separated using an Agilent ZORBAX Eclipse Plus C18 column (2.1 \times 100 mm) with a flow rate of 0.45 mL/min at 40 $^{\circ}$ C and a gradient of two mobile phases: phase A, consisting of 0.1% formic acid in water, and phase B, consisting of 0.1% formic acid in 90% acetonitrile. Polyphenols and phytohormones were detected using multiple reaction monitoring (MRM) scan on a QTRAP 6500+ mass spectrometer (Sciex, Framingham, MA, USA) operating with the IonDrive Turbo V electrospray ionization (ESI) source in positive and negative ion modes. For quantification, an external standard curve was prepared using a series of standard samples containing different concentrations of unlabeled compounds and fixed concentrations of the internal standards. Data analysis was processed using the Analyst 1.6.3 software (Sciex).

3.2.3.4.3 Statistical analysis

Data processing and statistical analysis were performed using MetaboAnalyst 5.0 software, an online statistical package available at <https://www.metaboanalyst.ca/> (Pang et al., 2021). For statistical analysis of polyphenols and phytohormones, concentration levels were considered. The data were normalized by Auto scaling to prevent variables with larger magnitudes from dominating the analysis, and heat maps were constructed to evaluate the relative levels between control and phosphorus treatments in both genotypes. One-way analysis of variance (ANOVA) with *p*-value cutoff (FDR α = 0.05) was used to test the significance of each compound between treatment and genotypes. The data was then submitted to Tukey's HSD Post-hoc analysis (*P* < 0.05, *n* = 3). The

heatmaps were constructed based on the Euclidean distance measure and the Ward clustering algorithm.

3.2.4 RESULTS

3.2.4.1 Physiological responses of popcorn to phosphorus deficiency

Under low P (LP), both inbred lines showed a significant reduction in shoot dry matter (68.96% and 82.24% for L80 and P7, respectively) (Figure 5A), and in P content (86.36% and 93.84% for L80 and P7, respectively) (Figure 5B), but an increase in PUE (98.41% and 97.24% for L80 and P7, respectively) (Figure 5C). The P-efficient inbred line (P7) showed higher shoot dry matter and P content compared to the P-inefficient inbred line (L80) at high P (HP) levels, and a significantly higher PUE compared at LP levels. At the V4 stage, even though the shoot dry matter content is not different between L80 and P7 at LP supply, L80 plants had yellowish leaves and wilted leaf tips, which are known signs of stress impact, whereas the P7 plants had purple and healthier leaves (Figure 6).

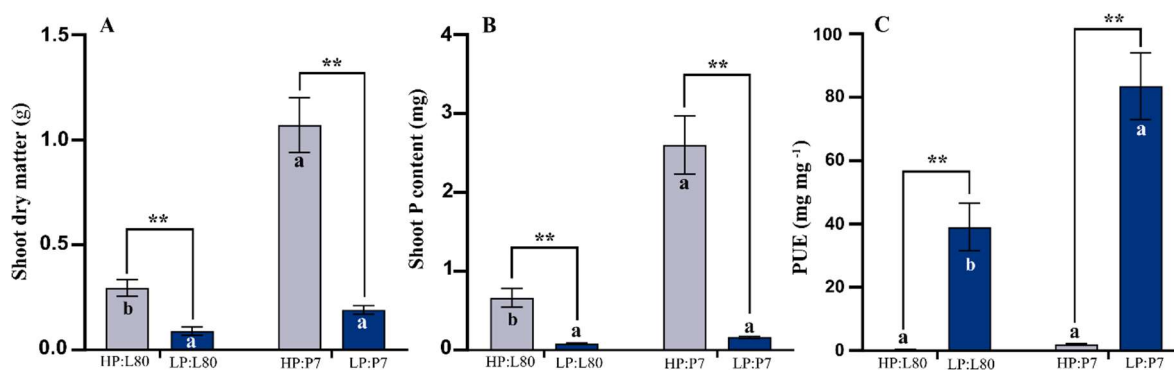


Figure 5. Dry matter accumulation (**A**) P content (**B**) and PUE (**C**) in shoot in the two popcorn inbred lines L80 and P7 under high (HP) and low (LP) phosphorus levels. Values with asterisks are statistically different by *F*-test at 1% (**), at 5% (*), or not significant (ns), and means followed by the same letter were not significantly different by *F*-test ($P < 0.05$). Asterisks indicate comparisons within the same genotype at different P levels, whereas letters indicate comparisons between two genotypes at the same P level. Values are expressed as mean \pm SD ($n = 3$).



Figure 6. A- Line L80 under low P supply. B- Line P7 under low P supply.

In Figures 7 and 8, the measurements of physiological traits in both strains indicated reduction in gas exchange and leaf pigments as a result of reduced P supply. Overall, they seem to follow the same response pattern regardless of tolerance level, except for the net CO₂ assimilation rate (*A*) and transpiration (*E*), which was higher in L80 at low P (Figure 7). Some of the major differences between P7 and L80 were in the chlorophyll and flavonoids content under low P (Figure 8). Concentration of flavonoids was twice as high in P7 at low P while chlorophyll content reduction is more apparent in P7 at low P.

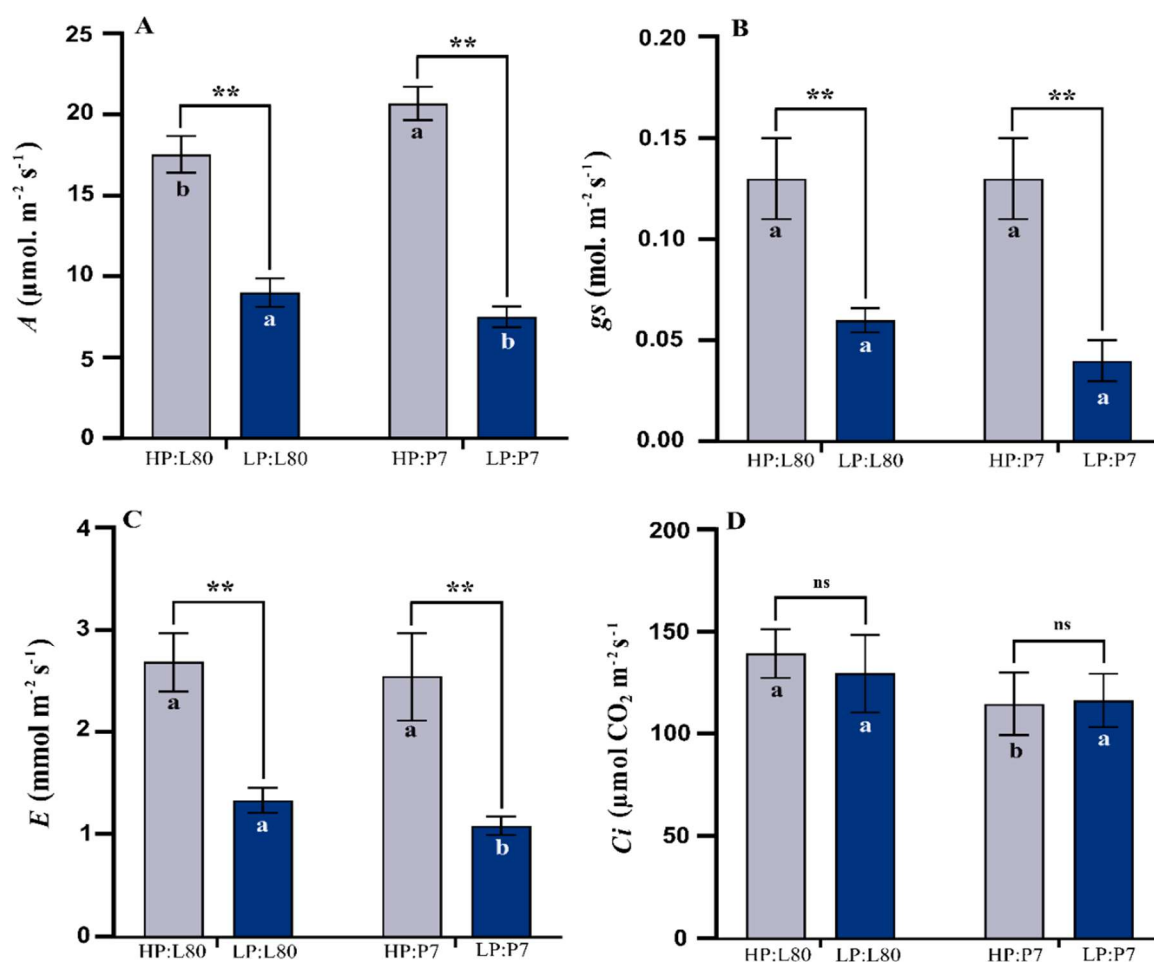


Figure 7. Photosynthetic traits in two popcorn inbred lines L80 and P7 under high (HP) and low (LP) phosphorus levels. **A**- net CO₂ assimilation rate (**A**); **g_s**- stomatal conductance (**B**); **E**- transpiration (**C**); **C_i**- internal CO₂ concentration (**D**). Values with asterisks are statistically different by *F*-test at 1% (**), at 5% (*), or not significant (ns), and means followed by the same letter were not significantly different by Tukey's test ($P < 0.05$). Asterisks indicate comparisons within the same genotype at different P levels, whereas letters indicate comparisons between two genotypes at the same P level. Values are expressed as mean \pm SD ($n = 6$).

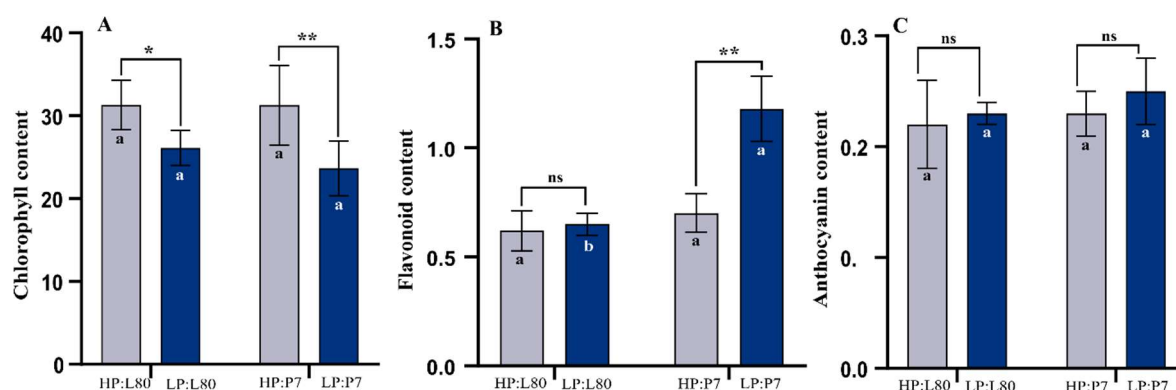


Figure 8. Chlorophyll (A) flavonoid (B) and anthocyanin content (C) in the leaves of the two popcorn inbred lines L80 and P7 under high (HP) and low (LP) phosphorus levels. Values with asterisks are statistically different by *F*-test at 1% (**), at 5% (*), or not significant (ns), and means followed by the same letter were not significantly different by Tukey's test ($P < 0.05$). Asterisks indicate comparisons within the same genotype at different P levels, whereas letters indicate comparisons between two genotypes at the same P level. Values are expressed as mean \pm SD ($n = 6$).

These results led to the hypothesis that mechanisms involved in photosynthesis and secondary metabolism might be involved in the difference in PUE between P7 and L80 and responsible for better P use efficiency. To address this hypothesis, comparative analyses of proteomics and metabolites were carried out to uncover the major intrinsic molecular mechanisms of each inbred line in response to P deficiency.

3.2.4.2 Proteome profile of popcorn leaves

A total of 2549 proteins were identified and quantified in popcorn leaves across the two inbred lines and the two P supplies: HP and LP (Figure 9). The heatmap showed that the protein profile grouped more similarly based on the treatment rather than the inbred line. In the comparison L80_LP/L80_HP, we detected 421 DEPs, with 166 down-regulated, and 255 up-regulated (Figure 10; Supplementary Table 3). For the P7_LP/P7_HP, 435 DEPs were identified, with 141 down-regulated, and 294 up-regulated (Figure 10; Supplementary Table 4).

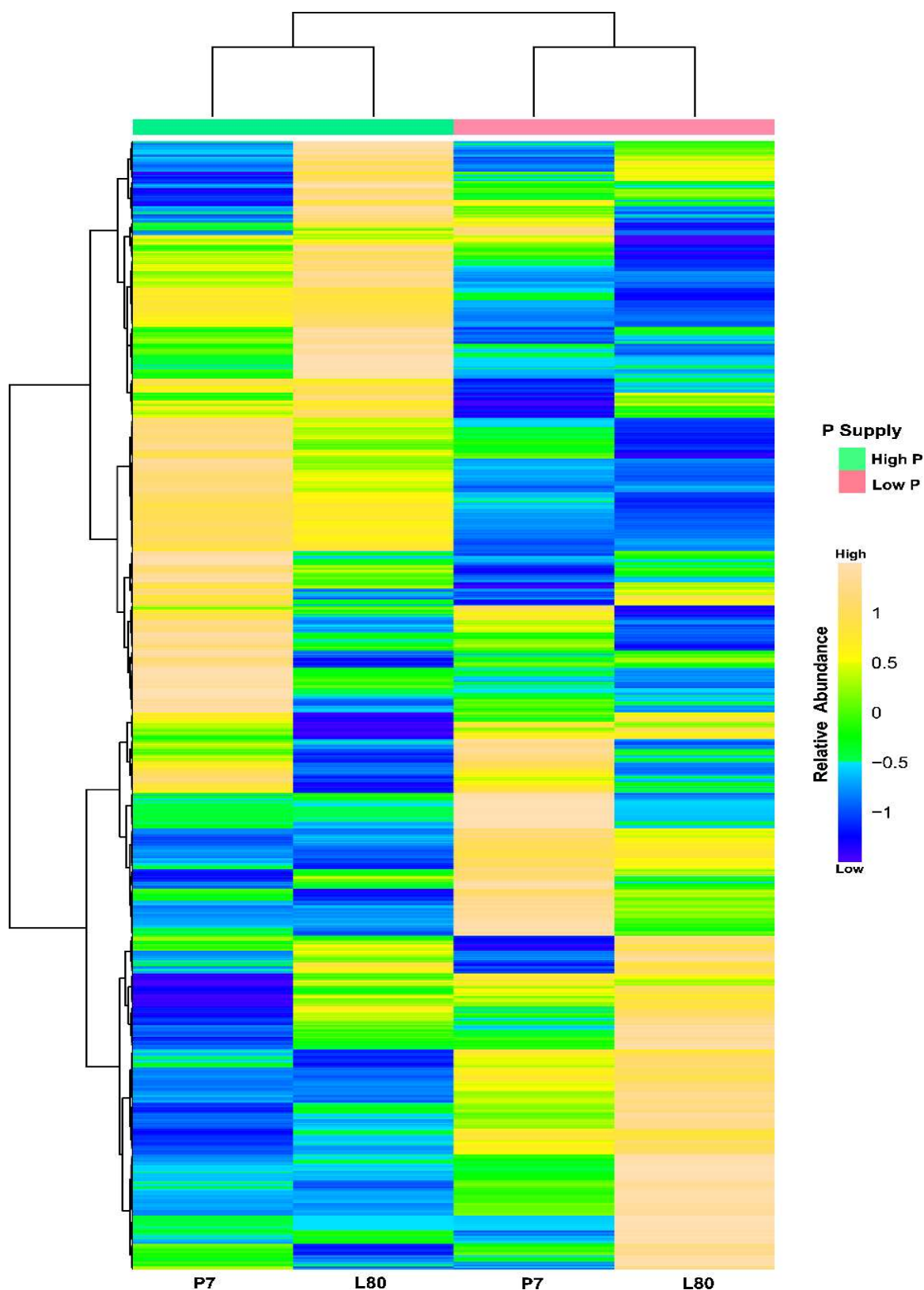


Figure 9. Heatmap of the 2549 proteins identified and quantified in L80 and P7 under high P and low P conditions. Yellow color represents higher protein abundance and blue color represents lower protein abundance. Green represents no protein change.

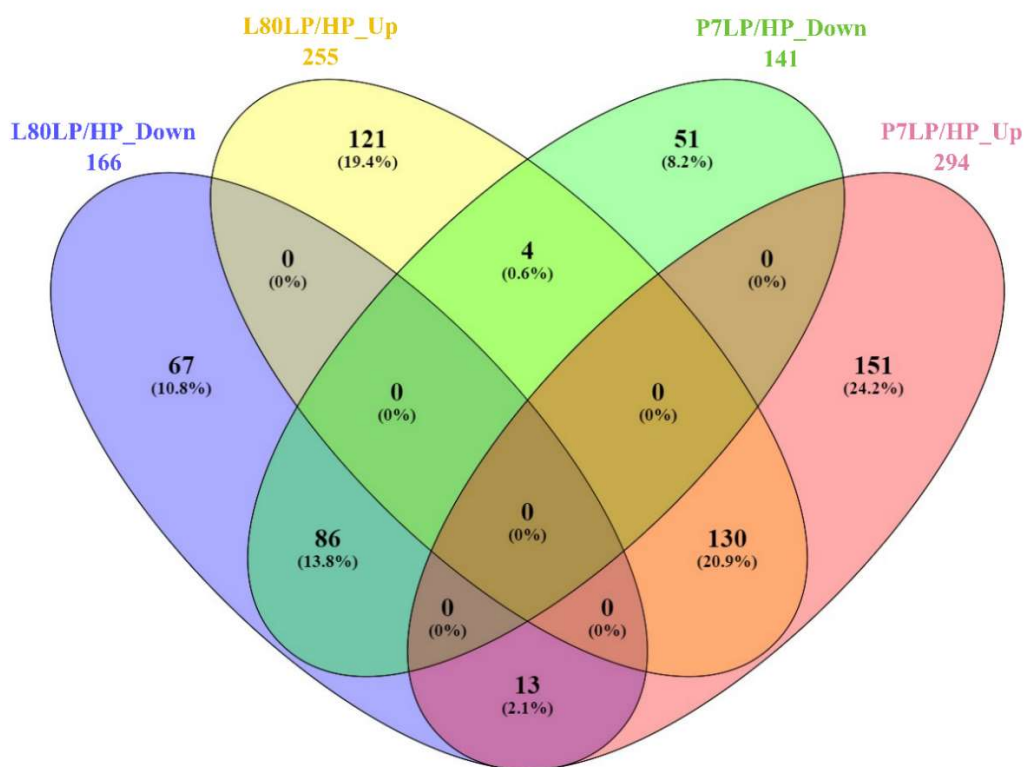


Figure 10. Venn diagram analysis of differentially expressed proteins (DEPs) in L80_LP/L80_HP and P7_LP/P7_HP, broken down as up- and down-regulated.

To detect potential candidate proteins that are responsive to PUE, the overlap of the DEPs (up- and down-regulated) identified under LP between L80 and P7 was displayed in a Venn Diagram (Figure 10). Only 51 down-regulated and 151 up-regulated proteins are unique in P7. While L80 presented only 121 and 67 exclusively up-regulated and down-regulated proteins, respectively (Figure 10).

3.2.4.3 Functional analysis of DEPs involved in the response to P deficiency

Based on the exclusive proteins identified in each line (Figure 10), a functional Gene Ontology (GO) enrichment analysis for these DEPs was performed (Figure 11; Supplemental Tables 5 to 8).

The main significant GO groups obtained with the down-regulated DEPs unique to L80 or P7 under LP are shown in Figure 11. The major functional classes down-regulated in L80 were photosynthesis (GO:0015979) and protein-chromophore linkage (GO:0018298) for biological processes; plastid (GO:0009536) and chloroplast (GO:0009507) for cellular component; and chlorophyll binding (GO:0016168) and rRNA binding (GO:0019843) for molecular function (Figure 11;

Supplementary Table 5). In P7 they were, response to cytokinin (GO:0009735) and photosynthesis (GO:0015979) for biological process, thylakoid membrane (GO:0042651) and photosynthetic membrane (GO:0034357) for cellular component; and electron carrier activity (GO:0009055) for molecular function (Figure 11; Supplementary Table 6).

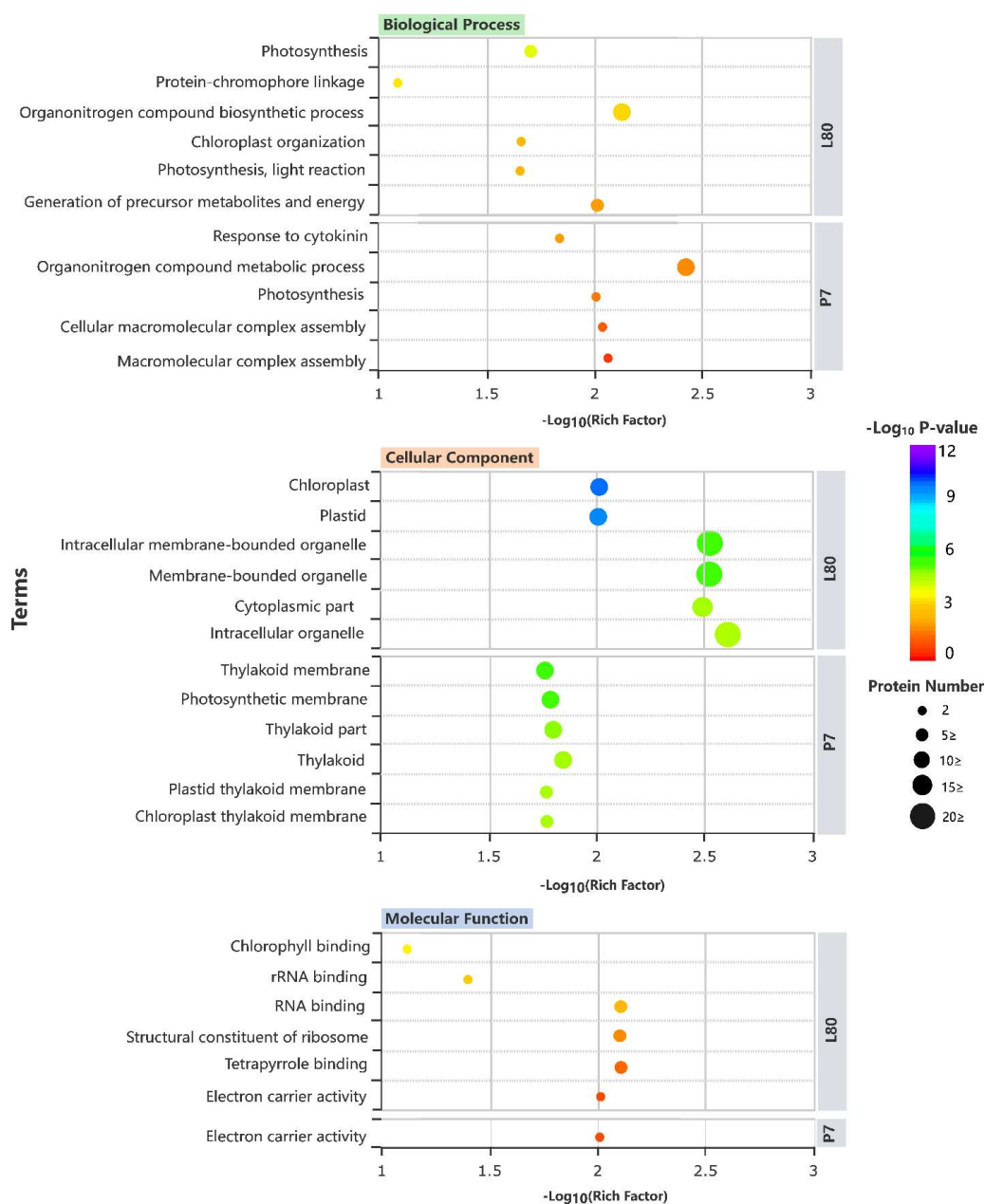


Figure 11. GO enrichment analysis of DEPs uniquely down-regulated in L80_LP or P7_LP. Rich factor measures the ratio of differentially expressed proteins annotated in a specific pathway term to the total number of annotated proteins. A higher enrichment factor indicates a higher level of intensity. The $-\log_{10}$ P value, ranging from 0 to 12, also reflects the intensity level, with higher values indicating greater intensity. Representation of the most significant DEPs in each group of enriched pathway terms with a $P < 0.05$.

The results of GO analysis obtained with up-regulation unique to L80 or P7 under LP are shown in Figure 12. The major functional classes in L80 were small molecule metabolic process (GO:0044281) and organonitrogen compound metabolic process (GO:1901564) for biological process; cytoplasm (GO:0005737) and cytoplasmic part (GO:0044444) for cellular component; and cofactor binding (GO:0048037) and pyridoxal phosphate binding (GO:0030170) for molecular function (Figure 12; Supplementary Table 7). For P7 they were small molecule metabolic process (GO:0044281) and cellular response to extracellular stimulus (GO:0031668) for biological process; cytoplasm (GO:0005737) and cytoplasmic part (GO:0044444) for cellular component and catalytic activity (GO:0003824); and glutathione binding (GO: 0043295) for molecular function (Figure 12; Supplementary Table 8).

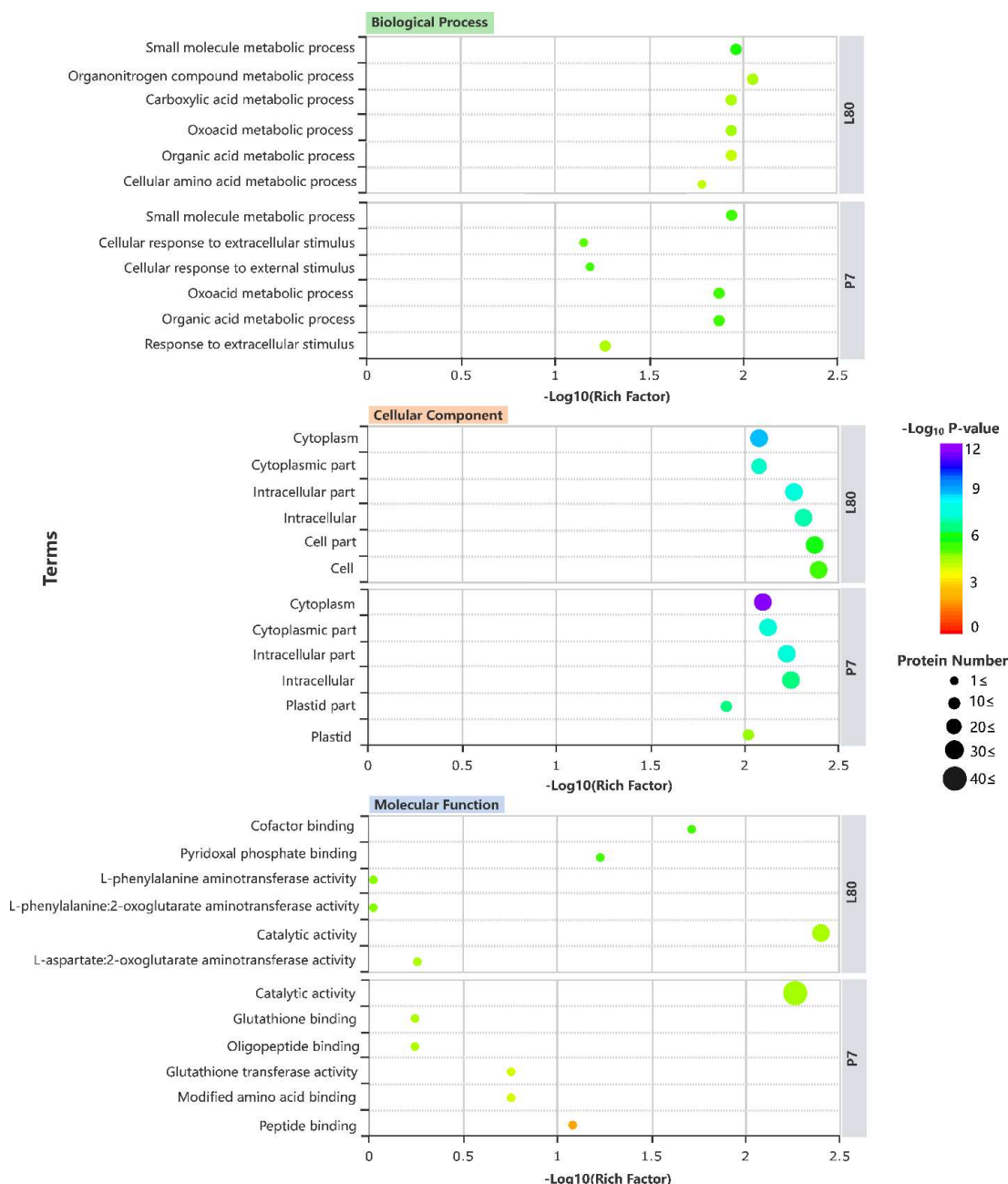


Figure 12. GO enrichment analysis of DEPs uniquely up-regulated in L80 or P7. Rich factor measures the ratio of differentially expressed proteins annotated in a specific pathway term to the total number of annotated proteins. A higher enrichment factor indicates a higher level of intensity. The $-\text{Log}_{10}$ P value, ranging from 0 to 12, also reflects the intensity level, with higher values indicating greater intensity. Representation of the most significant DEPs in each group of enriched pathway terms with a $P < 0.05$.

KEGG (Kyoto Encyclopedia of Genes and Genomes) pathway enrichment analysis was performed to investigate the major metabolic pathways in which the DEPs were involved. Only pathways with significant corrected P values ($p < 0.05$) were considered. A total of five pathways were identified with the down-regulated

DEPs in L80 (Supplementary Table 9), including "photosynthesis", "ribosome", and "photosynthesis - antenna proteins" (Figure 13), while in P7 "ribosome" was the unique significant pathway found (Figure 13; Supplementary Table 9).

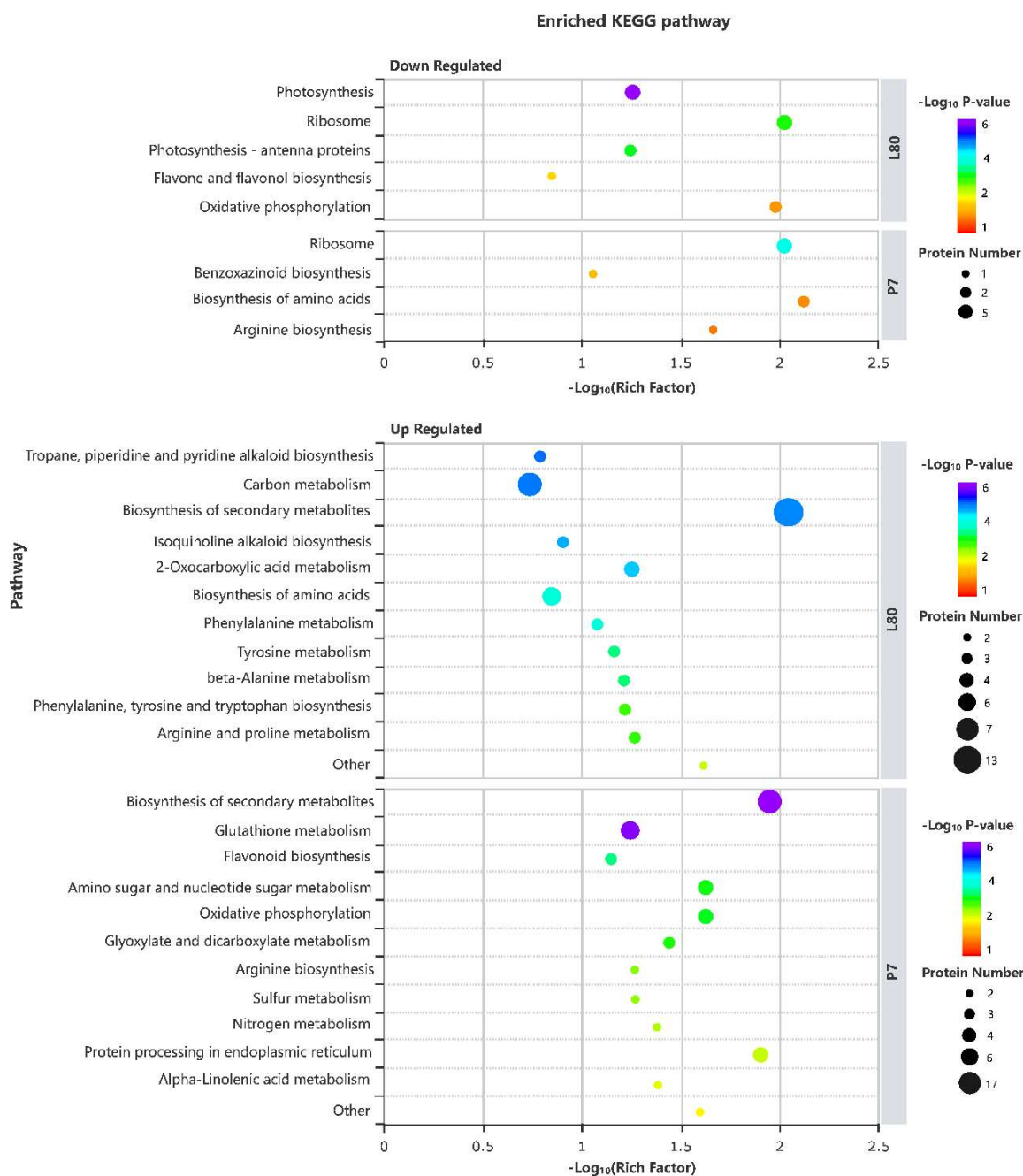


Figure 13. KEGG pathway enrichment analysis of the DEPs uniquely down- and up-regulated in L80 and P7. Rich factor measures the ratio of differentially expressed proteins annotated in a specific pathway term to the total number of annotated proteins. A higher enrichment factor indicates a higher level of intensity. The $-\text{Log}_{10}$ P value, ranging from 1 to 6, also reflects the intensity level, with higher values indicating greater intensity. Enriched pathway terms with $P < 0.05$ are shown.

A total of 28 significant pathways with up-regulated proteins were identified in the L80 (Supplementary Table 10). The most enriched pathways were "biosynthesis of secondary metabolites", "carbon metabolism", and "amino acid biosynthesis" (Figure 13). Most of the proteins enriched in the "secondary metabolite biosynthesis" pathway were also enriched in the "carbon metabolism" and "amino acid biosynthesis" pathways, suggesting that changes in these pathways are the main mechanisms of response to P deficiency in the L80 inbred line. In the P7, 16 enriched pathways were significant, consisting of "biosynthesis of secondary metabolites", "glutathione metabolism", and "flavonoid biosynthesis" being the most important pathways (Figure 13; Supplementary Table 10).

After performing KEGG enrichment analysis, these DEPs were categorized into four major different metabolic processes (Table 3).

Table 3. Selected differentially expressed proteins (DEPs) in leaves of popcorn lines treated with high and low P availability from the major enriched pathways identified by KEGG enrichment analysis.

| Process ^a | Protein ID# ^b | Protein name ^c | Folds changed (log2) | P-value | L80_LP / L80_HP | P7_LP / P7_HP |
|-----------------------------|--------------------------|---------------------------------------------------------|----------------------|----------|-----------------|---------------|
| Photosynthesis | | | | | | |
| | P1734 4 | ATP synthase subunit a, chloroplastic | -6.64 | 5.77E-17 | DOWN | - |
| | B4FRJ 4 | Photosystem II 11 kD protein | -6.64 | 5.77E-17 | DOWN | - |
| | B6SSN 3 | Chlorophyll a-b binding protein, chloroplastic | -1.89 | 7.35E-03 | DOWN | - |
| | P4818 7 | Photosystem II CP43 reaction center protein | -1.63 | 2.90E-02 | DOWN | - |
| | B4FXB 0 | Chlorophyll a-b binding protein, chloroplastic | -1.61 | 3.13E-02 | DOWN | - |
| | B4F9R 9 | Oxygen-evolving enhancer protein | -1.53 | 4.30E-02 | DOWN | - |
| | P6938 8 | Cytochrome b559 subunit alpha | -1.46 | 4.38E-02 | DOWN | - |
| | P2570 6 | NAD(P)H-quinone oxidoreductase subunit 1, chloroplastic | -2.01 | 4.73E-02 | DOWN | - |
| Protein biosynthesis | | | | | | |
| | P1233 9 | 30S ribosomal protein S7, chloroplastic | -6.64 | 5.77E-17 | DOWN | - |
| | P1778 8 | 50S ribosomal protein L2, chloroplastic | -6.64 | 5.77E-17 | DOWN | - |
| | P1770 3 | 30S ribosomal protein S15, chloroplastic | -2.06 | 1.49E-02 | DOWN | - |

Table 3. Cont.

| Process ^a | Protein ID# ^b | Protein name ^c | Folds changed (log2) | P-value | L80_LP / L80_HP | P7_LP / P7_HP |
|--------------------------|--------------------------|---------------------------------------------------------|----------------------|----------|-----------------|---------------|
| | B6TH42 | 60S ribosomal protein L9 | -2.06 | 1.49E-02 | DOWN | - |
| | P08530 | 30S ribosomal protein S8, chloroplastic | -1.86 | 4.29E-02 | DOWN | - |
| | B4FWR7 | 60S ribosomal protein L13 | -6.64 | 5.29E-17 | - | DOWN |
| | B6UE26 | 60S ribosomal protein L34 | -6.64 | 5.29E-17 | - | DOWN |
| | P25461 | 50S ribosomal protein L33 | -3.15 | 2.58E-04 | - | DOWN |
| | P08527 | 30S ribosomal protein S14, chloroplastic | -2.42 | 5.53E-03 | - | DOWN |
| | B4FUZ5 | 30S ribosomal protein S1 | -1.22 | 3.97E-02 | - | DOWN |
| Energy metabolism | | | | | | |
| | B4FTF9 | Isocitrate lyase | 6.64 | 5.77E-17 | UP | - |
| | B4F9G1 | Aspartate aminotransferase | 4.34 | 2.96E-05 | UP | - |
| | B4FUH2 | Aspartate aminotransferase | 3.2 | 6.90E-04 | UP | - |
| | B6SRL2 | Aconitate hydratase | 2.94 | 2.12E-02 | UP | - |
| | B4F8X3 | Acyl-coenzyme A oxidase | 2.81 | 2.42E-02 | UP | - |
| | A0A1D6 PUK8 | Aconitate hydratase | 2.17 | 2.69E-02 | UP | - |
| | C0P429 | UTP-glucose-1-phosphate uridylyltransferase | 6.64 | 5.29E-17 | - | UP |
| | A0A1D6 M1Y6 | UDP-glucuronate decarboxylase | 6.64 | 5.29E-17 | - | UP |
| | P46620 | NAD(P)H-quinone oxidoreductase subunit 5, chloroplastic | 6.64 | 5.29E-17 | - | UP |
| | B4FCR7 | Inorganic diphosphatases | 6.64 | 5.29E-17 | - | UP |
| | B4FWT5 | Inorganic diphosphatases | 2.62 | 9.12E-03 | - | UP |
| | C0PAU7 | Glucose-6-phosphate isomerase | 1.69 | 1.69E-02 | - | UP |
| | C4JAC1 | Mannose-1-phosphate guanylyltransferase | 3.24 | 2.54E-02 | - | UP |
| Defense response | | | | | | |
| | K7U2E4 | Amine oxidase | 3.62 | 2.61E-03 | UP | - |
| | C0PIW1 | Glucose-6-phosphate 1-dehydrogenase | 3.17 | 1.86E-02 | UP | - |
| | K7VCN5 | Peroxidase | 3.13 | 2.31E-02 | UP | - |
| | Q9FQB5 | Glutathione transferase | 6.64 | 5.29E-17 | - | UP |
| | C4J9Q3 | Glutathione transferase | 6.64 | 5.29E-17 | - | UP |
| | Q9ZP60 | Glutathione transferase | 6.64 | 5.29E-17 | - | UP |
| | B8A3K0 | Glutathione transferase | 6.64 | 5.29E-17 | - | UP |
| | P46420 | Glutathione transferase | 1.8 | 9.06E-03 | - | UP |

Table 3. Cont.

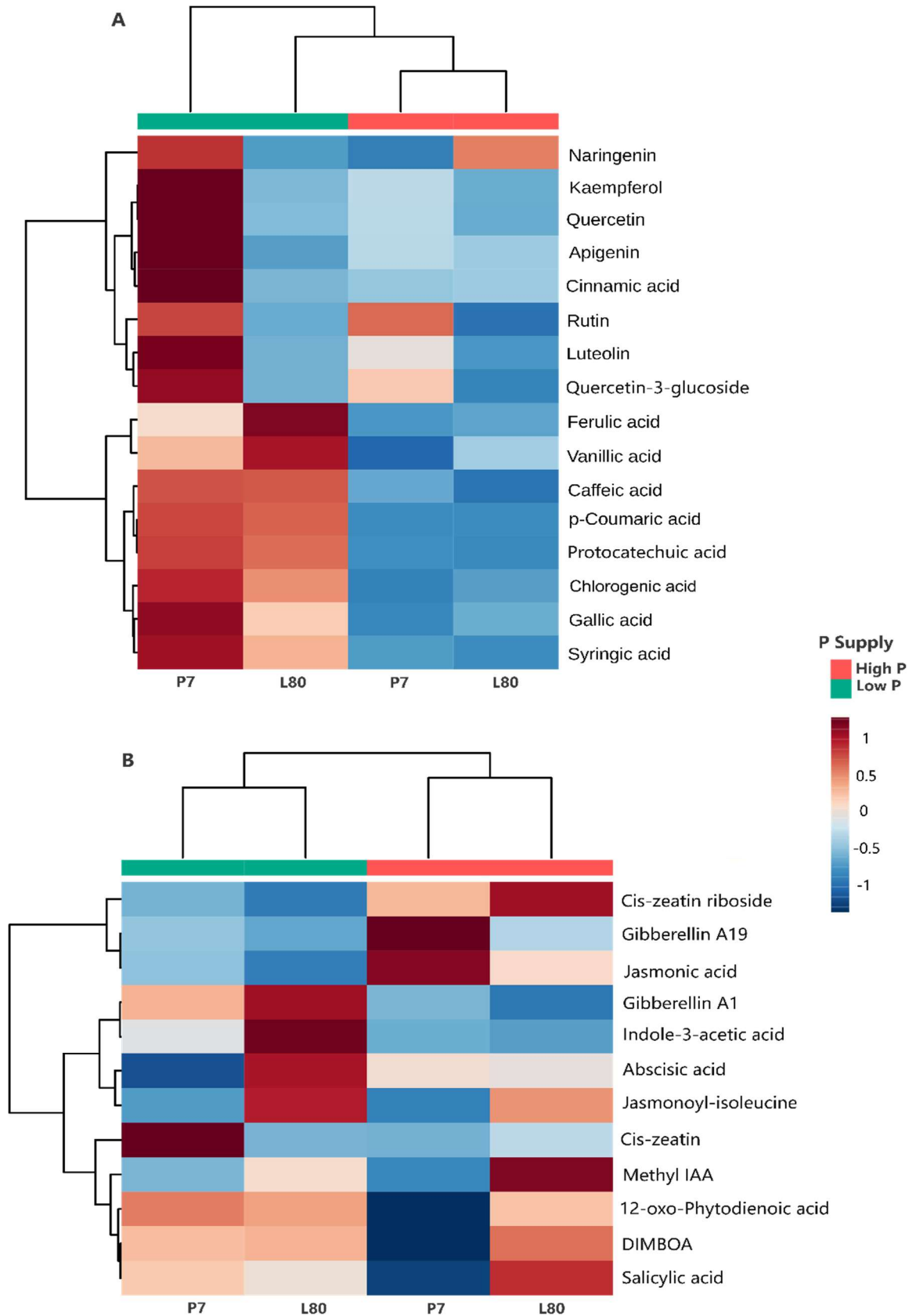
| Process ^a | Protein ID# ^b | Protein name ^c | Folds changed (log2) | P-value | L80_LP / L80_HP | P7_LP / P7_HP |
|----------------------|--------------------------|---------------------------------------------------|----------------------|----------|-----------------|---------------|
| | B6SYB7 | Arogenate dehydratase | 3.41 | 1.87E-02 | - | UP |
| | B4G1R6 | Chalcone-flavonone isomerase family protein | 2.03 | 3.56E-02 | - | UP |
| | A0A1D6 N1Z8 | 6-phosphogluconate dehydrogenase, decarboxylating | 1.54 | 3.79E-02 | - | UP |
| | B4F9P0 | Glycosyltransferase | 2.61 | 2.20E-02 | - | UP |
| | B4FRQ8 | Spermidine hydroxycinnamoyl transferase | 4.07 | 8.98E-05 | - | UP |
| | Q49HD7 | 12-oxo-phytodienoic acid reductase | 2.29 | 8.85E-03 | - | UP |

^a Main metabolic process enriched via KEGG; ^b Accession ID in the UniProt database and ^c Protein name identified by LC-MS-MS

3.2.4.4 Metabolite analysis

Targeted metabolomic analysis of phytohormone and polyphenols was performed in both inbred lines to investigate which flavonoids accumulate in P7 and to identify potential hormones involved in P stress and signaling. This analysis included a panel of 29 different phytohormones with well-known stress response hormones, such as abscisic acid (ABA) and salicylic acid (SA); and a panel of 28 polyphenols including flavonoids and phenolic acids.

P deficiency increased the concentration of flavonoids and phenolic acids in both inbred lines as shown by the heatmap (Figure 14A). However, differences in the pattern of accumulation of these polyphenols was observed between the two inbred lines. The flavone apigenin and flavonone naringenin had a higher accumulation in P7 under LP, while concentrations of flavone luteolin, and flavonoid glycosides quercetin-3-glycoside and rutin, are much higher in P7 compared to L80. Chlorogenic acid is the phenolic acid with the highest accumulation in P7 under LP.



P deficiency also led to changes in the concentration of phytohormones in both inbred lines (Figure 14B). It is worth noting from the heatmap that several hormones, SA, 12-oxo-phytodienoic acid (OPDA) and 2,4-dihydroxy-7-methoxy-1,4-benzoxazin-3-one (DIMBOA) are found in low concentrations in P7 under control conditions compared to L80. Their levels show the highest increase under low P in P7 to a similar level found in L80. The phytohormone IAA was higher accumulated in L80 under low P, while the accumulation pattern of GA19 and JA was reduced by P deficiency in both inbred lines (Figure 14B).

3.2.5 DISCUSSION

3.2.5.1 Effects of P deficiency and adaptation mechanisms

The lower PUE in L80, at low P, indicates that it is less capable of utilizing P from the substrate for biomass production than P7. The results indicate that P deficiency significantly affected the overall growth and health of the plants, reduced chlorophyll content, and consequently, reduced photosynthetic efficiency. The proteomics results complemented by the phytohormones and phenolic compounds analysis allowed for the mechanisms underlying the PUE difference in L80 and P7 to be characterized.

3.2.5.2 P deficiency impacts the photosynthesis, electron transfer chain and energy metabolism in L80

The P deficiency treatment negatively impacted carbon fixation and plant growth in both lines. The proteomics results revealed that several proteins involved in photochemical apparatus of photosynthesis were significantly altered by P deficiency. Photosystem II CP43 reaction center protein (P48187), cytochrome b559 subunit alpha (P69388), photosystem II 11 kD protein (B4FRJ4), oxygen-evolving enhancer protein (B4F9R9), and two chlorophyll a-b binding proteins chloroplastic (B4FXB0; B6SSN3), all associated with the photosystem II (PSII)

reaction center, were down-regulated under low P in L80, but not in P7 (Table 3; Supplementary Table 3).

The antenna proteins CP43 and CP47 are a key part of the energy conversion process and are responsible for transferring the excitation energy to the reaction center proteins D1 and D2 in PSII (Caffarri et al., 2014; Müh and Zouni 2020). The alpha subunit of cytochrome b559, in conjunction with the beta subunit, forms a crucial heme-binding heterodimer in the core of PSII. These subunits play a fundamental role in the assembly of PSII and probably participate in secondary electron transport mechanisms that protect PSII from light-induced damage (Burda et al., 2003; Chiu and Chu 2022). The oxygen-evolving complex (OEC) oxidizes water to provide protons for use by PSI (Chen et al., 2022). In addition, chlorophyll *a* plays a crucial role in the light-dependent reactions of photosynthesis (Govindjee, 2004), and chlorophyll *b* complements the action of chlorophyll *a* (Simkin et al., 2022). Therefore, negative regulation of the proteins that integrate these complexes can affect the function of both photosystems and compromise photosynthesis and plant growth.

Similarly, it was also found that NAD(P)H-quinone oxidoreductase subunit 1, chloroplastic (P25706) and ATP synthase subunit a, chloroplastic (P17344) (Table 3) were down-regulated only in the L80 under P starvation. Both enzymes are important for the electron transport chain and energy generation across membranes (Neupane et al., 2019; Yang et al., 2020). These enzymes are essential for plant growth and development, as it has been previously reported that P-deficiency decreases ATP synthase activity in maize (Zhang et al., 2014) and barley (Carstensen et al., 2018), with significant effects on photosynthesis.

These results indicate that P deficiency has significant effects on the regulation of key proteins involved in the processes of light capture, electron transfer, and energy conversion in photosynthesis in the P-inefficient inbred line. These perturbations, combined with reduced chlorophyll levels detected under low P, would explain the detrimental effect on photosynthesis and the growth of L80.

The carbon metabolism pathway was also one of the major enriched pathways in L80. Some of the proteins up-regulated comprise fatty acid β -oxidation, glyoxylate cycle and tricarboxylic acid (TCA) cycle, such as acyl-coenzyme A oxidase (B4F8X3), isocitrate lyase (ICL, B4FTF9), two aconitate hydratases (A0A1D6PUK8; B6SRL2) and two aspartate aminotransferases (ATT, B4F9G1; B4FUH2) (Table 3; Supplementary Table 10). Acyl-CoA (ACX) is the first enzyme involved in the β -oxidation of fatty acids in peroxisomes in plants (Graham and Eastmond, 2002). Its purpose is to degrade fatty acids to acetyl-CoA, the substrate

of the glyoxylate cycle, an alternative pathway of the TCA cycle (Eastmond and Graham, 2001; Kwon et al., 2021). ICL is involved in the decarboxylation steps of the TCA cycle to produce succinate. The increase of ICL has been previously observed in other plants in response to alkaline stress in tolerant grape hybrids (Guo et al., 2018) and in Chinese fir roots under P deficiency (Chen et al., 2021). The up-regulation of Acyl CoA and ICL in popcorn leaves suggests a conversion of stored lipids into carbohydrates to produce energy-rich molecules in L80 to cope with P deficiency. Additionally, ATT protein increase may be the result of plant adaptation to P deficiency as observed previously in other different environmental conditions (Han et al., 2021) to improve the energy generation by TCA cycle and amino acid metabolism. However, photosynthesis and plant growth is also impacted in P7 under low P, as also highlighted by the GO annotation (Figure 11). Interestingly, the abundance of the proteins involved in photosynthesis and energy metabolism affected in L80 by P deficiency are not in P7. This may mean that these proteins are more than just a consequence of stress and are indicators of P inefficiency of L80.

3.2.5.3 P starvation affects ribosomal protein biosynthesis

In the L80, P deficiency affected the abundance of chloroplast ribosomes and their structural integrity. The proteins 30S ribosomal protein S7, chloroplastic (P12339), 30S ribosomal protein S8, chloroplastic (P08530), 50S ribosomal protein L2, chloroplastic (P17788), 30S ribosomal protein S15, chloroplastic (P17703) and 60S ribosomal protein L9 (B6TH42), were down-regulated (Table 3; Supplementary Table 3). While in P7, the negatively regulated ribosomal proteins were mostly non-chloroplastic, namely 60S ribosomal protein L13 (B4FWR7), 30S ribosomal protein S1 (B4FUZ5), 50S ribosomal protein L33 (P25461), 60S ribosomal protein L34 (B6UE26) (Table 3; Supplementary Table 4).

The down-regulation of proteins involved in chloroplast ribosome assembly in the L80 suggests a decrease in the production of ribosomes, which are essential for protein synthesis, which may affect the ability of chloroplasts to synthesize proteins involved in various cellular processes, including those for photosynthesis (Daniell et al., 2016; Zoschke and Bock, 2018). This result corroborates the decrease in proteins involved in photosynthesis in L80 (Figure 13, Table 3). By reducing ribosome production and photosynthetic proteins, plants can minimize energy expenditure for protein synthesis and reallocate resources to other essential functions to cope with P limitation (Raven, 2013).

On the other hand, the decrease in ribosomal proteins in P7 suggests a reduction in ribosome abundance or efficiency, which may affect protein synthesis and cellular processes. However, this response may be beneficial for adaptation to environmental cues as long as the overall efficiency of translation is not compromised (Fakih et al., 2023). In contrast to L80, the reduction in ribosomal proteins in P7 suggests that the P-efficient inbred line has prioritized the synthesis of photosynthetic proteins that are more critical under low phosphorus conditions.

3.2.5.4 Protective mechanisms involved in the oxidative stress response

Distinct mechanisms of redox regulation and oxidative stress have been identified in the two inbred lines. In L80 only a few redox related proteins were up-regulated (Table 3; Supplementary Table 3). A peroxidase (K7VCN5), already well-known to participate to antioxidant defense in response to abiotic stresses (Kidwai et al., 2020; Su et al., 2020; Li et al., 2021), a glucose-6-phosphate 1-dehydrogenase (C0PIW1), first key enzyme in the oxidative pentose phosphate pathway (OPPP) producing NADPH (Corpas and Barroso 2014; Jiang et al., 2022) to maintain the oxidative-reductive balance (Yang et al., 2014; Zhao et al., 2020), and amine oxidase (AO, K7U2E4). AO is associated with oxidation of polyamine (PA) into reactive oxygen species (ROS) responsible for oxidative stress. Indeed, PA plays an essential role in growth and developmental processes (Gholizadeh and Mirzaghaderi, 2020), and acts as antioxidants to avoid oxidative stress (Napieraj et al., 2023).

In P7, five glutathione transferase (GSTs, Q9FQB5, C4J9Q3, Q9ZP60, P46420, B8A3K0), involved in the detoxification of ROS were identified (Table 3; Supplementary Table 4). GSTs have a crucial role in glutathione metabolism by catalyzing the conjugation of reduced glutathione (GSH) protecting cells from ROS accumulation and oxidative burst (Kumar and Trivedi, 2018). The up-regulation of GSTs in P7 indicates an adaptive response of this inbred line to the oxidative stress induced by P deficiency (Table 3). The increase of GSTs was observed in various species under low P conditions, such as maize (Zhang et al., 2014), wheat (Zheng et al., 2023), and barley (Nadira et al., 2016), supporting the induction of oxidative stress and response.

In addition to the GSTs direct ROS detoxification, the increase in flavonoids content observed in P7 (Figure 8) supported by the up-regulation of proteins involved in flavonoid biosynthesis (arogenate dehydratase (ADT, B6SYB7), chalcone-flavonone isomerase family protein (CHI, B4G1R6), and

glycosyltransferase (UGT, B4F9P0); Table 3) may also act as protecting mechanism against abiotic stress, including P deficiency as previously highlighted (Trejo-Téllez et al., 2019; Liu et al., 2020b). Amongst the phenolic compounds found with the highest concentrations in P7 under low P were chlorogenic acid, and the flavonoid glycosides quercetin-3-glucoside and rutin (Figure 14A). Chlorogenic acid and rutin are well characterized phenolic compounds for their antioxidant properties, and their role in defense response to abiotic stresses (Singh et al., 2017; Merewitz and Liu, 2019; Soviguidi et al, 2022). Therefore, the results suggest that the accumulation of specific flavonoids is a significant aspect of P7's response to this deficiency, enhancing its adaptive capacity and potentially mitigating the negative effects on plant growth and overall fitness. The deficiency of L80 to regulate the GSTs and enzymes involved in flavonoids biosynthesis is involved in the deficiency to cope with low P compared to P7.

3.2.6 CONCLUSIONS

Our results indicate that P7 has a more efficient response to P deficiency, with overall better performance in terms of physiological traits, which can be explained by specific proteome regulation, and metabolic adaptations compared to L80. The P-efficient inbred line with a high adjustment of photosynthetic apparatus and protein biosynthesis may influence biomass accumulation and P content in leaves, providing a higher performance of this inbred line under P starvation conditions. In addition, both enzymatic and non-enzymatic mechanisms of ROS scavenging are involved during P7 growth under this nutrient adverse condition. Flavonoids accumulation seems to play an important role in the adaptation mechanisms of P7 to P deficiency. Our results open new avenues into the understanding of molecular mechanisms of the tolerance of P deficiency that may be useful to breeding programs to develop resilient cultivars ensuring sustainable agricultural expansion and food supply.

REFERENCES

- Abbas, M., Shah, J. A., Irfan, M., Memon, M. Y. (2018) Remobilization and utilization of phosphorus in wheat cultivars under induced phosphorus deficiency. *Journal of Plant Nutrition*, v. 41, n. 12, p. 1522-1533.
- Alewell, C., Ringeval, B., Ballabio, C., Robinson, D. A., Panagos, P., Borrelli, P. (2020) Global phosphorus shortage will be aggravated by soil erosion. *Nature communications*, v. 11, n. 1, p. 4546.
- Almeida, V. C., Viana, J. M. S., Risso, L. A., Ribeiro, C., DeLima, R. O. (2018) Generation mean analysis for nitrogen and phosphorus uptake, utilization, and translocation indexes at vegetative stage in tropical popcorn. *Euphytica*, v. 214, p. 1-12.
- Aluko, O. O., Li, C., Wang, Q., Liu, H. (2021) Sucrose utilization for improved crop yields: A review article. *International Journal of Molecular Sciences*, v. 22, n. 9, p. 4704.
- Alvarez, S., Hicks, L. M., Pandey, S. (2011) ABA-dependent and-independent G-protein signaling in Arabidopsis roots revealed through an iTRAQ proteomics approach. *Journal of proteome research*, v. 10, n. 7, p. 3107-3122.
- Bechtaoui, N., Rabiou, M. K., Raklami, A., Oufdou, K., Hafidi, M., Jemo, M. (2021) Phosphate-dependent regulation of growth and stresses management in plants. *Frontiers in Plant Science*, v. 12, p. 679916.
- Bhatta, B. B., Panda, R. K., Anandan, A., Pradhan, N. S. N., Mahender, A., Rout, K. K., Patra, B. C., Ali, J. (2021) Improvement of phosphorus use efficiency in rice by adopting image-based phenotyping and tolerant indices. *Frontiers in plant science*, v. 12, p. 717107.

- Burda, K., Kruk, J., Borgstädt, R., Stanek, J., Strzałka, K., Schmid, G. H., Kruse, O. (2003) Mössbauer studies of the non-heme iron and cytochrome b559 in a *Chlamydomonas reinhardtii* PSI- mutant and their interactions with α -tocopherol quinone. *FEBS letters*, v. 535, n. 1-3, p. 159-165.
- Caffarri, S., Tibiletti, T., C Jennings, R., Santabarbara, S. (2014) A comparison between plant photosystem I and photosystem II architecture and functioning. *Current Protein and Peptide Science*, v. 15, n. 4, p. 296-331.
- Carstensen, A., Herdean, A., Schmidt, S. B., Sharma, A., Spetea, C., Pribil, M., Husted, S. (2018) The impacts of phosphorus deficiency on the photosynthetic electron transport chain. *Plant physiology*, v. 177, n. 1, p. 271-284.
- Carstensen, A., Szameitat, A. E., Frydenvang, J., Husted, S. (2019) Chlorophyll a fluorescence analysis can detect phosphorus deficiency under field conditions and is an effective tool to prevent grain yield reductions in spring barley (*Hordeum vulgare* L.). *Plant and Soil*, v. 434, p. 79-91.
- Chea, L., Meijide, A., Meinen, C., Pawelzik, E., Naumann, M. (2021) Cultivar-dependent responses in plant growth, leaf physiology, phosphorus use efficiency, and tuber quality of potatoes under limited phosphorus availability conditions. *Frontiers in Plant Science*, v. 12, p. 723862.
- Chen, G., Han, H., Yang, X., Du, R., Wang, X. (2022) Salt Tolerance of Rice Is Enhanced by the SS3 Gene, Which Regulates Ascorbic Acid Synthesis and ROS Scavenging. *International Journal of Molecular Sciences*, v. 23, n. 18, p. 10338.
- Chen, J., Xu, L., Cai, Y., Xu, J. (2008) QTL mapping of phosphorus efficiency and relative biologic characteristics in maize (*Zea mays* L.) at two sites. *Plant and Soil*, v. 313, n. 1-2, p. 251-266.
- Chen, W., Zhou, M., Zhao, M., Chen, R., Tigabu, M., Wu, P., Ma, X. (2021) Transcriptome analysis provides insights into the root response of Chinese fir to phosphorus deficiency. *BMC Plant Biology*, v. 21, p. 1-17.
- Chiu, Y. F., Chu, H. A. (2022) New Structural and Mechanistic Insights Into Functional Roles of Cytochrome b559 in Photosystem II. *Frontiers in Plant Science*, v. 13, p. 914922.
- Chu, S., Li, H., Zhang, X., Yu, K., Chao, M., Han, S., Zhang, D. (2018) Physiological and proteomics analyses reveal low-phosphorus stress affected the regulation of photosynthesis in soybean. *International Journal of Molecular Sciences*, v. 19, n. 6, p. 1688.

- Cordell, D., White, S. (2011) Peak phosphorus: clarifying the key issues of a vigorous debate about long-term phosphorus security. *Sustainability*, v. 3, n. 10, p. 2027-2049.
- Cordell, D., White, S. (2014) Life's bottleneck: sustaining the world's phosphorus for a food secure future. *Annual Review of Environment and Resources*, v. 39, p. 161-188.
- Corpas, F. J., Barroso, J. B. (2014) NADPH-generating dehydrogenases: their role in the mechanism of protection against nitro-oxidative stress induced by adverse environmental conditions. *Frontiers in Environmental Science*, v. 2, p. 55.
- Cruz, C. D. (2013) Genes: a software package for analysis in experimental statistics and quantitative genetics. *Acta Scientiarum. Agronomy*, v. 35, p. 271-276.
- Cruz, C. D., Carneiro, P. C. S., Regazzi, A. J. (2014) Modelos biométricos aplicados ao melhoramento genético. *Viçosa: Ed. da UFV*, 2.
- Curatti, L., and Rubio, L. M. (2014) Challenges to develop nitrogen-fixing cereals by direct nif-gene transfer. *Plant Science*, v. 225, p. 130-137.
- Da Silva Santos, L.; da Silva, L. S.; Griebeler, G. (2014) Ascorbic acid as a reducing agent for phosphorus analysis by colorimetry/Acido ascorbico como agente redutor para determinação de fósforo por colorimetria. *Ciencia Rural*, v. 44, n. 6, p. 1015-1019
- Daniell, H., Lin, C. S., Yu, M., Chang, W. J. (2016) Chloroplast genomes: diversity, evolution, and applications in genetic engineering. *Genome biology*, v. 17, p. 1-29.
- Delgado, A., Quemada, M., Villalobos, F. J., Mateos, L. (2016) Fertilization with phosphorus, potassium and other nutrients. *Principles of agronomy for sustainable agriculture*, p. 381-405.
- Dusenge, M. E., Duarte, A. G., Way, D. A. (2019) Plant carbon metabolism and climate change: elevated CO₂ and temperature impacts on photosynthesis, photorespiration and respiration. *New Phytologist*, v. 221, n. 1, p. 32-49.
- Eastmond, P. J., Graham, I. A. (2001) Re-examining the role of the glyoxylate cycle in oilseeds. *Trends in plant science*, v. 6, n. 2, p. 72-78.
- Eastmond, P. J., Graham, I. A. (2002) Pathways of straight and branched chain fatty acid catabolism in higher plants. *Progress in lipid research*, v. 41, n. 2, p. 156-181.
- Fakih, Z., Plourde, M. B., Germain, H. (2023) Differential Participation of Plant Ribosomal Proteins from the Small Ribosomal Subunit in Protein Translation under Stress. *Biomolecules*, v. 13, n. 7, p. 1160.

- Fontecilla-Camps, J. C. (2021) Primordial bioenergy sources: The two facets of adenosine triphosphate. *Journal of Inorganic Biochemistry*, v. 216, p. 111347.
- Fritsche-Neto, R., Miranda, G. V., DeLima, R. O., Souza, L. V. D., Silva, J. D. (2010) Inheritance of traits associated with phosphorus utilization efficiency in maize. *Pesquisa Agropecuária Brasileira*, v. 45, p. 465-471, 2010.
- Galindo-Castañeda, T., Brown, K. M., Lynch, J. P. (2018) Reduced root cortical burden improves growth and grain yield under low phosphorus availability in maize. *Plant, Cell & Environment*, v. 41, n. 7, p. 1579-1592.
- Gerhardt, I. F. S., Amaral Júnior, A. T., Guimarães, L. J. M., Schwantes, I. A., Santos, A., Kamphorst, S. H., Myers, G. O. (2017) Intraspecific variability of popcorn S7 lines for phosphorus efficiency in the soil. *Genetics and Molecular Research*, v. 16, n. 3.
- Gerhardt, I. F., Teixeira Do Amaral Junior, A., Ferreira Pena, G., Moreira Guimarães, L. J., De Lima, V. J., Vivas, M., Kamphorst, S. H. (2019) Genetic effects on the efficiency and responsiveness to phosphorus use in popcorn as estimated by diallel analysis. *PLoS one*, v. 14, n. 5, p. e0216980.
- Gholizadeh, F., Mirzaghaderi, G. (2020) Genome-wide analysis of the polyamine oxidase gene family in wheat (*Triticum aestivum* L.) reveals involvement in temperature stress response. *PLoS One*, v. 15, n. 8, p. e0236226.
- Govindjee, G. C. (2004) Chlorophyll a fluorescence: a bit of basics and history. In: Chlorophyll a fluorescence: a signature of photosynthesis. Dordrecht: *Springer Netherlands*, 2004. p. 1-41.
- Grieger, K., Merck, A., Deviney, A., Marshall, A. (2023) What are stakeholder views and needs for achieving phosphorus sustainability?. *Environment Systems and Decisions*, p.1-12.
- Griffing, B. (1956) Concept of general and specific combining ability in relation to diallel crossing systems. *Australian journal of biological sciences*, v. 9, n. 4, p. 463-493.
- Gu, R., Chen, F., Long, L., Cai, H., Liu, Z., Yang, J., Yuan, L. (2016) Enhancing phosphorus uptake efficiency through QTL-based selection for root system architecture in maize. *Journal of Genetics and Genomics*, v. 43, n. 11, p. 663-672.
- Guo, S. H., Niu, Y. J., Zhai, H., Han, N., Du, Y. P. (2018) Effects of alkaline stress on organic acid metabolism in roots of grape hybrid rootstocks. *Scientia Horticulturae*, v. 227, p. 255-260.

- Hallauer, A. R., Carena, M. J., Miranda Filho, J. D. (2010) Quantitative genetics in maize breeding. *Springer Science & Business Media*, v. 6, 577-653.
- Han, M., Xu, X., Li, X., Xu, M., Hu, M., Xiong, Y., Su, T. (2022) Spartate Metabolic Pathways in Populus: Linking the Root Responsive Isoenzymes with Amino Acid Biosynthesis during Incompatible Interactions of *Fusarium solani*. *International Journal of Molecular Sciences*, v. 23, n. 12, p. 6368.
- Heuer, S., Gaxiola, R., Schilling, R., Herrera-Estrella, L., López-Arredondo, D., Wissuwa, M., Rouached, H. (2017) Improving phosphorus use efficiency: a complex trait with emerging opportunities. *The Plant Journal*, v. 90, n. 5, p. 868-885.
- Hoagland, D. R., Arnon, D. I. (1950) The water-culture method for growing plants without soil. *Circular. California agricultural experiment station*, v. 347, n. 2nd edit.
- Hussain, M. A., Li, S., Gao, H., Feng, C., Sun, P., Sui, X., Li, H. (2023) Comparative analysis of physiological variations and genetic architecture for cold stress response in soybean germplasm. *Frontiers in Plant Science*, v. 13, p. 1095335.
- Iqbal, A., Gui, H., Zhang, H., Wang, X., Pang, N., Dong, Q., Song, M. (2019) Genotypic variation in cotton genotypes for phosphorus-use efficiency. *Agronomy*, v. 9, n. 11, p. 689.
- Irfan, M., Aziz, T., Maqsood, M. A., Bilal, H. M., Siddique, K. H., Xu, M. (2020) Phosphorus (P) use efficiency in rice is linked to tissue-specific biomass and P allocation patterns. *Scientific reports*, v. 10, n. 1, p. 4278.
- Jackson M. L. 1965. Soil chemical analysis New Jersey: Prentice Hall, 498p.
- Jele, P., Derera, J., Siwela, M. (2014) Assessment of popping ability of new tropical popcorn hybrids. *Australian Journal of Crop Science*, v. 8, n. 6, p. 831-839.
- Jiang, H., Zhang, J., Han, Z., Yang, J., Ge, C., Wu, Q. (2017) Revealing new insights into different phosphorus-starving responses between two maize (*Zea mays*) inbred lines by transcriptomic and proteomic studies. *Scientific Reports*, v. 7, n. 1, p. 44294.
- Jiang, Z., Wang, M., Nicolas, M., Ogé, L., Pérez-García, M. D., Crespel, L., Sakr, S. (2022) Glucose-6-Phosphate dehydrogenases: the hidden players of plant physiology. *International Journal of Molecular Sciences*, v. 23, n. 24, p. 16128.
- Kamphorst, S. H., do Amaral Júnior, A. T., Vergara-Díaz, O., Gracia-Romero, A., Fernández-Gallego, J. A., Chang-Espino, M. C., Ortega, J. L. A. (2022) Heterosis and reciprocal effects for physiological and morphological traits of popcorn plants under different water conditions. *Agricultural Water Management*, v. 261, p. 107371.

- Kayoumu, M., Iqbal, A., Muhammad, N., Li, X., Li, L., Wang, X., Dong, Q. (2023) Phosphorus Availability Affects the Photosynthesis and Antioxidant System of Contrasting Low-P-Tolerant Cotton Genotypes. *Antioxidants*, v. 12, n. 2, p. 466.
- Kidwai, M., Ahmad, I. Z., Chakrabarty, D. (2020) Class III peroxidase: An indispensable enzyme for biotic/abiotic stress tolerance and a potent candidate for crop improvement. *Plant cell reports*, v. 39, p. 1381-1393.
- Kist, B. B. Anuário Brasileiro do Milho. Santa Cruz: Editora Gazeta Santa Cruz, p. 72. 2019.
- Kramer, D. M., Johnson, G., Kiirats, O., Edwards, G. E. (2004) New fluorescence parameters for the determination of QA redox state and excitation energy fluxes. *Photosynthesis research*, v. 79, p. 209-218.
- Kumar, S., Chugh, C., Seem, K., Kumar, S., Vinod, K. K., Mohapatra, T. (2021) Characterization of contrasting rice (*Oryza sativa* L.) genotypes reveals the Pi-efficient schema for phosphate starvation tolerance. *BMC plant biology*, v. 21, p. 1-26.
- Kumar, S., Trivedi, P. K. (2018) Glutathione S-transferases: role in combating abiotic stresses including arsenic detoxification in plants. *Frontiers in Plant Science*, v. 9, p. 751.
- Kwon, S., Chun, H. L., Ha, H. J., Lee, S. Y., Park, H. H. (2021) Heterogeneous multimeric structure of isocitrate lyase in complex with succinate and itaconate provides novel insights into its inhibitory mechanism. *Plos one*, v. 16, n. 5, p. e0251067.
- Langhans, C., Beusen, A. H. W., Mogollón, J. M., Bouwman, A. F. (2022) Phosphorus for Sustainable Development Goal target of doubling smallholder productivity. *Nature Sustainability*, v. 5, n. 1, p. 57-63.
- Li, K., Xu, C., Li, Z., Zhang, K., Yang, A., Zhang, J. (2008) Comparative proteome analyses of phosphorus responses in maize (*Zea mays* L.) roots of wild-type and a low-P-tolerant mutant reveal root characteristics associated with phosphorus efficiency. *The Plant Journal*, v. 55, n. 6, p. 927-939.
- Li, W., Huai, X., Li, P., Raza, A., Mubarik, M. S., Habib, M., Khan, R. S. A. (2021) Genome-wide characterization of glutathione peroxidase (GPX) gene family in rapeseed (*Brassica napus* L.) revealed their role in multiple abiotic stress response and hormone signaling. *Antioxidants*, v. 10, n. 9, p. 1481.
- Li, X., Mang, M., Piepho, H. P., Melchinger, A., Ludewig, U. (2021) Decline of seedling phosphorus use efficiency in the heterotic pool of flint maize breeding lines since the

- onset of hybrid breeding. *Journal of Agronomy and Crop Science*, v. 207, n. 5, p. 857-872.
- Liu, D. (2021) Root developmental responses to phosphorus nutrition. *Journal of Integrative Plant Biology*, v. 63, n. 6, p. 1065-1090.
- Liu, X. L., Wang, L., Wang, X. W., Yan, Y., Yang, X. L., Xie, M. Y., Sun, S. B. (2020) Mutation of the chloroplast-localized phosphate transporter OsPHT2; 1 reduces flavonoid accumulation and UV tolerance in rice. *The Plant Journal*, v. 102, n. 1, p. 53-67.
- Liu, X., Chu, S., Sun, C., Xu, H., Zhang, J., Jiao, Y., Zhang, D. (2020) Genome-wide identification of low phosphorus responsive microRNAs in two soybean genotypes by high-throughput sequencing. *Functional & integrative genomics*, v. 20, p. 825-838.
- Lopez-Guerrero, M. G., Wang, P., Phares, F., Schachtman, D. P., Alvarez, S., van Dijk, K. (2022) A glass bead semi-hydroponic system for intact maize root exudate analysis and phenotyping. *Plant Methods*, v. 18, n. 1, p. 25.
- Lynch, J. P. (2007) Roots of the second green revolution. *Australian Journal of Botany*, v. 55, n. 5, p. 493-512.
- Mabagala, F. S. (2022) On the tropical soils; The influence of organic matter (OM) on phosphate bioavailability. *Saudi Journal of Biological Sciences*, v. 29, n. 5, p. 3635-3641.
- MacDonald, G. K., Bennett, E. M., Potter, P. A., Ramankutty, N. (2011) Agronomic phosphorus imbalances across the world's croplands. *Proceedings of the National Academy of Sciences*, v. 108, n. 7, p. 3086-3091.
- Maharajan, T., Ceasar, S. A., Krishna, T. P. A., Ignacimuthu, S. (2019) Phosphate supply influenced the growth, yield and expression of PHT1 family phosphate transporters in seven millets. *Planta*, v. 250, p. 1433-1448.
- Mahender, A., Anandan, A., Pradhan, S. K., Singh, O. N. (2018) Traits-related QTLs and genes and their potential applications in rice improvement under low phosphorus condition. *Archives of Agronomy and Soil Science*, v. 64, n. 4, p. 449-464.
- Malhotra, H., Vandana, Sharma, S., Pandey, R. (2018) Phosphorus nutrition: plant growth in response to deficiency and excess. *Plant nutrients and abiotic stress tolerance*, p. 171-190.
- Malhotra, H., Vandana, Sharma, S., Pandey, R. (2018) Phosphorus nutrition: plant growth in response to deficiency and excess. *Plant nutrients and abiotic stress tolerance*, p. 171-190.

- Manske, G. G. B., Ortiz-Monasterio, J. I., Van Ginkel, M., Gonzalez, R. M., Rajaram, S., Molina, E., Vlek, P. L. G. (2000) Traits associated with improved P-uptake efficiency in CIMMYT's semidwarf spring bread wheat grown on an acid Andisol in Mexico. *Plant and Soil*, v. 221, n. 2, p. 189-204.
- McClain, A. M., Sharkey, T. D. (2019) Triose phosphate utilization and beyond: from photosynthesis to end product synthesis. *Journal of experimental botany*, v. 70, n. 6, p. 1755-1766.
- Meena, R. K., Reddy, K. S., Gautam, R., Maddela, S., Reddy, A. R., Gudipalli, P. (2021) Improved photosynthetic characteristics correlated with enhanced biomass in a heterotic F 1 hybrid of maize (*Zea mays* L.). *Photosynthesis Research*, v. 147, p. 253-267.
- Mellacheruvu, D., Wright, Z., Couzens, A. L., Lambert, J. P., St-Denis, N. A., Li, T., ... & Nesvizhskii, A. I. (2013) The CRAPome: a contaminant repository for affinity purification–mass spectrometry data. *Nature methods*, v. 10, n. 8, p. 730-736.
- Merewitz, E. B., Liu, S. (2019) Improvement in heat tolerance of creeping Bentgrass with melatonin, Rutin, and silicon. *Journal of the American Society for Horticultural Science*, v. 144, n. 2, p. 141-148.
- Mpanga, I. K., Nkebiwe, P. M., Kuhlmann, M., Cozzolino, V., Piccolo, A., Geistlinger, J., Neumann, G. (2019) The form of N supply determines plant growth promotion by P-solubilizing microorganisms in maize. *Microorganisms*, v. 7, n. 2, p. 38.
- Müh, F., Zouni, A. (2020) Structural basis of light-harvesting in the photosystem II core complex. *Protein Science*, v. 29, n. 5, p. 1090-1119.
- Nadeem, M., Mollier, A., Morel, C., Vives, A., Prud'homme, L., Pellerin, S. (2011) Relative contribution of seed phosphorus reserves and exogenous phosphorus uptake to maize (*Zea mays* L.) nutrition during early growth stages. *Plant and Soil*, v. 346, n. 1-2, p. 231-244.
- Nadira, U. A., Ahmed, I. M., Zeng, J., Wu, F., Zhang, G. (2016) Identification of the differentially accumulated proteins associated with low phosphorus tolerance in a Tibetan wild barley accession. *Journal of plant physiology*, v. 198, p. 10-22.
- Napieraj, N., Janicka, M., Reda, M. (2023) Interactions of Polyamines and Phytohormones in Plant Response to Abiotic Stress. *Plants*, v. 12, n. 5, p. 1159.
- Neupane, P., Bhujju, S., Thapa, N., Bhattarai, H. K. (2019) ATP synthase: structure, function and inhibition. *Biomolecular concepts*, v. 10, n. 1, p. 1-10.

- Nguyen, V. L., Palmer, L., Stangoulis, J. (2021) Higher photochemical quenching and better maintenance of carbon dioxide fixation are key traits for phosphorus use efficiency in the wheat breeding line, RAC875. *Frontiers in Plant Science*, v. 12, p. 816211, 2022.
- Parentoni, S. N., Mendes, F. F., Guimarães, L. J. M. (2012) Breeding for phosphorus use efficiency. *Plant breeding for abiotic stress tolerance*, p. 67-85.
- Patel, M., Rangani, J., Kumari, A., Parida, A. K. (2020) Mineral nutrient homeostasis, photosynthetic performance, and modulations of antioxidative defense components in two contrasting genotypes of *Arachis hypogaea* L.(peanut) for mitigation of nitrogen and/or phosphorus starvation. *Journal of Biotechnology*, v. 323, p. 136-158.
- Pearce, R. B., Mock, J. J., Bailey, T. B. (1975) Rapid Method for Estimating Leaf Area Per Plant in Maize 1. *Crop Science*, v. 15, n. 5, p. 691-694.
- Perez-Riverol, Y., Bai, J., Bandla, C., Hewapathirana, S., García-Seisdedos, D., Kamatchinathan, S., Kundu, D., Prakash, A., et al. (2022) The PRIDE database resources in 2022: a hub for mass spectrometry-based proteomics evidences. *Nucleic acids research*, v. 50, n. D1, p. D543-D552.
- Pinit, S., Chadchawan, S., Chaiwanon, J. (2020) A simple high-throughput protocol for the extraction and quantification of inorganic phosphate in rice leaves. *Applications in Plant Sciences*, v. 8, n. 10, p. e11395.
- Rao, I. M., Terry, N. (1989) Leaf phosphate status, photosynthesis, and carbon partitioning in sugar beet: I. Changes in growth, gas exchange, and Calvin cycle enzymes. *Plant Physiology*, v. 90, n. 3, p. 814-819.
- Raven, J. A. (2013) RNA function and phosphorus use by photosynthetic organisms. *Frontiers in Plant Science*, v. 4, p. 536.
- Reich, P. B., Oleksyn, J., Wright, I. J. (2009) Leaf phosphorus influences the photosynthesis–nitrogen relation: a cross-biome analysis of 314 species. *Oecologia*, v. 160, p. 207-212.
- Riskin, S. H., Porder, S., Neill, C., Figueira, A. M. E. S., Tubbesing, C., Mahowald, N. (2013) The fate of phosphorus fertilizer in Amazon soya bean fields. *Philosophical Transactions of the Royal Society B: Biological Sciences*, v. 368, n. 1619, p. 20120154.
- Roberts, T. L., Johnston, A. E. (2015) Phosphorus use efficiency and management in agriculture. *Resources, conservation and recycling*, v. 105, p. 275-281.

- Sahoo, R. K., Ansari, M. W., Dangar, T. K., Mohanty, S., Tuteja, N. (2014) Phenotypic and molecular characterisation of efficient nitrogen-fixing *Azotobacter* strains from rice fields for crop improvement. *Protoplasma*, v. 251, p. 511-523.
- Santos, T. D. O., Amaral Junior, A. T. D., Bispo, R. B., Bernado, W. D. P., Simão, B. R., de Lima, V. J., Cruz, C. D. (2023) Exploring the Potential of Heterosis to Improve Nitrogen Use Efficiency in Popcorn Plants. *Plants*, v. 12, n. 11, p. 2135.
- Santos, T. D. O., F. T., Amaral Junior, A. T. D., de Almeida Filho, J. E., Bispo, R. B., de Freitas, M. S. M., Trindade, R. D. S. (2022) Additive and Non-Additive Effects on the Control of Key Agronomic Traits in Popcorn Lines under Contrasting Phosphorus Conditions. *Plants*, v. 11, n. 17, p. 2216.
- Schegoscheski Gerhardt, I. F., Teixeira do Amaral Junior, A., Ferreira Pena, G., Moreira Guimarães, L. J., de Lima, V. J., Vivas, M., Kamphorst, S. H. (2019) Genetic effects on the efficiency and responsiveness to phosphorus use in popcorn as estimated by diallel analysis. *PLoS one*, v. 14, n. 5, p. e0216980.
- Scholz, R. W., Ulrich, A. E., Eilittä, M., Roy, A. (2013) Sustainable use of phosphorus: a finite resource. *Science of the Total Environment*, v. 461, p. 799-803.
- Sherin, G., Aswathi, K. R., & Puthur, J. T. (2022) Photosynthetic functions in plants subjected to stresses are positively influenced by priming. *Plant Stress*, v. 4, p. 100079.
- Silva, D. A. D., Tsai, S. M., Chiorato, A. F., da Silva Andrade, S. C., Esteves, J. A. D. F., Recchia, G. H., Morais Carbonell, S. A. (2019) Analysis of the common bean (*Phaseolus vulgaris* L.) transcriptome regarding efficiency of phosphorus use. *PLoS one*, v. 14, n. 1, p. e0210428.
- Silva, T. R. C., do Amaral Júnior, A. T., de Almeida Filho, J. E., Freitas, M. S. M., Guimarães, A. G., Kamphorst, S. H. (2019) Contrasting phosphorus environments as indicators for popcorn breeding lines. *Functional Plant Breeding Journal*, v. 1, n. 1.
- Simkin, A. J., Kapoor, L., Doss, C. G. P., Hofmann, T. A., Lawson, T., Ramamoorthy, S. (2022) The role of photosynthesis related pigments in light harvesting, photoprotection and enhancement of photosynthetic yield in planta. *Photosynthesis Research*, v. 152, n. 1, p. 23-42.
- Sims, J. R., Jackson, G. D. (1971) Rapid analysis of soil nitrate with chromotropic acid. *Soil Science Society of America Journal*, v. 35, n. 4, p. 603-606.

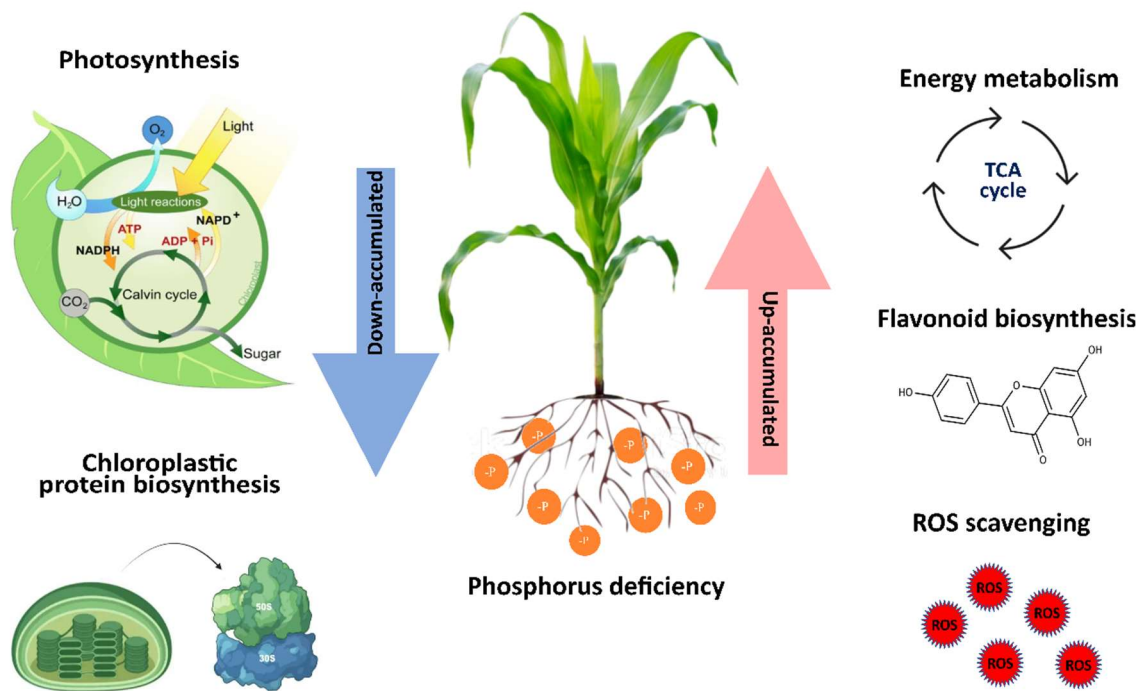
- Singh, A., Gupta, R., Pandey, R. (2017) Exogenous application of rutin and gallic acid regulate antioxidants and alleviate reactive oxygen generation in *Oryza sativa* L. *Physiology and Molecular Biology of Plants*, v. 23, p. 301-309.
- Song, J. (2021) Adenosine triphosphate energy-independently controls protein homeostasis with unique structure and diverse mechanisms. *Protein Science*, v. 30, n. 7, p. 1277-1293.
- Soviguidi, D. R. J., Pan, R., Liu, Y., Rao, L., Zhang, W., Yang, X. (2022) Chlorogenic acid metabolism: The evolution and roles in plant response to abiotic stress. *Phyton*, v. 91, n. 2, p. 239.
- Su, P., Yan, J., Li, W., Wang, L., Zhao, J., Ma, X., Kong, L. (2020) A member of wheat class III peroxidase gene family, TaPRX-2A, enhanced the tolerance of salt stress. *BMC plant biology*, v. 20, p. 1-15.
- Sun, Y., Mu, C., Liu, X. (2018) Key factors identified by proteomic analysis in maize (*Zea mays* L.) seedlings' response to long-term exposure to different phosphate levels. *Proteome Science*, v. 16, n. 1, p. 1-17.
- Suzuki, Y., Ishiyama, K., Yoon, D. K., Takegahara-Tamakawa, Y., Kondo, E., Suganami, M., Makino, A. (2022) Suppression of chloroplast triose phosphate isomerase evokes inorganic phosphate-limited photosynthesis in rice. *Plant physiology*, v. 188, n. 3, p. 1550-1562.
- Taghinasab, M., Imani, J., Steffens, D., Glaeser, S. P., Kogel, K. H. (2018) The root endophytes *Trametes versicolor* and *Piriformospora indica* increase grain yield and P content in wheat. *Plant and soil*, v. 426, p. 339-348.
- Thuynsma, R., Kleinert, A., Kossmann, J., Valentine, A. J., Hills, P. N. (2016) The effects of limiting phosphate on photosynthesis and growth of *Lotus japonicus*. *South African Journal of Botany*, v. 104, p. 244-248.
- Tietz, S., Hall, C. C., Cruz, J. A., Kramer, D. M. (2017) NPQ (T): a chlorophyll fluorescence parameter for rapid estimation and imaging of non-photochemical quenching of excitons in photosystem-II-associated antenna complexes. *Plant, cell & environment*, v. 40, n. 8, p. 1243-1255.
- Trejo-Télez, L. I., Estrada-Ortiz, E., Gómez-Merino, F. C., Becker, C., Krumbein, A., Schwarz, D. (2019) Flavonoid, nitrate and glucosinolate concentrations in Brassica species are differentially affected by photosynthetically active radiation, phosphate and phosphite. *Frontiers in Plant Science*, v. 10, p. 371.

- van de Wiel, C. C., van der Linden, C. G., Scholten, O. E. (2016) Improving phosphorus use efficiency in agriculture: opportunities for breeding. *Euphytica*, v. 207, p. 1-22.
- Vengavasi, K., Pandey, R., Abraham, G., Yadav, R. K. (2017) Comparative analysis of soybean root proteome reveals molecular basis of differential carboxylate efflux under low phosphorus stress. *Genes*, v. 8, n. 12, p. 341.
- Vu, D. C., Alvarez, S. (2021) Phenolic, carotenoid and saccharide compositions of vietnamese camellia sinensis teas and herbal teas. *Molecules*, v. 26, n. 21, p. 6496.
- Wacker-Fester, K., Uptmoor, R., Pfahler, V., Dehmer, K. J., Bachmann-Pfabe, S., Kavka, M. (2019) Genotype-specific differences in phosphorus efficiency of potato (*Solanum tuberosum* L.). *Frontiers in Plant Science*, v. 10, p. 1029.
- Wang, X., Shen, J., Liao, H. (2010) Acquisition or utilization, which is more critical for enhancing phosphorus efficiency in modern crops?. *Plant science*, v. 179, n. 4, p. 302-306.
- Wei, Y., Liu, S., Xiong, D., Xiong, Z., Zhang, Z., Wang, F., Huang, J. (2022) Genome-Wide Association Study for Non-Photochemical Quenching Traits in *Oryza sativa* L. *Agronomy*, v. 12, n. 12, p. 3216.
- Wellmer, F. W., Scholz, R. W. (2017) Putting phosphorus first: the need to know and right to know call for a revised hierarchy of natural resources. *Resources*, v. 6, n. 2, p. 20.
- Wen, Z., Li, H., Shen, J. (2017) Maize responds to low shoot P concentration by altering root morphology rather than increasing root exudation. *Plant and Soil*, v. 416, p. 377-389.
- Wingler, A., Henriques, R. (2022) Sugars and the speed of life—Metabolic signals that determine plant growth, development and death. *Physiologia Plantarum*, v. 174, n. 2, p. e13656.
- Yadav, H., Fatima, R., Sharma, A., Mathur, S. (2017) Enhancement of applicability of rock phosphate in alkaline soils by organic compost. *Applied Soil Ecology*, v. 113, p. 80-85.
- Yang, J. H., Williams, D., Kandiah, E., Fromme, P., Chiu, P. L. (2020) Structural basis of redox modulation on chloroplast ATP synthase. *Communications biology*, v. 3, n. 1, p. 482.
- Yang, S. Y., Huang, T. K., Kuo, H. F., Chiou, T. J. (2017) Role of vacuoles in phosphorus storage and remobilization. *Journal of experimental botany*, v. 68, n. 12, p. 3045-3055.

- Yang, Y., Fu, Z., Su, Y., Zhang, X., Li, G., Guo, J., Xu, L. (2014) A cytosolic glucose-6-phosphate dehydrogenase gene, ScG6PDH, plays a positive role in response to various abiotic stresses in sugarcane. *Scientific Reports*, v. 4, n. 1, p. 1-10.
- Yuan, Y., Gao, M., Zhang, M., Zheng, H., Zhou, X., Guo, Y., Li, S. (2017) QTL mapping for phosphorus efficiency and morphological traits at seedling and maturity stages in wheat. *Frontiers in plant science*, v. 8, p. 614.
- Zeng, H., Wang, G., Zhang, Y., Hu, X., Pi, E., Zhu, Y., Du, L. (2016) Genome-wide identification of phosphate-deficiency-responsive genes in soybean roots by high-throughput sequencing. *Plant and soil*, v. 398, p. 207-227.
- Zhang, K., Liu, H., Tao, P., Chen, H. (2014) Comparative proteomic analyses provide new insights into low phosphorus stress responses in maize leaves. *PLoS One*, v. 9, n. 5, p. e98215.
- Zhang, K., Liu, H., Tao, P., Chen, H. (2014b) Comparative proteomic analyses provide new insights into low phosphorus stress responses in maize leaves. *PLoS One*, v. 9, n. 5, p. e98215.
- Zhang, L. T., Li, J., Rong, T. Z., Gao, S. B., Wu, F. K., Xu, J., Li, M. L., Cao, M. J., Wang, J., Hu, E. L., Liu, Y. X. (2014a) Large-scale screening maize germplasm for low-phosphorus tolerance using multiple selection criteria. *Euphytica*, v. 197, p. 435-446.
- Zhao, Y., Cui, Y., Huang, S., Yu, J., Wang, X., Xin, D., Chen, Q. (2020) Genome-wide analysis of the glucose-6-phosphate dehydrogenase family in soybean and functional identification of GmG6PDH2 involvement in salt stress. *Frontiers in plant science*, v. 11, p. 214.
- Zheng, L., Wang, R., Zhou, P., Pan, Y., Shen, R., Lan, P. (2023) Comparative physiological and proteomic response to phosphate deficiency between two wheat genotypes differing in phosphorus utilization efficiency. *Journal of Proteomics*, v. 280, p. 104894.
- Zoschke, R., Bock, R. (2018) Chloroplast translation: structural and functional organization, operational control, and regulation. *The Plant Cell*, v. 30, n. 4, p. 745-770.

APPENDIX

Responses of popcorn plants to phosphorus deficiency



Supplementary Figure. Molecular adaptations of popcorn plants in response to phosphorus deficiency. Representation of the main pathways involved

Supplementary Table 1. Results of chemical and particle-size analysis of the substrate (sand) used to evaluate four lines and 12 hybrids of popcorn in a diallel under contrasting phosphorus conditions.

| Amostra | pH | S-SO ₄ | P | K | Ca | M | A | Na | H+A | C | MO | CTC | SB | V | m | ISN _a | Fe | Cu | Zn | Mn | B | N |
|---------|------------------|-------------------|--------------------|-----|-----|------------------------------------|---|-----|-----|-------------------|------|------------------------------------|-----|-----|---|------------------|-------|--------------------|-----|------|------|------|
| | H ₂ O | | mg/dm ³ | | | mmol _c /dm ³ | | | | g/dm ³ | | mmol _c /dm ³ | | % | % | % | | mg/dm ³ | | | % | |
| 1 | 7.0 | 6 | 9 | 0.3 | 2.7 | 1.2 | 0 | 0.5 | 0 | 0.3 | 0.52 | 4.7 | 4.7 | 100 | 0 | 11 | 162.1 | 0.20 | 2.2 | 31.5 | 0.11 | 0.07 |
| 2 | 7.2 | 5 | 10 | 0.3 | 2.9 | 1.3 | 0 | 0.5 | 0 | 0.3 | 0.52 | 5 | 5 | 100 | 0 | 10 | 201.1 | 0.22 | 2.6 | 36.6 | 0.10 | 0.07 |

Extractants: P, Na, K, Fe, Zn, Mn, Cu - Mehlich 1 extractant; Ca, Mg, Al - KCl extractant (1 mol/L); H + Al - Calcium acetate extractant (0.5 mol/L and pH 7.0); B - Hot water extractant; S - Monocalcium phosphate extractant. **Abbreviations:** SB - Sum of Exchangeable Bases; CEC - Cation Exchange Capacity at pH 7.0; V - Base Saturation Index; m - Aluminum Saturation Index; ISNa - Sodium Saturation Index; OM - Organic Matter (C Org × 1.724, Walkley-Black).

Supplementary Table 2. Analysis of variance and quadratic components for 31 traits evaluated in 16 popcorn genotypes under contrasting phosphorus conditions, according to the model proposed by Griffing (1956) for a diallel involving four lines, their F1s, and reciprocal hybrids.

| Traits | High P condition | | | | | | | | | | Low P condition | | | | | | | | | | | |
|--------------------|------------------|----------|------|-----|----------|------|-----|-----------|------|-------|-----------------|-----|----------|------|-----|----------|------|-----|-----------|------|-------|------|
| | GCA | | | SCA | | | REC | | | RES | | GCA | | | SCA | | | REC | | | RES | |
| | MS | ϕg | % | MS | ϕs | % | MS | ϕrc | % | Value | % | MS | ϕg | % | MS | ϕs | % | MS | ϕrc | % | Value | % |
| PH | ** | 6.57 | 16.3 | ** | 15.97 | 39.8 | ** | 5.04 | 12.5 | 12.50 | 31.1 | ** | 0.50 | 7.8 | ** | 3.11 | 48.1 | ** | 1.17 | 18.1 | 1.67 | 25.8 |
| SD | ** | 0.57 | 14.9 | ** | 1.42 | 37.0 | ** | 0.48 | 12.6 | 1.35 | 35.2 | ns | 0.01 | 2.3 | ** | 0.36 | 55.5 | ns | 0.04 | 7.1 | 0.22 | 35.0 |
| LL | ** | 15.50 | 14.8 | * | 27.88 | 26.6 | ** | 15.65 | 14.9 | 45.56 | 43.5 | ** | 1.20 | 4.0 | ** | 20.51 | 69.2 | ns | 1.11 | 3.7 | 6.79 | 22.9 |
| LW | ns | 0.00 | 1.8 | ns | 0.01 | 7.2 | ns | 0.02 | 11.5 | 0.16 | 79.4 | ** | 0.01 | 8.1 | ** | 0.08 | 55.7 | ns | -0.00 | 0.0 | 0.05 | 36.1 |
| LA | ns | 3549 | 12.6 | ** | 11224 | 40.0 | ns | 2495 | 8.89 | 2162 | 38.4 | ns | 56.84 | 3.4 | ** | 1034 | 63.5 | ns | 100 | 6.1 | 434 | 26.7 |
| LDM | ** | 0.30 | 15.5 | ** | 0.85 | 43.1 | ** | 0.47 | 24.1 | 0.34 | 17.1 | ** | 0.00 | 3.0 | ** | 0.01 | 65.5 | ** | 0.00 | 25.8 | 0.00 | 5.4 |
| SDM | ** | 0.12 | 12.6 | ** | 0.40 | 42.0 | ** | 0.22 | 23.4 | 0.21 | 21.8 | ** | 0.00 | 2.6 | ** | 0.03 | 66.2 | ** | 0.01 | 27.3 | 0.00 | 3.7 |
| RDM | ** | 0.01 | 9.2 | ** | 0.10 | 49.7 | ** | 0.04 | 22.6 | 0.03 | 18.2 | ** | 0.00 | 1.9 | ** | 0.00 | 70.5 | ** | 0.00 | 18.0 | 0.00 | 9.4 |
| R/S | ns | 0.00 | 0.6 | ** | -0.00 | 0.0 | * | 0.00 | 22.8 | 0.00 | 76.5 | ns | 0.00 | 2.7 | ** | 0.01 | 50.7 | ** | 0.00 | 33.4 | 0.00 | 13.0 |
| LPC | ns | 2.82 | 13.4 | ** | 11.94 | 56.8 | ** | 3.56 | 16.9 | 2.66 | 12.6 | ns | 0.00 | 2.9 | ** | 0.05 | 52.9 | ** | 0.02 | 31.1 | 0.01 | 12.9 |
| SPC | ns | 0.99 | 10.0 | ** | 4.28 | 43.3 | ** | 3.11 | 31.5 | 1.48 | 15.0 | ns | 0.00 | 3.9 | ** | 0.06 | 68.6 | ** | 0.02 | 23.1 | 0.00 | 4.2 |
| APC | ns | 6.53 | 12.2 | ** | 27.33 | 51.1 | ** | 12.35 | 23.1 | 7.24 | 13.5 | ns | 0.00 | 0.0 | ** | 0.12 | 63.7 | ** | 0.05 | 25.5 | 0.02 | 10.6 |
| RPC | ns | 0.04 | 13.9 | ** | 0.19 | 65.5 | ** | 0.03 | 12.3 | 0.02 | 8.1 | ns | 0.00 | 0.5 | ** | 0.00 | 73.4 | ** | 0.00 | 22.8 | 0.00 | 3.1 |
| PUE | ns | 0.00 | 11.5 | ** | 0.00 | 46.9 | ** | 0.00 | 19.4 | 0.00 | 22.1 | ns | 0.00 | 0.8 | ** | 0.12 | 70.2 | ** | 0.04 | 23.5 | 0.00 | 5.2 |
| PU ρ E | ns | 0.00 | 8.4 | ** | 0.00 | 42.6 | ** | 0.00 | 16.0 | 0.00 | 32.8 | ns | 0.00 | 0.2 | ns | 0.28 | 58.6 | ** | 0.10 | 22.1 | 0.09 | 18.9 |
| PU τ E | ns | 0.00 | 9.6 | ** | 0.00 | 50.5 | ** | 0.00 | 23.7 | 0.00 | 16.1 | ns | -0.00 | 0.0 | ** | 0.20 | 77.4 | ** | 0.04 | 16.6 | 0.01 | 5.8 |
| NPQt | ns | 0.00 | 1.4 | * | 0.00 | 30.8 | ns | 0.00 | 8.4 | 0.00 | 59.2 | ns | 3.29 | 8.0 | ns | 10.95 | 26.8 | ns | 24.94 | 61.1 | 1.56 | 3.8 |
| Φ PSII | * | 0.00 | 2.4 | ns | -0.00 | 0.0 | ns | -0.00 | 0.0 | 0.00 | 97.5 | ns | 0.00 | 4.6 | ** | 0.00 | 47.7 | ** | 0.00 | 28.7 | 0.00 | 18.9 |
| Φ NO | ns | 0.00 | 2.8 | ns | 0.00 | 16.4 | ns | 0.00 | 8.4 | 0.00 | 72.2 | ns | 0.00 | 6.5 | ** | 0.00 | 42.4 | ** | 0.00 | 43.2 | 0.00 | 7.7 |
| Φ NPQ | ** | 0.00 | 2.7 | ns | -0.00 | 0.0 | ns | -0.00 | 0.0 | 0.00 | 97.2 | ns | 0.00 | 4.4 | ns | 0.00 | 11.1 | ns | 0.00 | 1.6 | 0.02 | 82.8 |
| NPQt/ Φ NO | ns | 0.00 | 1.1 | ** | 0.06 | 43.0 | ns | 0.01 | 8.9 | 0.07 | 46.8 | ns | 1654 | 7.2 | ** | 7224 | 31.6 | ** | 13598 | 59.5 | 342 | 1.5 |
| Chi | * | 0.44 | 7.9 | ns | -0.45 | 0.0 | * | 1.28 | 22.7 | 3.91 | 69.3 | ns | 0.01 | 0.0 | ** | 5.25 | 32.4 | ** | 3.96 | 24.4 | 6.96 | 43.0 |
| Flav | ** | 0.00 | 14.2 | ** | 0.00 | 38.4 | ** | 0.00 | 31.4 | 0.00 | 15.8 | ** | 0.00 | 15.7 | ** | 0.03 | 62.5 | ** | 0.00 | 13.2 | 0.00 | 8.4 |
| NBI | ** | 3755 | 6.5 | ** | 30226 | 52.8 | ** | 18819 | 32.9 | 4386 | 7.6 | ** | 1986 | 13.8 | ** | 6035 | 42.0 | ** | 5434 | 37.8 | 899 | 6.2 |

Supplementary Table 2 - Cont.

| Traits | High P condition | | | | | | | | | | Low P condition | | | | | | | | | | | |
|--------------|------------------|-------------|-----|-----|-------------|------|-----|----------------|------|-------|-----------------|-----|-------------|------|-----|-------------|------|-----|----------------|------|-------|------|
| | GCA | | | SCA | | | REC | | | RES | | GCA | | | SCA | | | REC | | | RES | |
| | MS | φ_g | % | MS | φ_s | % | MS | φ_{rc} | % | Value | % | MS | φ_g | % | MS | φ_s | % | MS | φ_{rc} | % | Value | % |
| A | ns | -0.02 | 0.0 | ns | -0.13 | 0.0 | ** | 6.71 | 67.0 | 3.30 | 32.9 | ns | 1.66 | 11.2 | ** | 8.03 | 54.4 | ** | 4.07 | 27.6 | 0.97 | 6.6 |
| gs | ns | 0.00 | 3.3 | ns | -0.00 | 0.0 | * | 0.00 | 34.5 | 0.00 | 62.1 | ns | 0.00 | 6.5 | ** | 0.00 | 36.5 | ** | 0.00 | 34.4 | 0.00 | 22.4 |
| E | ns | -0.00 | 0.0 | ns | 0.00 | 6.0 | ** | 0.00 | 32.4 | 0.01 | 61.5 | ns | 0.00 | 5.0 | ** | 0.01 | 53.2 | ** | 0.00 | 17.3 | 0.00 | 24.4 |
| Ci | ns | 4.86 | 0.5 | ns | 175.12 | 19.1 | ** | 231 | 25.3 | 501 | 54.9 | ns | 3553 | 11.2 | ** | 17382 | 55.1 | ** | 7676 | 24.3 | 2884 | 9.1 |
| A/Ci | ns | 0.00 | 0.2 | * | 0.00 | 14.8 | ** | 0.00 | 48.7 | 0.00 | 36.1 | ns | 0.00 | 6.1 | ** | 0.00 | 57.9 | ** | 0.00 | 23.9 | 0.00 | 11.9 |
| A/CPF | ns | 0.07 | 8.2 | ** | 0.37 | 43.2 | ** | 0.31 | 36.5 | 0.10 | 12.0 | ns | 10.13 | 21.6 | ** | 28.60 | 60.9 | ** | 0.00 | 5.3 | 5.67 | 12.0 |

GCA- general combining ability; SCA- specific combining ability; REC- reciprocal effect; RES- residual effect; MS- mean square; φ_g , φ_s , and φ_{rc} - quadratic component associated with general and specific combining ability and reciprocal effects, respectively; PH – plant height (cm); SD – stem diameter (mm); LL – leaf length (cm); LW – leaf width (cm); LA – leaf area (cm²); LDM – leaf dry mass (g); SDM – stem dry mass (g); RDM – root dry mass (g); R/S- root to shoot ratio; LPC – leaf phosphorus content; SPC – stalk phosphorus content; APC – aboveground phosphorus content; RPC – root phosphorus content; PUE – phosphorus use efficiency; PUpE – phosphorus uptake efficiency; and PUE – phosphorus utilization efficiency; NPQt – non-photochemical quenching parameter; Φ PSII – quantum yield of PSII electron transport; Φ NO – non-regulated energy dissipation; Φ NPQ – regulated energy dissipation; NPQt/ Φ NO- non-photochemical quenching to non-regulated energy dissipation efficiency ratio; Chl – relative chlorophyll content; Flav – relative flavonoid content; and NBI – nitrogen balance index; A – net CO₂ assimilation rate ($\mu\text{mol CO}_2 \text{ m}^{-2} \text{ s}^{-1}$); gs – stomatal conductance ($\text{mol H}_2\text{O m}^{-2} \text{ s}^{-1}$); E – transpiration ($\text{mmol H}_2\text{O m}^{-2} \text{ s}^{-1}$); Ci – internal CO₂ concentration ($\mu\text{mol CO}_2 \text{ m}^{-2} \text{ s}^{-1}$); A/Ci – instantaneous carboxylation efficiency; A/LPC – carboxylation efficiency ratio to leaf phosphorus content; Significance levels: * $p < 0.05$; ** $p < 0.01$; ns = not significant.

Supplementary Table 3. List of differentially abundant proteins (DEPs) in the L80_LP / L80_HP comparison

| Accession | Description | Fold change (log2) | P value | DEPs: |
|------------|-----------------------------------------------------------------|--------------------|------------|-----------|
| A0A096RSU8 | Peptidase family M48 family protein | -6.64 | 5.7723E-17 | Unique HP |
| A0A1D6EFP8 | Fe-S cluster assembly factor HCF101 chloroplastic | -6.64 | 5.7723E-17 | Unique HP |
| A0A1D6F1Z5 | Serine/arginine-rich splicing factor SC35 | -6.64 | 5.7723E-17 | Unique HP |
| A0A1D6GIP9 | Adenylyl cyclase-associated protein | -6.64 | 5.7723E-17 | Unique HP |
| A0A1D6GVM7 | Delta-aminolevulinic acid dehydratase | -6.64 | 5.7723E-17 | Unique HP |
| A0A1D6HSW7 | Protein PXR1-like | -6.64 | 5.7723E-17 | Unique HP |
| A0A1D6I3E1 | Strictosidine synthase 3 | -6.64 | 5.7723E-17 | Unique HP |
| A0A1D6INZ7 | FSH1 domain-containing protein | -6.64 | 5.7723E-17 | Unique HP |
| A0A1D6JX93 | Peroxisomal nicotinamide adenine dinucleotide carrier | -6.64 | 5.7723E-17 | Unique HP |
| A0A1D6L4Z0 | Cytochrome b5 isoform A | -6.64 | 5.7723E-17 | Unique HP |
| A0A804LKZ4 | Uncharacterized protein | -6.64 | 5.7723E-17 | Unique HP |
| A0A804M3G2 | Alba domain-containing protein | -6.64 | 5.7723E-17 | Unique HP |
| A0A804PCB9 | xyloglucan:xyloglucosyl transferase | -6.64 | 5.7723E-17 | Unique HP |
| A0A804PES5 | Aha1_N domain-containing protein | -6.64 | 5.7723E-17 | Unique HP |
| A0A804PNN3 | TPR_REGION domain-containing protein | -6.64 | 5.7723E-17 | Unique HP |
| A0A804PTY4 | adenylate kinase | -6.64 | 5.7723E-17 | Unique HP |
| A0A804Q1R0 | Nucleosome assembly protein 1-like 1 | -6.64 | 5.7723E-17 | Unique HP |
| A0A804Q925 | phosphoglucomutase (alpha-D-glucose-1,6-bisphosphate-dependent) | -6.64 | 5.7723E-17 | Unique HP |
| A0A804R694 | Cytochrome c oxidase subunit 6b-1 | -6.64 | 5.7723E-17 | Unique HP |
| A0A804RFN4 | tyrosine--tRNA ligase | -6.64 | 5.7723E-17 | Unique HP |
| A0A804UCH1 | Glucose-1-phosphate adenylyltransferase | -6.64 | 5.7723E-17 | Unique HP |
| A0A804UH90 | Thiamine thiazole synthase, chloroplastic | -6.64 | 5.7723E-17 | Unique HP |
| A1JUJ0 | inositol-3-phosphate synthase | -6.64 | 5.7723E-17 | Unique HP |
| B4F8L1 | COP9 signalosome complex subunit 7 | -6.64 | 5.7723E-17 | Unique HP |
| B4F9B2 | Acetyl-CoA acetyltransferase, cytosolic 1 | -6.64 | 5.7723E-17 | Unique HP |
| B4FBE0 | Glycosyltransferase | -6.64 | 5.7723E-17 | Unique HP |
| B4FIL5 | Leucine-rich repeat (LRR) family protein | -6.64 | 5.7723E-17 | Unique HP |
| B4FRD6 | Peroxidase | -6.64 | 5.7723E-17 | Unique HP |
| B4FRJ4 | Photosystem II 11 kD protein | -6.64 | 5.7723E-17 | Unique HP |

Supplementary Table 3 - Cont.

| Accession | Description | Fold change (log2) | P value | DEPs: |
|-----------|----------------------------------------------------------------------------|--------------------|------------|-----------|
| B4FSA8 | GDSL esterase/lipase | -6.64 | 5.7723E-17 | Unique HP |
| B4FSJ1 | V-type proton ATPase subunit C | -6.64 | 5.7723E-17 | Unique HP |
| B4FSM7 | Hemoglobin1 | -6.64 | 5.7723E-17 | Unique HP |
| B4FT63 | Genomes uncoupled4-like protein | -6.64 | 5.7723E-17 | Unique HP |
| B4FWM3 | KH domain-containing protein | -6.64 | 5.7723E-17 | Unique HP |
| B4FZB8 | Signal recognition particle 54 kDa protein chloroplastic | -6.64 | 5.7723E-17 | Unique HP |
| B4FZL4 | Chlorophyll a-b binding protein, chloroplastic | -6.64 | 5.7723E-17 | Unique HP |
| B4G033 | peptidylprolyl isomerase | -6.64 | 5.7723E-17 | Unique HP |
| B4G0Z5 | 60S ribosomal protein L27a-3 | -6.64 | 5.7723E-17 | Unique HP |
| B4G1N1 | RmlD_sub_bind domain-containing protein | -6.64 | 5.7723E-17 | Unique HP |
| B4G1R9 | Glutamyl-tRNA(Gln) amidotransferase subunit C, chloroplastic/mitochondrial | -6.64 | 5.7723E-17 | Unique HP |
| B6SHZ1 | 40S ribosomal protein S5 | -6.64 | 5.7723E-17 | Unique HP |
| B6SJR3 | Mitochondrial import receptor subunit TOM7-1 | -6.64 | 5.7723E-17 | Unique HP |
| B6SM60 | 50S ribosomal protein L40 | -6.64 | 5.7723E-17 | Unique HP |
| B6SR25 | Maternal effect embryo arrest 59 | -6.64 | 5.7723E-17 | Unique HP |
| B6SUW7 | Protein LURP-one-related 5-like | -6.64 | 5.7723E-17 | Unique HP |
| B6SY86 | GATA-N domain-containing protein | -6.64 | 5.7723E-17 | Unique HP |
| B6SZF2 | DUF1995 domain-containing protein | -6.64 | 5.7723E-17 | Unique HP |
| B6T5I9 | Immature colon carcinoma transcript 1 protein | -6.64 | 5.7723E-17 | Unique HP |
| B6T6D2 | Dirigent protein | -6.64 | 5.7723E-17 | Unique HP |
| B6TDH3 | Protein MODIFIER OF SNC1 11 | -6.64 | 5.7723E-17 | Unique HP |
| B6TH42 | 60S ribosomal protein L9 | -6.64 | 5.7723E-17 | Unique HP |
| B6TSX9 | 4a-hydroxytetrahydrobiopterin dehydratase | -6.64 | 5.7723E-17 | Unique HP |
| B6TUB8 | Phospho-2-dehydro-3-deoxyheptonate aldolase | -6.64 | 5.7723E-17 | Unique HP |
| B6UB58 | Ubiquitin-like protein | -6.64 | 5.7723E-17 | Unique HP |
| B7ZZP2 | GTP-binding protein SAR1A | -6.64 | 5.7723E-17 | Unique HP |
| C0P4F3 | Multiple organellar RNA editing factor 9 chloroplastic | -6.64 | 5.7723E-17 | Unique HP |
| C0PEH3 | ThiC-associated domain-containing protein | -6.64 | 5.7723E-17 | Unique HP |
| C0PHM0 | Carboxypeptidase | -6.64 | 5.7723E-17 | Unique HP |
| C0PHM2 | Pollen receptor-like kinase 4 | -6.64 | 5.7723E-17 | Unique HP |

Supplementary Table 3 - Cont.

| Accession | Description | Fold change (log2) | P value | DEPs: |
|------------------|------------------------------------------------------------------|---------------------------|----------------|--------------|
| C0PN00 | Protein YLS3 | -6.64 | 5.7723E-17 | Unique HP |
| C0PKD9 | Chaperonin10 | -6.64 | 5.7723E-17 | Unique HP |
| K7TP80 | Zinc finger (C3HC4-type RING finger) family protein | -6.64 | 5.7723E-17 | Unique HP |
| K7TWH1 | peptidylprolyl isomerase | -6.64 | 5.7723E-17 | Unique HP |
| K7TZ17 | Glycosyltransferase | -6.64 | 5.7723E-17 | Unique HP |
| K7U9C9 | RNA helicase | -6.64 | 5.7723E-17 | Unique HP |
| K7UBG1 | peptidylprolyl isomerase | -6.64 | 5.7723E-17 | Unique HP |
| K7UR46 | Glutamyl-tRNA reductase-binding protein chloroplastic | -6.64 | 5.7723E-17 | Unique HP |
| K7USR3 | magnesium-protoporphyrin IX monomethyl ester (oxidative) cyclase | -6.64 | 5.7723E-17 | Unique HP |
| K7V5H2 | Copper ion binding protein | -6.64 | 5.7723E-17 | Unique HP |
| K7VDC0 | Peroxidase | -6.64 | 5.7723E-17 | Unique HP |
| K7W4T3 | Elongin-C | -6.64 | 5.7723E-17 | Unique HP |
| P10979 | Glycine-rich RNA-binding, abscisic acid-inducible protein | -6.64 | 5.7723E-17 | Unique HP |
| P12339 | 30S ribosomal protein S7, chloroplastic | -6.64 | 5.7723E-17 | Unique HP |
| P17344 | ATP synthase subunit a, chloroplastic | -6.64 | 5.7723E-17 | Unique HP |
| P17788 | 50S ribosomal protein L2, chloroplastic | -6.64 | 5.7723E-17 | Unique HP |
| P28523 | Casein kinase II subunit alpha | -6.64 | 5.7723E-17 | Unique HP |
| P42390 | Indole-3-glycerol phosphate lyase, chloroplastic | -6.64 | 5.7723E-17 | Unique HP |
| Q49HD9 | 12-oxo-phytodienoic acid reductase | -6.64 | 5.7723E-17 | Unique HP |
| Q4FZ48 | Cysteine proteinase inhibitor 5 | -6.64 | 5.7723E-17 | Unique HP |
| Q6JAD2 | Ferredoxin | -6.64 | 5.7723E-17 | Unique HP |
| Q84VG9 | Lycopene beta cyclase chloroplastic | -6.64 | 5.7723E-17 | Unique HP |
| B4FUZ9 | 50S ribosomal protein L15 chloroplastic | -5.91 | 1.73828E-12 | DOWN |
| B6T4J1 | 50S ribosomal protein L6 | -4.62 | 1.39549E-07 | DOWN |
| Q947B9 | Glucose-1-phosphate adenylyltransferase | -4 | 2.77536E-09 | DOWN |
| B4FGE5 | Uncharacterized protein | -3.55 | 0.000115671 | DOWN |
| B6U581 | Ribosome-like protein | -3.47 | 2.72187E-05 | DOWN |
| B6SWX3 | Anthocyanidin 3-O-glucosyltransferase | -3.42 | 0.000168642 | DOWN |
| B4FKB3 | 50S ribosomal protein L31 | -3.23 | 0.000114678 | DOWN |
| A0A1D6IKI2 | RNA binding protein 1 | -3.21 | 5.96291E-05 | DOWN |
| A0A804RV03 | Ribosomal_S3_C domain-containing protein | -3.12 | 0.000904049 | DOWN |
| B4F9J1 | Beta-galactosidase | -3.11 | 0.002677087 | DOWN |

Supplementary Table 3 - Cont.

| Accession | Description | Fold change (log2) | P value | DEPs: |
|------------------|------------------------------------------------------------------|---------------------------|----------------|--------------|
| B4FJG1 | Chlorophyll a-b binding protein, chloroplastic | -3.09 | 7.3467E-06 | DOWN |
| B6SUJ0 | 50S ribosomal protein L10 | -2.94 | 0.002790466 | DOWN |
| B4FU53 | 50S ribosomal protein L9, chloroplastic | -2.83 | 4.28461E-05 | DOWN |
| B4G1Q5 | 50S ribosomal protein L10 chloroplastic | -2.82 | 6.28178E-05 | DOWN |
| A5GZ73 | Glucose-1-phosphate adenylyltransferase | -2.79 | 0.000582698 | DOWN |
| P06588 | 30S ribosomal protein S19, chloroplastic | -2.76 | 5.23172E-05 | DOWN |
| B4FH16 | 30S ribosomal protein 3 chloroplastic | -2.72 | 0.002424688 | DOWN |
| B6TT66 | Ribosome-like protein | -2.67 | 0.000894703 | DOWN |
| A0A1D6FKD0 | Putative 3-hydroxyisobutyrate dehydrogenase-like 3 mitochondrial | -2.65 | 0.008096284 | DOWN |
| P16037 | 30S ribosomal protein S2, chloroplastic | -2.56 | 0.009295311 | DOWN |
| B4FMW6 | Aspartyl protease AED3 | -2.55 | 0.012526534 | DOWN |
| B6TEJ4 | Peptidase C15 pyroglutamyl peptidase I-like | -2.53 | 0.013760816 | DOWN |
| B6SST7 | 50S ribosomal protein L5, chloroplastic | -2.48 | 0.000467412 | DOWN |
| A0A804Q515 | PsbP domain-containing protein | -2.45 | 0.000472998 | DOWN |
| K7TXI5 | Chlorophyll a-b binding protein, chloroplastic | -2.43 | 0.000542772 | DOWN |
| P48183 | Photosystem II protein D1 | -2.42 | 0.00057908 | DOWN |
| P09387 | 50S ribosomal protein L23, chloroplastic | -2.41 | 0.002136721 | DOWN |
| B6SR22 | 50S ribosomal protein L12-1 | -2.41 | 0.003205514 | DOWN |
| P25459 | 30S ribosomal protein S18, chloroplastic | -2.39 | 0.012358193 | DOWN |
| B4FDG7 | RNA-binding (RRM/RBD/RNP motifs) family protein | -2.37 | 0.014044793 | DOWN |
| B6U8X9 | Glycerol-3-phosphate acyltransferase, chloroplastic | -2.33 | 0.025005051 | DOWN |
| A0A1D6JSL7 | inositol-3-phosphate synthase | -2.28 | 0.005425103 | DOWN |
| B4FLV6 | Protein translation factor SU11 | -2.28 | 0.021015021 | DOWN |
| P08529 | 50S ribosomal protein L14, chloroplastic | -2.26 | 0.00146273 | DOWN |
| B6U1J2 | 50S ribosomal protein L11 | -2.23 | 0.000875418 | DOWN |
| B4FL55 | Chlorophyll a-b binding protein, chloroplastic | -2.23 | 0.001722264 | DOWN |
| A0A804QDB7 | Chlorophyll a-b binding protein, chloroplastic | -2.22 | 0.001779289 | DOWN |
| B4FFI2 | Nitrilase-associated protein | -2.22 | 0.018986769 | DOWN |
| A0A804LKH5 | 50S ribosomal protein L6, chloroplastic | -2.2 | 0.001950986 | DOWN |
| A0A804MF05 | UBX domain-containing protein | -2.18 | 0.029963243 | DOWN |
| K7UTW6 | Plasminogen activator inhibitor 1 RNA-binding protein | -2.18 | 0.039304611 | DOWN |
| C4JA36 | Binding partner of ACD11 1 | -2.17 | 0.024375362 | DOWN |
| B4FZP0 | Mg-protoporphyrin IX chelatase | -2.16 | 0.019706593 | DOWN |

Supplementary Table 3 - Cont.

| Accession | Description | Fold change (log2) | P value | DEPs: |
|------------------|--------------------------------------------------------|---------------------------|----------------|--------------|
| A0A3L6E5Y7 | Plasma membrane ATPase | -2.15 | 0.027651766 | DOWN |
| A0A804M2J7 | 30S ribosomal protein S13, chloroplasic | -2.14 | 0.008766983 | DOWN |
| A0A804LV96 | 30S ribosomal protein S4, chloroplasic | -2.12 | 0.045514717 | DOWN |
| P08528 | 50S ribosomal protein L16, chloroplasic | -2.11 | 0.014863849 | DOWN |
| B4FXB9 | FLU | -2.08 | 0.034384128 | DOWN |
| P17703 | 30S ribosomal protein S15, chloroplasic | -2.06 | 0.014863849 | DOWN |
| B6U2H1 | Uncharacterized protein | -2.06 | 0.030757719 | DOWN |
| A0A1D6FDV3 | 50S ribosomal protein L29 chloroplasic | -2.06 | 0.041077423 | DOWN |
| P25706 | NAD(P)H-quinone oxidoreductase subunit 1, chloroplasic | -2.01 | 0.047270742 | DOWN |
| B4FA79 | Calcium-binding EF hand family protein | -1.99 | 0.017367986 | DOWN |
| A0A1X7YHF7 | Photosystem II D2 protein | -1.98 | 0.006088793 | DOWN |
| K7W010 | Phosphoglycerate mutase family protein | -1.97 | 0.034008825 | DOWN |
| A0A804R6R9 | Ribosomal_S10 domain-containing protein | -1.95 | 0.018855199 | DOWN |
| A0A1D6M323 | Ribosomal protein | -1.91 | 0.008665252 | DOWN |
| B6SSN3 | Chlorophyll a-b binding protein, chloroplasic | -1.89 | 0.007347957 | DOWN |
| P27723 | 30S ribosomal protein S16, chloroplasic | -1.89 | 0.018986769 | DOWN |
| B4FED9 | Ycf54-like protein | -1.86 | 0.00949216 | DOWN |
| P08530 | 30S ribosomal protein S8, chloroplasic | -1.86 | 0.042868793 | DOWN |
| A0A804P2H5 | 50S ribosomal protein L21 | -1.8 | 0.014103471 | DOWN |
| Q9TJN6 | 30S ribosomal protein S17, chloroplasic | -1.78 | 0.013658979 | DOWN |
| A0A1D6KJ07 | N-acyl-aliphatic-L-amino acid amidohydrolase | -1.77 | 0.04250011 | DOWN |
| B6T0F9 | Thylakoid soluble phosphoprotein TSP9 | -1.75 | 0.039149597 | DOWN |
| A0A804MRM8 | Oxygen-evolving enhancer protein 3-2, chloroplasic | -1.73 | 0.019468919 | DOWN |
| A0A804PCP6 | KOW domain-containing protein | -1.73 | 0.033336377 | DOWN |
| B4FYN6 | Iso_dh domain-containing protein | -1.73 | 0.041686196 | DOWN |
| B6SUJ3 | Plastid-specific 30S ribosomal protein 2 | -1.72 | 0.038972218 | DOWN |
| B4G1A1 | Photosystem II 5 kDa protein, chloroplasic | -1.71 | 0.021081212 | DOWN |
| B6UIC1 | 50S ribosomal protein L12-1 | -1.69 | 0.022382396 | DOWN |
| B4FSZ8 | Beta alanine synthase1 | -1.66 | 0.023893038 | DOWN |
| P48187 | Photosystem II CP43 reaction center protein | -1.63 | 0.029019142 | DOWN |
| B4FXB0 | Chlorophyll a-b binding protein, chloroplasic | -1.61 | 0.031273918 | DOWN |
| A0A804M4P0 | 30S ribosomal protein S9, chloroplasic | -1.6 | 0.026798941 | DOWN |
| B6T9H3 | Asparate aminotransferase | -1.6 | 0.03266098 | DOWN |
| Q41739 | Thiamine thiazole synthase 2, chloroplasic | -1.56 | 0.038100442 | DOWN |

Supplementary Table 3 - Cont.

| Accession | Description | Fold change (log2) | P value | DEPs: |
|------------------|----------------------------------------------------|---------------------------|----------------|--------------|
| B4G1J8 | 50S ribosomal protein L3-1 chloroplastic | -1.55 | 0.030398281 | DOWN |
| P24993 | Photosystem II reaction center protein H | -1.55 | 0.03922432 | DOWN |
| C0PEC4 | 30S ribosomal protein S5 chloroplastic | -1.54 | 0.041686196 | DOWN |
| B4F9R9 | Oxygen-evolving enhancer protein 1 | -1.53 | 0.043016018 | DOWN |
| Q41746 | Chlorophyll a-b binding protein, chloroplastic | -1.5 | 0.047265125 | DOWN |
| P05641 | Photosystem II CP47 reaction center protein | -1.5 | 0.048730517 | DOWN |
| A0A804RTY6 | FAD dependent oxidoreductase | -1.48 | 0.039281592 | DOWN |
| P69388 | Cytochrome b559 subunit alpha | -1.46 | 0.043796325 | DOWN |
| B4FVJ9 | glutathione transferase | 2.1 | 0.039570279 | UP |
| K7TJV6 | oxoglutarate dehydrogenase (succinyl-transferring) | 2.1 | 0.044307458 | UP |
| A0A1D6JMZ9 | Aconitate hydratase | 2.12 | 0.032784576 | UP |
| A0A1D6PUK8 | Aconitate hydratase | 2.17 | 0.026876277 | UP |
| A0A096RZN2 | carbonic anhydrase | 2.2 | 0.023783251 | UP |
| B4G1C2 | GH18 domain-containing protein | 2.31 | 0.021963287 | UP |
| C0P4M0 | Monodehydroascorbate reductase 1 peroxisomal | 2.39 | 0.018085913 | UP |
| B4FVL1 | 26S proteasome non-ATPase regulatory subunit 6 | 2.43 | 0.020614132 | UP |
| B4FL28 | Isovaleryl-CoA dehydrogenase mitochondrial | 2.44 | 0.027319943 | UP |
| A0A804P3Q9 | Glycosyltransferase | 2.45 | 0.020113738 | UP |
| A0A1D6I1V3 | phosphoenolpyruvate carboxylase | 2.48 | 0.006911522 | UP |
| B4G1B0 | Remorin | 2.49 | 0.027697554 | UP |
| B7ZWY9 | Citrate synthase | 2.54 | 0.017599973 | UP |
| A0A1D6PJL0 | Aconitate hydratase | 2.63 | 0.010840816 | UP |
| A6YSM3 | PL3K2 | 2.64 | 0.003049232 | UP |
| C0PMP2 | riboflavin kinase | 2.65 | 0.036327712 | UP |
| C0PFV4 | Chaperone protein ClpC1 chloroplastic | 2.69 | 0.002333133 | UP |
| B6TNF1 | Calnexin | 2.69 | 0.00404192 | UP |
| A0A1D6HR96 | Purple acid phosphatase | 2.71 | 0.037911504 | UP |
| B4F8X3 | Acyl-coenzyme A oxidase | 2.81 | 0.024153793 | UP |
| C0PHD8 | aldehyde dehydrogenase (NAD(+)) | 2.87 | 0.001431461 | UP |
| B4F7Z4 | glycerophosphodiester phosphodiesterase | 2.89 | 0.000806226 | UP |
| A0A804Q7K1 | Vesicle-associated membrane protein 726 | 2.9 | 0.040912659 | UP |
| A0A1D6H9K3 | Chaperone protein ClpD chloroplastic | 2.91 | 0.015003216 | UP |
| C4J473 | oligopeptidase A | 2.91 | 0.03766035 | UP |
| B4FLP7 | cysteine desulfurase | 2.93 | 0.031350162 | UP |
| B6SRL2 | Aconitate hydratase | 2.94 | 0.02120063 | UP |
| A0A804RBR8 | NTP_transferase domain-containing protein | 2.95 | 0.043796325 | UP |
| Q9FQA3 | Glutathione transferase GST 23 | 2.98 | 0.010124894 | UP |

Supplementary Table 3 – Cont.

| Accession | Description | Fold change (log2) | P value | DEPs: |
|------------------|--------------------------------------------------------------------------------------------|---------------------------|----------------|--------------|
| B4FZU9 | dihydropyrimidine dehydrogenase (NADP(+)) | 2.98 | 0.010858172 | UP |
| Q8LK07 | Histone H1 | 2.98 | 0.023872733 | UP |
| Q29SB6 | Pathogenesis-related protein 10 | 3 | 0.005714229 | UP |
| Q94F77 | Nucleosome/chromatin assembly factor C | 3 | 0.019049587 | UP |
| B6UC34 | glutamine--tRNA ligase | 3 | 0.037951957 | UP |
| A0A1D6F5G3 | Apyrase 1 | 3.04 | 0.031657093 | UP |
| C0PI30 | ribose-5-phosphate isomerase | 3.05 | 0.02930062 | UP |
| A0A1D6LPQ2 | Glycosyl hydrolase family 31 protein | 3.07 | 0.02307292 | UP |
| B6T484 | Mitogen-activated protein kinase | 3.07 | 0.031911851 | UP |
| B6TNK2 | 2-oxoglutarate (2OG) and Fe(II)-dependent oxygenase superfamily protein | 3.08 | 0.006372622 | UP |
| A0A804UHW9 | Heme-binding-like protein At3g10130, chloroplastic | 3.09 | 0.000288166 | UP |
| A0A1D6JNJ8 | Lethal leaf-spot 1 | 3.11 | 0.000206883 | UP |
| A0A1D6DSU2 | K(+) efflux antiporter 2 chloroplastic | 3.12 | 0.001445614 | UP |
| C0P8H3 | Cysteine proteinase | 3.13 | 0.008815813 | UP |
| K7VCN5 | Peroxidase | 3.13 | 0.023070518 | UP |
| C0P732 | Hsp70-Hsp90 organizing protein 3 | 3.14 | 0.009113496 | UP |
| C0PIW1 | Glucose-6-phosphate 1-dehydrogenase | 3.17 | 0.018569977 | UP |
| A0A1D6KCV3 | NAD(P)H-hydrate epimerase | 3.17 | 0.020802662 | UP |
| A0A1D6EC46 | Double Clp-N motif-containing P-loop nucleoside triphosphate hydrolase superfamily protein | 3.19 | 0.003871908 | UP |
| B4FUH2 | Aspartate aminotransferase | 3.2 | 0.000689736 | UP |
| B8A2L4 | Starch synthase, chloroplastic/amyloplastic | 3.23 | 0.000274182 | UP |
| A0A1D6K5D2 | Nucleoredoxin1 | 3.23 | 0.000514523 | UP |
| B4FNK8 | Chorismate mutase 1, chloroplastic | 3.23 | 0.009728915 | UP |
| A0A1D6FD96 | leucine--tRNA ligase | 3.24 | 0.009654925 | UP |
| K7VA33 | Kininogen-1 | 3.29 | 0.008164925 | UP |
| B4FRC6 | Peptidase A1 domain-containing protein | 3.31 | 0.000335786 | UP |
| A0A1D6EUJ1 | valine--tRNA ligase | 3.31 | 0.012559003 | UP |
| A0A804QH05 | Cysteine proteinase inhibitor | 3.31 | 0.027173267 | UP |
| A0A804PVC1 | EMC7_beta-sandw domain-containing protein | 3.33 | 0.014359128 | UP |
| K7UGR2 | Putative TCP-1/cpn60 chaperonin family protein isoform 1 | 3.35 | 0.002928229 | UP |
| B6T391 | Lichenase-2 | 3.39 | 0.011840187 | UP |
| Q6R9J5 | ATP synthase protein MI25 | 3.39 | 0.012635536 | UP |
| A0A1D6I6A1 | Isoamylase-type starch debranching enzyme3 | 3.42 | 0.028061515 | UP |
| A0A804U9Z6 | Glutamate--cysteine ligase | 3.5 | 1.5895E-05 | UP |
| A0A804RH46 | PG_binding_1 domain-containing protein | 3.5 | 0.004893231 | UP |
| A0A804NQX0 | methylcrotonoyl-CoA carboxylase | 3.5 | 0.019468919 | UP |

Supplementary Table 3 – Cont.

| Accession | Description | Fold change (log2) | P value | DEPs: |
|------------------|-------------------------------------------------------|---------------------------|----------------|--------------|
| B4FTQ1 | Arginase 1 mitochondrial | 3.51 | 0.001276901 | UP |
| A0A096RYW9 | alanine transaminase | 3.52 | 0.004831546 | UP |
| A0A804LI99 | GST N-terminal domain-containing protein | 3.52 | 0.016756307 | UP |
| B4FIH9 | Xylose isomerase | 3.59 | 0.003652026 | UP |
| B4FIA6 | Histone H2A | 3.59 | 0.015427004 | UP |
| B6TZD1 | Methylthioribose-1-phosphate isomerase | 3.61 | 0.002932149 | UP |
| B4FBK8 | 3-ketoacyl-CoA thiolase 2 peroxisomal | 3.62 | 0.000545361 | UP |
| K7U2E4 | Amine oxidase | 3.62 | 0.002607331 | UP |
| A0A804QPJ4 | Heat shock 70 kDa protein 14 | 3.62 | 0.003311564 | UP |
| A0A1D6EBS5 | 1,4-alpha-glucan branching enzyme | 3.67 | 0.000787236 | UP |
| Q9SAZ6 | phosphoenolpyruvate carboxylase | 3.7 | 9.97884E-06 | UP |
| P49105 | Glucose-6-phosphate isomerase, cytosolic | 3.7 | 6.03129E-05 | UP |
| P93629 | Alcohol dehydrogenase class-3 | 3.75 | 0.003072178 | UP |
| A0A1D6GNG8 | Nonspecific lipid-transfer protein | 3.78 | 0.001852353 | UP |
| B4FCX9 | alpha-L-fucosidase | 3.8 | 0.002928229 | UP |
| A0A1D6INR0 | Stress responsive protein | 3.83 | 0.001945942 | UP |
| A0A804RM97 | Dihydroorotate dehydrogenase (quinone), mitochondrial | 3.84 | 0.005089258 | UP |
| K7TY03 | Alanine--tRNA ligase | 4.02 | 0.000295049 | UP |
| A0A804MY67 | phosphoribosylaminoimidazole carboxylase | 4.04 | 9.69815E-05 | UP |
| A0A804N0J5 | Aspergillus nuclease S1 | 4.23 | 0.000189743 | UP |
| B4F9G1 | Aspartate aminotransferase | 4.34 | 2.95669E-05 | UP |
| K7VEU4 | Ubiquinone biosynthesis protein ubiB | 4.39 | 0.000234954 | UP |
| Q08275 | 17.0 kDa class II heat shock protein | 4.51 | 4.99622E-06 | UP |
| K7VYS6 | PLC-like phosphodiesterases superfamily protein | 4.56 | 9.44093E-07 | UP |
| A0A1D6HUN3 | D-2-hydroxyglutarate dehydrogenase mitochondrial | 4.56 | 3.25893E-05 | UP |
| B7ZWU3 | M20_dimer domain-containing protein | 4.73 | 1.23848E-05 | UP |
| B4FBD6 | Ribonuclease 1 | 4.75 | 1.75193E-08 | UP |
| C0HI30 | UDP-glucose 4-epimerase | 4.98 | 1.00564E-06 | UP |
| C0P472 | Protein TIC 55 chloroplastic | 5.02 | 3.72242E-06 | UP |
| A0A804QJX5 | 3-hydroxybutyryl-CoA epimerase | 5.07 | 2.05676E-06 | UP |
| A0A804QL16 | Salt stress root protein RS1 | 6.2 | 3.14582E-11 | UP |
| A0A1D6E7V9 | Malate synthase | 6.61 | 2.31446E-13 | UP |
| A0A096SRM5 | UDP-glycosyltransferase 708A6 | 6.64 | 5.7723E-17 | Unique LP |
| A0A1D6DQH1 | Acetyl-coenzyme A synthetase | 6.64 | 5.7723E-17 | Unique LP |
| A0A1D6DZR9 | AICARFT/IMPCHase bienzyme family protein | 6.64 | 5.7723E-17 | Unique LP |

Supplementary Table 3 – Cont.

| Accession | Description | Fold change (log2) | P value | DEPs: |
|------------------|-----------------------------------------------------|---------------------------|----------------|--------------|
| A0A1D6EC40 | Trihelix transcription factor ASR3 | 6.64 | 5.7723E-17 | Unique LP |
| A0A1D6ES79 | MLO-like protein | 6.64 | 5.7723E-17 | Unique LP |
| A0A1D6F8M1 | Coatomer subunit gamma | 6.64 | 5.7723E-17 | Unique LP |
| A0A1D6F9V3 | valine--tRNA ligase | 6.64 | 5.7723E-17 | Unique LP |
| A0A1D6FKF7 | Aspartic proteinase A1 | 6.64 | 5.7723E-17 | Unique LP |
| A0A1D6GBA2 | phosphoenolpyruvate carboxylase | 6.64 | 5.7723E-17 | Unique LP |
| A0A1D6GEY0 | Mitochondrial Rho GTPase | 6.64 | 5.7723E-17 | Unique LP |
| A0A1D6H4X4 | 3-hydroxybutyryl-CoA epimerase | 6.64 | 5.7723E-17 | Unique LP |
| A0A1D6H8S6 | UPF0548 protein | 6.64 | 5.7723E-17 | Unique LP |
| A0A1D6HKA8 | Arsenical pump-driving ATPase | 6.64 | 5.7723E-17 | Unique LP |
| A0A1D6I3N3 | Alpha-amylase | 6.64 | 5.7723E-17 | Unique LP |
| A0A1D6JA02 | Triglyceride lipases | 6.64 | 5.7723E-17 | Unique LP |
| A0A1D6K864 | Proline dehydrogenase | 6.64 | 5.7723E-17 | Unique LP |
| A0A1D6KV33 | acylaminoacyl-peptidase | 6.64 | 5.7723E-17 | Unique LP |
| A0A1D6L077 | Uncharacterized protein | 6.64 | 5.7723E-17 | Unique LP |
| A0A1D6L4K3 | Inosine-5'-monophosphate dehydrogenase | 6.64 | 5.7723E-17 | Unique LP |
| A0A1D6LVZ7 | Putative LIM-type zinc finger domain family protein | 6.64 | 5.7723E-17 | Unique LP |
| A0A1D6LY56 | galactinol--sucrose galactosyltransferase | 6.64 | 5.7723E-17 | Unique LP |
| A0A1D6LYR3 | arginine--tRNA ligase | 6.64 | 5.7723E-17 | Unique LP |
| A0A1D6M275 | Malic enzyme | 6.64 | 5.7723E-17 | Unique LP |
| A0A1D6MPN8 | Importin subunit alpha | 6.64 | 5.7723E-17 | Unique LP |
| A0A1D6MY33 | Glutathione transferase18 | 6.64 | 5.7723E-17 | Unique LP |
| A0A1D6N309 | Dynamamin-related protein 3A | 6.64 | 5.7723E-17 | Unique LP |
| A0A1D6N7A4 | Acyl-coenzyme A oxidase | 6.64 | 5.7723E-17 | Unique LP |
| A0A1D6NE76 | cytidine deaminase | 6.64 | 5.7723E-17 | Unique LP |
| A0A1D6NMU7 | Ubiquitin carboxyl-terminal hydrolase | 6.64 | 5.7723E-17 | Unique LP |
| A0A1D6NVZ6 | 3-phosphoshikimate 1-carboxyvinyltransferase | 6.64 | 5.7723E-17 | Unique LP |
| A0A1D6QK75 | Heat shock protein 90-5 chloroplastic | 6.64 | 5.7723E-17 | Unique LP |
| A0A1D6QNT3 | 3-hydroxybutyryl-CoA epimerase | 6.64 | 5.7723E-17 | Unique LP |
| A0A3L6EYR2 | Putrescine hydroxycinnamoyltransferase 1 | 6.64 | 5.7723E-17 | Unique LP |

Supplementary Table 3 – Cont.

| Accession | Description | Fold change (log2) | P value | DEPs: |
|------------------|---------------------------------------------------------|---------------------------|----------------|--------------|
| A0A804LLZ6 | SCP domain-containing protein | 6.64 | 5.7723E-17 | Unique LP |
| A0A804LMS8 | Ubiquitin domain-containing protein DSK2b | 6.64 | 5.7723E-17 | Unique LP |
| A0A804M6K4 | zf-Tim10_DDP domain-containing protein | 6.64 | 5.7723E-17 | Unique LP |
| A0A804M8T6 | Fe2OG dioxygenase domain-containing protein | 6.64 | 5.7723E-17 | Unique LP |
| A0A804M914 | Plasma membrane ATPase | 6.64 | 5.7723E-17 | Unique LP |
| A0A804MIN3 | Pullulanase 1, chloroplastic | 6.64 | 5.7723E-17 | Unique LP |
| A0A804MQX0 | Purple acid phosphatase | 6.64 | 5.7723E-17 | Unique LP |
| A0A804MS81 | 5-formyltetrahydrofolate cyclo-ligase | 6.64 | 5.7723E-17 | Unique LP |
| A0A804MST0 | Genome assembly, chromosome: II | 6.64 | 5.7723E-17 | Unique LP |
| A0A804MZU9 | AA_TRNA_LIGASE_II domain-containing protein | 6.64 | 5.7723E-17 | Unique LP |
| A0A804N3I3 | shikimate dehydrogenase (NADP(+)) | 6.64 | 5.7723E-17 | Unique LP |
| A0A804N9X8 | Pectinesterase | 6.64 | 5.7723E-17 | Unique LP |
| A0A804NJC9 | ATP citrate synthase | 6.64 | 5.7723E-17 | Unique LP |
| A0A804NKF2 | Acyl-coenzyme A oxidase | 6.64 | 5.7723E-17 | Unique LP |
| A0A804P9G2 | Chlorophyll(ide) b reductase NOL, chloroplastic | 6.64 | 5.7723E-17 | Unique LP |
| A0A804PH92 | AAA domain-containing protein | 6.64 | 5.7723E-17 | Unique LP |
| A0A804PNJ8 | Fe2OG dioxygenase domain-containing protein | 6.64 | 5.7723E-17 | Unique LP |
| A0A804Q6T0 | Short-chain dehydrogenase TIC 32, chloroplastic-like | 6.64 | 5.7723E-17 | Unique LP |
| A0A804QWE5 | Sucrose-phosphate synthase | 6.64 | 5.7723E-17 | Unique LP |
| A0A804R009 | Phostensin domain-containing protein | 6.64 | 5.7723E-17 | Unique LP |
| A0A804R5V2 | Asparagine synthetase [glutamine-hydrolyzing] | 6.64 | 5.7723E-17 | Unique LP |
| A0A804RDS0 | Laccase | 6.64 | 5.7723E-17 | Unique LP |
| A0A804RDU6 | Long-chain-fatty-acid--CoA ligase | 6.64 | 5.7723E-17 | Unique LP |
| A0A804RJC2 | Uncharacterized protein | 6.64 | 5.7723E-17 | Unique LP |
| A0A804RNZ5 | Trypsin family protein | 6.64 | 5.7723E-17 | Unique LP |
| A0A804U874 | Ubiquitin-like modifier-activating enzyme 5 | 6.64 | 5.7723E-17 | Unique LP |
| A0A804UB26 | dynamamin GTPase | 6.64 | 5.7723E-17 | Unique LP |
| A0A804UBU8 | phosphatidate phosphatase | 6.64 | 5.7723E-17 | Unique LP |
| B4F7W4 | Putative inactive shikimate kinase like 2 chloroplastic | 6.64 | 5.7723E-17 | Unique LP |
| B4F7Y5 | Acid phosphatase 1 | 6.64 | 5.7723E-17 | Unique LP |

Supplementary Table 3 – Cont.

| Accession | Description | Fold change (log2) | P value | DEPs: |
|------------------|-----------------------------------------------------------------------------------------|---------------------------|----------------|--------------|
| B4F8E3 | Electron transfer flavoprotein subunit alpha | 6.64 | 5.7723E-17 | Unique LP |
| B4F8U6 | Ornithine aminotransferase | 6.64 | 5.7723E-17 | Unique LP |
| B4F8V5 | NADH dehydrogenase [ubiquinone] iron-sulfur protein 1 mitochondrial | 6.64 | 5.7723E-17 | Unique LP |
| B4F8V5 | NADH dehydrogenase [ubiquinone] iron-sulfur protein 1 mitochondrial | 6.64 | 5.7723E-17 | Unique LP |
| B4F912 | Serine carboxypeptidase-like 19 | 6.64 | 5.7723E-17 | Unique LP |
| B4F976 | 17.4 kDa class I heat shock protein | 6.64 | 5.7723E-17 | Unique LP |
| B4FAB2 | Molecular chaperone Hsp40/DnaJ family protein | 6.64 | 5.7723E-17 | Unique LP |
| B4FAT6 | Glycosyltransferase | 6.64 | 5.7723E-17 | Unique LP |
| B4FBF9 | Pollen-specific leucine-rich repeat extensin-like protein 1 | 6.64 | 5.7723E-17 | Unique LP |
| B4FBW5 | Mannitol dehydrogenase | 6.64 | 5.7723E-17 | Unique LP |
| B4FDW3 | Rhodanese-like/PpiC domain-containing protein 12 chloroplastic | 6.64 | 5.7723E-17 | Unique LP |
| B4FG53 | Malate dehydrogenase | 6.64 | 5.7723E-17 | Unique LP |
| B4FIE4 | 2,4-dienoyl-CoA reductase [(3E)-enoyl-CoA-producing] | 6.64 | 5.7723E-17 | Unique LP |
| B4FL83 | Putative uridine nucleosidase 2 | 6.64 | 5.7723E-17 | Unique LP |
| B4FPG2 | Actin-1 | 6.64 | 5.7723E-17 | Unique LP |
| B4FRQ0 | MLP3.9 protein | 6.64 | 5.7723E-17 | Unique LP |
| B4FSH6 | Genome assembly, chromosome: II | 6.64 | 5.7723E-17 | Unique LP |
| B4FT62 | Putative aldo-keto reductase 4 | 6.64 | 5.7723E-17 | Unique LP |
| B4FTF9 | Isocitrate lyase | 6.64 | 5.7723E-17 | Unique LP |
| B4FTR1 | Alkyl transferase | 6.64 | 5.7723E-17 | Unique LP |
| B4FUC1 | 2-oxoisovalerate dehydrogenase subunit beta 1 mitochondrial | 6.64 | 5.7723E-17 | Unique LP |
| B4FUW7 | Uncharacterized conserved protein UCP022280 | 6.64 | 5.7723E-17 | Unique LP |
| B4FVB1 | Actin-7 | 6.64 | 5.7723E-17 | Unique LP |
| B4FVS8 | protein-serine/threonine phosphatase | 6.64 | 5.7723E-17 | Unique LP |
| B4FVU4 | Abhydrolase_3 domain-containing protein | 6.64 | 5.7723E-17 | Unique LP |
| B4FX20 | AKIN gamma | 6.64 | 5.7723E-17 | Unique LP |
| B4G0F3 | Probable bifunctional methylthioribulose-1-phosphate dehydratase/enolase-phosphatase E1 | 6.64 | 5.7723E-17 | Unique LP |
| B4G124 | 26S protease regulatory subunit 8 | 6.64 | 5.7723E-17 | Unique LP |

Supplementary Table 3 – Cont.

| Accession | Description | Fold change (log2) | P value | DEPs: |
|------------------|-------------------------------------------------------------------------|---------------------------|----------------|--------------|
| B6ETR5 | Asparagine synthetase [glutamine-hydrolyzing] | 6.64 | 5.7723E-17 | Unique LP |
| B6SIX0 | 16.9 kDa class I heat shock protein 1 | 6.64 | 5.7723E-17 | Unique LP |
| B6SLA5 | 2Fe-2S ferredoxin-like superfamily protein | 6.64 | 5.7723E-17 | Unique LP |
| B6SM26 | 3-oxoacyl-synthase III | 6.64 | 5.7723E-17 | Unique LP |
| B6SMQ8 | Histone H1 | 6.64 | 5.7723E-17 | Unique LP |
| B6SQD9 | Uncharacterized protein | 6.64 | 5.7723E-17 | Unique LP |
| B6SRI4 | 14-3-3-like protein | 6.64 | 5.7723E-17 | Unique LP |
| B6ST57 | DNA photolyase | 6.64 | 5.7723E-17 | Unique LP |
| B6SZ65 | Glycosyltransferase | 6.64 | 5.7723E-17 | Unique LP |
| B6T033 | glutathione transferase | 6.64 | 5.7723E-17 | Unique LP |
| B6T1E3 | Mitochondrial outer membrane protein porin 4 | 6.64 | 5.7723E-17 | Unique LP |
| B6T329 | Aspergillus nuclease S1 | 6.64 | 5.7723E-17 | Unique LP |
| B6T3Q3 | Adenine nucleotide alpha hydrolase-like superfamily protein | 6.64 | 5.7723E-17 | Unique LP |
| B6T563 | Nucleoside N-ribohydrolase 3 | 6.64 | 5.7723E-17 | Unique LP |
| B6T7L5 | THAP domain-containing protein 4 | 6.64 | 5.7723E-17 | Unique LP |
| B6TBM1 | Alpha-soluble NSF attachment protein | 6.64 | 5.7723E-17 | Unique LP |
| B6TDW7 | Secretory protein | 6.64 | 5.7723E-17 | Unique LP |
| B6TIQ8 | ATP/GTP binding protein | 6.64 | 5.7723E-17 | Unique LP |
| B6TJX4 | SnRK1-interacting protein 1 | 6.64 | 5.7723E-17 | Unique LP |
| B6TQ08 | Actin-1 | 6.64 | 5.7723E-17 | Unique LP |
| B6TWN7 | Elongation factor 1-alpha | 6.64 | 5.7723E-17 | Unique LP |
| B6TXN5 | Gibberellin receptor GID1L2 | 6.64 | 5.7723E-17 | Unique LP |
| B6TY16 | SUN domain protein2 | 6.64 | 5.7723E-17 | Unique LP |
| B6UHU1 | Catalase | 6.64 | 5.7723E-17 | Unique LP |
| B7ZXD5 | methenyltetrahydrofolate cyclohydrolase | 6.64 | 5.7723E-17 | Unique LP |
| B7ZZ71 | Cobalt ion binding | 6.64 | 5.7723E-17 | Unique LP |
| B8A1T1 | Peroxidase | 6.64 | 5.7723E-17 | Unique LP |
| C0HDZ4 | S-adenosyl-L-methionine-dependent methyltransferase superfamily protein | 6.64 | 5.7723E-17 | Unique LP |
| C0HIA5 | Eukaryotic initiation factor 4F subunit p150 isoform 1 | 6.64 | 5.7723E-17 | Unique LP |

Supplementary Table 3 – Cont.

| Accession | Description | Fold change (log2) | P value | DEPs: |
|------------------|----------------------------------------------------------|---------------------------|----------------|--------------|
| C0P5X3 | Cytokinin riboside 5'-monophosphate phosphoribohydrolase | 6.64 | 5.7723E-17 | Unique LP |
| C0P6C4 | 4HBT domain-containing protein | 6.64 | 5.7723E-17 | Unique LP |
| C0P6C5 | threonine synthase | 6.64 | 5.7723E-17 | Unique LP |
| C0P7E7 | Actin-interacting protein 1-2 | 6.64 | 5.7723E-17 | Unique LP |
| C0P820 | 3-ketoacyl-CoA thiolase 2 peroxisomal | 6.64 | 5.7723E-17 | Unique LP |
| C0P8C6 | CCT-theta | 6.64 | 5.7723E-17 | Unique LP |
| C0P8K0 | Enoyl-CoA hydratase 1, peroxisomal | 6.64 | 5.7723E-17 | Unique LP |
| C0P8L3 | Carboxypeptidase | 6.64 | 5.7723E-17 | Unique LP |
| C0P944 | 2,4-dienoyl-CoA reductase [(3E)-enoyl-CoA-producing] | 6.64 | 5.7723E-17 | Unique LP |
| C0PBF8 | FAD-dependent oxidoreductase family protein | 6.64 | 5.7723E-17 | Unique LP |
| C0PCK6 | adenylate kinase | 6.64 | 5.7723E-17 | Unique LP |
| C0PD54 | Molybdopterin synthase catalytic subunit | 6.64 | 5.7723E-17 | Unique LP |
| C0PDY0 | Purple acid phosphatase | 6.64 | 5.7723E-17 | Unique LP |
| C0PF34 | Heme-binding-like protein chloroplastic | 6.64 | 5.7723E-17 | Unique LP |
| C0PFA1 | Adenylosuccinate synthetase, chloroplastic | 6.64 | 5.7723E-17 | Unique LP |
| C0PGM6 | 26S protease regulatory subunit S10B homolog B | 6.64 | 5.7723E-17 | Unique LP |
| C0PJA6 | GTP cyclohydrolase II | 6.64 | 5.7723E-17 | Unique LP |
| C0PJM7 | Signal recognition particle 14 kDa protein | 6.64 | 5.7723E-17 | Unique LP |
| C0PPB8 | UDP-glycosyltransferase 76C1 | 6.64 | 5.7723E-17 | Unique LP |
| C6KEM4 | Aminoaldehyde dehydrogenase 2 | 6.64 | 5.7723E-17 | Unique LP |
| K7TFB6 | ABA-responsive protein | 6.64 | 5.7723E-17 | Unique LP |
| K7TNW2 | Leucoanthocyanidin reductase | 6.64 | 5.7723E-17 | Unique LP |
| K7TVE3 | Sucrose-phosphate synthase | 6.64 | 5.7723E-17 | Unique LP |
| K7U557 | dCTP pyrophosphatase 1 | 6.64 | 5.7723E-17 | Unique LP |
| K7U5A5 | 14-3-3-like protein | 6.64 | 5.7723E-17 | Unique LP |
| K7UAQ8 | Putative alcohol dehydrogenase superfamily protein | 6.64 | 5.7723E-17 | Unique LP |
| K7V4Q5 | Proteasome subunit alpha type | 6.64 | 5.7723E-17 | Unique LP |
| K7VJF3 | Heat shock 70 kDa protein 5 | 6.64 | 5.7723E-17 | Unique LP |
| K7VQ25 | Uncharacterized protein | 6.64 | 5.7723E-17 | Unique LP |

Supplementary Table 3 – Cont.

| Accession | Description | Fold change (log2) | P value | DEPs: |
|------------------|--------------------------------------------------|---------------------------|----------------|--------------|
| P04712 | Sucrose synthase 1 | 6.64 | 5.7723E-17 | Unique LP |
| P14640 | Tubulin alpha-1 chain | 6.64 | 5.7723E-17 | Unique LP |
| P24825 | Chalcone synthase C2 | 6.64 | 5.7723E-17 | Unique LP |
| P27787 | Ferredoxin-1, chloroplastic | 6.64 | 5.7723E-17 | Unique LP |
| P50472 | Probable glutathione S-transferase BZ2 | 6.64 | 5.7723E-17 | Unique LP |
| Q41815 | Heat shock protein 26 | 6.64 | 5.7723E-17 | Unique LP |
| Q4FZ53 | Cysteine proteinase inhibitor | 6.64 | 5.7723E-17 | Unique LP |
| Q8LT22 | Nicotianamine synthase | 6.64 | 5.7723E-17 | Unique LP |
| Q8W0V2 | Lipoxygenase | 6.64 | 5.7723E-17 | Unique LP |
| Q9XF14 | Protein BUNDLE SHEATH DEFECTIVE 2, chloroplastic | 6.64 | 5.7723E-17 | Unique LP |

Supplementary Table 4. List of differentially abundant proteins (DEPs) in the P7_LP / P7_HP comparison

| Accession | Description | Fold change (log2) | P value | DEPs: |
|------------|-------------------------------------------------------------------------------------------|--------------------|-------------|-----------|
| A0A1D6FKD0 | Putative 3-hydroxyisobutyrate dehydrogenase-like 3 mitochondrial | -6.64 | 5.28618E-17 | Unique HP |
| A0A1D6H0T6 | 26S proteasome non-ATPase regulatory subunit 2 homolog | -6.64 | 5.28618E-17 | Unique HP |
| A0A1D6I3E1 | Strictosidine synthase 3 | -6.64 | 5.28618E-17 | Unique HP |
| A0A1D6IBV1 | FAD/NAD(P)-binding oxidoreductase family protein | -6.64 | 5.28618E-17 | Unique HP |
| A0A1D6IMZ9 | Peroxidase | -6.64 | 5.28618E-17 | Unique HP |
| A0A1D6JX93 | Peroxisomal nicotinamide adenine dinucleotide carrier | -6.64 | 5.28618E-17 | Unique HP |
| A0A1D6JZU3 | Pathogenesis-related protein 10 | -6.64 | 5.28618E-17 | Unique HP |
| A0A1D6L4Z0 | Cytochrome b5 isoform A | -6.64 | 5.28618E-17 | Unique HP |
| A0A1D6L886 | Germin-like protein | -6.64 | 5.28618E-17 | Unique HP |
| A0A1D6NDZ0 | Tryptophan aminotransferase-related protein 4 | -6.64 | 5.28618E-17 | Unique HP |
| A0A804LK58 | HMA domain-containing protein | -6.64 | 5.28618E-17 | Unique HP |
| A0A804LKZ4 | Uncharacterized protein | -6.64 | 5.28618E-17 | Unique HP |
| A0A804MST0 | Genome assembly, chromosome: II | -6.64 | 5.28618E-17 | Unique HP |
| A0A804NBT6 | Cysteine synthase | -6.64 | 5.28618E-17 | Unique HP |
| A0A804PDB7 | chitinase | -6.64 | 5.28618E-17 | Unique HP |
| A0A804PES5 | Aha1_N domain-containing protein | -6.64 | 5.28618E-17 | Unique HP |
| A0A804PNN3 | TPR_REGION domain-containing protein | -6.64 | 5.28618E-17 | Unique HP |
| A0A804PZG8 | 4-hydroxy-7-methoxy-3-oxo-3,4-dihydro-2H-1,4-benzoxazin-2-yl glucoside beta-D-glucosidase | -6.64 | 5.28618E-17 | Unique HP |
| A0A804Q3Z6 | SCP domain-containing protein | -6.64 | 5.28618E-17 | Unique HP |
| A0A804QA42 | GDSL esterase/lipase | -6.64 | 5.28618E-17 | Unique HP |
| A0A804QUL8 | Integral membrane protein | -6.64 | 5.28618E-17 | Unique HP |
| A0A804RDS0 | Laccase | -6.64 | 5.28618E-17 | Unique HP |
| A0A804UH55 | UBP1-associated protein 2C | -6.64 | 5.28618E-17 | Unique HP |
| A1JUJ0 | inositol-3-phosphate synthase | -6.64 | 5.28618E-17 | Unique HP |
| B4F861 | IAA-amino acid hydrolase ILR1-like 4 | -6.64 | 5.28618E-17 | Unique HP |
| B4F8F0 | Nudix hydrolase 23 chloroplastic | -6.64 | 5.28618E-17 | Unique HP |
| B4FAQ2 | Pyridoxal phosphate homeostasis protein | -6.64 | 5.28618E-17 | Unique HP |
| B4FE28 | E2F transcription factor-like E2FE | -6.64 | 5.28618E-17 | Unique HP |
| B4FIE9 | S-adenosylmethionine synthase | -6.64 | 5.28618E-17 | Unique HP |

Supplementary Table 4 – Cont.

| Accession | Description | Fold change (log2) | P value | DEPs: |
|------------------|-----------------------------------------------------------|---------------------------|----------------|--------------|
| B4FKD5 | Eukaryotic translation initiation factor 6 | -6.64 | 5.29E-17 | Unique HP |
| B4FM15 | 60S ribosomal protein L28-1 | -6.64 | 5.28618E-17 | Unique HP |
| B4FSA8 | GDSL esterase/lipase | -6.64 | 5.28618E-17 | Unique HP |
| B4FV63 | Nuclear transport factor 2 (NTF2) family protein | -6.64 | 5.28618E-17 | Unique HP |
| B4FWC4 | Splicing factor CC1-like | -6.64 | 5.28618E-17 | Unique HP |
| B4FWR7 | 60S ribosomal protein L13 | -6.64 | 5.28618E-17 | Unique HP |
| B4G1N1 | RmlD_sub_bind domain-containing protein | -6.64 | 5.28618E-17 | Unique HP |
| B6SUW7 | Protein LURP-one-related 5-like | -6.64 | 5.28618E-17 | Unique HP |
| B6SZF2 | DUF1995 domain-containing protein | -6.64 | 5.28618E-17 | Unique HP |
| B6T144 | B12D protein | -6.64 | 5.28618E-17 | Unique HP |
| B6T5I9 | Immature colon carcinoma transcript 1 protein | -6.64 | 5.28618E-17 | Unique HP |
| B6TEJ4 | Peptidase C15 pyroglutamyl peptidase I-like | -6.64 | 5.28618E-17 | Unique HP |
| B6TVU2 | Prefoldin subunit 5 | -6.64 | 5.28618E-17 | Unique HP |
| B6UE26 | 60S ribosomal protein L34 | -6.64 | 5.28618E-17 | Unique HP |
| B8A324 | Carboxypeptidase | -6.64 | 5.28618E-17 | Unique HP |
| C0HFU7 | Phospholipase D | -6.64 | 5.28618E-17 | Unique HP |
| C0P6T4 | Uncharacterized protein | -6.64 | 5.28618E-17 | Unique HP |
| C0PD54 | Molybdopterin synthase catalytic subunit | -6.64 | 5.28618E-17 | Unique HP |
| K7U9C9 | RNA helicase | -6.64 | 5.28618E-17 | Unique HP |
| K7UBG1 | peptidylprolyl isomerase | -6.64 | 5.28618E-17 | Unique HP |
| K7UNY3 | Glycosyltransferase | -6.64 | 5.28618E-17 | Unique HP |
| K7UR46 | Glutamyl-tRNA reductase-binding protein chloroplastic | -6.64 | 5.28618E-17 | Unique HP |
| K7VDC0 | Peroxidase | -6.64 | 5.28618E-17 | Unique HP |
| P10979 | Glycine-rich RNA-binding, abscisic acid-inducible protein | -6.64 | 5.28618E-17 | Unique HP |
| P25459 | 30S ribosomal protein S18, chloroplastic | -6.64 | 5.28618E-17 | Unique HP |
| P28523 | Casein kinase II subunit alpha | -6.64 | 5.28618E-17 | Unique HP |
| P42390 | Indole-3-glycerol phosphate lyase, chloroplastic | -6.64 | 5.28618E-17 | Unique HP |
| Q6JAD2 | Ferredoxin | -6.64 | 5.28618E-17 | Unique HP |
| Q84VG9 | Lycopene beta cyclase chloroplastic | -6.64 | 5.28618E-17 | Unique HP |
| C0PEH3 | ThiC-associated domain-containing protein | -4.27 | 8.27699E-08 | DOWN |

Supplementary Table 4 – Cont.

| Accession | Description | Fold change (log2) | P value | DEPs: |
|------------------|----------------------------------------------------|---------------------------|----------------|--------------|
| A0A804UCH1 | Glucose-1-phosphate adenylyltransferase | -4.18 | 1.09551E-06 | DOWN |
| A0A096RSU8 | Peptidase family M48 family protein | -3.73 | 0.000217877 | DOWN |
| Q947B9 | Glucose-1-phosphate adenylyltransferase | -3.65 | 4.0334E-12 | DOWN |
| C0PHM2 | Pollen receptor-like kinase 4 | -3.2 | 0.001698148 | DOWN |
| P25461 | 50S ribosomal protein L33, chloroplastic | -3.15 | 0.000257683 | DOWN |
| A0A804RV03 | Ribosomal_S3_C domain-containing protein | -3 | 0.000110917 | DOWN |
| B4FKB3 | 50S ribosomal protein L31 | -2.98 | 4.17752E-06 | DOWN |
| B4FZL4 | Chlorophyll a-b binding protein, chloroplastic | -2.93 | 0.004538052 | DOWN |
| C0HGH7 | Universal stress family protein | -2.9 | 0.005974737 | DOWN |
| A0A1D6MBR0 | Serine/threonine-protein kinase STN7 chloroplastic | -2.8 | 0.001193318 | DOWN |
| B4FLV6 | Protein translation factor SUI1 | -2.79 | 0.004877888 | DOWN |
| P16037 | 30S ribosomal protein S2, chloroplastic | -2.74 | 0.000679908 | DOWN |
| A0A804QKD5 | Glutathione hydrolase | -2.59 | 0.013786182 | DOWN |
| A0A1D6JSL7 | inositol-3-phosphate synthase | -2.57 | 6.07444E-05 | DOWN |
| B4F9J1 | Beta-galactosidase | -2.46 | 0.027784646 | DOWN |
| P08527 | 30S ribosomal protein S14, chloroplastic | -2.42 | 0.005531953 | DOWN |
| B4FXB9 | FLU | -2.41 | 0.009779924 | DOWN |
| A0A804U9G4 | PAP_fibrillin domain-containing protein | -2.35 | 0.017633436 | DOWN |
| P06588 | 30S ribosomal protein S19, chloroplastic | -2.34 | 2.31598E-05 | DOWN |
| B4FUZ9 | 50S ribosomal protein L15 chloroplastic | -2.34 | 0.001994452 | DOWN |
| A0A1D6KJ07 | N-acyl-aliphatic-L-amino acid amidohydrolase | -2.3 | 0.000840316 | DOWN |
| A0A1D6IKI2 | RNA binding protein 1 | -2.29 | 0.000517293 | DOWN |
| B6U581 | Ribosome-like protein | -2.27 | 0.000555371 | DOWN |
| C0HHM6 | Thioredoxin family protein | -2.24 | 0.03133041 | DOWN |
| A0A804N941 | Secreted protein | -2.23 | 0.019602013 | DOWN |
| A0A3L6E5Y7 | Plasma membrane ATPase | -2.2 | 0.004113137 | DOWN |
| A0A804M2J7 | 30S ribosomal protein S13, chloroplastic | -2.18 | 0.000403618 | DOWN |
| A0A1D6QU12 | glutaminase | -2.14 | 0.040189866 | DOWN |
| B6SST7 | 50S ribosomal protein L5, chloroplastic | -2.12 | 0.000147936 | DOWN |
| B4G1Q5 | 50S ribosomal protein L10 chloroplastic | -2.07 | 0.000179128 | DOWN |
| A5GZ73 | Glucose-1-phosphate adenylyltransferase | -2.06 | 0.00015571 | DOWN |
| P09387 | 50S ribosomal protein L23, chloroplastic | -2.06 | 0.000313635 | DOWN |
| B4FJG1 | Chlorophyll a-b binding protein, chloroplastic | -2.03 | 0.000195509 | DOWN |
| B4FA79 | Calcium-binding EF hand family protein | -2.03 | 0.000778567 | DOWN |

Supplementary Table 4 – Cont.

| Accession | Description | Fold change (log2) | P value | DEPs: |
|------------------|-------------------------------------------------|---------------------------|----------------|--------------|
| B6U1J2 | 50S ribosomal protein L11 | -2.01 | 0.000228307 | DOWN |
| P08529 | 50S ribosomal protein L14, chloroplastic | -2.01 | 0.000237957 | DOWN |
| P08528 | 50S ribosomal protein L16, chloroplastic | -2 | 0.010665309 | DOWN |
| C0PF34 | Heme-binding-like protein chloroplastic | -1.95 | 0.012280495 | DOWN |
| B6TT66 | Ribosome-like protein | -1.94 | 0.002381582 | DOWN |
| A0A804R6R9 | Ribosomal_S10 domain-containing protein | -1.92 | 0.002993334 | DOWN |
| P27723 | 30S ribosomal protein S16, chloroplastic | -1.91 | 0.001777134 | DOWN |
| Q84TC2 | DIBOA-glucoside dioxygenase BX6 | -1.91 | 0.010613479 | DOWN |
| A0A804LKH5 | 50S ribosomal protein L6, chloroplastic | -1.89 | 0.000597802 | DOWN |
| B6SUJ3 | Plastid-specific 30S ribosomal protein 2 | -1.87 | 0.002885405 | DOWN |
| B4FU53 | 50S ribosomal protein L9, chloroplastic | -1.81 | 0.001065321 | DOWN |
| A0A1D6MMA5 | Multicopper oxidase LPR2 | -1.78 | 0.046079322 | DOWN |
| A0A1D6M323 | Ribosomal protein | -1.77 | 0.001478892 | DOWN |
| B6SUJ0 | 50S ribosomal protein L10 | -1.77 | 0.04931877 | DOWN |
| A0A1D6KLE2 | PWWP domain protein | -1.75 | 0.002993334 | DOWN |
| A0A804Q515 | PsbP domain-containing protein | -1.74 | 0.001745194 | DOWN |
| B4FV96 | Uncharacterized protein | -1.73 | 0.001880437 | DOWN |
| A0A804P2H5 | 50S ribosomal protein L21 | -1.72 | 0.002070105 | DOWN |
| A0A804PCP6 | KOW domain-containing protein | -1.72 | 0.002993334 | DOWN |
| Q9TJN6 | 30S ribosomal protein S17, chloroplastic | -1.71 | 0.002692246 | DOWN |
| B4FDG7 | RNA-binding (RRM/RBD/RNP motifs) family protein | -1.71 | 0.040982871 | DOWN |
| B6UIC1 | 50S ribosomal protein L12-1 | -1.66 | 0.003030973 | DOWN |
| B6T4J1 | 50S ribosomal protein L6 | -1.64 | 0.027066866 | DOWN |
| B4FL55 | Chlorophyll a-b binding protein, chloroplastic | -1.58 | 0.005329373 | DOWN |
| P48183 | Photosystem II protein D1 | -1.58 | 0.00533379 | DOWN |
| B7ZZM5 | Cell wall invertase | -1.57 | 0.013306096 | DOWN |
| B6SR22 | 50S ribosomal protein L12-1 | -1.54 | 0.023620353 | DOWN |
| B4FZP0 | Mg-protoporphyrin IX chelatase | -1.54 | 0.046108931 | DOWN |
| B4FH16 | 30S ribosomal protein 3 chloroplastic | -1.52 | 0.045048692 | DOWN |
| B4G1J8 | 50S ribosomal protein L3-1 chloroplastic | -1.46 | 0.010778841 | DOWN |
| B4FSZ8 | Beta alanine synthase1 | -1.46 | 0.013056584 | DOWN |
| C0PEC4 | 30S ribosomal protein S5 chloroplastic | -1.45 | 0.011444943 | DOWN |
| A0A804M4P0 | 30S ribosomal protein S9, chloroplastic | -1.45 | 0.014056594 | DOWN |
| A0A804UH90 | Thiamine thiazole synthase, chloroplastic | -1.45 | 0.01953458 | DOWN |
| A0A1X7YHF7 | Photosystem II D2 protein | -1.43 | 0.013333506 | DOWN |

Supplementary Table 4 – Cont.

| Accession | Description | Fold change (log2) | P value | DEPs: |
|------------|-----------------------------------------------------------------|--------------------|-------------|-------|
| A0A804UD88 | 30S ribosomal protein 2, chloroplastic | -1.36 | 0.019898142 | DOWN |
| B6T0F9 | Thylakoid soluble phosphoprotein TSP9 | -1.34 | 0.039659943 | DOWN |
| A0A804PJS0 | HMA domain-containing protein | -1.31 | 0.026176507 | DOWN |
| Q41746 | Chlorophyll a-b binding protein, chloroplastic | -1.31 | 0.026264039 | DOWN |
| B4FSD8 | plastoquinol--plastocyanin reductase | -1.28 | 0.030882655 | DOWN |
| K7TXI5 | Chlorophyll a-b binding protein, chloroplastic | -1.27 | 0.032717521 | DOWN |
| P05641 | Photosystem II CP47 reaction center protein | -1.26 | 0.03332418 | DOWN |
| P24993 | Photosystem II reaction center protein H | -1.26 | 0.033923926 | DOWN |
| B6SQV5 | Photosystem II 10 kDa polypeptide, chloroplastic | -1.23 | 0.040398137 | DOWN |
| B4FUZ5 | 30S ribosomal protein S1 | -1.22 | 0.039659943 | DOWN |
| Q41739 | Thiamine thiazole synthase 2, chloroplastic | -1.22 | 0.040985409 | DOWN |
| A0A1D6KCZ2 | alanine transaminase | -1.2 | 0.045166112 | DOWN |
| B4G1A1 | Photosystem II 5 kDa protein, chloroplastic | -1.19 | 0.04950119 | DOWN |
| C4J9R0 | PLAT domain-containing protein 3 | 1.51 | 0.044896291 | UP |
| A0A804RKJ9 | Ribulose bisphosphate carboxylase large chain | 1.53 | 0.040189866 | UP |
| A0A1D6N1Z8 | 6-phosphogluconate dehydrogenase, decarboxylating | 1.54 | 0.037903317 | UP |
| A0A1D6I1V3 | phosphoenolpyruvate carboxylase | 1.54 | 0.038363574 | UP |
| B5AK47 | Dhurrinase-like B-glucosidase | 1.54 | 0.038860476 | UP |
| A0A1D6KE93 | Purple acid phosphatase | 1.58 | 0.026722194 | UP |
| C0PAU7 | Glucose-6-phosphate isomerase | 1.69 | 0.016851853 | UP |
| C4JAX7 | UDP-sulfoquinovose synthase chloroplastic | 1.77 | 0.010521664 | UP |
| P46420 | Glutathione S-transferase 4 | 1.8 | 0.009060986 | UP |
| C0P4M0 | Monodehydroascorbate reductase 1 peroxisomal | 1.81 | 0.036720138 | UP |
| A0A1D6GVM3 | Delta-aminolevulinic acid dehydratase | 1.84 | 0.006999163 | UP |
| A0A804LY89 | TIC110 | 1.85 | 0.021708954 | UP |
| C0PAS9 | Alba DNA/RNA-binding protein | 1.9 | 0.013932701 | UP |
| B7ZWY9 | Citrate synthase | 1.9 | 0.026010865 | UP |
| B6TNF1 | Calnexin | 1.97 | 0.024307828 | UP |
| C4J410 | Heat shock 70 kDa protein | 2.01 | 0.002268263 | UP |
| A0A1R3QF47 | Chloroplast stem-loop binding protein of 41 kDa a chloroplastic | 2.01 | 0.010409623 | UP |
| B4G1R6 | Chalcone-flavonone isomerase family protein | 2.03 | 0.035608636 | UP |
| A0A804MG95 | Abscisic stress ripening protein 2 | 2.04 | 0.008972146 | UP |
| B4F9L9 | Elongated mesocotyl2 | 2.24 | 0.032982512 | UP |
| B6SRJ5 | sulfate adenyllyltransferase | 2.25 | 0.02222414 | UP |
| B4FLA2 | Chorismate synthase | 2.26 | 0.014823865 | UP |

Supplementary Table 4 – Cont.

| Accession | Description | Fold change (log2) | P value | DEPs: |
|------------|----------------------------------------------------|--------------------|-------------|-------|
| B6TEX0 | Inositol-1-monophosphatase | 2.27 | 0.000641509 | UP |
| A0A804U9S7 | Epimerase domain-containing protein | 2.29 | 0.0002779 | UP |
| Q49HD7 | 12-oxo-phytodienoic acid reductase | 2.29 | 0.008848019 | UP |
| A0A1D6K5D2 | Nucleoredoxin1 | 2.32 | 0.000215795 | UP |
| A0A1D6LCQ2 | SLH domain-containing protein | 2.36 | 0.004045389 | UP |
| B4FZW5 | Malate dehydrogenase | 2.37 | 0.028102949 | UP |
| B4F9L6 | Purple acid phosphatase | 2.38 | 0.000105749 | UP |
| B4FBK8 | 3-ketoacyl-CoA thiolase 2 peroxisomal | 2.38 | 0.025128191 | UP |
| A0A1D6JNJ8 | Lethal leaf-spot 1 | 2.46 | 0.000657495 | UP |
| A0A804UF48 | Peptidyl-prolyl cis-trans isomerase | 2.47 | 0.010026107 | UP |
| Q29SB6 | Pathogenesis-related protein 10 | 2.53 | 0.000458211 | UP |
| A0A804QL16 | Salt stress root protein RS1 | 2.53 | 0.004742669 | UP |
| C0PMP2 | riboflavin kinase | 2.53 | 0.034975061 | UP |
| A0A1D6H6F1 | Citrate synthase | 2.56 | 0.033174353 | UP |
| C4JBG7 | 3-isopropylmalate dehydratase | 2.57 | 0.001182769 | UP |
| B4F9P0 | Glycosyltransferase | 2.61 | 0.02204157 | UP |
| B4FWT5 | inorganic diphosphatase | 2.62 | 0.009119899 | UP |
| A0A804QPS7 | GTP cyclohydrolase II | 2.62 | 0.028231254 | UP |
| B4F7Z4 | glycerophosphodiester phosphodiesterase | 2.68 | 8.16333E-05 | UP |
| A0A1D6DSU2 | K(+) efflux antiporter 2 chloroplastic | 2.69 | 0.000569941 | UP |
| C0PFV4 | Chaperone protein ClpC1 chloroplastic | 2.89 | 1.1847E-05 | UP |
| B4FTQ1 | Arginase 1 mitochondrial | 2.89 | 0.022228171 | UP |
| Q9SAZ6 | phosphoenolpyruvate carboxylase | 2.96 | 1.97878E-05 | UP |
| A0A804PCL4 | Peroxidase | 2.96 | 0.040189866 | UP |
| A0A1D6HL18 | ER6 protein | 2.98 | 0.035548704 | UP |
| B4FWV7 | NAD(P)-binding Rossmann-fold superfamily protein | 3.02 | 0.039239078 | UP |
| A0A1D6ES79 | MLO-like protein | 3.02 | 0.049005992 | UP |
| C0P7Z0 | Peptidase A1 domain-containing protein | 3.05 | 0.004111996 | UP |
| P93629 | Alcohol dehydrogenase class-3 | 3.05 | 0.020323528 | UP |
| P49105 | Glucose-6-phosphate isomerase, cytosolic | 3.06 | 8.18011E-06 | UP |
| A0A804LSV9 | SHSP domain-containing protein | 3.07 | 0.001653767 | UP |
| C0PDB6 | HXXXD-type acyl-transferase family protein | 3.07 | 0.007359685 | UP |
| A0A804QPJ4 | Heat shock 70 kDa protein 14 | 3.09 | 0.038472778 | UP |
| A0A804R4S8 | ACB domain-containing protein | 3.1 | 0.003946784 | UP |
| C0P732 | Hsp70-Hsp90 organizing protein 3 | 3.1 | 0.032920186 | UP |
| A0A804UHW9 | Heme-binding-like protein At3g10130, chloroplastic | 3.13 | 7.49609E-08 | UP |
| B4FSG1 | Photosystem I assembly factor PSA3, chloroplastic | 3.16 | 0.046108931 | UP |

Supplementary Table 4 – Cont.

| Accession | Description | Fold change (log2) | P value | DEPs: |
|------------|--------------------------------------------------------------------------------------------|--------------------|-------------|-----------|
| B4FWI4 | D-3-phosphoglycerate dehydrogenase | 3.17 | 6.40804E-08 | UP |
| A0A1D6NVZ6 | 3-phosphoshikimate 1-carboxyvinyltransferase | 3.17 | 0.022600204 | UP |
| K7UGR2 | Putative TCP-1/cpn60 chaperonin family protein isoform 1 | 3.18 | 0.000618819 | UP |
| A0A804R5V2 | Asparagine synthetase [glutamine-hydrolyzing] | 3.18 | 0.042448234 | UP |
| B6SM26 | 3-oxoacyl-synthase III | 3.19 | 0.018698081 | UP |
| C4JAC1 | mannose-1-phosphate guanylyltransferase | 3.24 | 0.025412207 | UP |
| A0A1D6FD96 | leucine--tRNA ligase | 3.26 | 0.020666919 | UP |
| Q9FQA3 | Glutathione transferase GST 23 | 3.28 | 0.014327511 | UP |
| B4FI76 | adenylate kinase | 3.3 | 0.019324818 | UP |
| B8A230 | DUF1338 domain-containing protein | 3.37 | 0.000269368 | UP |
| B6SYB7 | Arogenate dehydratase | 3.41 | 0.018698081 | UP |
| A0A804MIN3 | Pullulanase 1, chloroplastic | 3.44 | 0.014006697 | UP |
| A0A1D6MY33 | Glutathione transferase18 | 3.44 | 0.022544798 | UP |
| A0A1D6EC46 | Double Clp-N motif-containing P-loop nucleoside triphosphate hydrolase superfamily protein | 3.48 | 0.000600646 | UP |
| A0A804QWE5 | Sucrose-phosphate synthase | 3.48 | 0.007436337 | UP |
| B6U0C2 | Phenazine biosynthesis PhzC/PhzF protein | 3.5 | 0.011703194 | UP |
| B6TZD1 | Methylthioribose-1-phosphate isomerase | 3.52 | 0.009915326 | UP |
| B6SH12 | Win1 | 3.54 | 0.004810443 | UP |
| A0A1D6EBS5 | 1,4-alpha-glucan branching enzyme | 3.58 | 7.22195E-07 | UP |
| O64960 | 23.6 kDa heat shock protein mitochondrial | 3.59 | 2.64095E-05 | UP |
| B4FBD6 | Ribonuclease 1 | 3.75 | 0.000161216 | UP |
| B6SP44 | Glutamate carboxypeptidase 2 | 3.75 | 0.005505017 | UP |
| A0A1D6N1P4 | Putative inactive purple acid phosphatase 16 | 3.79 | 0.000663098 | UP |
| K7VYS6 | PLC-like phosphodiesterases superfamily protein | 3.85 | 4.34758E-09 | UP |
| K7TWH1 | peptidylprolyl isomerase | 4 | 0.001109957 | UP |
| B4FRQ8 | Spermidine hydroxycinnamoyl transferase | 4.07 | 8.9818E-05 | UP |
| C0HI30 | UDP-glucose 4-epimerase | 4.09 | 0.000256914 | UP |
| Q6JN56 | Acc oxidase | 4.49 | 2.04719E-05 | UP |
| B6T2X7 | Histone H1 | 5.26 | 1.81462E-05 | UP |
| A0A804N0J5 | Aspergillus nuclease S1 | 5.44 | 1.47678E-09 | UP |
| B8A2L4 | Starch synthase, chloroplastic/amyloplastic | 5.98 | 5.28618E-17 | UP |
| B6T329 | Aspergillus nuclease S1 | 5.99 | 5.28618E-17 | UP |
| A0A096SFU6 | Lysine--tRNA ligase | 6.64 | 5.28618E-17 | Unique LP |
| A0A096SRM5 | UDP-glycosyltransferase 708A6 | 6.64 | 5.28618E-17 | Unique LP |

Supplementary Table 4 – Cont.

| Accession | Description | Fold change (log2) | P value | DEPs: |
|------------------|----------------------------------------------------------|---------------------------|----------------|--------------|
| A0A096TH11 | DEK domain-containing chromatin associated protein | 6.64 | 5.28618E-17 | Unique LP |
| A0A1D6DQH1 | Acetyl-coenzyme A synthetase | 6.64 | 5.28618E-17 | Unique LP |
| A0A1D6DUX6 | 26S proteasome non-ATPase regulatory subunit 7 homolog A | 6.64 | 5.28618E-17 | Unique LP |
| A0A1D6DZR9 | AICARFT/IMPCHase bienzyme family protein | 6.64 | 5.28618E-17 | Unique LP |
| A0A1D6E272 | Superoxide dismutase copper chaperone | 6.64 | 5.28618E-17 | Unique LP |
| A0A1D6EC40 | Trihelix transcription factor ASR3 | 6.64 | 5.28618E-17 | Unique LP |
| A0A1D6F9V3 | valine--tRNA ligase | 6.64 | 5.28618E-17 | Unique LP |
| A0A1D6FKF7 | Aspartic proteinase A1 | 6.64 | 5.28618E-17 | Unique LP |
| A0A1D6GBA2 | phosphoenolpyruvate carboxylase | 6.64 | 5.28618E-17 | Unique LP |
| A0A1D6GIP9 | Adenylyl cyclase-associated protein | 6.64 | 5.28618E-17 | Unique LP |
| A0A1D6HR96 | Purple acid phosphatase | 6.64 | 5.28618E-17 | Unique LP |
| A0A1D6I3N3 | Alpha-amylase | 6.64 | 5.28618E-17 | Unique LP |
| A0A1D6I6A1 | Isoamylase-type starch debranching enzyme3 | 6.64 | 5.28618E-17 | Unique LP |
| A0A1D6IIP0 | Cysteine proteinases superfamily protein | 6.64 | 5.28618E-17 | Unique LP |
| A0A1D6IPJ2 | Ketol-acid reductoisomerase chloroplastic | 6.64 | 5.28618E-17 | Unique LP |
| A0A1D6JA02 | Triglyceride lipases | 6.64 | 5.28618E-17 | Unique LP |
| A0A1D6JJ37 | Farnesylcysteine lyase | 6.64 | 5.28618E-17 | Unique LP |
| A0A1D6JSN1 | T-complex protein 1 subunit gamma | 6.64 | 5.28618E-17 | Unique LP |
| A0A1D6K7T5 | chitinase | 6.64 | 5.28618E-17 | Unique LP |
| A0A1D6K864 | Proline dehydrogenase | 6.64 | 5.28618E-17 | Unique LP |
| A0A1D6KV33 | acylaminoacyl-peptidase | 6.64 | 5.28618E-17 | Unique LP |
| A0A1D6LSA6 | Heme oxygenase2 | 6.64 | 5.28618E-17 | Unique LP |
| A0A1D6LTL9 | Alpha-glucan water dikinase 1 chloroplastic | 6.64 | 5.28618E-17 | Unique LP |
| A0A1D6LY56 | galactinol--sucrose galactosyltransferase | 6.64 | 5.28618E-17 | Unique LP |
| A0A1D6LYR3 | arginine--tRNA ligase | 6.64 | 5.28618E-17 | Unique LP |
| A0A1D6M1Y6 | UDP-glucuronate decarboxylase | 6.64 | 5.28618E-17 | Unique LP |
| A0A1D6M275 | Malic enzyme | 6.64 | 5.28618E-17 | Unique LP |
| A0A1D6MAK9 | Phosphotransferase | 6.64 | 5.28618E-17 | Unique LP |
| A0A1D6MPN8 | Importin subunit alpha | 6.64 | 5.28618E-17 | Unique LP |
| A0A1D6N309 | Dynammin-related protein 3A | 6.64 | 5.28618E-17 | Unique LP |

Supplementary Table 4 – Cont.

| Accession | Description | Fold change (log2) | P value | DEPs: |
|------------------|----------------------------------------------------------------------------|---------------------------|----------------|--------------|
| A0A1D6N7A4 | Acyl-coenzyme A oxidase | 6.64 | 5.28618E-17 | Unique LP |
| A0A1D6NE76 | cytidine deaminase | 6.64 | 5.28618E-17 | Unique LP |
| A0A1D6NMU7 | Ubiquitin carboxyl-terminal hydrolase | 6.64 | 5.28618E-17 | Unique LP |
| A0A1D6QK75 | Heat shock protein 90-5 chloroplastic | 6.64 | 5.28618E-17 | Unique LP |
| A0A1D6QNT3 | 3-hydroxybutyryl-CoA epimerase | 6.64 | 5.28618E-17 | Unique LP |
| A0A3L6EGC3 | Germin-like protein | 6.64 | 5.28618E-17 | Unique LP |
| A0A3L6EYR2 | Putrescine hydroxycinnamoyltransferase 1 | 6.64 | 5.28618E-17 | Unique LP |
| A0A804LD84 | 2Fe-2S ferredoxin-type domain-containing protein | 6.64 | 5.28618E-17 | Unique LP |
| A0A804M7G3 | Elongation factor Tu | 6.64 | 5.28618E-17 | Unique LP |
| A0A804M8K6 | Abhydrolase_2 domain-containing protein | 6.64 | 5.28618E-17 | Unique LP |
| A0A804M914 | Plasma membrane ATPase | 6.64 | 5.28618E-17 | Unique LP |
| A0A804MFI4 | Serine carboxypeptidase-like 18 | 6.64 | 5.28618E-17 | Unique LP |
| A0A804MJ55 | DUF6598 domain-containing protein | 6.64 | 5.28618E-17 | Unique LP |
| A0A804MJ71 | Expansin-like CBD domain-containing protein | 6.64 | 5.28618E-17 | Unique LP |
| A0A804MMD1 | D-isomer specific 2-hydroxyacid dehydrogenase family protein | 6.64 | 5.28618E-17 | Unique LP |
| A0A804MQX0 | Purple acid phosphatase | 6.64 | 5.28618E-17 | Unique LP |
| A0A804MS81 | 5-formyltetrahydrofolate cyclo-ligase | 6.64 | 5.28618E-17 | Unique LP |
| A0A804MZU9 | AA_TRNA_LIGASE_II domain-containing protein | 6.64 | 5.28618E-17 | Unique LP |
| A0A804N3I3 | shikimate dehydrogenase (NADP(+)) | 6.64 | 5.28618E-17 | Unique LP |
| A0A804NGD9 | UDPGT domain-containing protein | 6.64 | 5.28618E-17 | Unique LP |
| A0A804NH15 | Histone H2A | 6.64 | 5.28618E-17 | Unique LP |
| A0A804NKR4 | Sucrose-phosphate synthase | 6.64 | 5.28618E-17 | Unique LP |
| A0A804NLT9 | LRRNT_2 domain-containing protein | 6.64 | 5.28618E-17 | Unique LP |
| A0A804NR87 | MIR domain-containing protein | 6.64 | 5.28618E-17 | Unique LP |
| A0A804NU88 | Peroxisomal biogenesis factor 19 | 6.64 | 5.28618E-17 | Unique LP |
| A0A804NWX6 | Short-chain dehydrogenase/reductase SDR | 6.64 | 5.28618E-17 | Unique LP |
| A0A804NZC5 | Glutamyl-tRNA(Gln) amidotransferase subunit B, chloroplastic/mitochondrial | 6.64 | 5.28618E-17 | Unique LP |
| A0A804PH92 | AAA domain-containing protein | 6.64 | 5.28618E-17 | Unique LP |
| A0A804PQM0 | Enoyl reductase (ER) domain-containing protein | 6.64 | 5.28618E-17 | Unique LP |
| A0A804PV51 | chitinase | 6.64 | 5.28618E-17 | Unique LP |

Supplementary Table 4 – Cont.

| Accession | Description | Fold change (log2) | P value | DEPs: |
|------------------|---------------------------------------------------------|---------------------------|----------------|--------------|
| A0A804Q1R0 | Nucleosome assembly protein 1-like 1 | 6.64 | 5.28618E-17 | Unique LP |
| A0A804Q2Q4 | Clp R domain-containing protein | 6.64 | 5.28618E-17 | Unique LP |
| A0A804Q7P0 | Creatinase_N domain-containing protein | 6.64 | 5.28618E-17 | Unique LP |
| A0A804QGD4 | X8 domain-containing protein | 6.64 | 5.28618E-17 | Unique LP |
| A0A804QH05 | Cysteine proteinase inhibitor | 6.64 | 5.28618E-17 | Unique LP |
| A0A804QJX5 | 3-hydroxybutyryl-CoA epimerase | 6.64 | 5.28618E-17 | Unique LP |
| A0A804QJZ5 | Dihydrolipoyl dehydrogenase | 6.64 | 5.28618E-17 | Unique LP |
| A0A804QRA7 | Cofac_haem_bdg domain-containing protein | 6.64 | 5.28618E-17 | Unique LP |
| A0A804R266 | HP domain-containing protein | 6.64 | 5.28618E-17 | Unique LP |
| A0A804R7L0 | Serine/arginine-rich-splicing factor SR34 | 6.64 | 5.28618E-17 | Unique LP |
| A0A804R8U9 | Metallophos_C domain-containing protein | 6.64 | 5.28618E-17 | Unique LP |
| A0A804RBM1 | glutathione transferase | 6.64 | 5.28618E-17 | Unique LP |
| A0A804RBS0 | Ferritin | 6.64 | 5.28618E-17 | Unique LP |
| A0A804RDU6 | Long-chain-fatty-acid--CoA ligase | 6.64 | 5.28618E-17 | Unique LP |
| A0A804RFN4 | tyrosine--tRNA ligase | 6.64 | 5.28618E-17 | Unique LP |
| A0A804RJY8 | Pyruvate kinase | 6.64 | 5.28618E-17 | Unique LP |
| A0A804RKE9 | NAD(P)-binding Rossmann-fold superfamily protein | 6.64 | 5.28618E-17 | Unique LP |
| A0A804RNZ5 | Trypsin family protein | 6.64 | 5.28618E-17 | Unique LP |
| A0A804UAN7 | Tubulin beta chain | 6.64 | 5.28618E-17 | Unique LP |
| A0A804UB26 | dynamamin GTPase | 6.64 | 5.28618E-17 | Unique LP |
| A0A804UBB7 | J domain-containing protein | 6.64 | 5.28618E-17 | Unique LP |
| A0A804UL17 | Uncharacterized protein | 6.64 | 5.28618E-17 | Unique LP |
| A5H454 | Peroxidase 66 | 6.64 | 5.28618E-17 | Unique LP |
| B1P123 | TRIBOA-glucoside O-methyltransferase BX7 | 6.64 | 5.28618E-17 | Unique LP |
| B4F7W4 | Putative inactive shikimate kinase like 2 chloroplastic | 6.64 | 5.28618E-17 | Unique LP |
| B4F912 | Serine carboxypeptidase-like 19 | 6.64 | 5.28618E-17 | Unique LP |
| B4F976 | 17.4 kDa class I heat shock protein | 6.64 | 5.28618E-17 | Unique LP |
| B4F9B2 | Acetyl-CoA acetyltransferase, cytosolic 1 | 6.64 | 5.28618E-17 | Unique LP |
| B4F9C4 | HXXXD-type acyl-transferase family protein | 6.64 | 5.28618E-17 | Unique LP |
| B4FAB2 | Molecular chaperone Hsp40/DnaJ family protein | 6.64 | 5.28618E-17 | Unique LP |

Supplementary Table 4 – Cont.

| Accession | Description | Fold change (log2) | P value | DEPs: |
|------------------|-----------------------------------------------------------------------------------------|---------------------------|----------------|--------------|
| B4FAL8 | Methanethiol oxidase | 6.64 | 5.28618E-17 | Unique LP |
| B4FAT6 | Glycosyltransferase | 6.64 | 5.28618E-17 | Unique LP |
| B4FBW5 | Mannitol dehydrogenase | 6.64 | 5.28618E-17 | Unique LP |
| B4FCR7 | inorganic diphosphatase | 6.64 | 5.28618E-17 | Unique LP |
| B4FG53 | Malate dehydrogenase | 6.64 | 5.28618E-17 | Unique LP |
| B4FGY0 | Calcyclin-binding protein | 6.64 | 5.28618E-17 | Unique LP |
| B4FHX7 | Endo-1,31,4-beta-D-glucanase | 6.64 | 5.28618E-17 | Unique LP |
| B4FIE4 | 2,4-dienoyl-CoA reductase [(3E)-enoyl-CoA-producing] | 6.64 | 5.28618E-17 | Unique LP |
| B4FIH9 | Xylose isomerase | 6.64 | 5.28618E-17 | Unique LP |
| B4FIL5 | Leucine-rich repeat (LRR) family protein | 6.64 | 5.28618E-17 | Unique LP |
| B4FJN0 | Phosphoglucan phosphatase DSP4 chloroplastic | 6.64 | 5.28618E-17 | Unique LP |
| B4FKB8 | Palmitoyl-protein thioesterase 1 | 6.64 | 5.28618E-17 | Unique LP |
| B4FMW6 | Aspartyl protease AED3 | 6.64 | 5.28618E-17 | Unique LP |
| B4FPG2 | Actin-1 | 6.64 | 5.28618E-17 | Unique LP |
| B4FQL2 | SEC13-related protein | 6.64 | 5.28618E-17 | Unique LP |
| B4FRA6 | OSJNBb0091E11.19-like protein | 6.64 | 5.28618E-17 | Unique LP |
| B4FRD6 | Peroxidase | 6.64 | 5.28618E-17 | Unique LP |
| B4FT62 | Putative aldo-keto reductase 4 | 6.64 | 5.28618E-17 | Unique LP |
| B4FTR1 | Alkyl transferase | 6.64 | 5.28618E-17 | Unique LP |
| B4FUW7 | Uncharacterized conserved protein UCP022280 | 6.64 | 5.28618E-17 | Unique LP |
| B4FZ81 | Protein PLASTID TRANSCRIPTIONALLY ACTIVE 12, chloroplastic | 6.64 | 5.28618E-17 | Unique LP |
| B4FZB8 | Signal recognition particle 54 kDa protein chloroplastic | 6.64 | 5.28618E-17 | Unique LP |
| B4G0F3 | Probable bifunctional methylthioribulose-1-phosphate dehydratase/enolase-phosphatase E1 | 6.64 | 5.28618E-17 | Unique LP |
| B4G0U5 | Pectin lyase-like superfamily protein | 6.64 | 5.28618E-17 | Unique LP |
| B4G0Z5 | 60S ribosomal protein L27a-3 | 6.64 | 5.28618E-17 | Unique LP |
| B4G124 | 26S protease regulatory subunit 8 | 6.64 | 5.28618E-17 | Unique LP |
| B6ETR5 | Asparagine synthetase [glutamine-hydrolyzing] | 6.64 | 5.28618E-17 | Unique LP |
| B6SJR3 | Mitochondrial import receptor subunit TOM7-1 | 6.64 | 5.28618E-17 | Unique LP |
| B6SLA5 | 2Fe-2S ferredoxin-like superfamily protein | 6.64 | 5.28618E-17 | Unique LP |

Supplementary Table 4 – Cont.

| Accession | Description | Fold change (log2) | P value | DEPs: |
|------------------|-------------------------------------------------------------------------|---------------------------|----------------|--------------|
| B6SMW8 | Succinate dehydrogenase assembly factor 2 mitochondrial | 6.64 | 5.28618E-17 | Unique LP |
| B6SP43 | ABC family1 | 6.64 | 5.28618E-17 | Unique LP |
| B6ST57 | DNA photolyase | 6.64 | 5.28618E-17 | Unique LP |
| B6SVI8 | Cytochrome P450 13 | 6.64 | 5.28618E-17 | Unique LP |
| B6T033 | glutathione transferase | 6.64 | 5.28618E-17 | Unique LP |
| B6T1E3 | Mitochondrial outer membrane protein porin 4 | 6.64 | 5.28618E-17 | Unique LP |
| B6T3Q3 | Adenine nucleotide alpha hydrolase-like superfamily protein | 6.64 | 5.28618E-17 | Unique LP |
| B6T484 | Mitogen-activated protein kinase | 6.64 | 5.28618E-17 | Unique LP |
| B6T563 | Nucleoside N-ribohydrolase 3 | 6.64 | 5.28618E-17 | Unique LP |
| B6T8F6 | ATP synthase subunit | 6.64 | 5.28618E-17 | Unique LP |
| B6T9P0 | UDP-glucose 6-dehydrogenase | 6.64 | 5.28618E-17 | Unique LP |
| B6TF38 | Tubulin beta chain | 6.64 | 5.28618E-17 | Unique LP |
| B6TIQ8 | ATP/GTP binding protein | 6.64 | 5.28618E-17 | Unique LP |
| B6TJX4 | SnRK1-interacting protein 1 | 6.64 | 5.28618E-17 | Unique LP |
| B6TLS0 | Ubiquitin carboxyl-terminal hydrolase | 6.64 | 5.28618E-17 | Unique LP |
| B6TM36 | Energy transducer TonB | 6.64 | 5.28618E-17 | Unique LP |
| B6TQ08 | Actin-1 | 6.64 | 5.28618E-17 | Unique LP |
| B6U3A0 | Glycine-rich RNA-binding protein 7 | 6.64 | 5.28618E-17 | Unique LP |
| B6UHU1 | Catalase | 6.64 | 5.28618E-17 | Unique LP |
| B7ZXD5 | methenyltetrahydrofolate cyclohydrolase | 6.64 | 5.28618E-17 | Unique LP |
| B7ZZ71 | Cobalt ion binding | 6.64 | 5.28618E-17 | Unique LP |
| B8A1T1 | Peroxidase | 6.64 | 5.28618E-17 | Unique LP |
| B8A2W3 | Peptidase_M28 domain-containing protein | 6.64 | 5.28618E-17 | Unique LP |
| B8A3K0 | glutathione transferase | 6.64 | 5.28618E-17 | Unique LP |
| B8A3M0 | Glutamine synthetase | 6.64 | 5.28618E-17 | Unique LP |
| C0HDZ4 | S-adenosyl-L-methionine-dependent methyltransferase superfamily protein | 6.64 | 5.28618E-17 | Unique LP |
| C0HFI5 | ATP-dependent 6-phosphofructokinase | 6.64 | 5.28618E-17 | Unique LP |
| C0P429 | UTP--glucose-1-phosphate uridylyltransferase | 6.64 | 5.28618E-17 | Unique LP |
| C0P6C4 | 4HBT domain-containing protein | 6.64 | 5.28618E-17 | Unique LP |
| C0P7E7 | Actin-interacting protein 1-2 | 6.64 | 5.28618E-17 | Unique LP |

Supplementary Table 4 – Cont.

| Accession | Description | Fold change (log2) | P value | DEPs: |
|------------------|------------------------------------------------------------------------------------|---------------------------|----------------|--------------|
| C0P820 | 3-ketoacyl-CoA thiolase 2 peroxisomal | 6.64 | 5.28618E-17 | Unique LP |
| C0P8C6 | CCT-theta | 6.64 | 5.28618E-17 | Unique LP |
| C0PC61 | transaldolase | 6.64 | 5.28618E-17 | Unique LP |
| C0PCK6 | adenylate kinase | 6.64 | 5.28618E-17 | Unique LP |
| C0PDR3 | 4-hydroxy-3-methylbut-2-enyl diphosphate reductase | 6.64 | 5.28618E-17 | Unique LP |
| C0PDY0 | Purple acid phosphatase | 6.64 | 5.28618E-17 | Unique LP |
| C0PFA1 | Adenylosuccinate synthetase, chloroplastic | 6.64 | 5.28618E-17 | Unique LP |
| C0PFM8 | Protein RETICULATA-RELATED 3 chloroplastic | 6.64 | 5.28618E-17 | Unique LP |
| C0PHQ1 | cysteine--tRNA ligase | 6.64 | 5.28618E-17 | Unique LP |
| C0PJA6 | GTP cyclohydrolase II | 6.64 | 5.28618E-17 | Unique LP |
| C0PJM7 | Signal recognition particle 14 kDa protein | 6.64 | 5.28618E-17 | Unique LP |
| C0PN00 | Protein YLS3 | 6.64 | 5.28618E-17 | Unique LP |
| C0PPB8 | UDP-glycosyltransferase 76C1 | 6.64 | 5.28618E-17 | Unique LP |
| C4J240 | NADH dehydrogenase [ubiquinone] 1 alpha subcomplex subunit 12 | 6.64 | 5.28618E-17 | Unique LP |
| C4J9Q3 | glutathione transferase | 6.64 | 5.28618E-17 | Unique LP |
| C4JB33 | Calmodulin-7 | 6.64 | 5.28618E-17 | Unique LP |
| K7TEL4 | Purple acid phosphatase | 6.64 | 5.28618E-17 | Unique LP |
| K7TFB6 | ABA-responsive protein | 6.64 | 5.28618E-17 | Unique LP |
| K7TLJ6 | valine--tRNA ligase | 6.64 | 5.28618E-17 | Unique LP |
| K7TNW2 | Leucoanthocyanidin reductase | 6.64 | 5.28618E-17 | Unique LP |
| K7TQX2 | Kinesin motor domain-containing protein | 6.64 | 5.28618E-17 | Unique LP |
| K7TTX0 | Plant UBX domain-containing protein 4 | 6.64 | 5.28618E-17 | Unique LP |
| K7TZ17 | Glycosyltransferase | 6.64 | 5.28618E-17 | Unique LP |
| K7U557 | dCTP pyrophosphatase 1 | 6.64 | 5.28618E-17 | Unique LP |
| K7U5A5 | 14-3-3-like protein | 6.64 | 5.28618E-17 | Unique LP |
| K7U8I5 | NEP-interacting protein 1 | 6.64 | 5.28618E-17 | Unique LP |
| K7UC48 | 3-isopropylmalate dehydratase | 6.64 | 5.28618E-17 | Unique LP |
| K7V4Q5 | Proteasome subunit alpha type Eukaryotic translation initiation factor 3 subunit F | 6.64 | 5.28618E-17 | Unique LP |
| K7V686 | factor 3 subunit F | 6.64 | 5.28618E-17 | Unique LP |
| K7V6J0 | Dirigent protein | 6.64 | 5.28618E-17 | Unique LP |

Supplementary Table 4 – Cont.

| Accession | Description | Fold change (log2) | P value | DEPs: |
|------------------|---------------------------------------------------------|---------------------------|----------------|--------------|
| K7VJF3 | Heat shock 70 kDa protein 5 | 6.64 | 5.28618E-17 | Unique LP |
| K7VNE0 | phosphoenolpyruvate carboxykinase (ATP) | 6.64 | 5.28618E-17 | Unique LP |
| K7VQ25 | Uncharacterized protein | 6.64 | 5.28618E-17 | Unique LP |
| K7VQ98 | Class I heat shock protein 3 | 6.64 | 5.28618E-17 | Unique LP |
| K7VUU0 | Protein DJ-1 homolog B | 6.64 | 5.28618E-17 | Unique LP |
| P04712 | Sucrose synthase 1 | 6.64 | 5.28618E-17 | Unique LP |
| P18026 | Tubulin beta-2 chain | 6.64 | 5.28618E-17 | Unique LP |
| P24825 | Chalcone synthase C2 | 6.64 | 5.28618E-17 | Unique LP |
| P38559 | Glutamine synthetase root isozyme 1 | 6.64 | 5.28618E-17 | Unique LP |
| P46620 | NAD(P)H-quinone oxidoreductase subunit 5, chloroplastic | 6.64 | 5.28618E-17 | Unique LP |
| P50472 | Probable glutathione S-transferase BZ2 | 6.64 | 5.28618E-17 | Unique LP |
| Q08275 | 17.0 kDa class II heat shock protein | 6.64 | 5.28618E-17 | Unique LP |
| Q41815 | Heat shock protein 26 | 6.64 | 5.28618E-17 | Unique LP |
| Q43264 | Alcohol dehydrogenase 1 | 6.64 | 5.28618E-17 | Unique LP |
| Q5EUD6 | Protein disulfide isomerase | 6.64 | 5.28618E-17 | Unique LP |
| Q6R9J5 | ATP synthase protein MI25 | 6.64 | 5.28618E-17 | Unique LP |
| Q8GT71 | Ubiquinol oxidase | 6.64 | 5.28618E-17 | Unique LP |
| Q8W0V2 | Lipoxygenase | 6.64 | 5.28618E-17 | Unique LP |
| Q9FQB5 | glutathione transferase | 6.64 | 5.28618E-17 | Unique LP |
| Q9XF14 | Protein BUNDLE SHEATH DEFECTIVE 2, chloroplastic | 6.64 | 5.28618E-17 | Unique LP |
| Q9XGD6 | Caffeoyl-CoA O-methyltransferase 1 | 6.64 | 5.28618E-17 | Unique LP |
| Q9ZP60 | glutathione transferase | 6.64 | 5.28618E-17 | Unique LP |

Supplementary Table 5. List of differentially abundant proteins (DEPs) down regulated in L80 LP enriched by GO antology analysis

| GO ID | Functional Class | Annotated | Input number | Expected | Aspect | p-value | q-value | Rich Factor | Log (Rich Factor) | Log P-value |
|------------|------------------------------------------|-----------|--------------|----------|--------------------|----------|----------|-------------|-------------------|-------------|
| GO:0009507 | chloroplast | 1592 | 14 | 1.95 | Cellular Component | 5.90E-11 | 3.82E-08 | 0.00879397 | 2.055815 | 10.22915 |
| GO:0009536 | plastid | 1669 | 14 | 2.05 | Cellular Component | 1.10E-10 | 3.82E-08 | 0.008388256 | 2.076328 | 9.958607 |
| GO:0043231 | intracellular membrane-bounded organelle | 6349 | 17 | 7.78 | Cellular Component | 6.80E-06 | 1.18E-03 | 0.002677587 | 2.572256 | 5.167491 |
| GO:0043227 | membrane-bounded organelle | 6351 | 17 | 7.78 | Cellular Component | 6.80E-06 | 1.18E-03 | 0.002676744 | 2.572393 | 5.167491 |
| GO:0044444 | cytoplasmic part | 5088 | 15 | 6.23 | Cellular Component | 3.10E-05 | 3.38E-03 | 0.002948113 | 2.530456 | 4.508638 |
| GO:0043229 | intracellular organelle | 7014 | 17 | 8.6 | Cellular Component | 3.40E-05 | 3.38E-03 | 0.002423724 | 2.615517 | 4.468521 |
| GO:0043226 | organelle | 7018 | 17 | 8.6 | Cellular Component | 3.40E-05 | 3.38E-03 | 0.002422343 | 2.615764 | 4.468521 |
| GO:0005737 | cytoplasm | 5580 | 15 | 6.84 | Cellular Component | 0.00011 | 9.56E-03 | 0.002688172 | 2.570543 | 3.958607 |
| GO:0009579 | thylakoid | 468 | 5 | 0.57 | Cellular Component | 2.00E-04 | 1.54E-02 | 0.010683761 | 1.971276 | 3.69897 |
| GO:0044424 | intracellular part | 8058 | 17 | 9.87 | Cellular Component | 0.00032 | 2.22E-02 | 0.002109705 | 2.675778 | 3.49485 |
| GO:0005622 | intracellular | 8394 | 17 | 10.29 | Cellular Component | 0.00061 | 3.85E-02 | 0.002025256 | 2.69352 | 3.21467 |
| GO:0044434 | chloroplast part | 955 | 6 | 1.17 | Cellular Component | 7.00E-04 | 4.05E-02 | 0.006282723 | 2.201852 | 3.154902 |
| GO:0044435 | plastid part | 972 | 6 | 1.19 | Cellular Component | 0.00077 | 4.12E-02 | 0.00617284 | 2.209515 | 3.113509 |
| GO:0009534 | chloroplast thylakoid | 367 | 4 | 0.45 | Cellular Component | 0.00089 | 4.12E-02 | 0.010899183 | 1.962606 | 3.05061 |
| GO:0031976 | plastid thylakoid | 367 | 4 | 0.45 | Cellular Component | 0.00089 | 4.12E-02 | 0.010899183 | 1.962606 | 3.05061 |
| GO:0010287 | plastoglobule | 67 | 2 | 0.08 | Cellular Component | 0.00299 | 1.15E-01 | 0.029850746 | 1.525045 | 2.524329 |

Supplementary Table 5 – Cont.

| GO ID | Functional Class | Annotated | Input number | Expected | Aspect | p-value | q-value | Rich Factor | Log (Rich Factor) | Log P-value |
|------------|--------------------------------|-----------|--------------|----------|--------------------|---------|----------|-------------|-------------------|-------------|
| GO:0044464 | cell part | 9180 | 17 | 11.25 | Cellular Component | 0.00248 | 1.08E-01 | 0.001851852 | 2.732394 | 2.605548 |
| GO:0005623 | cell | 9301 | 17 | 11.4 | Cellular Component | 0.00305 | 1.15E-01 | 0.00182776 | 2.738081 | 2.5157 |
| GO:0009570 | chloroplast stroma | 518 | 4 | 0.63 | Cellular Component | 0.00315 | 1.15E-01 | 0.007722008 | 2.11227 | 2.501689 |
| GO:0009532 | plastid stroma | 533 | 4 | 0.65 | Cellular Component | 0.0035 | 1.17E-01 | 0.00750469 | 2.124667 | 2.455932 |
| GO:0031984 | organelle subcompartment | 542 | 4 | 0.66 | Cellular Component | 0.00371 | 1.17E-01 | 0.007380074 | 2.131939 | 2.430626 |
| GO:0009523 | photosystem II | 81 | 2 | 0.1 | Cellular Component | 0.00434 | 1.31E-01 | 0.024691358 | 1.607455 | 2.36251 |
| GO:0009535 | chloroplast thylakoid membrane | 296 | 3 | 0.36 | Cellular Component | 0.00528 | 1.44E-01 | 0.010135135 | 1.99417 | 2.277366 |
| GO:0055035 | plastid thylakoid membrane | 298 | 3 | 0.37 | Cellular Component | 0.00538 | 1.44E-01 | 0.010067114 | 1.997095 | 2.269218 |
| GO:0032991 | macromolecular complex | 2033 | 7 | 2.49 | Cellular Component | 0.00758 | 1.88E-01 | 0.003443187 | 2.463039 | 2.120331 |
| GO:0042651 | thylakoid membrane | 339 | 3 | 0.42 | Cellular Component | 0.00769 | 1.88E-01 | 0.008849558 | 2.053078 | 2.114074 |
| GO:0009521 | photosystem | 110 | 2 | 0.13 | Cellular Component | 0.00786 | 1.88E-01 | 0.018181818 | 1.740363 | 2.104577 |
| GO:0034357 | photosynthetic membrane | 360 | 3 | 0.44 | Cellular Component | 0.00906 | 2.03E-01 | 0.008333333 | 2.079181 | 2.042872 |
| GO:0044436 | thylakoid part | 374 | 3 | 0.46 | Cellular Component | 0.01006 | 2.12E-01 | 0.00802139 | 2.09575 | 1.997402 |
| GO:0098796 | membrane protein complex | 407 | 3 | 0.5 | Cellular Component | 0.01264 | 2.53E-01 | 0.007371007 | 2.132473 | 1.898253 |
| GO:0009941 | chloroplast envelope | 408 | 3 | 0.5 | Cellular Component | 0.01273 | 2.53E-01 | 0.007352941 | 2.133539 | 1.895172 |
| GO:0009526 | plastid envelope | 424 | 3 | 0.52 | Cellular Component | 0.01411 | 2.65E-01 | 0.007075472 | 2.150245 | 1.850473 |
| GO:0044446 | intracellular organelle part | 2917 | 8 | 3.57 | Cellular Component | 0.01555 | 2.79E-01 | 0.002742544 | 2.561846 | 1.80827 |

Supplementary Table 5 – Cont.

| GO ID | Functional Class | Annotated | Input number | Expected | Aspect | p-value | q-value | Rich Factor | Log (Rich Factor) | Log P-value |
|------------|------------------------------------------------|-----------|--------------|----------|--------------------|---------|----------|-------------|-------------------|-------------|
| GO:0044422 | organelle part | 2920 | 8 | 3.58 | Cellular Component | 0.01565 | 2.79E-01 | 0.002739726 | 2.562293 | 1.805486 |
| GO:0005840 | ribosome | 605 | 3 | 0.74 | Cellular Component | 0.03577 | 6.22E-01 | 0.004958678 | 2.304634 | 1.446481 |
| GO:0031967 | organelle envelope | 690 | 3 | 0.85 | Cellular Component | 0.04976 | 7.63E-01 | 0.004347826 | 2.361728 | 1.30312 |
| GO:0016168 | chlorophyll binding | 34 | 2 | 0.04 | Molecular Function | 0.00073 | 1.00E+00 | 0.058823529 | 1.230449 | 3.136677 |
| GO:0019843 | rRNA binding | 54 | 2 | 0.06 | Molecular Function | 0.00183 | 1.00E+00 | 0.037037037 | 1.431364 | 2.737549 |
| GO:0003723 | RNA binding | 713 | 4 | 0.84 | Molecular Function | 0.009 | 1.00E+00 | 0.005610098 | 2.25103 | 2.045757 |
| GO:0003735 | structural constituent of ribosome | 526 | 3 | 0.62 | Molecular Function | 0.0231 | 1.00E+00 | 0.005703422 | 2.243864 | 1.636388 |
| GO:0046906 | tetrapyrrole binding | 557 | 3 | 0.66 | Molecular Function | 0.0268 | 1.00E+00 | 0.005385996 | 2.268734 | 1.571865 |
| GO:0009055 | electron carrier activity | 236 | 2 | 0.28 | Molecular Function | 0.03119 | 1.00E+00 | 0.008474576 | 2.071882 | 1.505985 |
| GO:0005198 | structural molecule activity | 592 | 3 | 0.7 | Molecular Function | 0.03134 | 1.00E+00 | 0.005067568 | 2.2952 | 1.503901 |
| GO:0015979 | photosynthesis | 216 | 4 | 0.31 | Biological Process | 0.00022 | 1.00E+00 | 0.018518519 | 1.732394 | 3.657577 |
| GO:0018298 | protein-chromophore linkage | 37 | 2 | 0.05 | Biological Process | 0.00123 | 1.00E+00 | 0.054054054 | 1.267172 | 2.910095 |
| GO:1901566 | organonitrogen compound biosynthetic process | 1349 | 7 | 1.91 | Biological Process | 0.00193 | 1.00E+00 | 0.005189029 | 2.284914 | 2.714443 |
| GO:0009658 | chloroplast organization | 104 | 2 | 0.15 | Biological Process | 0.00938 | 1.00E+00 | 0.019230769 | 1.716003 | 2.027797 |
| GO:0019684 | photosynthesis, light reaction | 104 | 2 | 0.15 | Biological Process | 0.00938 | 1.00E+00 | 0.019230769 | 1.716003 | 2.027797 |
| GO:0006091 | generation of precursor metabolites and energy | 323 | 3 | 0.46 | Biological Process | 0.0102 | 1.00E+00 | 0.009287926 | 2.032081 | 1.9914 |
| GO:1901564 | organonitrogen compound metabolic process | 1843 | 7 | 2.61 | Biological Process | 0.01105 | 1.00E+00 | 0.003798155 | 2.420427 | 1.956638 |

Supplementary Table 5 – Cont.

| GO ID | Functional Class | Annotated | Input number | Expected | Aspect | p-value | q-value | Rich Factor | Log (Rich Factor) | Log P-value |
|------------|----------------------------------------|-----------|--------------|----------|--------------------|---------|----------|-------------|-------------------|-------------|
| GO:0009657 | plastid organization | 151 | 2 | 0.21 | Biological Process | 0.01905 | 1.00E+00 | 0.013245033 | 1.877947 | 1.720105 |
| GO:0008152 | metabolic process | 11940 | 21 | 16.89 | Biological Process | 0.0228 | 1.00E+00 | 0.001758794 | 2.754785 | 1.642065 |
| GO:0006412 | translation | 792 | 4 | 1.12 | Biological Process | 0.02346 | 1.00E+00 | 0.005050505 | 2.296665 | 1.629672 |
| GO:0051188 | cofactor biosynthetic process | 171 | 2 | 0.24 | Biological Process | 0.02404 | 1.00E+00 | 0.011695906 | 1.931966 | 1.619066 |
| GO:0043043 | peptide biosynthetic process | 804 | 4 | 1.14 | Biological Process | 0.02464 | 1.00E+00 | 0.004975124 | 2.303196 | 1.608359 |
| GO:0006518 | peptide metabolic process | 821 | 4 | 1.16 | Biological Process | 0.02638 | 1.00E+00 | 0.004872107 | 2.312283 | 1.578725 |
| GO:0043604 | amide biosynthetic process | 836 | 4 | 1.18 | Biological Process | 0.02797 | 1.00E+00 | 0.004784689 | 2.320146 | 1.553308 |
| GO:0044237 | cellular metabolic process | 8634 | 17 | 12.21 | Biological Process | 0.03015 | 1.00E+00 | 0.00196896 | 2.705763 | 1.520713 |
| GO:0044711 | single-organism biosynthetic process | 1286 | 5 | 1.82 | Biological Process | 0.03085 | 1.00E+00 | 0.003888025 | 2.410271 | 1.510745 |
| GO:0071704 | organic substance metabolic process | 9451 | 18 | 13.37 | Biological Process | 0.03124 | 1.00E+00 | 0.00190456 | 2.720205 | 1.505289 |
| GO:0043603 | cellular amide metabolic process | 874 | 4 | 1.24 | Biological Process | 0.03226 | 1.00E+00 | 0.004576659 | 2.339451 | 1.491336 |
| GO:0044249 | cellular biosynthetic process | 4133 | 10 | 5.85 | Biological Process | 0.04378 | 1.00E+00 | 0.00241955 | 2.616265 | 1.358724 |
| GO:1901576 | organic substance biosynthetic process | 4195 | 10 | 5.93 | Biological Process | 0.04811 | 1.00E+00 | 0.00238379 | 2.622732 | 1.317765 |

Supplementary Table 6. List of differentially abundant proteins (DEPs) down regulated in P7 LP enriched by GO ontology analysis

| GO ID | Functional Class | Annotated | Input number | Expected | Aspect | p-value | q-value | Rich Factor | Log (Rich Factor) | Log P-value |
|------------|--------------------------------|-----------|--------------|----------|-----------------------|----------|----------|-------------|-------------------|-------------|
| GO:0042651 | thylakoid membrane | 339 | 6 | 0.39 | Cellular Component | 1.40E-06 | 6.02E-04 | 0.02 | 1.752048448 | 5.853872 |
| GO:0034357 | photosynthetic membrane | 360 | 6 | 0.42 | Cellular Component | 2.00E-06 | 6.02E-04 | 0.02 | 1.77815125 | 5.69897 |
| GO:0044436 | thylakoid part | 374 | 6 | 0.43 | Cellular Component | 2.60E-06 | 6.02E-04 | 0.02 | 1.794720352 | 5.585027 |
| GO:0009579 | thylakoid | 468 | 6 | 0.54 | Cellular Component | 9.30E-06 | 1.62E-03 | 0.01 | 1.892094603 | 5.031517 |
| GO:0009535 | chloroplast thylakoid membrane | 296 | 5 | 0.34 | Cellular Component | 1.60E-05 | 1.97E-03 | 0.02 | 1.772321707 | 4.79588 |
| GO:0055035 | plastid thylakoid membrane | 298 | 5 | 0.34 | Cellular Component | 1.70E-05 | 1.97E-03 | 0.02 | 1.77524626 | 4.769551 |
| GO:0009507 | chloroplast | 1592 | 9 | 1.84 | Cellular Component | 2.20E-05 | 2.18E-03 | 0.01 | 2.247700554 | 4.657577 |
| GO:0009536 | plastid | 1669 | 9 | 1.93 | Cellular Component | 3.20E-05 | 2.78E-03 | 0.01 | 2.268213827 | 4.49485 |
| GO:0009534 | chloroplast thylakoid | 367 | 5 | 0.42 | Cellular Component | 4.60E-05 | 3.20E-03 | 0.01 | 1.86569606 | 4.337242 |
| GO:0031976 | plastid thylakoid | 367 | 5 | 0.42 | Cellular Component | 4.60E-05 | 3.20E-03 | 0.01 | 1.86569606 | 4.337242 |
| GO:0005737 | cytoplasm | 5580 | 14 | 6.46 | Cellular Component | 0.00024 | 1.52E-02 | 0.00 | 2.600506163 | 3.619789 |
| GO:0031984 | organelle subcompartment | 542 | 5 | 0.63 | Cellular Component | 0.00029 | 1.68E-02 | 0.01 | 2.035029282 | 3.537602 |
| GO:0044434 | chloroplast part | 955 | 6 | 1.11 | Cellular Component | 0.00049 | 2.39E-02 | 0.01 | 2.201852121 | 3.309804 |
| GO:0044444 | cytoplasmic part | 5088 | 13 | 5.89 | Cellular Component | 0.00052 | 2.39E-02 | 0.00 | 2.59260375 | 3.283997 |
| GO:0044435 | plastid part | 972 | 6 | 1.12 | Cellular Component | 0.00054 | 2.39E-02 | 0.01 | 2.209515015 | 3.267606 |
| GO:0044424 | intracellular part | 8058 | 16 | 9.33 | Cellular Component | 0.00055 | 2.39E-02 | 0.00 | 2.70210728 | 3.259637 |
| GO:0005622 | intracellular | 8394 | 16 | 9.71 | Cellular Component | 0.00101 | 4.13E-02 | 0.00 | 2.719848982 | 2.995679 |
| GO:0044446 | intracellular organelle part | 2917 | 9 | 3.38 | Cellular Component | 0.00244 | 8.96E-02 | 0.00 | 2.51069392 | 2.61261 |

Supplementary Table 6 – Cont.

| GO ID | Functional Class | Annotated | Input number | Expected | Aspect | p-value | q-value | Rich Factor | Log (Rich Factor) | Log P-value |
|------------|-------------------------------------------|-----------|--------------|----------|--------------------|---------|----------|-------------|-------------------|-------------|
| GO:0044422 | organelle part | 2920 | 9 | 3.38 | Cellular Component | 0.00245 | 8.96E-02 | 0.00 | 2.511140342 | 2.610834 |
| GO:0044464 | cell part | 9180 | 16 | 10.62 | Cellular Component | 0.00378 | 1.31E-01 | 0.00 | 2.758722699 | 2.422508 |
| GO:0005623 | cell | 9301 | 16 | 10.76 | Cellular Component | 0.00457 | 1.51E-01 | 0.00 | 2.764409662 | 2.340084 |
| GO:0043229 | intracellular organelle | 7014 | 13 | 8.12 | Cellular Component | 0.0156 | 4.54E-01 | 0.00 | 2.732022409 | 1.806875 |
| GO:0043226 | organelle | 7018 | 13 | 8.12 | Cellular Component | 0.01568 | 4.54E-01 | 0.00 | 2.732270012 | 1.804654 |
| GO:0043231 | intracellular membrane-bounded organelle | 6349 | 12 | 7.35 | Cellular Component | 0.02116 | 5.67E-01 | 0.00 | 2.723524081 | 1.674484 |
| GO:0043227 | membrane-bounded organelle | 6351 | 12 | 7.35 | Cellular Component | 0.02122 | 5.67E-01 | 0.00 | 2.723660867 | 1.673255 |
| GO:0005730 | nucleolus | 236 | 2 | 0.27 | Cellular Component | 0.02983 | 7.63E-01 | 0.01 | 2.071882007 | 1.525347 |
| GO:0005840 | ribosome | 605 | 3 | 0.7 | Cellular Component | 0.03073 | 7.63E-01 | 0.00 | 2.30463412 | 1.512437 |
| GO:0009055 | electron carrier activity | 236 | 2 | 0.17 | Molecular Function | 0.01204 | 1.00E+00 | 0.01 | 2.071882007 | 1.919374 |
| GO:0009735 | response to cytokinin | 140 | 2 | 0.15 | Biological Process | 0.01 | 1.00E+00 | 0.01 | 1.84509804 | 2 |
| GO:1901564 | organonitrogen compound metabolic process | 1843 | 6 | 2.01 | Biological Process | 0.0107 | 1.00E+00 | 0.00 | 2.487374085 | 1.970616 |
| GO:0015979 | photosynthesis | 216 | 2 | 0.24 | Biological Process | 0.0228 | 1.00E+00 | 0.01 | 2.033423755 | 1.642065 |
| GO:0034622 | cellular macromolecular complex assembly | 271 | 2 | 0.3 | Biological Process | 0.0346 | 1.00E+00 | 0.01 | 2.131939295 | 1.460924 |
| GO:0065003 | macromolecular complex assembly | 314 | 2 | 0.34 | Biological Process | 0.0453 | 1.00E+00 | 0.01 | 2.195899652 | 1.343902 |

Supplementary Table 7. List of differentially abundant proteins (DEPs) Up regulated in L80 LP enriched by GO antology analysis

| GO ID | Functional Class | Annotated | Input number | Expected | Aspect | p-value | q-value | Rich Factor | Log (Rich Factor) | Log P-value |
|------------|------------------------------------------|-----------|--------------|----------|--------------------|----------|----------|-------------|-------------------|-------------|
| GO:0005737 | cytoplasm | 5580 | 31 | 13.68 | Cellular Component | 3.40E-09 | 2.36E-06 | 0.005556 | 2.255273 | 8.468521 |
| GO:0044444 | cytoplasmic part | 5088 | 28 | 12.47 | Cellular Component | 1.50E-07 | 4.17E-05 | 0.005503 | 2.259389 | 6.823909 |
| GO:0044424 | intracellular part | 8058 | 34 | 19.75 | Cellular Component | 1.80E-07 | 4.17E-05 | 0.004219 | 2.374748 | 6.744727 |
| GO:0005622 | intracellular | 8394 | 34 | 20.57 | Cellular Component | 6.70E-07 | 1.16E-04 | 0.004051 | 2.39249 | 6.173925 |
| GO:0044464 | cell part | 9180 | 35 | 22.5 | Cellular Component | 9.90E-07 | 1.38E-04 | 0.003813 | 2.418775 | 6.004365 |
| GO:0005623 | cell | 9301 | 35 | 22.8 | Cellular Component | 1.50E-06 | 1.74E-04 | 0.003763 | 2.424462 | 5.823909 |
| GO:0005777 | peroxisome | 129 | 5 | 0.32 | Cellular Component | 1.50E-05 | 1.30E-03 | 0.038760 | 1.41162 | 4.823909 |
| GO:0042579 | microbody | 129 | 5 | 0.32 | Cellular Component | 1.50E-05 | 1.30E-03 | 0.038760 | 1.41162 | 4.823909 |
| GO:0043231 | intracellular membrane-bounded organelle | 6349 | 26 | 15.56 | Cellular Component | 4.00E-04 | 2.85E-02 | 0.004095 | 2.387732 | 3.39794 |
| GO:0043227 | membrane-bounded organelle | 6351 | 26 | 15.57 | Cellular Component | 0.00041 | 2.85E-02 | 0.004094 | 2.387869 | 3.387216 |
| GO:0005829 | cytosol | 1094 | 9 | 2.68 | Cellular Component | 0.00102 | 6.45E-02 | 0.008227 | 2.084775 | 2.9914 |
| GO:0043229 | intracellular organelle | 7014 | 26 | 17.19 | Cellular Component | 0.00252 | 1.20E-01 | 0.003707 | 2.430992 | 2.598599 |
| GO:0043226 | organelle | 7018 | 26 | 17.2 | Cellular Component | 0.00255 | 1.20E-01 | 0.003705 | 2.43124 | 2.59346 |
| GO:0009506 | plasmodesma | 404 | 5 | 0.99 | Cellular Component | 0.00287 | 1.20E-01 | 0.012376 | 1.907411 | 2.542118 |
| GO:0055044 | symplast | 404 | 5 | 0.99 | Cellular Component | 0.00287 | 1.20E-01 | 0.012376 | 1.907411 | 2.542118 |
| GO:0005911 | cell-cell junction | 405 | 5 | 0.99 | Cellular Component | 0.0029 | 1.20E-01 | 0.012346 | 1.908485 | 2.537602 |
| GO:0030054 | cell junction | 406 | 5 | 1 | Cellular Component | 0.00293 | 1.20E-01 | 0.012315 | 1.909556 | 2.533132 |

Supplementary Table 7 – Cont.

| GO ID | Functional Class | Annotated | Input number | Expected | Aspect | p-value | q-value | Rich Factor | Log (Rich Factor) | Log P-value |
|------------|----------------------------------------------------------|-----------|--------------|----------|--------------------|----------|----------|-------------|-------------------|-------------|
| GO:0009536 | plastid | 1669 | 10 | 4.09 | Cellular Component | 0.00552 | 2.02E-01 | 0.005992 | 2.222456 | 2.258061 |
| GO:0005773 | vacuole | 493 | 5 | 1.21 | Cellular Component | 0.00666 | 2.31E-01 | 0.010142 | 1.993877 | 2.176526 |
| GO:0009507 | chloroplast | 1592 | 9 | 3.9 | Cellular Component | 0.01264 | 4.18E-01 | 0.005653 | 2.247701 | 1.898253 |
| GO:0000502 | proteasome complex | 75 | 2 | 0.18 | Cellular Component | 0.01449 | 4.58E-01 | 0.026667 | 1.574031 | 1.838932 |
| GO:0000786 | nucleosome | 103 | 2 | 0.25 | Cellular Component | 0.02628 | 7.57E-01 | 0.019417 | 1.711807 | 1.580375 |
| GO:0005739 | mitochondrion | 954 | 6 | 2.34 | Cellular Component | 0.02698 | 7.57E-01 | 0.006289 | 2.201397 | 1.568958 |
| GO:0044815 | DNA packaging complex | 105 | 2 | 0.26 | Cellular Component | 0.02723 | 7.57E-01 | 0.019048 | 1.720159 | 1.564952 |
| GO:0032993 | protein-DNA complex | 110 | 2 | 0.27 | Cellular Component | 0.02967 | 7.93E-01 | 0.018182 | 1.740363 | 1.527682 |
| GO:0000785 | chromatin | 128 | 2 | 0.31 | Cellular Component | 0.03914 | 1.00E+00 | 0.015625 | 1.80618 | 1.407379 |
| GO:0048037 | cofactor binding | 530 | 9 | 1.28 | Molecular Function | 4.10E-06 | 3.34E-03 | 0.016981 | 1.770033 | 5.387216 |
| GO:0030170 | pyridoxal phosphate binding | 103 | 5 | 0.25 | Molecular Function | 4.80E-06 | 3.34E-03 | 0.048544 | 1.313867 | 5.318759 |
| GO:0070546 | L-phenylalanine aminotransferase activity | 2 | 2 | 0 | Molecular Function | 5.70E-06 | 3.34E-03 | 1.000000 | 0 | 5.244125 |
| GO:0080130 | L-phenylalanine:2-oxoglutarate aminotransferase activity | 2 | 2 | 0 | Molecular Function | 5.70E-06 | 3.34E-03 | 1.000000 | 0 | 5.244125 |
| GO:0003824 | catalytic activity | 9657 | 38 | 23.26 | Molecular Function | 9.00E-06 | 4.22E-03 | 0.003935 | 2.405059 | 5.045757 |
| GO:0004069 | L-aspartate:2-oxoglutarate aminotransferase activity | 5 | 2 | 0.01 | Molecular Function | 5.70E-05 | 2.23E-02 | 0.400000 | 0.39794 | 4.244125 |
| GO:0008483 | transaminase activity | 46 | 3 | 0.11 | Molecular Function | 0.00018 | 5.27E-02 | 0.065217 | 1.185637 | 3.744727 |

Supplementary Table 7 – Cont.

| GO ID | Functional Class | Annotated | Input number | Expected | Aspect | p-value | q-value | Rich Factor | Log (Rich Factor) | Log P-value |
|------------|------------------------------------------------------------------------|-----------|--------------|----------|--------------------|---------|----------|-------------|-------------------|-------------|
| GO:0016769 | transferase activity, transferring nitrogenous groups | 46 | 3 | 0.11 | Molecular Function | 0.00018 | 5.27E-02 | 0.065217 | 1.185637 | 3.744727 |
| GO:0051536 | iron-sulfur cluster binding | 132 | 3 | 0.32 | Molecular Function | 0.00395 | 6.61E-01 | 0.022727 | 1.643453 | 2.403403 |
| GO:0051540 | metal cluster binding | 132 | 3 | 0.32 | Molecular Function | 0.00395 | 6.61E-01 | 0.022727 | 1.643453 | 2.403403 |
| GO:0016799 | hydrolase activity, hydrolyzing N-glycosyl compounds | 41 | 2 | 0.1 | Molecular Function | 0.00439 | 6.63E-01 | 0.048780 | 1.311754 | 2.357535 |
| GO:0005507 | copper ion binding | 146 | 3 | 0.35 | Molecular Function | 0.00523 | 6.81E-01 | 0.020548 | 1.687232 | 2.281498 |
| GO:0016798 | hydrolase activity, acting on glycosyl bonds | 498 | 5 | 1.2 | Molecular Function | 0.00674 | 7.68E-01 | 0.010040 | 1.998259 | 2.17134 |
| GO:0016491 | oxidoreductase activity | 1790 | 10 | 4.31 | Molecular Function | 0.00911 | 8.65E-01 | 0.005587 | 2.252853 | 2.040482 |
| GO:0016903 | oxidoreductase activity, acting on the aldehyde or oxo group of donors | 65 | 2 | 0.16 | Molecular Function | 0.01072 | 8.73E-01 | 0.030769 | 1.511883 | 1.969805 |
| GO:0004812 | aminoacyl-tRNA ligase activity | 71 | 2 | 0.17 | Molecular Function | 0.0127 | 8.73E-01 | 0.028169 | 1.550228 | 1.896196 |
| GO:0016875 | ligase activity, forming carbon-oxygen bonds | 71 | 2 | 0.17 | Molecular Function | 0.0127 | 8.73E-01 | 0.028169 | 1.550228 | 1.896196 |
| GO:0016876 | ligase activity, forming aminoacyl-tRNA and related compounds | 71 | 2 | 0.17 | Molecular Function | 0.0127 | 8.73E-01 | 0.028169 | 1.550228 | 1.896196 |
| GO:0016627 | oxidoreductase activity, acting on the CH-CH group of donors | 72 | 2 | 0.17 | Molecular Function | 0.01304 | 8.73E-01 | 0.027778 | 1.556303 | 1.884722 |
| GO:0035251 | UDP-glucosyltransferase activity | 104 | 2 | 0.25 | Molecular Function | 0.02603 | 1.00E+00 | 0.019231 | 1.716003 | 1.584526 |
| GO:0046527 | glucosyltransferase activity | 105 | 2 | 0.25 | Molecular Function | 0.02649 | 1.00E+00 | 0.019048 | 1.720159 | 1.576918 |
| GO:0043168 | anion binding | 3484 | 14 | 8.39 | Molecular Function | 0.03128 | 1.00E+00 | 0.004018 | 2.39595 | 1.504733 |

Supplementary Table 7 – Cont.

| GO ID | Functional Class | Annotated | Input number | Expected | Aspect | p-value | q-value | Rich Factor | Log (Rich Factor) | Log P-value |
|------------|----------------------------------------------|-----------|--------------|----------|--------------------|----------|----------|-------------|-------------------|-------------|
| GO:0016835 | carbon-oxygen lyase activity | 140 | 2 | 0.34 | Molecular Function | 0.04478 | 1.00E+00 | 0.014286 | 1.845098 | 1.348916 |
| GO:0016829 | lyase activity | 342 | 3 | 0.82 | Molecular Function | 0.04913 | 1.00E+00 | 0.008772 | 2.056905 | 1.308653 |
| GO:0044281 | small molecule metabolic process | 1473 | 16 | 4.07 | Biological Process | 8.60E-07 | 4.10E-03 | 0.010862 | 1.964083 | 6.065502 |
| GO:1901564 | organonitrogen compound metabolic process | 1843 | 16 | 5.1 | Biological Process | 1.60E-05 | 2.77E-02 | 0.008681 | 2.061405 | 4.79588 |
| GO:0019752 | carboxylic acid metabolic process | 897 | 11 | 2.48 | Biological Process | 2.30E-05 | 2.77E-02 | 0.012263 | 1.9114 | 4.638272 |
| GO:0043436 | oxoacid metabolic process | 916 | 11 | 2.53 | Biological Process | 2.80E-05 | 2.77E-02 | 0.012009 | 1.920503 | 4.552842 |
| GO:0006082 | organic acid metabolic process | 918 | 11 | 2.54 | Biological Process | 2.90E-05 | 2.77E-02 | 0.011983 | 1.92145 | 4.537602 |
| GO:0006520 | cellular amino acid metabolic process | 431 | 7 | 1.19 | Biological Process | 0.00016 | 1.27E-01 | 0.016241 | 1.789379 | 3.79588 |
| GO:0009308 | amine metabolic process | 128 | 4 | 0.35 | Biological Process | 0.00042 | 2.62E-01 | 0.031250 | 1.50515 | 3.376751 |
| GO:0010035 | response to inorganic substance | 507 | 7 | 1.4 | Biological Process | 0.00044 | 2.62E-01 | 0.013807 | 1.85991 | 3.356547 |
| GO:0044710 | single-organism metabolic process | 4290 | 22 | 11.86 | Biological Process | 0.00088 | 4.66E-01 | 0.005128 | 2.290035 | 3.055517 |
| GO:0046686 | response to cadmium ion | 191 | 4 | 0.53 | Biological Process | 0.00187 | 7.77E-01 | 0.020942 | 1.678973 | 2.728158 |
| GO:0006098 | pentose-phosphate shunt | 26 | 2 | 0.07 | Biological Process | 0.00233 | 7.77E-01 | 0.076923 | 1.113943 | 2.632644 |
| GO:0051156 | glucose 6-phosphate metabolic process | 27 | 2 | 0.07 | Biological Process | 0.00251 | 7.77E-01 | 0.074074 | 1.130334 | 2.600326 |
| GO:0019682 | glyceraldehyde-3-phosphate metabolic process | 33 | 2 | 0.09 | Biological Process | 0.00373 | 8.78E-01 | 0.060606 | 1.217484 | 2.428291 |
| GO:1901565 | organonitrogen compound catabolic process | 118 | 3 | 0.33 | Biological Process | 0.00421 | 8.78E-01 | 0.025424 | 1.594761 | 2.375718 |

Supplementary Table 7 – Cont.

| GO ID | Functional Class | Annotated | Input number | Expected | Aspect | p-value | q-value | Rich Factor | Log (Rich Factor) | Log P-value |
|------------|--------------------------------------------------------|-----------|--------------|----------|--------------------|---------|----------|-------------|-------------------|-------------|
| GO:0006739 | NADP metabolic process | 36 | 2 | 0.1 | Biological Process | 0.00443 | 8.78E-01 | 0.055556 | 1.255273 | 2.353596 |
| GO:0008152 | metabolic process | 11940 | 40 | 33.02 | Biological Process | 0.00505 | 8.78E-01 | 0.003350 | 2.474944 | 2.296709 |
| GO:0010038 | response to metal ion | 254 | 4 | 0.7 | Biological Process | 0.0052 | 8.78E-01 | 0.015748 | 1.802774 | 2.283997 |
| GO:0009309 | amine biosynthetic process | 42 | 2 | 0.12 | Biological Process | 0.00599 | 8.93E-01 | 0.047619 | 1.322219 | 2.222573 |
| GO:0042401 | cellular biogenic amine biosynthetic process | 42 | 2 | 0.12 | Biological Process | 0.00599 | 8.93E-01 | 0.047619 | 1.322219 | 2.222573 |
| GO:0055086 | nucleobase-containing small molecule metabolic process | 437 | 5 | 1.21 | Biological Process | 0.00685 | 9.90E-01 | 0.011442 | 1.941511 | 2.164309 |
| GO:0009605 | response to external stimulus | 627 | 6 | 1.73 | Biological Process | 0.00718 | 1.00E+00 | 0.009569 | 2.019116 | 2.143876 |
| GO:0072350 | tricarboxylic acid metabolic process | 50 | 2 | 0.14 | Biological Process | 0.00841 | 1.00E+00 | 0.040000 | 1.39794 | 2.075204 |
| GO:0044712 | single-organism catabolic process | 479 | 5 | 1.32 | Biological Process | 0.00997 | 1.00E+00 | 0.010438 | 1.981366 | 2.001305 |
| GO:0010150 | leaf senescence | 60 | 2 | 0.17 | Biological Process | 0.01194 | 1.00E+00 | 0.033333 | 1.477121 | 1.922996 |
| GO:0010260 | organ senescence | 60 | 2 | 0.17 | Biological Process | 0.01194 | 1.00E+00 | 0.033333 | 1.477121 | 1.922996 |
| GO:0006081 | cellular aldehyde metabolic process | 63 | 2 | 0.17 | Biological Process | 0.01311 | 1.00E+00 | 0.031746 | 1.498311 | 1.882397 |
| GO:0009414 | response to water deprivation | 180 | 3 | 0.5 | Biological Process | 0.01341 | 1.00E+00 | 0.016667 | 1.778151 | 1.872571 |
| GO:0009415 | response to water | 185 | 3 | 0.51 | Biological Process | 0.01442 | 1.00E+00 | 0.016216 | 1.79005 | 1.841035 |
| GO:0006418 | tRNA aminoacylation for protein translation | 70 | 2 | 0.19 | Biological Process | 0.01601 | 1.00E+00 | 0.028571 | 1.544068 | 1.795609 |
| GO:0043648 | dicarboxylic acid metabolic process | 70 | 2 | 0.19 | Biological Process | 0.01601 | 1.00E+00 | 0.028571 | 1.544068 | 1.795609 |
| GO:0007568 | aging | 72 | 2 | 0.2 | Biological Process | 0.01689 | 1.00E+00 | 0.027778 | 1.556303 | 1.77237 |

Supplementary Table 7 – Cont.

| GO ID | Functional Class | Annotated | Input number | Expected | Aspect | p-value | q-value | Rich Factor | Log (Rich Factor) | Log P-value |
|------------|----------------------------------------------|-----------|--------------|----------|--------------------|---------|----------|-------------|-------------------|-------------|
| GO:0098542 | defense response to other organism | 359 | 4 | 0.99 | Biological Process | 0.01698 | 1.00E+00 | 0.011142 | 1.953034 | 1.770062 |
| GO:0042742 | defense response to bacterium | 197 | 3 | 0.54 | Biological Process | 0.01704 | 1.00E+00 | 0.015228 | 1.817345 | 1.76853 |
| GO:0043038 | amino acid activation | 73 | 2 | 0.2 | Biological Process | 0.01734 | 1.00E+00 | 0.027397 | 1.562293 | 1.760951 |
| GO:0043039 | tRNA aminoacylation | 73 | 2 | 0.2 | Biological Process | 0.01734 | 1.00E+00 | 0.027397 | 1.562293 | 1.760951 |
| GO:0042221 | response to chemical | 1481 | 9 | 4.1 | Biological Process | 0.01815 | 1.00E+00 | 0.006077 | 2.216313 | 1.741123 |
| GO:0031669 | cellular response to nutrient levels | 77 | 2 | 0.21 | Biological Process | 0.01917 | 1.00E+00 | 0.025974 | 1.585461 | 1.717378 |
| GO:0006576 | cellular biogenic amine metabolic process | 78 | 2 | 0.22 | Biological Process | 0.01964 | 1.00E+00 | 0.025641 | 1.591065 | 1.706859 |
| GO:0016054 | organic acid catabolic process | 82 | 2 | 0.23 | Biological Process | 0.02157 | 1.00E+00 | 0.024390 | 1.612784 | 1.66615 |
| GO:0046395 | carboxylic acid catabolic process | 82 | 2 | 0.23 | Biological Process | 0.02157 | 1.00E+00 | 0.024390 | 1.612784 | 1.66615 |
| GO:0044106 | cellular amine metabolic process | 87 | 2 | 0.24 | Biological Process | 0.02408 | 1.00E+00 | 0.022989 | 1.638489 | 1.618344 |
| GO:0009617 | response to bacterium | 233 | 3 | 0.64 | Biological Process | 0.0264 | 1.00E+00 | 0.012876 | 1.890235 | 1.578396 |
| GO:0031667 | response to nutrient levels | 92 | 2 | 0.25 | Biological Process | 0.02672 | 1.00E+00 | 0.021739 | 1.662758 | 1.573164 |
| GO:0031668 | cellular response to extracellular stimulus | 92 | 2 | 0.25 | Biological Process | 0.02672 | 1.00E+00 | 0.021739 | 1.662758 | 1.573164 |
| GO:0044270 | cellular nitrogen compound catabolic process | 94 | 2 | 0.26 | Biological Process | 0.0278 | 1.00E+00 | 0.021277 | 1.672098 | 1.555955 |
| GO:0045333 | cellular respiration | 94 | 2 | 0.26 | Biological Process | 0.0278 | 1.00E+00 | 0.021277 | 1.672098 | 1.555955 |
| GO:0046700 | heterocycle catabolic process | 94 | 2 | 0.26 | Biological Process | 0.0278 | 1.00E+00 | 0.021277 | 1.672098 | 1.555955 |
| GO:0071496 | cellular response to external stimulus | 96 | 2 | 0.27 | Biological Process | 0.0289 | 1.00E+00 | 0.020833 | 1.681241 | 1.539102 |

Supplementary Table 7 – Cont.

| GO ID | Functional Class | Annotated | Input number | Expected | Aspect | p-value | q-value | Rich Factor | Log (Rich Factor) | Log P-value |
|------------|-----------------------------------------------------|-----------|--------------|----------|--------------------|---------|----------|-------------|-------------------|-------------|
| GO:0016053 | organic acid biosynthetic process | 429 | 4 | 1.19 | Biological Process | 0.03023 | 1.00E+00 | 0.009324 | 2.030397 | 1.519562 |
| GO:0046394 | carboxylic acid biosynthetic process | 429 | 4 | 1.19 | Biological Process | 0.03023 | 1.00E+00 | 0.009324 | 2.030397 | 1.519562 |
| GO:0044248 | cellular catabolic process | 663 | 5 | 1.83 | Biological Process | 0.03511 | 1.00E+00 | 0.007541 | 2.122544 | 1.454569 |
| GO:0055114 | oxidation-reduction process | 1936 | 10 | 5.35 | Biological Process | 0.03531 | 1.00E+00 | 0.005165 | 2.286905 | 1.452102 |
| GO:0009991 | response to extracellular stimulus | 108 | 2 | 0.3 | Biological Process | 0.03587 | 1.00E+00 | 0.018519 | 1.732394 | 1.445269 |
| GO:0015980 | energy derivation by oxidation of organic compounds | 110 | 2 | 0.3 | Biological Process | 0.03709 | 1.00E+00 | 0.018182 | 1.740363 | 1.430743 |
| GO:0043207 | response to external biotic stimulus | 465 | 4 | 1.29 | Biological Process | 0.03891 | 1.00E+00 | 0.008602 | 2.065393 | 1.409939 |
| GO:0051707 | response to other organism | 465 | 4 | 1.29 | Biological Process | 0.03891 | 1.00E+00 | 0.008602 | 2.065393 | 1.409939 |
| GO:0044282 | small molecule catabolic process | 113 | 2 | 0.31 | Biological Process | 0.03895 | 1.00E+00 | 0.017699 | 1.752048 | 1.409493 |
| GO:0009056 | catabolic process | 920 | 6 | 2.54 | Biological Process | 0.03962 | 1.00E+00 | 0.006522 | 2.185637 | 1.402086 |
| GO:0009607 | response to biotic stimulus | 482 | 4 | 1.33 | Biological Process | 0.04347 | 1.00E+00 | 0.008299 | 2.080987 | 1.36181 |
| GO:0019693 | ribose phosphate metabolic process | 285 | 3 | 0.79 | Biological Process | 0.04389 | 1.00E+00 | 0.010526 | 1.977724 | 1.357634 |
| GO:1901361 | organic cyclic compound catabolic process | 126 | 2 | 0.35 | Biological Process | 0.0474 | 1.00E+00 | 0.015873 | 1.799341 | 1.324222 |
| GO:0048827 | phyllome development | 298 | 3 | 0.82 | Biological Process | 0.04899 | 1.00E+00 | 0.010067 | 1.997095 | 1.309893 |
| GO:0006952 | defense response | 502 | 4 | 1.39 | Biological Process | 0.04919 | 1.00E+00 | 0.007968 | 2.098644 | 1.308123 |

Supplementary Table 8. List of differentially abundant proteins (DEPs) Up regulated in P7 LP enriched by GO antology analysis

| GO ID | Functional Class | Annotated | Input number | Expected | Aspect | p-value | q-value | Rich Factor | Log (Rich Factor) | Log P-value |
|------------|------------------------------------------|-----------|--------------|----------|--------------------|----------|----------|-------------|-------------------|-------------|
| GO:0005737 | cytoplasm | 5580 | 35 | 14.44 | Cellular Component | 3.90E-12 | 2.71E-09 | 0.006272 | 2.202566 | 11.40894 |
| GO:0044444 | cytoplasmic part | 5088 | 30 | 13.16 | Cellular Component | 2.80E-08 | 9.73E-06 | 0.005896 | 2.229426 | 7.552842 |
| GO:0044424 | intracellular part | 8058 | 36 | 20.85 | Cellular Component | 6.10E-08 | 1.41E-05 | 0.004468 | 2.349925 | 7.21467 |
| GO:0005622 | intracellular | 8394 | 36 | 21.72 | Cellular Component | 2.40E-07 | 4.17E-05 | 0.004289 | 2.367666 | 6.619789 |
| GO:0044435 | plastid part | 972 | 13 | 2.51 | Cellular Component | 4.90E-07 | 6.81E-05 | 0.013374 | 1.873723 | 6.309804 |
| GO:0009536 | plastid | 1669 | 16 | 4.32 | Cellular Component | 1.40E-06 | 1.30E-04 | 0.009587 | 2.018336 | 5.853872 |
| GO:0044446 | intracellular organelle part | 2917 | 21 | 7.55 | Cellular Component | 1.40E-06 | 1.30E-04 | 0.007199 | 2.142717 | 5.853872 |
| GO:0044422 | organelle part | 2920 | 21 | 7.55 | Cellular Component | 1.50E-06 | 1.30E-04 | 0.007192 | 2.143164 | 5.823909 |
| GO:0044434 | chloroplast part | 955 | 12 | 2.47 | Cellular Component | 3.00E-06 | 2.32E-04 | 0.012565 | 1.900822 | 5.522879 |
| GO:0009507 | chloroplast | 1592 | 15 | 4.12 | Cellular Component | 4.30E-06 | 2.97E-04 | 0.009422 | 2.025852 | 5.366532 |
| GO:0044464 | cell part | 9180 | 36 | 23.75 | Cellular Component | 4.70E-06 | 2.97E-04 | 0.003922 | 2.40654 | 5.327902 |
| GO:0009532 | plastid stroma | 533 | 9 | 1.38 | Cellular Component | 6.50E-06 | 3.77E-04 | 0.016886 | 1.772485 | 5.187087 |
| GO:0005623 | cell | 9301 | 36 | 24.06 | Cellular Component | 7.30E-06 | 3.90E-04 | 0.003871 | 2.412227 | 5.136677 |
| GO:0009570 | chloroplast stroma | 518 | 8 | 1.34 | Cellular Component | 4.40E-05 | 2.18E-03 | 0.015444 | 1.81124 | 4.356547 |
| GO:0043229 | intracellular organelle | 7014 | 29 | 18.15 | Cellular Component | 0.00031 | 1.35E-02 | 0.004135 | 2.383568 | 3.508638 |
| GO:0043226 | organelle | 7018 | 29 | 18.16 | Cellular Component | 0.00031 | 1.35E-02 | 0.004132 | 2.383815 | 3.508638 |
| GO:0043231 | intracellular membrane-bounded organelle | 6349 | 27 | 16.42 | Cellular Component | 0.00048 | 1.85E-02 | 0.004253 | 2.371342 | 3.318759 |

Supplementary Table 8 – Cont.

| GO ID | Functional Class | Annotated | Input number | Expected | Aspect | p-value | q-value | Rich Factor | Log (Rich Factor) | Log P-value |
|------------|----------------------------------------------|-----------|--------------|----------|--------------------|---------|----------|-------------|-------------------|-------------|
| GO:0043227 | membrane-bounded organelle | 6351 | 27 | 16.43 | Cellular Component | 0.00048 | 1.85E-02 | 0.004251 | 2.371478 | 3.318759 |
| GO:0005829 | cytosol | 1094 | 9 | 2.83 | Cellular Component | 0.00155 | 5.67E-02 | 0.008227 | 2.084775 | 2.809668 |
| GO:0070469 | respiratory chain | 106 | 3 | 0.27 | Cellular Component | 0.00256 | 8.90E-02 | 0.028302 | 1.548185 | 2.59176 |
| GO:0043234 | protein complex | 1303 | 8 | 3.37 | Cellular Component | 0.01656 | 4.80E-01 | 0.00614 | 2.211854 | 1.78094 |
| GO:0005746 | mitochondrial respiratory chain | 79 | 2 | 0.2 | Cellular Component | 0.01772 | 4.93E-01 | 0.025316 | 1.596597 | 1.751536 |
| GO:0098803 | respiratory chain complex | 81 | 2 | 0.21 | Cellular Component | 0.01857 | 4.96E-01 | 0.024691 | 1.607455 | 1.731188 |
| GO:0098800 | inner mitochondrial membrane protein complex | 98 | 2 | 0.25 | Cellular Component | 0.0265 | 6.82E-01 | 0.020408 | 1.690196 | 1.576754 |
| GO:0098798 | mitochondrial protein complex | 104 | 2 | 0.27 | Cellular Component | 0.02958 | 6.82E-01 | 0.019231 | 1.716003 | 1.529002 |
| GO:0031967 | organelle envelope | 690 | 5 | 1.79 | Cellular Component | 0.03139 | 6.82E-01 | 0.007246 | 2.139879 | 1.503209 |
| GO:0009505 | plant-type cell wall | 108 | 2 | 0.28 | Cellular Component | 0.03171 | 6.82E-01 | 0.018519 | 1.732394 | 1.498804 |
| GO:0031975 | envelope | 694 | 5 | 1.8 | Cellular Component | 0.03207 | 6.82E-01 | 0.007205 | 2.142389 | 1.493901 |
| GO:0005739 | mitochondrion | 954 | 6 | 2.47 | Cellular Component | 0.03429 | 6.82E-01 | 0.006289 | 2.201397 | 1.464833 |
| GO:0005773 | vacuole | 493 | 4 | 1.28 | Cellular Component | 0.03763 | 6.82E-01 | 0.008114 | 2.090787 | 1.424466 |
| GO:1990204 | oxidoreductase complex | 124 | 2 | 0.32 | Cellular Component | 0.04079 | 6.82E-01 | 0.016129 | 1.792392 | 1.389446 |
| GO:0005777 | peroxisome | 129 | 2 | 0.33 | Cellular Component | 0.0438 | 6.82E-01 | 0.015504 | 1.80956 | 1.358526 |
| GO:0042579 | microbody | 129 | 2 | 0.33 | Cellular Component | 0.0438 | 6.82E-01 | 0.015504 | 1.80956 | 1.358526 |
| GO:0005774 | vacuolar membrane | 306 | 3 | 0.79 | Cellular Component | 0.04419 | 6.82E-01 | 0.009804 | 2.0086 | 1.354676 |

Supplementary Table 8 – Cont.

| GO ID | Functional Class | Annotated | Input number | Expected | Aspect | p-value | q-value | Rich Factor | Log (Rich Factor) | Log P-value |
|------------|----------------------------------------|-----------|--------------|----------|--------------------|----------|----------|-------------|-------------------|-------------|
| GO:0044437 | vacuolar part | 307 | 3 | 0.79 | Cellular Component | 0.04455 | 6.82E-01 | 0.009772 | 2.010017 | 1.351152 |
| GO:0005777 | peroxisome | 129 | 2 | 0.33 | Cellular Component | 0.0438 | 6.82E-01 | 0.015504 | 1.80956 | 1.358526 |
| GO:0042579 | microbody | 129 | 2 | 0.33 | Cellular Component | 0.0438 | 6.82E-01 | 0.015504 | 1.80956 | 1.358526 |
| GO:0005774 | vacuolar membrane | 306 | 3 | 0.79 | Cellular Component | 0.04419 | 6.82E-01 | 0.009804 | 2.0086 | 1.354676 |
| GO:0044437 | vacuolar part | 307 | 3 | 0.79 | Cellular Component | 0.04455 | 6.82E-01 | 0.009772 | 2.010017 | 1.351152 |
| GO:0005874 | microtubule | 131 | 2 | 0.34 | Cellular Component | 0.04503 | 6.82E-01 | 0.015267 | 1.816241 | 1.346498 |
| GO:0044455 | mitochondrial membrane part | 131 | 2 | 0.34 | Cellular Component | 0.04503 | 6.82E-01 | 0.015267 | 1.816241 | 1.346498 |
| GO:0003824 | catalytic activity | 9657 | 43 | 27.22 | Molecular Function | 1.20E-05 | 2.81E-02 | 0.004453 | 2.351374 | 4.920819 |
| GO:0043295 | glutathione binding | 4 | 2 | 0.01 | Molecular Function | 4.70E-05 | 3.67E-02 | 0.5 | 0.30103 | 4.327902 |
| GO:1900750 | oligopeptide binding | 4 | 2 | 0.01 | Molecular Function | 4.70E-05 | 3.67E-02 | 0.5 | 0.30103 | 4.327902 |
| GO:0004364 | glutathione transferase activity | 11 | 2 | 0.03 | Molecular Function | 0.00042 | 1.97E-01 | 0.181818 | 0.740363 | 3.376751 |
| GO:0072341 | modified amino acid binding | 11 | 2 | 0.03 | Molecular Function | 0.00042 | 1.97E-01 | 0.181818 | 0.740363 | 3.376751 |
| GO:0042277 | peptide binding | 26 | 2 | 0.07 | Molecular Function | 0.00243 | 6.00E-01 | 0.076923 | 1.113943 | 2.614394 |
| GO:1901681 | sulfur compound binding | 26 | 2 | 0.07 | Molecular Function | 0.00243 | 6.00E-01 | 0.076923 | 1.113943 | 2.614394 |
| GO:0005200 | structural constituent of cytoskeleton | 28 | 2 | 0.08 | Molecular Function | 0.00281 | 6.00E-01 | 0.071429 | 1.146128 | 2.551294 |
| GO:0003993 | acid phosphatase activity | 31 | 2 | 0.09 | Molecular Function | 0.00344 | 6.71E-01 | 0.064516 | 1.190332 | 2.463442 |

Supplementary Table 8 – Cont.

| GO ID | Functional Class | Annotated | Input number | Expected | Aspect | p-value | q-value | Rich Factor | Log (Rich Factor) | Log P-value |
|------------|-------------------------------------------------------------------------------------|-----------|--------------|----------|--------------------|---------|----------|-------------|-------------------|-------------|
| GO:0033218 | amide binding | 35 | 2 | 0.1 | Molecular Function | 0.00437 | 6.94E-01 | 0.057143 | 1.243038 | 2.359519 |
| GO:0003954 | NADH dehydrogenase activity | 43 | 2 | 0.12 | Molecular Function | 0.00654 | 6.96E-01 | 0.046512 | 1.332438 | 2.184422 |
| GO:0008137 | NADH dehydrogenase (ubiquinone) activity | 43 | 2 | 0.12 | Molecular Function | 0.00654 | 6.96E-01 | 0.046512 | 1.332438 | 2.184422 |
| GO:0033218 | amide binding | 35 | 2 | 0.1 | Molecular Function | 0.00437 | 6.94E-01 | 0.057143 | 1.243038 | 2.359519 |
| GO:0003954 | NADH dehydrogenase activity | 43 | 2 | 0.12 | Molecular Function | 0.00654 | 6.96E-01 | 0.046512 | 1.332438 | 2.184422 |
| GO:0008137 | NADH dehydrogenase (ubiquinone) activity | 43 | 2 | 0.12 | Molecular Function | 0.00654 | 6.96E-01 | 0.046512 | 1.332438 | 2.184422 |
| GO:0050136 | NADH dehydrogenase (quinone) activity | 43 | 2 | 0.12 | Molecular Function | 0.00654 | 6.96E-01 | 0.046512 | 1.332438 | 2.184422 |
| GO:0016835 | carbon-oxygen lyase activity | 140 | 3 | 0.39 | Molecular Function | 0.00722 | 7.35E-01 | 0.021429 | 1.669007 | 2.141463 |
| GO:0016655 | oxidoreductase activity, acting on NAD(P)H, quinone or similar compound as acceptor | 53 | 2 | 0.15 | Molecular Function | 0.0098 | 7.74E-01 | 0.037736 | 1.423246 | 2.008774 |
| GO:0016597 | amino acid binding | 63 | 2 | 0.18 | Molecular Function | 0.01365 | 8.42E-01 | 0.031746 | 1.498311 | 1.864867 |
| GO:0016829 | lyase activity | 342 | 4 | 0.96 | Molecular Function | 0.01568 | 8.53E-01 | 0.011696 | 1.931966 | 1.804654 |
| GO:0016836 | hydro-lyase activity | 70 | 2 | 0.2 | Molecular Function | 0.01667 | 8.53E-01 | 0.028571 | 1.544068 | 1.778064 |
| GO:0004812 | aminoacyl-tRNA ligase activity | 71 | 2 | 0.2 | Molecular Function | 0.01712 | 8.53E-01 | 0.028169 | 1.550228 | 1.766496 |
| GO:0016875 | ligase activity, forming carbon-oxygen bonds | 71 | 2 | 0.2 | Molecular Function | 0.01712 | 8.53E-01 | 0.028169 | 1.550228 | 1.766496 |
| GO:0016876 | ligase activity, forming aminoacyl-tRNA and related compounds | 71 | 2 | 0.2 | Molecular Function | 0.01712 | 8.53E-01 | 0.028169 | 1.550228 | 1.766496 |

Supplementary Table 8 – Cont.

| GO ID | Functional Class | Annotated | Input number | Expected | Aspect | p-value | q-value | Rich Factor | Log (Rich Factor) | Log P-value |
|------------|-----------------------------------------------------------------------------|-----------|--------------|----------|--------------------|----------|----------|-------------|-------------------|-------------|
| GO:0016627 | oxidoreductase activity, acting on the CH-CH group of donors | 72 | 2 | 0.2 | Molecular Function | 0.01758 | 8.58E-01 | 0.027778 | 1.556303 | 1.754981 |
| GO:0016779 | nucleotidyltransferase activity | 208 | 3 | 0.59 | Molecular Function | 0.02087 | 9.58E-01 | 0.014423 | 1.840942 | 1.680478 |
| GO:0016765 | transferase activity, transferring alkyl or aryl (other than methyl) groups | 84 | 2 | 0.24 | Molecular Function | 0.02346 | 9.79E-01 | 0.02381 | 1.623249 | 1.629672 |
| GO:0031406 | carboxylic acid binding | 87 | 2 | 0.25 | Molecular Function | 0.02505 | 9.79E-01 | 0.022989 | 1.638489 | 1.601192 |
| GO:0043177 | organic acid binding | 87 | 2 | 0.25 | Molecular Function | 0.02505 | 9.79E-01 | 0.022989 | 1.638489 | 1.601192 |
| GO:0016491 | oxidoreductase activity | 1790 | 10 | 5.05 | Molecular Function | 0.02645 | 1.00E+00 | 0.005587 | 2.252853 | 1.577574 |
| GO:0016791 | phosphatase activity | 232 | 3 | 0.65 | Molecular Function | 0.02767 | 1.00E+00 | 0.012931 | 1.888367 | 1.557991 |
| GO:0016874 | ligase activity | 239 | 3 | 0.67 | Molecular Function | 0.02985 | 1.00E+00 | 0.012552 | 1.901277 | 1.525056 |
| GO:0016651 | oxidoreductase activity, acting on NAD(P)H | 109 | 2 | 0.31 | Molecular Function | 0.03789 | 1.00E+00 | 0.018349 | 1.736397 | 1.421475 |
| GO:0016787 | hydrolase activity | 3046 | 14 | 8.59 | Molecular Function | 0.03984 | 1.00E+00 | 0.004596 | 2.337602 | 1.399681 |
| GO:0042578 | phosphoric ester hydrolase activity | 293 | 3 | 0.83 | Molecular Function | 0.04963 | 1.00E+00 | 0.010239 | 1.989746 | 1.304256 |
| GO:0044281 | small molecule metabolic process | 1473 | 16 | 4.36 | Biological Process | 2.40E-06 | 9.54E-03 | 0.010862 | 1.964083 | 5.619789 |
| GO:0031668 | cellular response to extracellular stimulus | 92 | 5 | 0.27 | Biological Process | 7.40E-06 | 9.54E-03 | 0.054348 | 1.264818 | 5.130768 |
| GO:0071496 | cellular response to external stimulus | 96 | 5 | 0.28 | Biological Process | 9.10E-06 | 9.54E-03 | 0.052083 | 1.283301 | 5.040959 |
| GO:0043436 | oxoacid metabolic process | 916 | 12 | 2.71 | Biological Process | 9.80E-06 | 9.54E-03 | 0.0131 | 1.882714 | 5.008774 |
| GO:0006082 | organic acid metabolic process | 918 | 12 | 2.72 | Biological Process | 1.00E-05 | 9.54E-03 | 0.013072 | 1.883661 | 5 |

Supplementary Table 8 – Cont.

| GO ID | Functional Class | Annotated | Input number | Expected | Aspect | p-value | q-value | Rich Factor | Log (Rich Factor) | Log P-value |
|------------|-------------------------------------------|-----------|--------------|----------|--------------------|----------|----------|-------------|-------------------|-------------|
| GO:0006082 | organic acid metabolic process | 918 | 12 | 2.72 | Biological Process | 1.00E-05 | 9.54E-03 | 0.013072 | 1.883661 | 5 |
| GO:0009991 | response to extracellular stimulus | 108 | 5 | 0.32 | Biological Process | 1.60E-05 | 1.27E-02 | 0.046296 | 1.334454 | 4.79588 |
| GO:0009267 | cellular response to starvation | 67 | 4 | 0.2 | Biological Process | 4.50E-05 | 2.74E-02 | 0.059701 | 1.224015 | 4.346787 |
| GO:0019752 | carboxylic acid metabolic process | 897 | 11 | 2.65 | Biological Process | 4.60E-05 | 2.74E-02 | 0.012263 | 1.9114 | 4.337242 |
| GO:0042594 | response to starvation | 74 | 4 | 0.22 | Biological Process | 6.60E-05 | 3.50E-02 | 0.054054 | 1.267172 | 4.180456 |
| GO:0031669 | cellular response to nutrient levels | 77 | 4 | 0.23 | Biological Process | 7.70E-05 | 3.67E-02 | 0.051948 | 1.284431 | 4.113509 |
| GO:0031667 | response to nutrient levels | 92 | 4 | 0.27 | Biological Process | 0.00015 | 6.50E-02 | 0.043478 | 1.361728 | 3.823909 |
| GO:0016036 | cellular response to phosphate starvation | 41 | 3 | 0.12 | Biological Process | 0.00024 | 9.54E-02 | 0.073171 | 1.135663 | 3.619789 |
| GO:0044763 | single-organism cellular process | 5424 | 27 | 16.04 | Biological Process | 0.00081 | 2.97E-01 | 0.004978 | 2.302956 | 3.091515 |
| GO:0044283 | small molecule biosynthetic process | 548 | 7 | 1.62 | Biological Process | 0.00105 | 3.37E-01 | 0.012774 | 1.893683 | 2.978811 |
| GO:0044711 | single-organism biosynthetic process | 1286 | 11 | 3.8 | Biological Process | 0.00106 | 3.37E-01 | 0.008554 | 2.067848 | 2.974694 |
| GO:0016053 | organic acid biosynthetic process | 429 | 6 | 1.27 | Biological Process | 0.00157 | 4.24E-01 | 0.013986 | 1.854306 | 2.8041 |
| GO:0046394 | carboxylic acid biosynthetic process | 429 | 6 | 1.27 | Biological Process | 0.00157 | 4.24E-01 | 0.013986 | 1.854306 | 2.8041 |
| GO:0006520 | cellular amino acid metabolic process | 431 | 6 | 1.27 | Biological Process | 0.0016 | 4.24E-01 | 0.013921 | 1.856326 | 2.79588 |
| GO:0009605 | response to external stimulus | 627 | 7 | 1.85 | Biological Process | 0.00228 | 5.30E-01 | 0.011164 | 1.95217 | 2.642065 |
| GO:0046686 | response to cadmium ion | 191 | 4 | 0.56 | Biological Process | 0.00241 | 5.30E-01 | 0.020942 | 1.678973 | 2.617983 |
| GO:0033554 | cellular response to stress | 468 | 6 | 1.38 | Biological Process | 0.00243 | 5.30E-01 | 0.012821 | 1.892095 | 2.614394 |

Supplementary Table 8 – Cont.

| GO ID | Functional Class | Annotated | Input number | Expected | Aspect | p-value | q-value | Rich Factor | Log (Rich Factor) | Log P-value |
|------------|-----------------------------------------------------|-----------|--------------|----------|--------------------|---------|----------|-------------|-------------------|-------------|
| GO:0045333 | cellular respiration | 94 | 3 | 0.28 | Biological Process | 0.00269 | 5.30E-01 | 0.031915 | 1.496007 | 2.570248 |
| GO:0008652 | cellular amino acid biosynthetic process | 203 | 4 | 0.6 | Biological Process | 0.003 | 5.30E-01 | 0.019704 | 1.705436 | 2.522879 |
| GO:0050896 | response to stimulus | 3255 | 18 | 9.63 | Biological Process | 0.00368 | 6.27E-01 | 0.00553 | 2.257278 | 2.434152 |
| GO:0000302 | response to reactive oxygen species | 107 | 3 | 0.32 | Biological Process | 0.00388 | 6.38E-01 | 0.028037 | 1.552263 | 2.411168 |
| GO:0015980 | energy derivation by oxidation of organic compounds | 110 | 3 | 0.33 | Biological Process | 0.00419 | 6.66E-01 | 0.027273 | 1.564271 | 2.377786 |
| GO:0006950 | response to stress | 1815 | 12 | 5.37 | Biological Process | 0.00539 | 8.05E-01 | 0.006612 | 2.179695 | 2.268411 |
| GO:0050896 | response to stimulus | 3255 | 18 | 9.63 | Biological Process | 0.00368 | 6.27E-01 | 0.00553 | 2.257278 | 2.434152 |
| GO:0000302 | response to reactive oxygen species | 107 | 3 | 0.32 | Biological Process | 0.00388 | 6.38E-01 | 0.028037 | 1.552263 | 2.411168 |
| GO:0015980 | energy derivation by oxidation of organic compounds | 110 | 3 | 0.33 | Biological Process | 0.00419 | 6.66E-01 | 0.027273 | 1.564271 | 2.377786 |
| GO:0006950 | response to stress | 1815 | 12 | 5.37 | Biological Process | 0.00539 | 8.05E-01 | 0.006612 | 2.179695 | 2.268411 |
| GO:0044710 | single-organism metabolic process | 4290 | 21 | 12.69 | Biological Process | 0.00656 | 8.53E-01 | 0.004895 | 2.310238 | 2.183096 |
| GO:0010038 | response to metal ion | 254 | 4 | 0.75 | Biological Process | 0.00662 | 8.53E-01 | 0.015748 | 1.802774 | 2.179142 |
| GO:0042221 | response to chemical | 1481 | 10 | 4.38 | Biological Process | 0.01004 | 1.00E+00 | 0.006752 | 2.170555 | 1.998266 |
| GO:0044699 | single-organism process | 7726 | 31 | 22.85 | Biological Process | 0.01148 | 1.00E+00 | 0.004012 | 2.396593 | 1.940058 |
| GO:1901607 | alpha-amino acid biosynthetic process | 159 | 3 | 0.47 | Biological Process | 0.01154 | 1.00E+00 | 0.018868 | 1.724276 | 1.937794 |
| GO:0009628 | response to abiotic stimulus | 1067 | 8 | 3.16 | Biological Process | 0.01211 | 1.00E+00 | 0.007498 | 2.125074 | 1.916856 |

Supplementary Table 8 – Cont.

| GO ID | Functional Class | Annotated | Input number | Expected | Aspect | p-value | q-value | Rich Factor | Log (Rich Factor) | Log P-value |
|------------|-------------------------------------------------|-----------|--------------|----------|--------------------|---------|----------|-------------|-------------------|-------------|
| GO:0009073 | aromatic amino acid family biosynthetic process | 58 | 2 | 0.17 | Biological Process | 0.01274 | 1.00E+00 | 0.034483 | 1.462398 | 1.894831 |
| GO:0006081 | cellular aldehyde metabolic process | 63 | 2 | 0.19 | Biological Process | 0.01491 | 1.00E+00 | 0.031746 | 1.498311 | 1.826522 |
| GO:0006091 | generation of precursor metabolites and energy | 323 | 4 | 0.96 | Biological Process | 0.01503 | 1.00E+00 | 0.012384 | 1.907143 | 1.823041 |
| GO:0007154 | cell communication | 897 | 7 | 2.65 | Biological Process | 0.01551 | 1.00E+00 | 0.007804 | 2.107694 | 1.809388 |
| GO:0010035 | response to inorganic substance | 507 | 5 | 1.5 | Biological Process | 0.01648 | 1.00E+00 | 0.009862 | 2.006038 | 1.783043 |
| GO:0009648 | photoperiodism | 67 | 2 | 0.2 | Biological Process | 0.01675 | 1.00E+00 | 0.029851 | 1.525045 | 1.775985 |
| GO:0006418 | tRNA aminoacylation for protein translation | 70 | 2 | 0.21 | Biological Process | 0.0182 | 1.00E+00 | 0.028571 | 1.544068 | 1.739929 |
| GO:0043648 | dicarboxylic acid metabolic process | 70 | 2 | 0.21 | Biological Process | 0.0182 | 1.00E+00 | 0.028571 | 1.544068 | 1.739929 |
| GO:0043038 | amino acid activation | 73 | 2 | 0.22 | Biological Process | 0.01969 | 1.00E+00 | 0.027397 | 1.562293 | 1.705754 |
| GO:0043039 | tRNA aminoacylation | 73 | 2 | 0.22 | Biological Process | 0.01969 | 1.00E+00 | 0.027397 | 1.562293 | 1.705754 |
| GO:0006417 | regulation of translation | 75 | 2 | 0.22 | Biological Process | 0.02072 | 1.00E+00 | 0.026667 | 1.574031 | 1.68361 |
| GO:0034248 | regulation of cellular amide metabolic process | 75 | 2 | 0.22 | Biological Process | 0.02072 | 1.00E+00 | 0.026667 | 1.574031 | 1.68361 |
| GO:1901135 | carbohydrate derivative metabolic process | 548 | 5 | 1.62 | Biological Process | 0.02227 | 1.00E+00 | 0.009124 | 2.039811 | 1.65228 |
| GO:0009117 | nucleotide metabolic process | 372 | 4 | 1.1 | Biological Process | 0.02388 | 1.00E+00 | 0.010753 | 1.968483 | 1.621966 |
| GO:0006753 | nucleoside phosphate metabolic process | 378 | 4 | 1.12 | Biological Process | 0.02514 | 1.00E+00 | 0.010582 | 1.975432 | 1.599635 |
| GO:0016311 | dephosphorylation | 215 | 3 | 0.64 | Biological Process | 0.02559 | 1.00E+00 | 0.013953 | 1.855317 | 1.59193 |

Supplementary Table 8 – Cont.

| GO ID | Functional Class | Annotated | Input number | Expected | Aspect | p-value | q-value | Rich Factor | Log (Rich Factor) | Log P-value |
|------------|--------------------------------------------------------|-----------|--------------|----------|--------------------|---------|----------|-------------|-------------------|-------------|
| GO:0006979 | response to oxidative stress | 382 | 4 | 1.13 | Biological Process | 0.026 | 1.00E+00 | 0.010471 | 1.980003 | 1.585027 |
| GO:0009072 | aromatic amino acid family metabolic process | 87 | 2 | 0.26 | Biological Process | 0.02731 | 1.00E+00 | 0.022989 | 1.638489 | 1.563678 |
| GO:0019637 | organophosphate metabolic process | 586 | 5 | 1.73 | Biological Process | 0.02871 | 1.00E+00 | 0.008532 | 2.068928 | 1.541967 |
| GO:0051716 | cellular response to stimulus | 1259 | 8 | 3.72 | Biological Process | 0.02977 | 1.00E+00 | 0.006354 | 2.196936 | 1.526221 |
| GO:0032787 | monocarboxylic acid metabolic process | 407 | 4 | 1.2 | Biological Process | 0.03181 | 1.00E+00 | 0.009828 | 2.007534 | 1.497436 |
| GO:0009553 | embryo sac development | 97 | 2 | 0.29 | Biological Process | 0.03337 | 1.00E+00 | 0.020619 | 1.685742 | 1.476644 |
| GO:0008299 | isoprenoid biosynthetic process | 100 | 2 | 0.3 | Biological Process | 0.03528 | 1.00E+00 | 0.02 | 1.69897 | 1.452471 |
| GO:0071214 | cellular response to abiotic stimulus | 102 | 2 | 0.3 | Biological Process | 0.03657 | 1.00E+00 | 0.019608 | 1.70757 | 1.436875 |
| GO:0006090 | pyruvate metabolic process | 104 | 2 | 0.31 | Biological Process | 0.03789 | 1.00E+00 | 0.019231 | 1.716003 | 1.421475 |
| GO:0009793 | embryo development ending in seed dormancy | 251 | 3 | 0.74 | Biological Process | 0.03792 | 1.00E+00 | 0.011952 | 1.922552 | 1.421132 |
| GO:1901605 | alpha-amino acid metabolic process | 254 | 3 | 0.75 | Biological Process | 0.03907 | 1.00E+00 | 0.011811 | 1.927712 | 1.408157 |
| GO:0048229 | gametophyte development | 255 | 3 | 0.75 | Biological Process | 0.03945 | 1.00E+00 | 0.011765 | 1.929419 | 1.403953 |
| GO:0055086 | nucleobase-containing small molecule metabolic process | 437 | 4 | 1.29 | Biological Process | 0.03972 | 1.00E+00 | 0.009153 | 2.038421 | 1.400991 |
| GO:1901564 | organonitrogen compound metabolic process | 1843 | 10 | 5.45 | Biological Process | 0.04014 | 1.00E+00 | 0.005426 | 2.265525 | 1.396423 |
| GO:0009790 | embryo development | 271 | 3 | 0.8 | Biological Process | 0.04588 | 1.00E+00 | 0.01107 | 1.955848 | 1.338377 |

Supplementary Table 8 – Cont.

| GO ID | Functional Class | Annotated | Input number | Expected | Aspect | p-value | q-value | Rich Factor | Log (Rich Factor) | Log P-value |
|------------|------------------------------|-----------|--------------|----------|--------------------|---------|----------|-------------|-------------------|-------------|
| GO:0042440 | pigment metabolic process | 116 | 2 | 0.34 | Biological Process | 0.04615 | 1.00E+00 | 0.017241 | 1.763428 | 1.335828 |
| GO:0006720 | isoprenoid metabolic process | 117 | 2 | 0.35 | Biological Process | 0.04686 | 1.00E+00 | 0.017094 | 1.767156 | 1.329198 |
| GO:0046939 | nucleotide phosphorylation | 119 | 2 | 0.35 | Biological Process | 0.04831 | 1.00E+00 | 0.016807 | 1.774517 | 1.315963 |

Supplementary Table 9. Pathways enriched by Kyoto Encyclopedia of Genes and Genomes (KEGG) analysis

| Proteins down regulated in L80 LP | | | | | | | | |
|-----------------------------------|-----------------------------------------------------|--------------|-------------------|-------------|-------------------|-------------|-------------------|-------------|
| ID | Pathway | Input number | Background number | P-Value | Corrected P-Value | Rich Factor | Log (Rich Factor) | Log P-value |
| zma00195 | Photosynthesis | 5 | 117 | 8.71E-07 | 1.57E-05 | 0.042735043 | 1.369215857 | 6.060154434 |
| zma01100 | Metabolic pathways | 12 | 2906 | 0.000599726 | 0.00539753 | 0.004129387 | 2.384114364 | 3.222047428 |
| zma03010 | Ribosome | 5 | 577 | 0.0014153 | 0.008491801 | 0.008665511 | 2.062205809 | 2.849151432 |
| zma00196 | Photosynthesis - antenna proteins | 2 | 47 | 0.002264559 | 0.010190517 | 0.042553191 | 1.371067862 | 2.645016286 |
| zma00944 | Flavone and flavonol biosynthesis | 1 | 7 | 0.011422426 | 0.041120735 | 0.142857143 | 0.84509804 | 1.94224163 |
| zma00190 | Oxidative phosphorylation | 2 | 197 | 0.033139172 | 0.099417515 | 0.010152284 | 1.99343623 | 1.47965835 |
| zma01110 | Biosynthesis of secondary metabolites | 5 | 1478 | 0.059820081 | 0.143596146 | 0.00338295 | 2.47070443 | 1.223153006 |
| zma00592 | alpha-Linolenic acid metabolism | 1 | 55 | 0.077329606 | 0.143596146 | 0.018181818 | 1.740362689 | 1.111654202 |
| zma01230 | Biosynthesis of amino acids | 2 | 327 | 0.080850355 | 0.143596146 | 0.006116208 | 2.213517757 | 1.092318068 |
| zma00400 | Phenylalanine, tyrosine and tryptophan biosynthesis | 1 | 59 | 0.082624055 | 0.143596146 | 0.016949153 | 1.770852012 | 1.082893495 |
| zma00970 | Aminoacyl-tRNA biosynthesis | 1 | 64 | 0.089200424 | 0.143596146 | 0.015625 | 1.806179974 | 1.049633081 |
| zma00860 | Porphyrin and chlorophyll metabolism | 1 | 69 | 0.095730764 | 0.143596146 | 0.014492754 | 1.838849091 | 1.018948476 |
| zma01210 | 2-Oxocarboxylic acid metabolism | 1 | 80 | 0.109937034 | 0.152220509 | 0.0125 | 1.903089987 | 0.958855982 |
| zma00020 | Citrate cycle (TCA cycle) | 1 | 91 | 0.123925354 | 0.159332598 | 0.010989011 | 1.959041392 | 0.906839833 |
| zma00561 | Glycerolipid metabolism | 1 | 106 | 0.14265498 | 0.171185975 | 0.009433962 | 2.025305865 | 0.845713064 |
| zma00564 | Glycerophospholipid metabolism | 1 | 141 | 0.184850301 | 0.207956588 | 0.007092199 | 2.149219113 | 0.733179838 |
| zma04141 | Protein processing in endoplasmic reticulum | 1 | 312 | 0.363540599 | 0.38492534 | 0.003205128 | 2.494154594 | 0.439447082 |
| zma01200 | Carbon metabolism | 1 | 358 | 0.404676337 | 0.404676337 | 0.002793296 | 2.553883027 | 0.39289219 |
| Proteins down regulated in P7 LP | | | | | | | | |
| zma03010 | Ribosome | 5 | 577 | 9.52E-05 | 0.001427799 | 0.008665511 | 2.062205809 | 4.0214241 |
| zma00402 | Benzoxazinoid biosynthesis | 1 | 15 | 0.013049277 | 0.097869577 | 0.066666667 | 1.176091259 | 1.884413554 |
| zma01230 | Biosynthesis of amino acids | 2 | 327 | 0.029569714 | 0.135328617 | 0.006116208 | 2.213517757 | 1.529152882 |
| zma00220 | Arginine biosynthesis | 1 | 44 | 0.036286276 | 0.135328617 | 0.022727273 | 1.643452676 | 1.440257604 |

Supplementary Table 9 – Cont.

| ID | Pathway | Input number | Background number | P-Value | Corrected P-Value | Rich Factor | Log (Rich Factor) | Log P-value |
|-----------|---------------------------------------------|---------------------|--------------------------|----------------|--------------------------|--------------------|--------------------------|--------------------|
| zma00250 | Alanine, aspartate and glutamate metabolism | 1 | 69 | 0.055896523 | 0.135328617 | 0.014492754 | 1.838849091 | 1.252615205 |
| zma00052 | Galactose metabolism | 1 | 76 | 0.061318495 | 0.135328617 | 0.013157895 | 1.880813592 | 1.21240851 |
| zma01210 | 2-Oxocarboxylic acid metabolism | 1 | 80 | 0.064403354 | 0.135328617 | 0.0125 | 1.903089987 | 1.191091514 |
| zma03050 | Proteasome | 1 | 98 | 0.078165393 | 0.135328617 | 0.010204082 | 1.991226076 | 1.106985483 |
| zma00710 | Carbon fixation in photosynthetic organisms | 1 | 102 | 0.08119717 | 0.135328617 | 0.009803922 | 2.008600172 | 1.090459108 |
| zma00195 | Photosynthesis | 1 | 117 | 0.092481451 | 0.138722177 | 0.008547009 | 2.068185862 | 1.033945363 |
| zma00270 | Cysteine and methionine metabolism | 1 | 150 | 0.116841235 | 0.159328957 | 0.006666667 | 2.176091259 | 0.93240386 |
| zma00500 | Starch and sucrose metabolism | 1 | 186 | 0.142700617 | 0.178375771 | 0.005376344 | 2.269512944 | 0.84557415 |
| zma01100 | Metabolic pathways | 4 | 2906 | 0.211484867 | 0.244021001 | 0.001376462 | 2.861235619 | 0.674720703 |
| zma01200 | Carbon metabolism | 1 | 358 | 0.256557016 | 0.274882517 | 0.002793296 | 2.553883027 | 0.590816104 |
| zma01110 | Biosynthesis of secondary metabolites | 1 | 1478 | 0.712238195 | 0.712238195 | 0.00067659 | 3.169674434 | 0.147374741 |

Supplementary Table 10. Pathways enriched by Kyoto Encyclopedia of Genes and Genomes (KEGG) analysis

| Proteins up regulated in L80 LP | | | | | | | | |
|---------------------------------|--------------------------------------------------------|--------------|-------------------|-------------|-------------------|-------------|-------------------|-------------|
| ID | Pathway | Input number | Background number | P-Value | Corrected P-Value | Rich Factor | Log (Rich Factor) | Log P-value |
| zma01100 | Metabolic pathways | 25 | 2906 | 1.60E-09 | 7.21E-08 | 0.008602891 | 2.065355601 | 8.795348498 |
| zma00960 | Tropane, piperidine and pyridine alkaloid biosynthesis | 3 | 18 | 1.41E-05 | 0.000268723 | 0.166666667 | 0.77815125 | 4.850502528 |
| zma01200 | Carbon metabolism | 7 | 358 | 1.82E-05 | 0.000268723 | 0.019553073 | 1.708784987 | 4.739345856 |
| zma01110 | Biosynthesis of secondary metabolites | 13 | 1478 | 2.39E-05 | 0.000268723 | 0.00879567 | 2.055731082 | 4.621846911 |
| zma00950 | Isoquinoline alkaloid biosynthesis | 3 | 24 | 3.07E-05 | 0.000276576 | 0.125 | 0.903089987 | 4.512427845 |
| zma01210 | 2-Oxocarboxylic acid metabolism | 4 | 80 | 3.96E-05 | 0.000296865 | 0.05 | 1.301029996 | 4.402502088 |
| zma01230 | Biosynthesis of amino acids | 6 | 327 | 0.000105562 | 0.000615935 | 0.018348624 | 1.736396502 | 3.976491073 |
| zma00360 | Phenylalanine metabolism | 3 | 38 | 0.0001095 | 0.000615935 | 0.078947368 | 1.102662342 | 3.960587423 |
| zma00350 | Tyrosine metabolism | 3 | 48 | 0.000210501 | 0.001052504 | 0.0625 | 1.204119983 | 3.676746199 |
| zma00410 | beta-Alanine metabolism | 3 | 58 | 0.000357989 | 0.001536497 | 0.051724138 | 1.286306739 | 3.446130131 |
| zma00400 | Phenylalanine, tyrosine and tryptophan biosynthesis | 3 | 59 | 0.000375588 | 0.001536497 | 0.050847458 | 1.293730757 | 3.425288209 |
| zma00330 | Arginine and proline metabolism | 3 | 63 | 0.000451529 | 0.001693235 | 0.047619048 | 1.322219295 | 3.345314154 |
| zma00750 | Vitamin B6 metabolism | 2 | 16 | 0.000747189 | 0.002586425 | 0.125 | 0.903089987 | 3.126569331 |
| zma00260 | Glycine, serine and threonine metabolism | 3 | 82 | 0.000945329 | 0.003038559 | 0.036585366 | 1.436692598 | 3.024416827 |
| zma00630 | Glyoxylate and dicarboxylate metabolism | 3 | 89 | 0.001188517 | 0.003565552 | 0.033707865 | 1.472268752 | 2.924994536 |
| zma00640 | Propanoate metabolism | 2 | 42 | 0.004448834 | 0.012512345 | 0.047619048 | 1.322219295 | 2.351753808 |
| zma00220 | Arginine biosynthesis | 2 | 44 | 0.004853309 | 0.012846993 | 0.045454545 | 1.342422681 | 2.313962093 |
| zma00280 | Valine, leucine and isoleucine degradation | 2 | 59 | 0.00839712 | 0.0209928 | 0.033898305 | 1.469822016 | 2.075869649 |
| zma00970 | Aminoacyl-tRNA biosynthesis | 2 | 64 | 0.009771747 | 0.023143611 | 0.03125 | 1.505149978 | 2.010027783 |
| zma00250 | Alanine, aspartate and glutamate metabolism | 2 | 69 | 0.011239307 | 0.02528844 | 0.028985507 | 1.537819095 | 1.949260471 |
| zma00240 | Pyrimidine metabolism | 2 | 84 | 0.016177841 | 0.034666802 | 0.023809524 | 1.62324929 | 1.791079445 |

Supplementary Table 10 – Cont.

| ID | Pathway | Input number | Background number | P-Value | Corrected P-Value | Rich Factor | Log (Rich Factor) | Log P-value |
|----------|---------------------------------------------|--------------|-------------------|-------------|-------------------|-------------|-------------------|-------------|
| zma01212 | Fatty acid metabolism | 2 | 91 | 0.018745826 | 0.036676615 | 0.021978022 | 1.658011397 | 1.727095429 |
| zma00020 | Citrate cycle (TCA cycle) | 2 | 91 | 0.018745826 | 0.036676615 | 0.021978022 | 1.658011397 | 1.727095429 |
| zma03050 | Proteasome | 2 | 98 | 0.021473591 | 0.040262983 | 0.020408163 | 1.69019608 | 1.668095324 |
| zma00710 | Carbon fixation in photosynthetic organisms | 2 | 102 | 0.023101939 | 0.04158349 | 0.019607843 | 1.707570176 | 1.636351566 |
| zma04146 | Peroxisome | 2 | 113 | 0.027831539 | 0.048169971 | 0.017699115 | 1.752048448 | 1.555462783 |
| zma00230 | Purine metabolism | 2 | 119 | 0.030561434 | 0.049964808 | 0.016806723 | 1.774516966 | 1.514826268 |
| zma04122 | Sulfur relay system | 1 | 13 | 0.031089214 | 0.049964808 | 0.076923077 | 1.113943352 | 1.507390261 |
| zma00480 | Glutathione metabolism | 2 | 126 | 0.033874815 | 0.052564368 | 0.015873016 | 1.799340549 | 1.470123073 |
| zma00511 | Other glycan degradation | 1 | 18 | 0.041960196 | 0.062940294 | 0.055555556 | 1.255272505 | 1.377162494 |
| zma00270 | Cysteine and methionine metabolism | 2 | 150 | 0.046219969 | 0.067093503 | 0.013333333 | 1.875061263 | 1.335170351 |
| zma00730 | Thiamine metabolism | 1 | 35 | 0.078030663 | 0.10973062 | 0.028571429 | 1.544068044 | 1.107734704 |
| zma01040 | Biosynthesis of unsaturated fatty acids | 1 | 37 | 0.082185303 | 0.112070868 | 0.027027027 | 1.568201724 | 1.085205839 |
| zma00770 | Pantothenate and CoA biosynthesis | 1 | 42 | 0.092491407 | 0.122415097 | 0.023809524 | 1.62324929 | 1.033898614 |
| zma00062 | Fatty acid elongation | 1 | 51 | 0.110755967 | 0.142400529 | 0.019607843 | 1.707570176 | 0.955632868 |
| zma00592 | alpha-Linolenic acid metabolism | 1 | 55 | 0.118756885 | 0.144434049 | 0.018181818 | 1.740362689 | 0.925341204 |
| zma00071 | Fatty acid degradation | 1 | 55 | 0.118756885 | 0.144434049 | 0.018181818 | 1.740362689 | 0.925341204 |
| zma00061 | Fatty acid biosynthesis | 1 | 65 | 0.138450315 | 0.16395432 | 0.015384615 | 1.812913357 | 0.858706052 |
| zma00030 | Pentose phosphate pathway | 1 | 76 | 0.159612673 | 0.184168469 | 0.013157895 | 1.880813592 | 0.796932629 |
| zma04145 | Phagosome | 1 | 123 | 0.244412825 | 0.274964428 | 0.008130081 | 2.089905111 | 0.61187601 |
| zma00520 | Amino sugar and nucleotide sugar metabolism | 1 | 183 | 0.340516473 | 0.373737593 | 0.005464481 | 2.26245109 | 0.467861873 |
| zma00190 | Oxidative phosphorylation | 1 | 197 | 0.361147009 | 0.386943224 | 0.005076142 | 2.294466226 | 0.442315977 |
| zma03013 | RNA transport | 1 | 226 | 0.401880721 | 0.420572847 | 0.004424779 | 2.354108439 | 0.395902828 |
| zma00940 | Phenylpropanoid biosynthesis | 1 | 245 | 0.427169982 | 0.436878391 | 0.004081633 | 2.389166084 | 0.369399274 |
| zma04141 | Protein processing in endoplasmic reticulum | 1 | 312 | 0.508224676 | 0.508224676 | 0.003205128 | 2.494154594 | 0.293944252 |

Supplementary Table 10 – Cont.

| Proteins up regulated in P7 LP | | | | | | | | |
|--------------------------------|---------------------------------------------|--------------|-------------------|-------------|-------------------|-------------|-------------------|-------------|
| ID | Pathway | Input number | Background number | P-Value | Corrected P-Value | Rich Factor | Log (Rich Factor) | Log P-value |
| zma01100 | Metabolic pathways | 30 | 2906 | 9.12E-13 | 4.65E-11 | 0.010323469 | 1.986174355 | 12.04000723 |
| zma01110 | Biosynthesis of secondary metabolites | 17 | 1478 | 5.90E-08 | 1.50E-06 | 0.01150203 | 1.939225513 | 7.229220122 |
| zma00480 | Glutathione metabolism | 6 | 126 | 7.72E-07 | 1.31E-05 | 0.047619048 | 1.322219295 | 6.112440754 |
| zma00941 | Flavonoid biosynthesis | 3 | 58 | 0.000425547 | 0.00542572 | 0.051724138 | 1.286306739 | 3.37105277 |
| zma00520 | Amino sugar and nucleotide sugar metabolism | 4 | 183 | 0.001060611 | 0.010261178 | 0.021857923 | 1.660391098 | 2.974444049 |
| zma00190 | Oxidative phosphorylation | 4 | 197 | 0.001383863 | 0.010261178 | 0.020304569 | 1.692406235 | 2.858906802 |
| zma00630 | Glyoxylate and dicarboxylate metabolism | 3 | 89 | 0.001408397 | 0.010261178 | 0.033707865 | 1.472268752 | 2.851274907 |
| zma00220 | Arginine biosynthesis | 2 | 44 | 0.00544107 | 0.030832729 | 0.045454545 | 1.342422681 | 2.264315696 |
| zma00920 | Sulfur metabolism | 2 | 44 | 0.00544107 | 0.030832729 | 0.045454545 | 1.342422681 | 2.264315696 |
| zma00910 | Nitrogen metabolism | 2 | 50 | 0.006906918 | 0.032291807 | 0.04 | 1.397940009 | 2.160715673 |
| zma04141 | Protein processing in endoplasmic reticulum | 4 | 312 | 0.0069649 | 0.032291807 | 0.012820513 | 1.892094603 | 2.157085138 |
| zma00592 | alpha-Linolenic acid metabolism | 2 | 55 | 0.008249752 | 0.035061448 | 0.036363636 | 1.439332694 | 2.083559084 |
| zma00500 | Starch and sucrose metabolism | 3 | 186 | 0.010536676 | 0.041336189 | 0.016129032 | 1.792391689 | 1.977296393 |
| zma00250 | Alanine, aspartate and glutamate metabolism | 2 | 69 | 0.012572398 | 0.04579945 | 0.028985507 | 1.537819095 | 1.900581878 |
| zma00030 | Pentose phosphate pathway | 2 | 76 | 0.015031333 | 0.049081779 | 0.026315789 | 1.579783597 | 1.823002507 |
| zma00900 | Terpenoid backbone biosynthesis | 2 | 77 | 0.015398205 | 0.049081779 | 0.025974026 | 1.58546073 | 1.812529897 |
| zma04070 | Phosphatidylinositol signaling system | 2 | 106 | 0.027628563 | 0.082885688 | 0.018867925 | 1.72427587 | 1.55864171 |
| zma00230 | Purine metabolism | 2 | 119 | 0.034036422 | 0.09643653 | 0.016806723 | 1.774516966 | 1.468056095 |
| zma00402 | Benzoxazinoid biosynthesis | 1 | 15 | 0.037557353 | 0.100811842 | 0.066666667 | 1.176091259 | 1.425305026 |
| zma00261 | Monobactam biosynthesis | 1 | 18 | 0.044442925 | 0.10829616 | 0.055555556 | 1.255272505 | 1.35219737 |
| zma01230 | Biosynthesis of amino acids | 3 | 327 | 0.044592537 | 0.10829616 | 0.009174312 | 2.037426498 | 1.350737823 |

Supplementary Table 10 – Cont.

| ID | Pathway | Input number | Background number | P-Value | Corrected P-Value | Rich Factor | Log (Rich Factor) | Log P-value |
|----------|-------------------------------------------------------|--------------|-------------------|-------------|-------------------|-------------|-------------------|-------------|
| zma00270 | Cysteine and methionine metabolism | 2 | 150 | 0.051337553 | 0.119009782 | 0.013333333 | 1.875061263 | 1.289564836 |
| zma01200 | Carbon metabolism | 3 | 358 | 0.055493339 | 0.123050447 | 0.008379888 | 2.076761772 | 1.255759146 |
| zma00450 | Selenocompound metabolism | 1 | 29 | 0.069277102 | 0.147213842 | 0.034482759 | 1.462397998 | 1.159410288 |
| zma00945 | Stilbenoid, diarylheptanoid and gingerol biosynthesis | 1 | 31 | 0.073723553 | 0.150396048 | 0.032258065 | 1.491361694 | 1.132393744 |
| zma00010 | Glycolysis / Gluconeogenesis | 2 | 197 | 0.08212647 | 0.155934824 | 0.010152284 | 1.99343623 | 1.085516844 |
| zma00730 | Thiamine metabolism | 1 | 35 | 0.08255373 | 0.155934824 | 0.028571429 | 1.544068044 | 1.083263298 |
| zma00906 | Carotenoid biosynthesis | 1 | 44 | 0.10211938 | 0.186003156 | 0.022727273 | 1.643452676 | 0.990891832 |
| zma00460 | Cyanoamino acid metabolism | 1 | 48 | 0.11068265 | 0.187930476 | 0.020833333 | 1.681241237 | 0.95592045 |
| zma00350 | Tyrosine metabolism | 1 | 48 | 0.11068265 | 0.187930476 | 0.020833333 | 1.681241237 | 0.95592045 |
| zma00062 | Fatty acid elongation | 1 | 51 | 0.117052225 | 0.187930476 | 0.019607843 | 1.707570176 | 0.931620326 |
| zma00940 | Phenylpropanoid biosynthesis | 2 | 245 | 0.117917161 | 0.187930476 | 0.008163265 | 2.088136089 | 0.928422984 |
| zma00071 | Fatty acid degradation | 1 | 55 | 0.125475086 | 0.193916042 | 0.018181818 | 1.740362689 | 0.901442497 |
| zma00400 | Phenylalanine, tyrosine and tryptophan biosynthesis | 1 | 59 | 0.133818735 | 0.198518964 | 0.016949153 | 1.770852012 | 0.87348308 |
| zma03040 | Spliceosome | 2 | 268 | 0.136238505 | 0.198518964 | 0.007462687 | 2.127104798 | 0.865700132 |
| zma00970 | Aminoacyl-tRNA biosynthesis | 1 | 64 | 0.144138021 | 0.204195529 | 0.015625 | 1.806179974 | 0.841221446 |
| zma00053 | Ascorbate and aldarate metabolism | 1 | 67 | 0.150271324 | 0.207130744 | 0.014925373 | 1.826074803 | 0.823123886 |
| zma00860 | Porphyrin and chlorophyll metabolism | 1 | 69 | 0.154336103 | 0.207135296 | 0.014492754 | 1.838849091 | 0.81153247 |
| zma00052 | Galactose metabolism | 1 | 76 | 0.168412465 | 0.220231685 | 0.013157895 | 1.880813592 | 0.773625768 |
| zma00040 | Pentose and glucuronate interconversions | 1 | 84 | 0.18421708 | 0.234603541 | 0.011904762 | 1.924279286 | 0.734670106 |
| zma00051 | Fructose and mannose metabolism | 1 | 90 | 0.195875885 | 0.234603541 | 0.011111111 | 1.954242509 | 0.708019029 |
| zma01212 | Fatty acid metabolism | 1 | 91 | 0.197802985 | 0.234603541 | 0.010989011 | 1.959041392 | 0.703767158 |
| zma00020 | Citrate cycle (TCA cycle) | 1 | 91 | 0.197802985 | 0.234603541 | 0.010989011 | 1.959041392 | 0.703767158 |
| zma00562 | Inositol phosphate metabolism | 1 | 98 | 0.211165813 | 0.244760374 | 0.010204082 | 1.991226076 | 0.675376392 |

Supplementary Table 10 – Cont.

| ID | Pathway | Input number | Background number | P-Value | Corrected P-Value | Rich Factor | Log (Rich Factor) | Log P-value |
|-----------|---------------------------------------------|---------------------|--------------------------|----------------|--------------------------|--------------------|--------------------------|--------------------|
| zma00562 | Inositol phosphate metabolism | 1 | 98 | 0.211165813 | 0.244760374 | 0.010204082 | 1.991226076 | 0.675376392 |
| zma00710 | Carbon fixation in photosynthetic organisms | 1 | 102 | 0.218702948 | 0.247863341 | 0.009803922 | 2.008600172 | 0.660145363 |
| zma00620 | Pyruvate metabolism | 1 | 121 | 0.253545977 | 0.279006166 | 0.008264463 | 2.08278537 | 0.595943276 |
| zma04145 | Phagosome | 1 | 123 | 0.257123329 | 0.279006166 | 0.008130081 | 2.089905111 | 0.589858517 |
| zma04626 | Plant-pathogen interaction | 1 | 214 | 0.403189692 | 0.425605141 | 0.004672897 | 2.330413773 | 0.39449058 |
| zma04144 | Endocytosis | 1 | 218 | 0.408914744 | 0.425605141 | 0.004587156 | 2.338456494 | 0.38836723 |
| zma03013 | RNA transport | 1 | 226 | 0.420202927 | 0.428529359 | 0.004424779 | 2.354108439 | 0.376540927 |
| zma04016 | MAPK signaling pathway - plant | 1 | 232 | 0.428529359 | 0.428529359 | 0.004310345 | 2.365487985 | 0.368019419 |